

**МІНІСТЕРСТВО ОСВІТИ І НАУКИ, МОЛОДІ ТА СПОРТУ УКРАЇНИ  
ПРИКАРПАТСЬКИЙ НАЦІОНАЛЬНИЙ УНІВЕРСИТЕТ  
ІМЕНІ ВАСИЛЯ СТЕФАНІКА**

Фізико-хімічний інститут  
Бердянський державний педагогічний університет  
Івано-Франківський національний технічний університет нафти і газу

**ДЕРЖАВНЕ АГЕНТСТВО З ПИТАНЬ НАУКИ, ІННОВАЦІЇ ТА  
ІНФОРМАЦІЇ УКРАЇНИ**

Державний фонд фундаментальних досліджень

**НАЦІОНАЛЬНА АКАДЕМІЯ НАУК УКРАЇНИ**

Інститут фізики напівпровідників ім. В.Є. Лашкарьова  
Інститут металофізики ім. Г.В. Курдюмова  
Інститут загальної і неорганічної хімії ім. В.І. Вернадського  
Інститут хімії поверхні ім. О.О.Чуйка

УКРАЇНСЬКЕ ФІЗИЧНЕ ТОВАРИСТВО  
АСОЦІАЦІЯ "ВЧЕНІ ПРИКАРПАТТЯ"  
ЛЮБЛІНСЬКИЙ ТЕХНІЧНИЙ УНІВЕРСИТЕТ (ПОЛЬЩА)  
УНІВЕРСИТЕТ ГАЗІ (ТУРЕЧЧИНА)

# **ФІЗИКА І ТЕХНОЛОГІЯ ТОНКИХ ПЛІВОК ТА НАНОСИСТЕМ**

**Матеріали XIII Міжнародної конференції**

**МКФТТПН-XIII**

**Т О М 2**

*16-21 травня 2011 р.*

Івано-Франківськ  
Україна

УДК 539.2  
ББК 22.373.1  
Ф 83

**Фізика і технологія тонких плівок та наносистем. Матеріали XIII Міжнародної конференції: У 2 т. – Т. 2.** / За заг. ред. заслуженого діяча науки і техніки України, д.х.н., проф. **Фреїка Д.М.** – Івано-Франківськ: Видавництво Прикарпатського національного університету імені Василя Стефаника, 2011. – 300 с.

Представлено результати теоретичних і експериментальних досліджень з питань: технологія тонких плівок (метали, напівпровідники, діелектрики, провідні полімери) і методи їх дослідження; фізико-хімічні властивості плівок; нанотехнології і наноматеріали, квантово-розмірні структури; тонкоплівкові елементи електронних пристроїв.

Матеріали підготовлено до друку Організаційним комітетом та Редакційною колегією конференції і подано в авторській редакції.

Для наукових та інженерних працівників з проблем тонкоплівкового матеріалознавства та мікроелектроніки.

Рекомендовано до друку науково-технічною радою Фізико-хімічного інституту Прикарпатського національного університету імені Василя Стефаника.

**Рецензенти:**

**Литовченко В.Г.**

*чл.-кор. НАН України, Інститут фізики напівпровідників  
ім. В.Є. Лашкарьова НАН України*

**Уваров В.М.**

*чл.-кор. НАН України, Інститут металофізики  
ім. Г.В. Курдюмова НАН України*

**Харченко М.Ф.**

*академік НАН України, Фізико-технічний інститут низьких температур  
ім. Б.І. Веркіна НАН України*

**УДК 539.2  
ББК 22.373.1**

© Прикарпатський  
національний університет  
імені Василя Стефаника  
вул. Шевченка, 57,  
м. Івано-Франківськ,  
76025, Україна  
Тел. (0342) 503752  
Факс (03422) 31574  
E-mail: [freik@pu.if.ua](mailto:freik@pu.if.ua)

**MINISTRY OF EDUCATION AND SCIENCE, YOUTH AND SPORT OF UKRAINE  
'VASYL STEFANYK' PRECARPATHIAN NATIONAL UNIVERSITY**

Physico-Chemical Institute

Berdyansk State Pedagogical University

Ivano-Frankivsk National Technical University of Oil and Gas

STATE AGENCY OF SCIENCE, INNOVATION AND INFORMATION OF UKRAINE

STATE FUND OF FUNDAMENTAL RESEARCH

**NATIONAL ACADEMY OF SCIENCE OF UKRAINE**

'V.E. Lashkarev' Institute of Semiconductor Physics

Institute of Surface Chemistry

'G.V. Kurdyumov' Institute of the Physics of Metals

'V.I. Vernadsky' Institute of General and Inorganic Chemistry

Chuiko Institute of Surface Chemistry

UKRAINE PHYSICS SOCIETY

"SCIENTISTS OF THE PRECARPATHIAN" ASSOCIATION

LUBLIN TECHNICAL UNIVERSITY (POLAND)

GAZY UNIVERSITY (TURKEY)

**PHYSICS AND TECHNOLOGY OF THIN FILMS  
AND NANOSYSTEMS**

***XIII INTERNATIONAL CONFERENCE***

**Materials**

*16-21, May, 2011*

Ivano-Frankivsk, Ukraine

---

---

**МИНИСТЕРСТВО ПРОСВЕЩЕНИЯ И НАУКИ, МОЛОДИ И СПОРТА УКРАИНЫ  
ПРИКАРПАТСКИЙ НАЦИОНАЛЬНЫЙ УНИВЕРСИТЕТ ИМЕНИ ВАСИЛИЯ СТЕФАНИКА**

Физико-химический институт

Бердянский государственный педагогический университет

Ивано-Франковский национальный технический университет нефти и газа

**ГОСУДАРСТВЕННОЕ АГЕНТСТВО ПО ВОПРОСАМ НАУКИ, ИННОВАЦИИ И  
ИНФОРМАЦИИ УКРАИНЫ**

Государственный фонд фундаментальных исследований

**НАЦИОНАЛЬНАЯ АКАДЕМИЯ НАУК УКРАИНЫ**

Институт физики полупроводников имени В.Е. Лашкарева

Институт химии поверхности

Институт металлофизики имени Г.В. Курдюмова

Институт общей и неорганической химии имени В.И. Вернадского

Институт химии поверхности им. О.О.Чуйка

УКРАИНСКОЕ ФИЗИЧЕСКОЕ ОБЩЕСТВО

АССОЦИАЦИЯ "УЧЕНЫЕ ПРИКАРПАТЬЯ"

ЛЮБЛИНСКИЙ ТЕХНИЧЕСКИЙ УНИВЕРСИТЕТ (ПОЛЬША)

**УНИВЕРСИТЕТ ГАЗИ (ТУРЕЧЧИНА)**

**ФИЗИКА И ТЕХНОЛОГИЯ ТОНКИХ  
ПЛЁНОК И НАНОСИСТЕМ  
XII МЕЖДУНАРОДНАЯ КОНФЕРЕНЦИЯ**

**Материалы**

16-21 мая 2011 года

Ивано-Франковск, Украина

**Physics and Technology of Thin Films and Nanosystems. Materials of XIII International Conference: On 2 V. – V. 2. / Ed by Honored engineer and techniques of Ukraine, Dr.Chem.Sci., Prof. Freik D.M. – Ivano-Frankivsk: A publishn-designing department of ‘Vasyl Stefanyk’ Precarpathian National University, 2011. – 300 c.**

The results of theoretical and experimental researches in directions are submitted: technology of thin films (metals, semiconductors, dielectrics, and carrying out polymers) and methods of their investigation; physic-chemical properties of thin films; nanotechnology and nanomaterials, quantum-size structures; thin-film devices of electronics.

The materials preformed for printing by Organizational Committee and Editorial Board of Conference, are conveyed in authoring edition.

For the scientific and engineering workers on thin-film material sciences and microelectronics.

It is recommended for printing by Scientific and Technical Advice of Physico-Chemical Institute at the ‘Vasyl Stefanyk’ Precarpathian National University.

---

---

**Физика и технология тонких пленок и наносистем. Материалы XIII Международной конференции: В 2 т. – Т. 2. / Под общ. ред. заслуженного деятеля науки и техники Украины, д.х.н., проф. Фрейка Д.М. – Ивано-Франковск: Издательство Прикарпатского национального университета имени Василия Стефаника, 2011. – 300 с.**

Предоставлены результаты теоретических и экспериментальных исследований в направлениях: технология тонких пленок (металлы, полупроводники, диэлектрики, проводящие полимеры) и методы их исследования; физико-химические свойства пленок; нанотехнологии и наноматериалы, квантово-размерные структуры; тонкопленочные элементы электронных приборов.

Материалы подготовлены к печати Организационным комитетом и редакционной коллегией конференции, поданы в авторской редакции.

Для научных и инженерных работников по вопросам тонкопленочного материаловедения и микроэлектроники.

Рекомендовано к печати научно-техническим советом Физико-химического института Прикарпатского национального университета имени Василия Стефаника.

## ОРГАНІЗАЦІЙНИЙ КОМІТЕТ

### Бюро

Литовченко В.Г., Миронюк І.Ф., Остафійчук Б.К., Сукач Г.О., Фреїк Д.М.

### Міжнародний

Анатичук Л. (Україна), Ахиска Р. (Туреччина), Бабанли М. (Азербайджан), Беляєв О. (Україна), Блонський І. (Україна), Бродин М. (Україна), Булавін Л. (Україна), Власенко О. (Україна), Волков С. (Україна), Вуйцік В. (Польща), Галушак М. (Україна), Горбик П. (Україна), Готра З. (Україна), Грігоніс А. (Литва), Гриньов Б. (Україна), Гуревич Ю. (Мексика), Гончаренко М. (Україна), Жуковські П. (Польща) Зломанов В. (Росія), Івасишин О. (Україна), Калінкін І. (Росія), Картель М. (Україна), Кияк Б. (Україна), Кікінеші О. (Угорщина), Комаров Ф. (Білорусь), Кумар М. (Індія), Кучмій С. (Україна), Мазуренко Є. (Україна), Малашкевич Г. (Білорусь), Мачулін В. (Україна), Мітгова І. (Росія), Младенов Г. (Болгарія), Мовчан Б. (Україна), Наумовець А. (Україна), Находкін М. (Україна), Нікіфоров К. (Росія), Новиков М. (Україна), Панасюк В. (Україна), Птушинський Ю. (Україна), Раренко І. (Україна), Свечніков С. (Україна), Сидоренко С. (Україна), Сизов Ф. (Україна), Скатков Л. (Ізраїль), Солонін Ю. (Україна), Стасюк І. (Україна), Стріха М. (Україна), Харченко М. (Україна) Челідзе Т. (Грузія), Чобанюк В. (Україна), Тигиняну І. (Молдова), Тодоран Р. (Румунія), Томчук П. (Україна), Уваров В. (Україна), Фірстов С. (Україна), Фістуль В. (Росія), Шпак А. (Україна), Шпілевський Е. (Білорусь), Шпотюк О. (Україна)

### Національний

Бойчук В. (Дрогобич), Буджак Я. (Львів), Гасюк І. (Івано-Франківськ), **Гладких М.** (Харків), Давидюк Г. (Луцьк), Дзундза Б. (Івано-Франківськ), Дмитрук М. (Київ), Дружинін А. (Львів), Запухляк Р. (Івано-Франківськ), Зауличний Я. (Київ), Зінченко В. (Одеса), Зиман З. (Харків), Ігнатенко П. (Донецьк), Кідалов В. (Бердянськ), Кланічка В. (Івано-Франківськ), Коваленко О. (Дніпропетровськ), Корбутяк Д. (Київ), Куницький Ю. (Київ), Лашкарьов Г. (Київ), Лепіх Я. (Одеса), Ліщинський І. (Івано-Франківськ), Лоп'янко М. (Івано-Франківськ), Матвеева Л. (Київ), Мельничук О. (Ніжин), Миколайчук О. (Львів), Никируй Л. (Івано-Франківськ), Похмурський В. (Львів), Прокопів В. (Івано-Франківськ), Проценко І. (Суми), Прокопенко І. (Київ), Птащенко О. (Одеса), Рогачова О. (Харків), Рубіш В. (Ужгород), Рувінський М. (Івано-Франківськ), Середа Б. (Запоріжжя), Смертенко П. (Київ), Стасюк З. (Львів), Стронський О. (Київ), Студеняк І. (Ужгород), Ткач М. (Чернівці), Томашик В. (Київ), Чуйко Г. (Херсон)

### Секретаріат

Межиловська Л.Й. – вчений секретар конференції  
Борик В.В., Гургула Г.Я., Дзумедзей Р.О.,  
Соколов О.Л., Потяк В.Ю. – секретарі

## ORGANIZING COMMITTEE

### Bureau

**D. Freik, V. Lytovchenko, I. Myronyuk, B. Ostafiychuk, G. Sukach**

### International

**R. Ahiska** (Turkey), **L. Anatychyk** (Ukraine), **M. Babanly** (Azerbaijan), **O. Belyaev** (Ukraine), **I. Blonskiy** (Ukraine), **M. Brodyn** (Ukraine), **L. Bulavin** (Ukraine), **V. Chobanyuk** (Ukraine), **S. Firstov** (Ukraine), **V. Fistulj** (Russia), **M. Galushchak** (Ukraine), **M. Goncharenko** (Ukraine), **P. Gorbyk** (Ukraine), **Z. Gotra** (Ukraine), **A. Grigonis** (Lithuania), **B. Grynyov** (Ukraine), **Yu. Gurevich** (Mexico), **O. Ivasyshyn** (Ukraine), **I. Kalinkin** (Russia), **M. Kartel** (Ukraine), **M. Kharchenko** (Ukraine), **O. Kikineshi** (Hungary), **F. Komarov** (Belarus), **S. Kuchmij** (Ukraine), **B. Kyyak** (Ukraine), **M. Kumar** (India), **V. Machulin** (Ukraine), **G. Malashkevich** (Belarus), **Ye. Mazurenko** (Ukraine), **I. Mittova** (Russia), **G. Mladenov** (Bulgaria), **B. Movchan** (Ukraine), **A. Naumovetsj** (Ukraine), **M. Nahodkin** (Ukraine), **K. Nikiforov** (Russia), **M. Novykov** (Ukraine), **V. Panasjuk** (Ukraine), **Yu. Ptushynskiy** (Ukraine), **I. Rarenko** (Ukraine), **A. Shpak** (Ukraine), **E. Shpilevsky** (Belarus), **O. Shpotyuk** (Ukraine), **F. Sizov** (Ukraine), **L. Skatkov** (Israel), **Yu. Solonin** (Ukraine), **I. Stasjuk** (Ukraine), **M. Striha** (Ukraine), **S. Svechnikov** (Ukraine), **S. Sydorenko** (Ukraine), **T. Tchelidze** (Georgia), **R. Todoran** (Romania), **P. Tomchuk** (Ukraine), **I. Tiginyanu** (Moldova), **V. Uvarov** (Ukraine), **O. Vlasenko** (Ukraine), **S. Volkov** (Ukraine), **V. Wojcik** (Poland), **V. Zlomanov** (Russia), **P. Zukowski** (Poland)

### National

**V. Boychuk** (Drogobych), **Ya. Budzhak** (Lviv), **G. Chuyko** (Kherson), **G. Davydyuk** (Lutsk), **B. Dzundza** (Ivano-Frankivsk), **M. Dmytruk** (Kyiv), **A. Druzhynin** (Lviv), **I. Gasyuk** (Ivano-Frankivsk), **M. Gladkykh** (Kharkiv), **P. Ignatenko** (Donetsk), **V. Kidalov** (Berdyansk), **V. Klanichka** (Ivano-Frankivsk), **D. Korbutyak** (Kyiv), **O. Kovalenko** (Dnipropetrovsk), **Yu. Kunitskiy** (Kyiv), **G. Lashkaryov** (Kyiv), **I. Lepikh** (Odesa), **I. Lishchynskyy** (Ivano-Frankivsk), **M. Lopyanko** (Ivano-Frankivsk), **L. Matveeva** (Kyiv), **Yu. Melnychuk** (Nizhyn), **O. Mykolaychuk** (Lviv), **L. Nykyruy** (Ivano-Frankivsk), **V. Pohmursjkyy** (Lviv), **V. Prokopiv** (Ivano-Frankivsk), **I. Protsenko** (Sumy), **I. Prokopenko** (Kyiv), **O. Ptashchenko** (Odesa), **O. Rogachova** (Kharkiv), **V. Rubish** (Uzhgorod), **M. Ruvinskyy** (Ivano-Frankivsk), **B. Sereda** (Zaporizzhya), **P. Smertenko** (Kyiv), **Z. Stasyuk** (Lviv), **O. Stronsjkyy** (Kyiv), **I. Studenyak** (Uzhgorod), **M. Tkach** (Chernivtsi), **V. Tomashyk** (Kyiv), **R. Zapykhlyak** (Ivano-Frankivsk), **I. Zaulychnyy** (Kyiv), **Z. Zyman** (Kharkiv), **V. Zinchenko** (Odesa)

### Secretariate

Scientific Secretary – **L. Mezhylovska**

Secretaries – **V. Boryk, G. Gurgula, R. Dzumedzey, O. Sokolov, V. Potyak**

**Вельмишановні пані та  
панове! Друзі! Колеги!  
Учасники  
XIII МКФТТПН – 2011!**

Історія розвитку подій часто повторюється! Це не обійшло стороною і нашу міжнародну конференцію! Маю на увазі місце її проведення у серці Гуцульщини – смт. Верховині! Постійним учасникам, нашим друзям, буде приємно згадати минулі роки, коли ми були молодими. Отож юнацького запалу всім Вам у науковому пошуку, спілкуванні!

Сподіваюся, що наша зустріч сприятиме насамперед консолідації діяльності провідних науковців і молоді України та інших держав, зміцнить наукові дослідження у нових стратегічних напрямках.

***Оптимізму і успіхів Вам!***

**З великою повагою,  
голова Оргкомітету  
МКФТТПН-ХІІІ**

**Дмитро Фреїк**



*с.м.т. Верховина, Івано-  
Франківська обл., Україна  
16 травня 2011 р.*



**Ladies and Gentlemen, Friends!  
Colleagues  
Participants  
XIII ICPTTFN – 2011!**

History of events often repeats! This is not spared our international conference! I mean the venue in the heart Hutsulshchyna – town Verkhovyna! Regular members, our friends, be nice to remember the years when we were young. So youthful enthusiasm to all of You in scientific research, communication!

I hope that our meeting will first consolidate the work of scholars and youth of Ukraine and other countries, strengthen scientific research in new strategic directions.

***Optimism and good luck to You!***

**With great respect,  
Chairman of the Organizing Committee  
ICPTTFN-XIII**

**Dmytro Freik**



*Town Verkhovyna, Ivano-Frankivsk  
region, Ukraine  
May, 16, 2011.*

**СЕКЦІЯ 3 (усні доповіді)  
ФІЗИКО-ХІМІЧНІ ВЛАСТИВОСТІ ПЛІВОК  
ТА НАНОСТРУКТУР**

17-20 травня 2011 р.

**SESSION 3 (oral)  
NANOTECHNOLOGIES AND NANOMATERIALS,  
QUANTUM-SIZE STRUCTURES**

May, 17-20, 2011

## Photoluminescence of thin films of ZnO obtained from chelate compounds

Baskevich A.S.<sup>1</sup>, Bezpalchenko A.V.<sup>2</sup>, Bulanyi M.F.<sup>2</sup>, Dyadenko A.I.<sup>2</sup>,  
Skuratovskaya O.V.<sup>2</sup>, Omelchuk A.R.<sup>2</sup>

<sup>1</sup>*Ukrainian State University of Chemical Technology, Dnipropetrovsk, Ukraine*

<sup>2</sup>*Oles Honchar Dnipropetrovsk National University, Dnipropetrovsk, Ukraine*

In this study we investigated the properties of the ZnO films, obtained from the chelate compounds in flowing gas-phase reactor. Zinc oxide is one of the most attractive materials for the development of optical and optoelectronic devices for next-generation operating in the near ultraviolet spectral range. Using chelating compounds as starting materials allows obtaining films with high stoichiometry of various materials, including materials with semiconducting properties. The  $A_2B_6$  films were obtained by reactor of slit-flow gas phase, as a carrier gas were used Ar,  $O_2$  and their mixtures. Acetylacetonates of zinc, which were synthesized from reagent grade materials, were used for obtaining ZnO films. The mixture of Ar +  $O_2$  with the  $O_2$  concentration within the  $8 \div 10\%$  was used for ZnO films. The substrate temperature for obtaining ZnO films was  $290 \div 310$  °C. The gas's flow velocity was determined visually through the quartz sight glass and was chosen in the laminar regime to ensure the uniform of film deposition. The standard substrate  $20 \times 15$  mm of ceramics condenser and glass LC-7 were used as the substrates.

According to the X-ray diffraction analyzing, films which was deposited are characterized by fine-grained polycrystalline structure with grain sizes from 90 to 110 nm, have a hexagonal structure with unit cell parameters  $a = 3,2811$  Å,  $c = 5,2066$  Å and with a low degree of microstrain  $M = 1,09 \cdot 10^{-3}$  %. Spectra of the X-ray phase analyzing and photoluminescence of the obtained films are shown in fig. 1 and fig. 2 respectively.

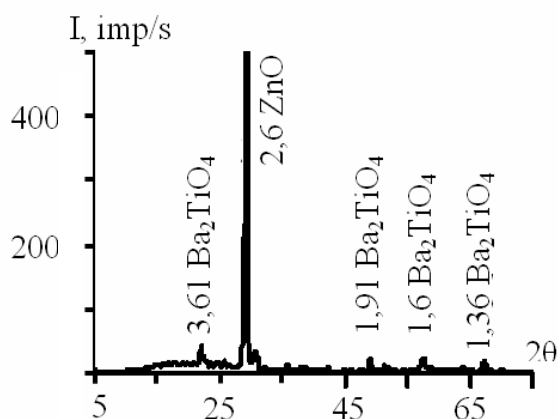


Fig. 1.

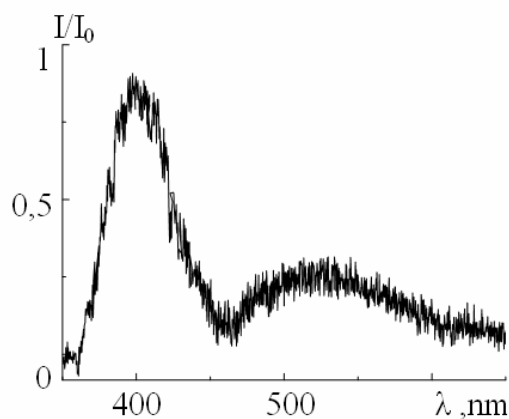


Fig. 2.

## Phase formation during temperature cycling of metal nanoparticles of different shapes

Bilgorodskyy Y.S.<sup>1</sup>, Shirinyan A.S.<sup>2</sup>, Wilde G.<sup>3</sup>

<sup>1</sup>*Department of Physics, Cherkasy B. Khmelnytskyi National University, Cherkasy, Ukraine*

<sup>2</sup>*Department of Physics, Kiev Taras Shevchenko National University, Kiev, Ukraine*

<sup>3</sup>*Institut für Materialphysik, Westfälische Wilhelms-Universität Münster, Munster, Germany*

We present a description of the evolution of a polymorphically transforming metal nanoparticles of different shapes subjected to a temperature cycling [1-2]. The theoretical and computer experimental findings of the present work put new insight into the intensively discussed topic of size-induced phase transitions and hysteresis phenomena in nanomaterials:

1) The calculations of the time dependence of the volume fraction of the new phase show the existence of size-induced hysteresis and its main features.

2) The size-dependent critical supersaturation and critical supercooling and a linear dependence of the width of hysteresis loop on the logarithm of the number of atoms in the nanopowder particles.

3) The thermodynamic relations between the energy of transition and the size and shape of nanoparticles.

4) The thermodynamics and kinetics of transition phenomena in a nanopowder taking into account the possible size distribution of the nanoparticles.

Work is partially supported by the Ministry of Education and Science. Part of the work have been done in the framework of the grant of Ukrainian Government (Cabinet of Ministers of Ukraine) for young scientists: Award of State Committee in Science and Technology dated 11 October 2010.

1. Shirinyan A., Pasichnyy M. // *Nanotechnology*. – 2005. – T.16. – 1724.
2. Shirinyan A. S., Bilgorodskyy Y. S. “Size-induced thermal thermodynamic hysteresis in nanopowder undergoing structural transitions – from particular case to general behaviour” // *Journal of Phase Transitions*. – 2009. – T.82. – 551.

## Electron transport in nanocomposite SiO<sub>2</sub>(Si) films

Bratus' O., Evtukh A., Kizjak A.

*V. Lashkaryov Institute of Semiconductor Physics, Kiev, Ukraine*

Nanocomposite films containing silicon nanocrystals in insulating matrix are under intensive investigations for their further applications in various branches of industry, for example, in nonvolatile memory cells and optoelectronics. One problem that restricts the application is preparation of the structures with required parameters.

The aim of this work is research of electron transport mechanisms in nanocomposite SiO<sub>2</sub>(Si) films, obtained by ion-plasma sputtering (IPS) and Low pressure chemical vapour deposition (LP CVD) methods with following high-temperature annealing.

The mechanisms of electron transport through nanocomposite films have been proposed. The electron hopping processes and trap-assisted tunneling through insulator sublayers between nanocrystals dominate in IPS and LP CVD deposited films respectively (Fig.1, Fig.2).

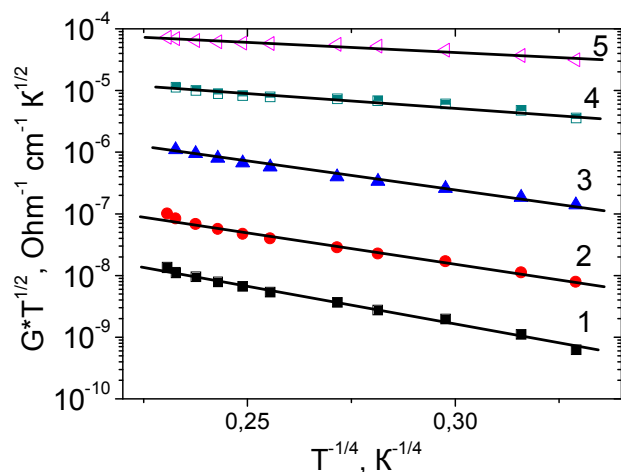


Fig. 1. Temperature dependences of electrical conductivity of nanocomposite SiO<sub>2</sub>(Si) films obtained by IPS method in Mott coordinates with electric field as a parameter: (1-  $E = 9 \times 10^{-3}$  V/cm; 2-  $E = 2.6 \times 10^{-4}$  V/cm; 3-  $E = 8.3 \times 10^{-4}$  V/cm; 4-  $E = 2.3 \times 10^{-5}$  V/cm; 5-  $E = 6.2 \times 10^{-5}$  V/cm.

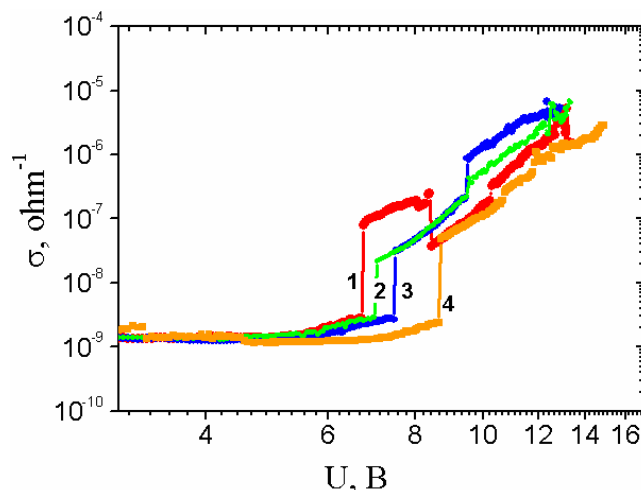


Fig. 2. Electrical conductivity of nanocomposite SiO<sub>2</sub>(Si) films obtained by LP CVD method on applied voltage dependences with temperature as a parameter: (1- 261 K; 2- 314 K; 3- 287 K; 4- 341 K.

## **Influence of TiO<sub>2</sub> structure modifications on its sorption properties**

Budzulyak I.M., Gumenyuk L.M., Solovko Y.T., Ilnytsky R.V.

*Vasyl Stefanyk Precarpathian National University, Ivano-Frankivsk, Ukraine*

The mass of sorption water in the nanodispersed titanium dioxide, which are used as cathode materials for lithium power sources, is very important factor which significantly influence on their energy characteristics [1]. This is explained by the fact that sorption water prevents lithium ion intercalation into TiO<sub>2</sub> structure and organic electrolytes, that are used in lithium power sources, are very sensitive to the water availability within them (limit of water in electrolyte is not more than 0,002 % by mass). We used such methods as thermogravimetry (TG) and differential thermal analysis (DTA) which were carried out on Leading Thermal Analysis STA 449 F3 Jupiter in liner heating regime at a heating rate of 10 °C/min in temperature range of 25-1000 °C for investigation of water behavior in rutile and anatase of the nanodispersed polymorfy TiO<sub>2</sub>. Change of mass was determined with accuracy 10<sup>-6</sup> kg, noise of DTA signal was less than 50 nV. Crystalline modification of rutile Dupon R-706 and anatase Aldrich of titanium dioxide were investigated.

It was found that:

1) adsorption water is present on rutile structure and completely lost at heating to 200 °C. Thus decreasing of H<sub>2</sub>O mass is more than 0,4 % for rutile and is about 0,1 % for anatase;

2) the mass of crystalline water in rutile structure is 0,6 % for the original sample mass. DTA curve didn't change at temperature ranges from 200 °C to 450 °C, that's explained by the absent of any physical changes and material structure reconstruction;

3) enthalpy of adsorption and crystalline water is -46,8 J/g and -95,6 J/g respectively as the sorption process are better for crystalline water. That's why adsorption water on rutile structure is less comparatively with crystalline water;

4) heating rutile over than 450 °C results in the growth of structure defects due to the loss of oxygen, that negatively affects on electrochemical properties of cells formed on their base;

5) the mass doesn't change at temperature ranges from 200 °C to 1000 °C. At the heating above 600 °C anatase is converted into rutile, and at 1000 °C anatase phase content is less than 4,0 % (from the data of X-ray diffractometry, done on the device of DRON 3.0).

1. Chuan Cai and Ying Wang. Novel Nanocomposite Materials for Advanced Li-Ion Rechargeable Batteries // *Materials*. – 2009. – Vol. 2, N 3. – P.1205-1238.

## Structural and optical properties of photocatalytic active TiO<sub>2</sub>/ZrO<sub>2</sub>/SiO<sub>2</sub> and TiO<sub>2</sub>/ZrO<sub>2</sub>/SiO<sub>2</sub>/Au films.

Busko T.O.<sup>1</sup>, Dmytrenko O.P.<sup>1</sup>, Kulish M.P.<sup>1</sup>, Vityuk N.V.<sup>2</sup>, Eremenko A.M.<sup>2</sup>.

<sup>1</sup>Kiev National Shevchenko University, Kyev, Ukraine

<sup>2</sup>Chuiko Institute of Surface Chemistry of NAS of Ukraine, Kyiv, Ukraine

Titanium dioxide are the most actively investigated photocatalysts for applications in materials that can effectively decompose of environmental pollution [1]. However, TiO<sub>2</sub> uses of only 5% of sunlight. The increase in the photocatalytic activity of TiO<sub>2</sub> systems has been achieved by the synthesis of semiconductor nanoparticles, where the quantum size effects arise [2]. In metal-semiconductor nanocomposites, the recombination processes are suppressed due to the electron transfer to the metal nanoparticles, that leads to the spatial and energy separation of charges as well as to the accumulation of electrons by metal atoms. To improve the redox processes is an increasing the specific surface of TiO<sub>2</sub> particles while maintaining the structure of anatase. This seems to be possible using heterophase composites of TiO<sub>2</sub> with other oxides, such as ZrO<sub>2</sub> or SiO<sub>2</sub>, which contribute to slowing down the sintering of TiO<sub>2</sub> nanoparticles during the annealing. Mixed oxide materials can be more efficient photocatalysts than pure oxide [3].

In this work, TiO<sub>2</sub>/ZrO<sub>2</sub>/SiO<sub>2</sub> and TiO<sub>2</sub>/ZrO<sub>2</sub>/SiO<sub>2</sub> (doped with Au) films have been prepared using the sol-gel method. X-ray diffraction measurements were performed with a DRON-3M system with radiation wavelength of 1.5406 Å (Cu k<sub>α</sub>). The XRD study of ternary films TiO<sub>2</sub>/ZrO<sub>2</sub>/SiO<sub>2</sub> undoped and doped with Au NPs indicates an amorphous state of the predominant part of oxide TiO<sub>2</sub> nanocrystals in anatase phase SiO<sub>2</sub> and srilankite Ti<sub>2</sub>ZrO<sub>6</sub>.

Spectroscopic ellipsometry measurements of the undoped TiO<sub>2</sub>/ZrO<sub>2</sub>/SiO<sub>2</sub> films show no significant absorption in a spectral range 300-1000 nm. Doping with gold results in appearance of an absorption band at 600 nm. It related to the surface plasmon resonance of Au nanoparticles.

Optical absorption spectra of organic dye Rhodamine B solutions in the presence of the photocatalytic activ films were recorded in a spectral range of 1.24-6.2 eV using Perkin-Elmer Lambda Bio-40 spectrometer. From the kinetic curves were calculated the rate constants of photodecomposition of Rhodamine B in the presence of the films, that equal  $k_1=0.14 \times 10^{-2} \text{ min}^{-1}$  and  $k_2 = 1.02 \times 10^{-2} \text{ min}^{-1}$  for TiO<sub>2</sub>/ZrO<sub>2</sub>/SiO<sub>2</sub> and TiO<sub>2</sub>/ZrO<sub>2</sub>/SiO<sub>2</sub>/Au films, respectively.

1. Diebold U. The surface science of titanium dioxide // *Surf. Sci. rep.* – 2003.– V.48 – P .53-229.
2. Khairutdinov R F. Chemistry of semiconductor nanoparticles // *RUSS Chem. rev.* – 1998. – V. 67 – P.109-122.
3. Andrulevičius M., Tamulevičius S., Gnatyuk Yu., Vityuk N., Smirnova N., Eremenko A. XPS investigation of TiO<sub>2</sub>/ZrO<sub>2</sub>/SiO<sub>2</sub> films modified with Ag/Au nanoparticles // *Materials science (Medziagotyra)* – 2008 – V.14 – P. 8-14.

## Structure and hardness of worn layer

Danylenko M.I.<sup>1</sup>, Chernega S.M.<sup>2</sup>, Mameka N.O.<sup>1</sup>, Velychko A.<sup>2</sup>

<sup>1</sup>*Institute for Problems of Materials Science, Kyiv, Ukraine*

<sup>2</sup>*National Technical University of Ukraine “Kyiv Polytechnic Institute”, Kyiv, Ukraine*

Shear deformation is realized by methods of severe plastic deformations such as equal channel angular pressures (ECAP), twist extrusion (TE) et al. for producing nanostructures with unique high properties [1]. However, these methods can be used only for strengthening of “soft” one-component materials.

Methods of surface deformation processing realize shear deformation in surface layers and widely used for strengthening of complex-alloyed alloys and composites. The most detailed analysis of surface severe plastic deformations (SSPD) was done by K.Lu and co-workers who investigated the changes of structural state in SSPD-processed near-surface layers of steel articles [2]. Authors [3] studied the gradient nanostructure on “cross-section” samples of steel 65Г after severe surface plastic deformation. They revealed the dissolution of cementite Fe<sub>3</sub>C and carbon redistribution on cell boundaries during plastic deformation. The free carbon on cell boundaries suppresses the recovery processes. Cell size in surface layer is about 20-30 nm and hardness in near-surface layer is about 12 GPa.

Samples of steel 20 after wear have been studied. Initial structure consists of ferrite and perlite grains and microhardness is in range 3-6 GPa. Hardness of worn layer is presented on Fig. 1. Different level and depth of hardening of worn layer is presented on Fig.2.

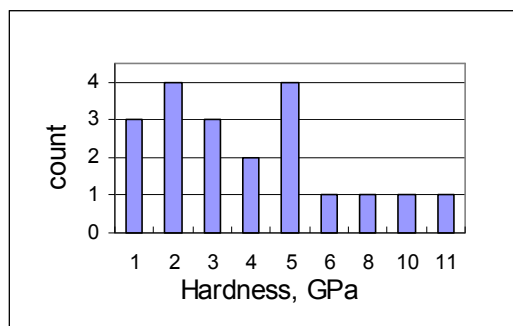


Fig. 1. Hardness of worn layer.

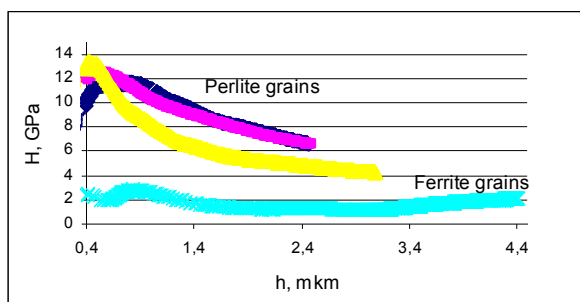


Fig. 2. Hardness vs indentation depth.

1. Segal V.M., Reznikov V.I., Kopylov V.I., *Procesy Plasticheskogo Structuroobrazovania Metallov. // Sci Eng. Minsk. – 1994. – 231 p.*
2. K. Lu, H. Zhahg, Y. Zhong, H. J. Fecht // *J.Mater. Res.* – 1997. – V. 12 – P. 923.
3. M.Danylenko, V. Gorban, Yu. Podrezov, S. Firstov, O. Rozenberg, S.Sheykin, Y. Yamabe-Mitarai, F.Morito, *Materials Science Forum Vols.* – 2006. – № 503-504. – P. 787.

## Scattering mechanisms of carriers in crystals doped PbTe: Ga (In, Tl)

Dzumedzey R.O.

*Vasyl Stefanyk Precarpathian National University, Ivano-Frankivsk, Ukraine*

Semiconductors IV-VI have proved as reliable material for building on the basis of active infrared devices, elements and techniques of thermoelectric energy converters. Properties of lead chalcogenides can be modified by alloying elements of the periodic table group III, which form deep resonance impurity states. Thus, indium creates impurity states in the conduction band near its edge with the energy  $(0.07 \pm 0.01)$  eV at  $T = 0$  K. Thallium in lead chalcogenides are deep acceptor, and Tl impurity states are single-electron character. Power distance from waist level to the valence band is 0.22 eV PbTe at temperatures close to 0 K.

The research, based on a variational principle defined temperature and concentration dependences of charge carrier mobility for crystal PbTe, doped with indium and thallium. Some of the results obtained are presented in tables.

Electrical parameters of PbTe, doped with indium at different concentrations of impurity

0.002 at.% In				0.02 at.% In			
T, K	$\sigma, \text{Ohm}^{-1}\text{cm}^{-1}$	$n, 10^{18} \text{cm}^{-3}$	$\mu, \text{cm}^2/\text{Vs}$	T, K	$\sigma, \text{Ohm}^{-1}\text{cm}^{-1}$	$n 10^{18}, \text{cm}^{-3}$	$\mu, \text{cm}^2/\text{Vs}$
423	342	2.6	822	623	170	4.6	231
473	263	2.8	587	673	164	5.6	197
523	207	3	431	723	156	6.1	160
573	197	3.6	342	773	150	7.2	130
623	179	4.3	253	823	145	8.1	112

Electrical parameters of PbTe, doped with thallium at temperatures of 77 K and 300 K

at.% Tl	77 K			300 K		
	$\sigma, \text{Ohm}^{-1}\text{cm}^{-1}$	$p 10^{-18}, \text{cm}^{-3}$	$\mu, \text{cm}^2/\text{Vs}$	$\sigma, \text{Ohm}^{-1}\text{cm}^{-1}$	$p 10^{-18}, \text{cm}^{-3}$	$\mu, \text{cm}^2/\text{Vs}$
0.01	4874	2.97	10235	282	2.7	648
0.2	7135	5.7	7849	336	4.8	437
0.4	1852	10.4	1111	211	8.9	148

In this work the calculation of charge carrier mobility of crystalline PbTe:In content for different impurity indium (0.002-0.02) at. % In and crystalline p-PbTe:Tl impurity content depending on the waist (0.01-0.4) at. % Tl. The temperature and concentration ranges dominance of individual scattering mechanisms of charge carriers: the acoustic and optical phonons in short-range potential vacancies and impurity potential.

*Work partially funded by State Committee of Science and Notice of Ukraine (state registration number 0110U007675).*

## **Size effects and electrical parameters of nanostructured lead chalcogenides films**

Dzundza B.S.

*Vasyl Stefanyk PreCarpathian National University, Ivano-Frankivsk, Ukraine*

Size effects of electrical conduction of nanostructured lead chalcogenides films grown from the vapor phase by hot-wall method and open evaporation in a vacuum were investigated.

In the approximation of the average free path of current carriers electrical resistance of nanostructured lead chalcogenides films with different structural perfection (monocrystal, polycrystal) dependence on their thickness and temperature were investigated; kinetic parameters were calculated. It was determined that the average length of free path of current carriers in monocrystalline specimens by orders of magnitude (depending on temperature) greater than corresponding values for polycrystalline specimens, and the temperature increase due to the influence of scattering on crystal lattice vibrations leads to its reduction.

Based on experimental researches of profiles of effective and local values of electrical parameters of lead chalcogenides films and the use of phenomenological mathematical Petrits' model it was shown that by annealing in vacuum and oxygen atmosphere, due to diffusion processes of donor and acceptor centers, there is a significant redistribution of both elemental composition and changed of whole complex of physical-chemical properties of condensate.

It was shown that barrier effects in polycrystalline nanostructured lead chalcogenides films are the dominant forms of influence on transport processes. Based on analysis of temperature dependence of the current carrier mobility the influence of crystal structure, annealing temperatures in vacuum and oxygen atmosphere on the conditions of formation of potential grain barriers was investigated; their values were determined.

It was determined that vacuum annealing of both freshly grown and aged in the air films leads to complicated nature of changes of conductivity with temperature due to desorption processes of oxygen and chalcogen and the effect of its own conductivity.

The optimized technology of growing of lead chalcogenides and tin telluride films from the vapor phase and conditions of following annealing in vacuum and oxygen atmosphere provide defined structure and complex of physical-chemical properties necessary for the development and the operation of active device structures of infrared technology and thermoelectricity.

*This work is partially financed by NAS of Ukraine (State registration № 0110U006281) and Ministry of education and science, youth and sport of Ukraine (State registration № 0110U001766).*

## The Sb adsorption on Si and Ge surfaces

Fedorchenko M.I., Nakhodkin M.G.

*Taras Shevchenko National University, Kyiv, Ukraine*

The Sb adsorption on Si and Ge surfaces is intensively studied owing to Sb significance as effective surfactant for growing of quantum-dimensional heterostructures.

In this work are presented the results of experimental research of Sb interface formation with Si(100), Si(111), Ge(100), Ge(111) and Ge(113) crystal surfaces. An attempt have been made to correlate between the structures and electronic properties of such interfaces depending on thicknesses of adsorbed Sb films and their annealing temperatures.

The experiments were done in a homebuilt ultra-high vacuum chamber with a base pressure  $\approx 2 \times 10^{-10}$  Torr. Auger electron spectroscopy, low-energy electron diffraction, ultra-violet photoelectron spectroscopy were used for analyzing the interfaces.

Experimental investigations showed that adsorption of Sb atoms on these surfaces at room temperature leads to Sb film formation by mechanism of Stranski-Krastanov. Increasing of the surface coverage of Sb atoms ( $\Theta_{Sb}$ ) leads to saturation of surface states and amorfisation of near surface region. Annealing the surfaces with  $\Theta_{Sb} \leq 1$  ML results in to formation of the ordered superstructures wich depend on  $\Theta_{Sb}$  and have different electronic properties. The Sb films with  $\Theta_{Sb} > 1$  ML manufactured near room temperature display amorphous semiconductor properties. Low temperature annealing ( $T \approx 120^\circ\text{C}$ ) results in arrangement of such films and their metallization. In the time of increasing of annealing temperature (higher then  $120\text{-}200^\circ\text{C}$ ) the Sb atoms partly desorb and  $\Theta_{Sb}$  decrease to value nearly of 1 ML. The covering whith  $\Theta_{Sb} \approx 1$  ML keeps in the annealing temperature range about  $160\text{-}700^\circ\text{C}$ .

The Sb adsorption affect strongly on the work function  $\phi$  of the investigated surfaces and band bending  $\Delta Y$  nearly these surfaces. The Sb deposition on the surfaces Si and Ge amorfisated by Ar ion bombardment lead to monotonous decreasing  $\phi$  of these surfaces to value wich is closely related to  $\phi$  of the Sb volume specimen surface. The  $\phi$  behaviour of the Si and Ge crystal surfaces in depending on the  $\Theta_{Sb}$  and the temperatures of the interfaces formation for the most part caused by the changes of the  $\Delta Y$  nearly the surfaces. For the annealed surfaces with  $\Theta_{Sb} \approx 1$  the bands bend down for the Si surfases, and up for the Ge surfaces. It can be possibly as a result of formation of different tipe of near surface electronic states wich caused of different character build-in of Sb atoms into Si and Ge lattices.

The model that provides the explanation of correlation between structures and electronic properties of Sb/Si and Sb/Ge interfaces are discussed.

## **X-rays diffractometry methods for polymer-containing nanocomposites investigation**

Gomza Yu.P., Klepko V.V.

*Institute of macromolecular chemistry NAS of Ukraine, Kyiv, Ukraine*

The most of polymer-containing composites at the short-range ordering level (0.1-10 nm) are amorphous materials and at long-range ordering level (1 – 100 nm) are characterized by nearly random distribution of nanosized filler particles. That is why investigation of such systems demands of appropriate adaptation of the experimental X-rays diffraction methods and the data interpretation. In this report we represent the examples of application of small angle (SAXS) and wide angle (SAXS) X-rays diffractometry for structure peculiarities investigation of polymer-containing nanocomposites.

Organic-inorganic nanocomposites based on polymer matrix and inorganic nanofiller are as a rule a weak-ordered systems and are characterized by hierarchy of structural levels. Conventional X-rays diffractometry as developed for determination of crystalline structure peculiarities for high-ordering mono- and polycrystalline materials are non-effective in above mentioned cases. We developed the experimental approach for obtaining, processing and interpretation of wide-angles (WAXS) and small-angles (SAXS) X-rays scattering in terms of peculiarities of short-range ordering and nanoscale aggregations of weak-ordered polymer-containing nanocomposites determination.

The method of interpreting X-ray scattering data is based on the analysis of the scattering curve, which shows the dependence of the scattering intensity,  $I$ , on the scattering angle,  $\theta$ , or the wave vector,  $q$ . The experimental X-rays data obtained from the nanocomposites contain a large amount of information hidden in the structure of measured X-ray spectra. So the wide-angle X-rays scattering was used by as for primary estimation of short-ordering level – i.e. are the investigated material amorphous or partial crystalline. The second main application of WAXS for nanocomposites is the establishing of different stages of organoclay dispersion in polymeric matrix – i.e. differentiated the three canonical cases: i) phase separation; ii) intercalation, iii) exfoliation of primary inorganic sheets in polymeric matrix. But the most informative for structure peculiarities determination for nanocomposites is the small-angle X-rays scattering (SAXS)/ The method enables the structure peculiarities determination in the range of structural elements sizes from 1-2 to 100-200 nm. The character of the SAXS scattering curve enables us to differentiated the nanoscale-ordered structures (the presence of discrete maxima) from disordered (diffuse character of scattering) ones. The integral SAXS intensity in all cases of ordering is the measure of degree of microphase separation of investigated material at

nanoscale level. If the SAXS curve is maxima-less (i.e. diffuse one) we must represent the corresponding SAXS data in *log-log* coordinates.

The scattering profiles exhibit a straight-line behaviour over a range of  $q$  indicating fractal nature of the structure of the samples. Also, profiles in the entire  $q$ -range may be divided into few (2-3) regions each with a different slope for the lines. This indicates different nature of structural features on different length-scales of observation. It is known [1] that the SAXS intensity  $I(q)$  for a fractal object exhibits a power-law described by the following equation:

$$I = C \cdot q^{-\alpha}$$

In practice, this is observed in the  $q$ -range  $\zeta^{-1} < q < l^{-1}$  where  $\zeta$  and  $l$  are the upper and lower cutoff lengths. For mass-fractals,  $\alpha \leq 3.0$  with fractal dimension  $D_m = \alpha$  whereas for fractally rough particle interfaces,  $\alpha$  varies between 3.0 and 4.0 and the surface-fractal dimension  $D_s = 6 - \alpha$ . Likewise, for particles with smooth surfaces,  $\alpha = 4.0$  whereas for diffuse or fuzzy particle interface  $\alpha > 4.0$  (i.e., the slope of the lines is steeper than -4) [2]. For systems having different structures on different length scales, the scattering data can be analyzed using a unified theory [G. Beaucage, J. Appl. Cryst. 28 (1995) 717.]. According to this formalism, the intensity  $I(q)$  can be represented by the equation:

$$I(q) = \sum_{i=1}^n (G_i \exp(-q^2 R_{g_i}^2 / 3) + B_i \exp(-q^2 R_{g_{(i+1)}}^2 / 3) \times \left\{ \left[ \text{erf}(q R_{g_i} / 6^{1/2}) \right]^3 / q \right\}^{-P_i} )$$

where  $R_{g_i}$  are the average radii of gyration of the aggregates and the primary particles (in the aggregate).

The  $R_{g_i}$  values are determined using Guinier's approximate law [3],

$$I(q) = (\Delta\rho)^2 \exp(R^2 q^2 / 3),$$

where  $q = 4\pi \sin\theta / \lambda$ , and  $(\Delta\rho)$  is the difference in electron densities between particle and surrounding medium. The average radius of gyration  $\langle R_g \rangle$  in the Guinier formula is calculated from the slope of the linear fit of  $\log I$  vs.  $q^2$  curve. The average particle diameter is then deduced, using  $\langle D_p \rangle = 2(5/3)^{1/2} \langle R_g \rangle$  ( $2.58 \cdot \langle R_g \rangle$ ) for particles of spherical shape. Nature of the structures in the respective regions can be known from the values of the exponents  $P_i$  determined from the rectilinear parts of scattering curves, as discussed above.

This approach has been successfully used for studying the structures peculiarities of the nano-sized powders-, clay minerals- and carbon nanotubes and polymer-based nanocomposites filled by them. It was established the correlation of functional characteristics of such materials (i.e. ionic conductivity and catalytic activity levels etc) and their structure peculiarities.

1. Schmidt P.W. // J. Appl. Cryst. – 1991. – V.24. – P. 414.
2. Schmidt P.W., Anvir D., Levy D., et al. // J. Chem. Phys. – 1991. – V.94 P. 1474.
3. Guinier A. // Ann Phys Paris. – 1939. – V.12. – P.161.

## The peculiarities of organic layers growth and electroconductivity in (vitamin B1 or analgine)-patterned silicon hybrids

Gorbach T.Ya., Smertenko P.S.

*V. Lashkarev Institute of Semiconductors Physics, NAS of Ukraine, Kyiv, Ukraine*

Organic layers deposited at room temperature from aqueous solution of medical materials of thiamine diphosphide, TD (pH=1÷2) and metamizole sodium, MS (pH = 6 ÷ 7) [1] modified the surface morphology, chemical composition and physical properties of porous patterned substrates. The modification was found to be determined by deposition time, i.e. layer thickness and do not depend on solution chemistry. For thin organic layers ( $\leq 100 \mu\text{m}$ ) the layer contour is the same as substrate and terrace-step-kink growth mechanism is realized. For more thick layers (up to micrometer) self organized assemblies are formed but with preference of pre-pattern substrate.

Analysis of current-voltage characteristics was made on the base of injection [2] and differential [3] approaches.

For example, the I-V characteristics for TD – Si hybrid solution were asymmetric. The ratio of forward to reverse currents was about 40 at  $V=0.75 \text{ V}$  for the layer deposited during 100 min. It decreased to 6 for deposition process during 20 hours. The sensitivity of hybrids with TD is recognized to be higher than with MS and in both cases it decreases with increase of layer thickness. In the TD (MS) – porous patterned hybrids the transport is determined by some processes but mainly by the high injection of charge carriers in dielectric organic layers. The barrier is formed at the interface of TD layer – porous patterned substrate and PV characteristic is observed. The increase of the layer thickness leads to decrease of open circuit voltage and short circuit current.

Thus, the chemical solution deposition at room temperature is newly simple technological process useful for realization of hybrid organic-inorganic structures.

1. Gorbach T.Ya., Kostylyov V.P., Smertenko P.S. New organic materials for organic-inorganic silicon-based solar cells // *Mol. Cryst. Liq.Cryst.* – 2011. – V.535. – P. 174-178.
2. Injection Technique for Study of Solar Cells Test Structures / R.Ciach, Yu.P.Dotsenko, V.V.Naumov, A.N.Shmyryeva, P.S.Smertenko // *Solar Energy Materials & Solar Cells.* – 2003. – V.76/4. – P. 613-624.
3. Differential approach to the study of integral characteristics in polymer films / P. Smertenko, L. Fenenko, L. Brehmer and S. Schrader / *Advances in Colloid and Interface Science.* – 2005. – V. 116, №1-3. – P. 255-261.

## Quantum-chemical and thermodynamic calculation of formation energies of vacancies in diamond-like semiconductors

Gorichok I.V.

*Precarpathion National University named after V. Stefanyk, Ivano-Frankivsk, Ukraine*

Vacancies in semiconductors are the most important point defects, as they almost always present in crystals and largely determine their thermodynamic and electrical properties. That is why the definition energy formation of these defects has a great practical importance.

Existing methods of determining the numerical values of  $h$  in most cases can be realized only with computers, as they based mainly on the solution Hartree-Fock-Ruthan equations. But in spirit of great in development of computer, some problems in the theory of defects still remain difficult solved, and sometimes are even practically undecided. Therefore, the search of relatively simple analytical methods for determination energy formation of defects is important.

In this work for determine energy formation of point defects in diamond-like semiconductors was made the calculation of these quantities using semi-empirical quantum method Hyukelya (RMH) [1], the thermodynamic method, taking into account deformation in the vicinity of vacancies [2], and method of formation of Schottky's defects entalpiy using pair interaction potentials [3].

During the investigation it is determinated the Hryunayzen parameters and the parameters of Mi-Lennard-Jones potential for semiconductor crystals. It is established that the most energetically favorable is the formation of Schottky's defects in crystals of compounds  $A^{IV}B^{VI}$ , the less energetically favourable is the formation of Schottky's defects in compounds  $A^{II}B^{VI}$  and  $A^{III}B^V$ . Established that the deformation in the vicinity of neutral vacancies are not significant and do not significantly affect to the value of energies formation of these defects.

The calculated values of formation energies of vacancies consistent with the literature data, and can be used for calculation of these defects concentrations in semiconductors.

*This work is partially financed by State Fund of Fundamental Researches of State Agency for Science, Innovation and Information of Ukraine (State registration № 0110U007675).*

1. Ганина Н.В., Шмугуров В.А., Фистуль В.И. Квантово-химический метод определения энтальпий образования моновакансий в полупроводниках // Фізика і хімія твердого тіла. – 2004. –Т. 5, № 3. – С. 430-435.
2. Вернер В.Д., Ничуговский Д.К. Энергия образования вакансий атомов металлов в арсениде галлия и в антимониде индия // ФТТ. – 1973. –Т. 15, № 10. – С. 2012-2013.
3. Магомедов М.Н. Энтальпия образования дефекта Шоттки в ионном кристалле // ФТТ, 1992, Т. 34, № 12. – С. 3724-3729.

## The relaxation under thermal noise in the spin-crossover film

Gudyma Iu.V., Maksymov A.Iu.

Chernivtsi National University, Chernivtsi, Ukraine

Today become an actual investigation of new nanomaterials for satisfying the growing requirements in the field of informational technology. The more suitable for it is the spin-crossover molecular compounds which possess two stable spin states: the ground so-called low spin (LS) state with total spin number  $S=0$ , and the metastable high spin (HS) state with  $S=2$ , which make possible to design a memory cell with  $4 \text{ nm}^3$ . Due to action of external field such as light irradiation, pressure and temperature changes or thermal fluctuations, is possible transition between LS and HS states.

In this work we have carried out the Langevin and Fokker-Planck description of noise driven transition in spin-crossover compounds described by the phenomenological model in term of photoexcitation and relaxation rates. The general form of equation with noise term is the next:

$$\frac{dn_H}{dt} = \beta(1 - n_H) - n_H \exp(-\alpha n_H) + \xi(t) \equiv f_{exc} - f_{rel} + \xi(t), \quad (1)$$

where,  $n_H$  – is concentration of HS fraction;  $\beta$  – is photoexcitation term;  $\alpha$  – is self-accelerating factor of relaxation;  $\xi(t)$  – noise induced by environment. An idealized treatment assumes the random force in phenomenological equation as a white Gaussian noise with zero means and a zero-ranged correlation functions:

$$\langle \xi(t)\xi(t + \Delta t) \rangle = 2\sigma^2 \delta(\Delta t). \quad (2)$$

where  $\sigma$  is the noise strength. Eq. (1) and the requirements (2) define the evolution of system completely. The state diagram of the system with multiplicative and additive cross-correlated noises has been obtained in [1].

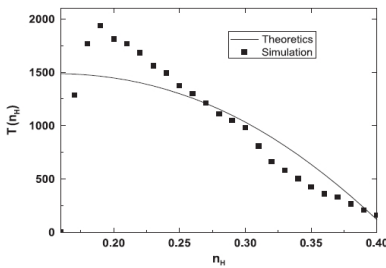


Fig.1. The mean of the first passage time vs  $n_H$  for fixed values of  $\beta = 0.085$ .

In result we have obtained time of escape from metastable state by using mean first passage time (MFPT) technique in Kramer-like approximation take into account the noise term as described in [2]. On the figure is depicted the numerical results for the MFPT together with the corresponding theoretical curves and shows that the MFPT decreases monotonously at the increase of  $n_H$ . The value of MFPT can be used to estimate the switching time in bistable electronic devices based on spin-crossover nanomaterials.

1. Gudyma Iu.V., Maksymov A.Iu. Theoretical analysis of the states of spin-crossover solids under cross-correlated noises // *Physica B*, – 2010 – V.405, P. 2534 – 2537.
2. Iu. Gudyma, A. Maksymov, C. Enachescu. Decay of a metastable high-spin state in spin-crossover compounds: mean first passage time analysis // *Eur. Phys. J. B*, – 2010 – V.78 – P. 167-172.

## Crystal defects and their complexes in crystals doped zinc chalcogenides

Gurgula G.Y.

*Vasyl Stefanyk Precarpathian National University*

Zinc chalcogenides are prospective materials of optoelectronics, because their working range corresponds to the light blue zone of optical spectrum [1]. It has been determined, that the spectral composition of photoluminescence bands ZnX significantly depends on the doping impurities [1,2]., Three different bands of the cathode luminescence identified in the literature as SA SA(I), SAL(II) i III [3] are typical in the presence of the background oxygen impurities in the crystals AІІBVI. Additional alloying of copper is associated with the centers Cu (I), Cu (II) and Cu (III) accordingly.

In the article the crystalquasichemical formulae of the clean and alloyed crystals ZnSe by a copper are offered, which contain the selfactivated oxygen for formation of the SA(I) – Cu(I) complexes, SAL(II) – Cu(II), III – Cu(III). Dependences of concentration of defects, Hall concentration of transmitters of current are figured out on maintenance of the alloying admixture Cu for different values of concentration of background oxygen, both in stoichiometric zinc selenide and n- and p-ZnSe. The role of oxygen and copper in forming of electronic subsystem of crystals of zinc selenide and realization at them thermodynamics p-n – transitions is identified.

Generalized quasi-chemical formula for ZnX crystals (X = S, Se) with O and Cu admixtures, taking into account both intrinsic point defects and complexes formed with the doping elements, are proposed. It is shown that if  $[O] > [Cu]$ , for crystals with n-type conductivity  $V_{Zn}^{//}$ ,  $V_X^\bullet$  and  $Zn_i^\bullet$  point defects and their complexes  $(O_X^\times Zn_i^\bullet V_{Zn}^{//})'$ ,  $(O_X^\times Cu_i^\bullet V_{Zn}^{//})'$  prevail, whereas for p-type crystals,  $V_{Zn}^{//}$ ,  $(O_X^\times Zn_i^{\bullet\bullet} V_{Zn}^{//})^\bullet$  and  $(O_X^\times Cu_i^{\bullet\bullet} V_{Zn}^{//})^\bullet$  dominate. If  $[Cu] > [O]$ , for n-ZnX  $V_{Zn}^{//}$ ,  $V_X^\bullet$ ,  $Zn_i^\bullet$  point defects and  $(O_X^\times Cu_i^\bullet V_{Zn}^{//})'$  complex prevail, while for p-type crystals  $V_{Zn}^{//}$ ,  $V_X^\bullet$  and  $(O_X^\times Cu_i^{\bullet\bullet} V_{Zn}^{//})^\bullet$  are found.

*This work to execute according department project (State registration № 0107U006768).*

1. Георгобиани А.Н., Котляревский М.Б. // Изв. АН СССР, Сер. Физ. – 1985. – Т.49, №10. – С. 1916-1922.
2. Бабич В.М., Блукан Н.И., Венгер Е.Ф. *Кислород в монокристаллах кремния*. Интерпресс ЛТД, Киев. 240 с. (1997).
3. Морозова Н.К., Каретников И.А. // Физ. Техн. Полупровод. – 2001. – Т.35, №1. – С. 25-33.

## **Synchrotron radiation photoelectron and surface-enhanced Raman spectroscopy of As<sub>2</sub>S<sub>3</sub> nanolayers under laser irradiation**

Holomb R.

*Research Institute of Solid State Physics and Chemistry, Uzhhorod National University,  
Uzhhorod, Ukraine*

Since the discovering the non-crystalline chalcogenides have come out as the materials of choice for infrared optics because of their excellent IR transparency. Further studies of chalcogenides particularly in their glassy and amorphous states revealed remarkable structural, electronic and optical properties of these materials. Furthermore, being sensitive to near-bandgap light they have been of great interest demonstrating a wide range of potential applications. The IR transparency, the light sensitivity, the large refractive indexes and third-order optical nonlinearities exhibiting by these materials are the main advantages of modern chalcogenide nanotechnology making attractive these materials and one of the ideal candidates as photonic devices for ultrafast all-optical switching and data processing. From other hand, modern technology requires the quantitative knowledge about the structure and its changes at the atomic scale. Therefore, the study of induced structural changes at the so called short- and medium-range order (SRO and MRO) scales of nanostructured amorphous semiconductors is an important scientific and applied task.

The goal of this study is a quantitative investigation of laser assisted photostructural transformations in thin As<sub>2</sub>S<sub>3</sub> nanolayers by using different spectroscopical methods in order to refine our current understanding of photo-induced phenomena. As a probe and quantification of SRO structures the ordinary X-ray photoelectron spectroscopy (XPS) was used together with the high surface sensitive synchrotron-radiation photoelectron spectroscopy (SRPES). In addition, the widely used Raman spectroscopy was combined with the surface-enhanced Raman spectroscopy and used for characterization of both SRO and MRO structures using the cluster approach.

The high resolution As 3d and S 2p core level spectra of amorphous As<sub>2</sub>S<sub>3</sub> film before and after near bandgap laser irradiation are reported and the contribution of different structural units (s.u.) into the experimental photoemission spectra is analysed. Also, the measured Raman and surface-enhanced Raman spectra of the samples are interpreted in terms of different nanoclusters built up from these s.u. using the results of *ab initio* vibrational spectra calculations. The contribution of different building blocks (s.u. and clusters) to the experimental spectra and their couplings to the structure of As<sub>2</sub>S<sub>3</sub> nanolayers before and after laser irradiation is analyzed and discussed in detail.

## Production and physical properties of nanostructured films Co-Cu/Cu

Ivanova S.E., Omelchenko S.A., Yurchenko N.P.,  
Khmelenko O.V., Gorban A.A., Lokot S.A.

*Dnipropetrovsk National University named by Oles Gonchar, Dnipropetrovsk, Ukraine*

Nanostructured multilayered films are widely used in such devices as magnetic hard disk drives, the read-out heads, magnetic field sensors, pressure sensors etc. Multilayered structures consist of alternate metallic ferromagnetic and non-magnetic layers. They exhibit the giant magnetoresistance (GMR) effect [1]. The devices based on multilayered structures with GMR effect have been widely manufactured by the expensive and difficult physical deposition methods [2]. In the current paper is reported about the development of cheaper and less difficult technology of electrochemical deposition which is capable of producing Co-Cu/Cu multilayered magnetic nanostructured films exhibiting the GMR effect [3]. The results of physical properties of such films are given to determine the interaction between the factors of electrochemical deposition and the magnetic properties, nanostructure and characteristics of GMR. As the substrates of the nanostructures were used Au and In that were sputtered on the silicon surface.

The main problems in production and investigation of physical properties of the Co-Cu/Cu layered structures are the measurement of the layer thickness and the thickness of the whole deposit (the difficulty in determination each layer thickness with the theoretical methods) and the complexity in production of smooth homogeneous layer in the film structure.

It is reported about the results of the investigation of ferromagnetic resonance spectra of Co-Cu/Cu films sputtered on the Au substrates. These results permit to make a conclusion that the Co layers manufactured by the method of electrochemical deposition are homogeneous.

1. Butler B., Zhang X., Nicholson D. Giant Magnetoresistance in Layered Magnetic Materials. Published online at <http://www.ornl.gov/info/ornlreview/v30n3-4/giant.htm>.
2. Farrow RFC. The role of molecular beam epitaxy in research on giant magnetoresistance and interlayer exchange coupling // IBM J Res Dev. – 1998. – №42. – P. 43-52.
3. Bakonyi I., Péter L. Electrodeposited multilayer films with giant magnetoresistance (GMR): Progress and problems // Progress in Materials Science. – 2010. – №55. – P. 107-245.

## Investigation of free volume in glasses, polymer and glass-polymer nanocomposite by positron annihilation technique

Kavetsky T.S.

*Solid State Microelectronics Laboratory, Drohobych Ivan Franko State Pedagogical University, Drohobych, Ukraine*

In the present work the results of investigation of free volume in chalcogenide glasses of  $As_2S_3$ -Ag/AgI,  $As_2Se_3$ -Bi, and  $As_2Se_3$ -Bi<sub>2</sub>Se<sub>3</sub> systems, polymer (ureasilicate or “ureasil”) and  $As_2S_3$ -polymer nanocomposite using positron annihilation technique are reported and discussed.

The concept of the free-volume structure of solids and subsequently the correlation between the free volume and the atomic structure and the physical properties of solids and its interpretation is a very useful and actual idea in the physics of disordered systems and especially of polymers [1]. Positron annihilation lifetime spectroscopy or, for simplicity, positron annihilation technique, is known as a powerful experimental tool for the investigation of free volume in solids despite their structural hierarchy. This method possesses a high sensitivity to the pore size in the range of 1-10 nm and is non-destructive.

In the last few years, the study of the free volume using positron annihilation technique has significantly increased for metals, polymers and topologically disordered materials (glasses, fine-grained ceramics, thin films). The method is based on the fact that the lifetime of a positron and its bound form, positronium (Ps), is very sensitive to the presence of defects and structural inhomogeneities in the matrix. Thermalized positrons can be trapped and annihilated in vacancy-type defects (free volume) with the surrounding electrons, giving information on the local electronic environment around the defects.

The purpose of the present work is the investigation of free volume in glasses, polymer and glass-polymer nanocomposite by positron annihilation technique. The chalcogenide glasses from  $As_2S_3$ -Ag/AgI [2],  $As_2Se_3$ -Bi, and  $As_2Se_3$ -Bi<sub>2</sub>Se<sub>3</sub> systems, polymer (ureasilicate or “ureasil”) and  $As_2S_3$ -polymer nanocomposite are selected for the research and comparative analysis.

1. Kristiak J., Bartos J., Kristiakova K., Sausa O., Bandzuch P. Free-volume microstructure of amorphous polycarbonate at low temperatures determined by positron-annihilation-lifetime spectroscopy // *Phys. Rev. B.* – 1994. – V.49, N.10. – P. 6601-6607.
2. Kavetsky T., Borc J., Petkov P., Kolev K., Petkova T. Free-volume defects and microstructure in ion-conducting Ag/AgI- $As_2S_3$  glasses as revealed from positron annihilation and microhardness measurements // *Solid State Ionics.* – 2011. – V.183. – P. 16-19.

## Synthesis and characterization of Ce<sub>2</sub>O<sub>3</sub> nanoparticles in silica shell

Khottchenkova T.<sup>1</sup>, Malashkevich G.<sup>1</sup>, Kiisk V.<sup>2</sup>, Sildos I.<sup>2</sup>

<sup>1</sup>*B.I. Stepanov Institute of Physics of National Academy of Sciences, Minsk, Belarus*

<sup>2</sup>*Institute of Physics, Tartu University, Tartu, Estonia*

It is known [1] that in silica gel-glasses doped with cerium after annealing in air at 1200°C predominant share of cerium ions are in non-luminescent quadruply charged state. At that triply charged ions form two main types of optical centers with luminescence bands maxima at 380 and 450 nm. In [2] it is shown that the annealing of such glasses in hydrogen at temperatures from 800 to 1000°C leads to reduction of Ce<sup>4+</sup> to Ce<sup>3+</sup> and to forming of optical centers with weak dependence of their luminescence and its excitation bands shapes and positions on excitation and recording wavelengths. In [2] it is also shown that at annealing in hydrogen of highly activated glasses that are characterized by the presence of Ce-containing clusters the forming of new two types optical centers takes place. The appearance of these new centers is connected with the rearrangement of the clusters structure conditioned by relaxation of the local environment of reduced (Ce<sup>4+</sup>)<sup>-</sup> ions in the clusters to the equilibrium state.

The purpose of a synthesis of Ce<sub>2</sub>O<sub>3</sub> nanopowders in silica shell and an investigation of their structural and spectral-luminescence properties was set in the present work.

The synthesis process involved Si(OC<sub>2</sub>H<sub>5</sub>)<sub>4</sub> hydrolysis in hydrochloric acid as a catalyst presence, doping of the sol obtained by adding cerium nitrate salt solution, drying to the polymerisation process finishing and grinding of the gel. Activated powders obtained were annealed in air and than in hydrogen.

X-ray diffractometer DRON-2, Andor SR303i spectrograph equipped with Andor ICCD camera and scanning electron microscope LEO-1420REM were used for investigations.

It was established that individual grains of the powders annealed in air are CeO<sub>2</sub> nanocrystals with ‘diameter’ about 50 nm in silica shell. Hydrogen annealing of the powders at temperatures >1250°C leads to reduction of cerium ions to the triply charged state and to appearance of new luminescence centers of two types which could be connected with a formation of Ce<sub>2</sub>O<sub>3</sub> nanocrystals.

Powders synthesized could be used as phosphors at a creation of LED-Phosphor hybrid light sources, as additives to printer's inks to increase a level of protection of securities.

This research was supported by European Social Fund's Doctoral Studies and Internationalisation Programme DoRa.

1. Malshkevich G.E. at. el. // J. Non-Cryst. Solids. – 1995. – 188,– 107.
2. Malashkevich G.E. at. el. // J. Non-Cryst. Solids. – 1999. – 260, – 141.

## **Melting and crystallization of Bi, Sn, In films in Al matrix**

Kolendovskiy M.M., Bogatyrenko S.I., Kryshtal A.P.

*V.N. Karazin Kharkiv National University, Kharkiv, Ukraine*

The development of new technologies for production and employment of nanodevices are of current importance. Thin-film technologies are among them. They are based on sequential deposition of films of various materials on a substrate with the simultaneous formation of required structures, e.g. X-ray mirrors, superhard coatings etc. One of the key issues of such technology is thermal and diffusion stability of the formed structures. Moreover the decreasing in film thickness leads to various kinds of size effects which in general intensify these processes, change stoichiometry, and as a result, degrade the characteristics of devices based of such film structures.

The formation and thermal stability of liquid phase in the layered film systems, that is, in systems in which one component is located between films of the second component is insufficiently studied. There are several experimental data on the size variation the melting/eutectic temperature of embedded particles or films. The studies of temperature stability of the supercooled liquid phase in such systems are quite limited. This is probably due to experimental difficulties in detecting of phase transitions in such systems. For example, the high-resolution transmission electron microscopy method can't precisely measure the temperature during phase transformations, differential scanning nanocalorimetry and electrical resistance measurements are well suited for materials with high thermal and electrical conductivity. A new approach to study phase transitions of melting-crystallization in film systems, based on the use of quartz crystal as a substrate for thin-film systems was proposed in [1]. It was shown that the change of frequency and quality factor of quartz crystal during heating and cooling can give information about formation and temperature stability of liquid phase in Bi/C system.

We applied this method to study phase transitions in Al/Sn/Al, Al/Bi/Al and Al/In/Al layered film systems (each film was 100nm thick). Film systems were prepared by successive condensation of components from independent sources in a high vacuum on a quartz plate with pre-deposited carbon film. The variation of the resonant frequency and quality factor of quartz crystal with the system under study was recorded during heating-cooling cycles. The measured values of melting and crystallization temperatures correlate with data available in literature for two component systems.

1. Kolendovskiy M.M., Bogatyrenko S.I., Kryshtal A.P. New method for studying of melting-crystallization temperature hysteresis in nanosized film systems // Ultradispersed powders, nanostructures, materials: Russian science and technical conference with international participations, 15-16 October 2009, Krasnoyarsk. – P. 252-256.

## **XPS investigation of laser-induced structural changes in As<sub>50</sub>Se<sub>50</sub> nanolayers**

Kondrat O.<sup>1</sup>, Popovich N.<sup>1</sup>, Holomb R.<sup>1</sup>, Mitsa V.<sup>1</sup>, Petrachenkov O.<sup>1</sup>,  
Lyamaev V.<sup>2</sup>, Tsud N.<sup>3</sup>

<sup>1</sup>*Institute of Solid State Physics and Chemistry, Uzhhorod National University,  
Uzhhorod, Ukraine*

<sup>2</sup>*Sincrotrone Trieste, Area Science Park, Basovizza (Trieste), Italy*

<sup>3</sup>*Charles University, Faculty of Mathematics and Physics, Department of Surface and  
Plasma Science, Prague, Czech Republic*

The amorphous chalcogenides have been of great interest due to their remarkable structural, electronic and optical properties demonstrating a wide range of potential applications [1]. Chalcogenide glasses are known for being sensitive to near-bandgap light, which produces several types of photoinduced changes in structure and properties. Many researchers consider that due to the nano-phase separation in as deposited films the manufacturing of holographic gratings and rewritable optical disks, using the optomechanical effect discovered in g-As<sub>50</sub>Se<sub>50</sub> will be possible. Therefore, the study of structural changes at the atomic scale in nanostructured amorphous semiconductors induced by laser irradiation is an important scientific and applied task.

The bulk As<sub>50</sub>Se<sub>50</sub> samples were prepared by conventional melt-quenching route in evacuated quartz ampoules from a mixture of high purity 99.999 % As and Se precursors. Amorphous As<sub>50</sub>Se<sub>50</sub> thin films with thickness of about 500 Å were prepared by thermal evaporation from bulk glass on the (100) silicon crystal wafer substrates. The irradiation of amorphous As<sub>50</sub>Se<sub>50</sub> thin film was carried out by using a He-Ne (632.8 nm) laser of 50 mW/cm<sup>2</sup> intensity. The high resolution photoemission spectra were taken using the Mg K-α (hν = 1253.6 eV) X-rays source. The photoelectron As 3d, Se 3d, C 1s and O 1s core-level spectra of as-prepared and laser irradiated As<sub>50</sub>Se<sub>50</sub> films before and after Ar-ion sputtering were measured and analyzed.

The obtained experimental results on influence of near bandgap laser irradiation on the structure of As<sub>50</sub>Se<sub>50</sub> nanolayer films are reported. The analysis of Se3d core level spectra shows that the laser illumination leads to increase of concentration of Se-rich structural units. The As3d core level spectrum is also transformed when the sample was irradiated in air. In addition, the laser induced diffusion of O and C into the deeper layers is observed.

1. R. Holomb, V. Mitsa, Solid. St. Commun. – 2004. – V.129. – P. 655.

## **Influence of heavy metal ions on absorption spectra and structure of polyaminoarene films**

Konopelnyk O.I., Aksimentyeva O.I., Demchenko P.Yu.

*Ivan Franko National University of Lviv, Lviv, Ukraine*

The study of the changes in optical and structural film characteristics under the influence of chemical factors (gases, ions, organic substances) is necessary for creating new environment optical sensors. Conjugated polyaminoarenes are quite sensitive to chemical environments, including the pH, polar gases, solvents [1, 2]. We studied the optical properties of the polyaminoarene films in solutions of heavy metals salts - Fe, Ni and Cu to create a visual "express" – control sensors for determination of small quantities of these metals.

The effect of heavy metals on the changes in polyaminoarenes films coloration that represent the spectral changes in the optical region spectrum has been established. Under the action of  $\text{Cu}^{2+}$  ions there is a general increase in optical absorption of the films. The interaction of ions with the polymer chain causes a reducing of  $\text{Cu}^{2+}$  to  $\text{Cu}^{1+}$  with generation of positive charges (holes) in the conjugated chain. Such processes lead to the increasing of charge carrier's concentration - polarons and correspondently of optical absorption in polaron and bipolaron bands. An interaction of  $\text{Fe}^{3+}$  with conjugated polymers leads to easy reduction to the  $\text{Fe}^{2+}$ . It can form a complex with charge transfer type  $[\text{PANI}]^+[\text{FeCl}_4]^-$ , which leading to changes in the electronic structure of the polymer and in the supramolecular structure of the film.

X-ray diffractograms of polyaminoarenes doped by metal ions indicate the formation of almost amorphous phase of doped polymer. The average size of domains (crystallites) is 5,79 Å. It is interesting fact of appearance a group of narrow, well-formed peaks, which correspond to inter plane distance of  $d \sim 13,46$  Å and 3,43 Å at the angles of  $2\theta = 8,25^\circ$  and  $32,83^\circ$  respectively, which indicate the phase formation with a high degree of crystallinity. We can assume that for polyaniline the process of the phase formation by type  $[\text{PANI}^+ \text{FeCl}_4^-]$  takes a place, which gives own diffraction picture is not similar to X-ray for  $\text{FeCl}_3$ ,  $\text{FeCl}_2$ , and others compounds.

Thus, the effect of heavy metal ions causes the changes in the electronic structure of conjugated polymers and their supramolecular structure as a result of acceptor doping and the formation of charge transfer complexes.

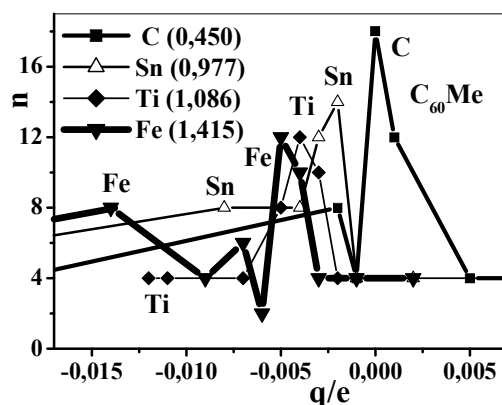
1. Konopelnyk O.I., Aksimentyeva O.I., Tsizh B.R., Chokhan M.I. Physical and Technological Properties of the Sensor Materials Based on Conjugated Polyaminoarenes // Physics and Chemistry of Solid State – 2007. – V.8, №4. – P. 786-790.
2. Tsizh B.R., Chokhan M.I., Aksimentyeva O.I., Konopelnyk O.I., Poliovyi D.O. Sensors based on conducting polyaminoarenes to control the animal food freshness // Mol. Cryst. Liq. Cryst. – 2008. – V.497. – P. 254-260.

## Collective chemical bonds of atoms of metals with fullerene molecules C<sub>60</sub>: theory and experiment

Korniyenko N., Kulish N., Dmytrenko O., Pavlenko O., Brusentsov V., Strelchuk V.

*Kyiv National Taras Shevchenko University, Kyiv, Ukraine*

Systematic experimental and theoretical study of chemical interaction of metal atoms of Ti, Fe, Sn (Me) etc. with fullerenes C<sub>60</sub> was performed. Numerical calculations of geometrical configurations, binding energy, vibration frequencies and intensities of all bands in the IR and Raman spectrums are calculated with Gaussian-98 program for systems C<sub>60</sub>Me and C<sub>60</sub>MeC<sub>60</sub>. Restricted Hartree-Fock method with 3-21G basis was applied. Registration of Raman spectra was made by Horiba Jobin Yvon T64000 spectrometer. Thin films of C<sub>60</sub> with metals were prepared by vacuum sublimation and deposition on Si(111) substrates.



It is shown that electron density from metal atom to fullerene is transferred not only to one atom C of the molecule, but also to the other atoms. Moreover these charges are distributed nonhomogeneously, that characterizes collective properties of bonds. For collective bonds formed by C<sub>60</sub> molecules with the metal atoms is typical decrease of the double bonds by 1,3%, and single ones by 0.75%, despite of Coulomb repulsion of the charges. Length of bonds for studied metals is 1,9-2,2 Å, that is more than length of C-C bonds. All multiplets of observed and calculated splitted bands H<sub>g</sub>(i) and F<sub>u</sub>(k) (I = 1-8; k = 1-4) were performed. For case of systems C<sub>60</sub> with Fe and Ti is observed anomalous increase of intensities for many silent bands for C<sub>60</sub>.

## The kinetic of the formation of magnetite and lepidocrocite on the steel surface depending on the pH values of dispersion medium

Lavrynenko O.M., Netroba S.V., Prokopenko V.A.

*F.D. Ovcharenko Institute of Bio-Colloid Chemistry NAS of Ukraine, Kiev, Ukraine*

The investigation of processes connected with formation of nanosized para- and ferry magnetic particles is actual problem of colloidal chemistry. Iron oxides and hydroxides of different structural modification are used for medical-biological application, such as magnetic carriers for drug delivery, target therapy, diagnostic of a range of diseases [1]. The properties of nanosized particles are defined by the range of the physical-chemical factors of phase formation, particularly by the pH values of dispersion medium. The formation of iron-oxygen nanosized minerals has carried out on the surface of steel electrode by its contact with air oxygen and dispersion medium. The methodic of experiment was described in [2]. The steel electrode was made of the carbon steel (St3); as the dispersion medium there was chosen water solutions at the range of pH values from 1.5 to 11.0. The main method of investigation there was X-ray diffraction *in situ*. The obtained results have shown that on steel surface are formed mainly the phases of Green Rust, lepidocrocite  $\gamma$ -FeOOH and magnetite  $\text{FeFe}_2\text{O}_4$ . By contact the steel with acid dispersion medium (pH = 1.5) after 2 h the particles of  $\gamma$ -FeOOH (020) and (120) are formed on surface. The intensity and quantity of the X-ray reflexes gradually increase, but  $\gamma$ -FeOOH stays as the single phase to the stationary state of the system (72 h). By the pH value 4.0 after 1 h particles of  $\gamma$ -FeOOH are formed on steel surface. Magnetite is reflected on XRD-pattern after 5 h and its intensity is increasing more than three times to the stationary state of the system (48 h). At the pH value 6.5 after 2 h  $\gamma$ -FeOOH appears on steel surface and after 5 h there appears  $\text{FeFe}_2\text{O}_4$ . The accumulation of  $\text{FeFe}_2\text{O}_4$  on steel surface in such condition is faster than the accumulation of  $\gamma$ -FeOOH. The system is stabilized after 48 hours of contact. At the pH = 11.0 the surface structures are weakly crystallized and diffraction patterns show low intensity peaks of  $\gamma$ -FeOOH. After 24 hours on steel surface there appear two peaks of  $\text{FeFe}_2\text{O}_4$  (311) and (220), which intensity is insignificantly growing. The optimal conditions for the formation on steel surface of lepidocrocite are acid dispersion medium and for formation of magnetite is neutral dispersion medium.

1. Mornet S., Vasseur S., Grasset F., Duguet E. Magnetic nanoparticle design for medical diagnosis and therapy // J. Mater. Chem. – 2004. – V.14. – P. 2161-217.
2. Lavrynenko O.M., Korol Ya.D., Netroba S.V., Prokopenko V.A. Kinetic regularity of the formation of Fe (II)–Fe(III) LDH structures (Green Rust) on the steel surface in presence of the  $\text{FeSO}_4$  and  $\text{Fe}_2(\text{SO}_4)_3$  water solutions // Хімія, фізика та технол. поверхні. – 2010. – Т. 1, № 3. – С. 338-342.

## Heterostructure p (Pb<sub>1-x</sub>Sn<sub>x</sub>Se)-n (CdSe) films for far ir spectrum photodetectors

Lepikh Ya. I., Ivanchenko I. A., Budiyanskaya L. M.

*Odessa Mechnikov National University, Odessa, Ukraine*

In the far IR spectral region ( $\lambda > 10 \text{ m}$ ) the highest sensitivity is possessed by cooled to liquid helium temperature photodetectors (PhD) based on A<sub>3</sub>B<sub>5</sub> compounds with a detectivity level  $D^* = 10^9 \dots 10^{10} \text{ cm}\cdot\text{Hz}^{1/2}/\text{W}$  [1].

Since the application of cooled PhD causes some difficulties, for example, as an indicator of sensors, the creation of uncooled PhD in this spectral region is quite up-to-date.

Considerable interest for the purposes of creation of such photodetectors has been seen recently to the narrow-gap semiconductors, which have intrinsic conductivity in the far-infrared region.

As a functional material of uncooled PhD we investigated the solid solution of tin and lead chalcogenides Pb<sub>1-x</sub>Sn<sub>x</sub>Se ( $0 < x < 0,3$ ) with a spectral sensitivity peak in the field  $\lambda = 10 \text{ }\mu\text{m}$  at a temperature close to room temperature.

This material electrical properties which depend on band gap  $E_g$  on the composition and temperature, that indicates the band inversion are provided.

The mechanism of the sensitivity origin of the samples in the infrared spectrum, which consists of minority carriers injection from the narrow-gap semiconductor, which absorbs IR-radiation, into the wide-gap semiconductor with a space charge current limitation mechanism has been researched.

A method for obtaining narrow-band semiconductor compound Pb<sub>1-x</sub>Sn<sub>x</sub>Se polycrystalline ingots with a composition sensitive in the field  $\lambda = 10 \text{ }\mu\text{m}$  at room temperature has been developed.

The possibility of creating an uncooled self PhD in the field  $\lambda = 10 \text{ }\mu\text{m}$  on the basis of Pb<sub>1-x</sub>Sn<sub>x</sub>Se based on the fact that the inversion zone is observed at temperatures of 77, 195 and 300 K and the compositions  $x = 0,19, 0,25$  and  $0,30$ , respectively, has been proved.

The design and manufacturing technology of film bilayer photohetero resistors based on p-n junction p(Pb<sub>1-x</sub>Sn<sub>x</sub>Se)-n(CdSe) with a threshold sensitivity  $P_N = 10^{-6} \dots 10^{-7} \text{ W/Hz}^{1/2}$  has been developed.

Also a film matrix PhD sensitive in region of 10,6 microns, with the element threshold sensitivity not worse than  $10^{-6} \text{ W/Hz}^{1/2}$  has been developed.

1. Козелкин В.В., Усольцев И.Ф. Основы инфракрасной техники. Машиностроение, М. 1997.

## Effect of deposition rate on properties of thin Ge films on GaAs

Mitin V.F.<sup>1</sup>, Lazarov V.K.<sup>2</sup>, Lytvyn P.M.<sup>1</sup>, Kholevchuk V.V.<sup>1</sup>, Matveeva L.A.<sup>1</sup>,  
Kotenko I.E.<sup>3</sup>, Mitin V.V.<sup>3</sup>, Venger E.F.<sup>1</sup>

<sup>1</sup>*V. Lashkaryov Institute of Semiconductor Physics, National Academy of Sciences of Ukraine,  
Kyiv, Ukraine*

<sup>2</sup>*Department of Physics, The University of York, Heslington, York, UK*

<sup>3</sup>*National Technical University of Ukraine “Kyiv Polytechnic Institute”, Kyiv, Ukraine*

When depositing thin Ge films onto the semi-insulating GaAs(100) substrates using thermal evaporation of Ge in the vacuum, we have found strong effect of deposition rate on their electrical properties, surface and heteroboundary morphology, as well as the intrinsic stresses due to misfit of the Ge and GaAs lattice constants.

In this work the temperature of GaAs substrate remained constant ( $490 \pm 10$  °C) in the course of Ge film deposition. The film thickness was  $130 \pm 30$  nm. The deposition rate varied from 0.025 up to 0.37 nm/s.

At rather high deposition rates ( $\sim 0.4$  nm/s), the films are heavily doped and of *n*-type. The film resistivity is  $\sim 0.01$  Ω·cm. The temperature dependence of conductivity is very weak and of non-activation type, which is characteristic of semiconductors with degenerate charge carriers. The electronic properties of films changed drastically as the deposition rate was decreased. At low deposition rates ( $\sim 0.03$  nm/s), the temperature dependence of resistivity becomes of activation type (exponential, with activation energy close to  $E_g/2$ ), i.e., a metal–insulator transition occurs. In this case, the film resistivity increases up to  $\sim 100$  Ω·cm. Such films are heavily doped and strongly (in particular, fully) compensated and are of *p*-type. The intrinsic stresses in the films (due to misfit of the Ge and GaAs lattice constants) go down as the deposition rate is decreased. The structure of all the films under investigation is single-crystalline. The film–substrate interface is coherent, and the film surface is granular. As the deposition rate increased, the most probable value of grain diameter decreased and the distribution of those values acquires Gaussian type.

*This work was partially funded under Ukrainian State Program “Nanotechnologies and nanomaterials”, Projects No. 2.2.6.15 and 3.6.1.10.*

## **Contact angle changes at spreading of liquid metals on the surface of amorphous alloys**

Mudry S., Boruh I.

*Faculty of Physics, Ivan Franko Lviv National University, Lviv, Ukraine*

Liquid metallic alloys with low melting temperature are widely used as solder materials and on that reason it is important to know how changes the surface properties during soldering process. New Pb-free solder alloys consist of Sn, Bi, In, and other low melting point metals, which maintain the contact between crystalline or amorphous materials of various kind. If the information on behavior of such melts on the surface of crystalline materials is available, the data for spreading of such liquids over the surface of amorphous alloys are poor.

In this work the changes of contact angle with time for liquid Sn, Bi, In and Ga on the surface of  $\text{Co}_{70}\text{Fe}_3\text{Mn}_{3,5}\text{Mo}_{1,5}\text{Si}_{11}\text{B}_{11}$  amorphous alloy have been studied. Measurements were carried out with using of equipment for surface tension measurements. We have obtained the results on change of contact angle also for alloys, which was crystallized from amorphous phase by heating. These results were compared and analyzed. For example for liquid In, placed on the surface of  $\text{Co}_{70}\text{Fe}_3\text{Mn}_{3,5}\text{Mo}_{1,5}\text{Si}_{11}\text{B}_{11}$  amorphous alloy the decrease of contact angle is observed at  $T=600^\circ\text{K}$  and higher temperatures, whereas for crystalline alloy a contact angle is in fact unchangeable at this temperature. Similar behavior was also observed for liquid Bi and Sn but the temperatures, when intense interaction between liquid and solid substrate starts are equal about  $645^\circ\text{K}$  for liquid Bi, whereas for liquid Sn it is the same as for In. Significantly different is the behavior of contact angle for liquid Ga. In this case at  $T=600^\circ\text{K}$  the rapid decrease of contact change is observed both for amorphous and crystalline substrate, but for last it is not so intensive.

## **Influence of oxygen state in crystalline Si on the implanted Fe and Ti gettering by Al layer**

Naseka V., Melnik V., Sarikov A., Oberemok O., Romanyuk B.,  
Litovchenko V., Zlobin S., Popov V.

*V. Lashkarev Institute of Semiconductor Physics NAS Ukraine, Kiev, Ukraine*

The efficiency of solar energy photo converters is determined by a number of factors related to the material properties, element design, and formation technology. High values of the life time of minority charge carriers are to be provided in the first turn both in the initial material and during the photo converter production. Recombination active heavy metal impurities such as Fe, Ti, V, Cu et al. play an important role in Si. Their total concentration in the initial material should not exceed 1 ppm. Such impurities as V, Cr, Fe, Ti decrease the solar element efficiency beginning from the concentrations as low as 0,3 ppm [1]. An important factor influencing the impurity gettering is the presence of SiO<sub>2</sub> precipitates in Si bulk. During the high temperature (700-900°C) technological processes the SiO<sub>2</sub> precipitates in Cz-Si act as the centres of internal gettering leading to the decrease of the efficiency of external gettering procedure.

This work presents the results of the theoretical and the experimental study of impurity gettering in Si wafers with SiO<sub>2</sub> precipitates by the Al layer. Single crystalline (100) 400 μm thick Si wafers were the object of investigations. Three step anneals (3 h 1150°C, 5 h 700°C, and 10 h 1000°C) were applied for the precipitate formation. The thickness of Al layer on the back side of Si wafers was 3 μm. Fe and Ti were implanted in Si with doses in the range of 10<sup>11</sup> to 10<sup>13</sup> cm<sup>-2</sup> at the implantation energy of 35 keV. Obtained samples were annealed at the temperatures in the range of 800 to 1100°C. The efficiency of impurity removal from the Si wafers was controlled by measuring the diffusion length of minority charge carriers  $L_D$  as well as from the thickness distribution of Fe and Ti on the front (being implanted) and back sides of Si wafers. The formation of SiO<sub>2</sub> precipitates was controlled by IR spectroscopy.

The theoretical model analyses three processes, namely: (i) precipitate growth/dissolution, (ii) impurity diffusion under point defect injection, and (iii) impurity capture by Al getter and SiO<sub>2</sub> precipitates.

The study resulted in the elaboration of optimum regimes for the gettering of impurities from the crystalline Si wafers. A physical model is proposed that describes the kinetics of Fe and Ti gettering influenced by the SiO<sub>2</sub> precipitates. A number of characteristics of Al+SiO<sub>2</sub> combined getter were obtained from the comparison of experimental data with theoretical results.

1. Popov V.G. Solar cells based on multicrystalline silicon // *Semicond. Phys., Quantum Electronics & Optoelectronics*. – 2000. – V.3, №4. – P. 479-488.

## Defects creation in the LPE $\text{Cd}_{1-x}\text{Zn}_x\text{Te}$ thin films under $\gamma$ -irradiation

Naseka Yu.M., Rashkovetskyi L.V., Strilchuk O.M., Danilchenko B.O.

*V.E. Lashkaryov Institute of semiconductor physics of NAS of Ukraine, Kyiv, Ukraine;*

<sup>2</sup>*Institute of physics of NAS of Ukraine, Kyiv, Ukraine*

For today it is given much attention to the study of the post growth methods for changing of the physical properties of CdTe based compounds: chemical etching [1], thermal treatment,  $\gamma$ -irradiation [2], laser irradiation [3]. The great interest of such kind of research works is caused by great suitability of Cd(Zn)Te single crystals for production X- and  $\gamma$ -ray semiconductor sensors. But there no information about the influence of the noted treatments on the physical properties of the thin layers of CdTe based compounds. However, CdZnTe thin films also got more applications in biophysics, solar cells production and growth of CdHgTe for the infrared detectors. Therefore in this work we will investigate the influence of different dose  $\gamma$ -quanta irradiation on the physical and in particular structural and photoluminescence properties of  $\text{Cd}_{0.9}\text{Zn}_{0.1}\text{Te}$  thin films grown by liquid phase epitaxy (LPE) on CdTe (111) substrates. Low-temperature photoluminescence was used as the main tool in the investigated of radiation-stimulated changes in the optical properties and defect structure of  $\text{Cd}_{0.9}\text{Zn}_{0.1}\text{Te}$  thin films. It was obtained that  $\gamma$ -irradiation in the dose range of 10 – 100 kGy leads to the substantial changes in the photoluminescence properties of the  $\text{Cd}_{0.9}\text{Zn}_{0.1}\text{Te}/\text{CdTe}$  system. At first, it induces the rise of the intensities of the photoluminescence emission lines related to the radiate transitions including Cd-vacancies due to effective creation of the Cd-vacancies in all volume of studied samples. Secondly,  $\gamma$ -irradiation leads to the decrease in the intensity of the donor bound exciton emission line which is caused by decrease in the concentration of isolated donors which is related with compensation of the pointed donor atoms and  $\gamma$ -stimulated Cd-vacancies [2]. And thirdly, it leads to the red shift in the energy peak positions of the both free and bound exciton lines. We suppose it is related with the change in the content of the ternary compound thin film which can be explained by  $\gamma$ -stimulated migration of the Zn atoms in the volume of the CdTe substrate on Cd-vacancies.

1. Chan H., Tong J., Hu Z., Shi D.T., Wu G.H., Chan K.-T., George M.A., Collins W.E., Burger A., James R.B., Stahle C.M., Bartlett L.M. // *J. Appl. Phys.* 80. – 1996. – P. 3509.
2. Krylyuk S.G., Korbutyak D.V., Kryuchenko Yu.V., Kupchak I.M., Vakhnyak N.D. // *J. of All. and Comp.* – 2003. - V. 371. - P. 142.
3. Medvid A., Mychko A., Strilchuk O., Litovchenko N., Naseka Yu., Onufrijevs P., Pludonis A. // *Phys. Stat. Sol. (c)* 1.6/ - 2009. – P. 209.

## Magnetothermopower and the Magnetoresistivity of Bi Nanowires in Weak and Strong Magnetic Fields

Nikolaeva A.<sup>1,2</sup>, Konopko L.<sup>1,2</sup>, Huber T.<sup>3</sup>, Para Gh.<sup>1</sup>

<sup>1</sup>Institute of Electronic Engineering and Industrial Technologies, AS of Moldova

<sup>2</sup>International Laboratory of High Magnetic Fields and Low Temperatures, Wroclaw, Poland

<sup>3</sup>Department of Chemistry, Howard University, Washington, U.S.A

The aim of this work was to study the effect of magnetic fields on the thermopower  $\alpha(H)$  and the resistance  $R(H)$  of Bi nanowires in the region of occurrence of the classical and quantum size effects, which were shown in the "semiconductor" dependence of the resistance  $R(T)$  and the anomalous dependence of the thermopower  $\alpha(T)$  at  $d < 80$  nm [1].

Figure 1 shows the field dependences the resistance  $R(H), H \parallel I$  (left) and of magnetothermopower  $\alpha(H, H \parallel \Delta T)$  (right) Bi- wire with  $d = 70$  nm at various temperatures.

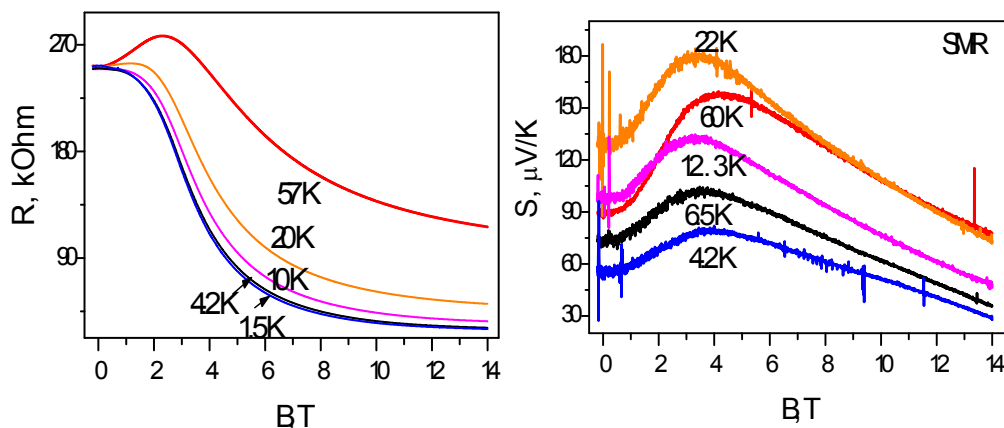


Fig. 1.

The displacement of  $H_{\max}$  to the range of higher temperatures in the  $R(H)$  dependences, which characterizes the law of variation in the carrier mobility with temperature, shows that  $\mu \sim T^{-1}$ . The weak magnetic field  $\mu H < 1$  leads to an enhancement of the positive contribution to the thermopower. The Power factor ( $P.f = \alpha^2 \sigma = 2.9 \cdot 10^{-4} \text{ W/cm} \cdot \text{K}^2$ ) reaches maximum values at for Bi wire,  $d = 70$  nm,  $T = 20$  K. The appearance of the thermopower sign reversal depending on Bi-wire diameter  $d$  in a magnetic field ( $H \parallel I$ ) leads to an increase in  $\alpha$  in the positive range and to a shift of the sign reversal point to higher temperatures. The fact that the thermopower and magnetothermopower in Bi nanowires have a positive value at low temperatures, unlike bulk samples, can serve a trigger for the optimization of using these nanowires as p-branches of thermoelectric converters.

*This work was supported by SCOPES IZ73ZO\_127968.*

1. D. Gitsu, L. Konopko, A. Nikolaeva, and T. Huber // J. Appl. Phys. Lett. – 2005. – V 86. – P. 10210.

## Scattering mechanisms in crystals PbSe p-type conductivity

Nyzhnykevych V.V. Galuschak M.O.

*Ivano-Frankivsk National University of Oil and Gas, Ivano- Ivankivsk Ukraine*

The theoretical analysis of scattering mechanisms of carriers by thermal vibrations of crystal lattice is done. The calculation provided of the mobility of carriers in a wide temperature (4,2 – 300 K) and concentration ( $10^{16} - 10^{20} \text{ sm}^{-3}$ ) bands in view of interacting conduction of holes of deformation potential acoustic and optical phonons and polarization potential of optical phonons.

Kinetic parameters of semiconductor materials are largely determined by the scattering mechanisms of carriers. Scattering mechanisms of carriers in lead chalcogenides have been studied repeatedly by different authors. But despite this, at present there is no consensus on the concentration and temperature limits the dominance of certain types of scattering. In this paper, based on comparison of theoretical calculations with the experimental Hall mobility data of specified concentration and temperature limits the use of approximate models of the band structure and the prevailing scattering mechanisms of charge carriers in lead selenide crystals p-type conductivity.

The dominant scattering mechanisms of carriers in hole lead selenide crystals are the scattering of short-range potential vacancies for the concentrations of  $10^{19} - 10^{20} \text{ sm}^{-3}$  and the lattice thermal vibrations.

Scattering of phonons gives a correct picture of the quality necessary to characterize transport phenomena. The role of polar optical phonon significant at temperatures of 77 and 300 K for concentrations of  $10^{16} - 10^{18} \text{ sm}^{-3}$ . When increasing the concentration scattering on optical phonons is reduced due to screening.

At high concentrations (higher  $10^{19} \text{ sm}^{-3}$ ) scattering on optical phonons is manifested through their deformation potential, whose influence on the total scattering at certain concentrations is very essential at room temperature. Scattering of carriers by acoustic phonons significant for all temperatures in the considering the whole studied concentration range. For temperature 77 K influence on the total scattering dominates deformation potential scattering on optical phonons.

1. Ravich Yu.L., Efimova B.A., Tamarchenko V.I. Scattering of current carriers and transport phenomena in lead chalcogenides. I. Theory // Phys. Stat. Sol. – 1971. – Vol.43, № 1. – P. 11-33.
2. Freik D.M., Nykyruy L.I., Ruvinsky M.A., Shperun V.M., Nyzhnykevych V.V. Scattering of charge carriers in lead chalcogenides crystals n-type // Physics and Chemistry of Solids. – 2001. – Vol.2, № 4. – P. 681-685.

## Theoretical basis of thermoelectric parameters calculation of the doped lead chalcogenides crystals

Nykyruy L.I.<sup>1</sup>, Mazur M.P.<sup>2</sup>

<sup>1</sup>*Vasyl Stefanyk PreCarpathion National University, Ivano-Frankivsk, Ukraine*

<sup>2</sup>*Ivano-Frankivsk National Technical University of Oil and Gas, Ivano-Frankivsk, Ukraine*

Semiconductor substitutional solid solutions have attracted the attention of the possibility of changes in wide range of options for changing the composition. Experimental studies have shown that, despite the random arrangement of atoms of different varieties in the crystal lattice, the electronic spectrum of solid solutions is characterized by relatively well-defined structure.

Properties of binary compounds IV-VI, including transport phenomena have been studied quite well and presented in several reviews [1]. However, in solid solution, despite the large number of experimental data, theoretical analysis of such processes is not investigated. Therefore, special importance is the modeling of their properties, to predict the characteristics of the solid solution  $A_xB_{1-x}C$ , based on the measured parameters of its constituent components A, B and C.

In paper study the influence of composition fluctuations in the density of states of electrons and holes in solid solution, as well as the electronic properties of solid solutions based on IV-VI narrow-gap semiconductors.

Random potential  $V(z)$ , due to compositional fluctuations, leads to the tail states decaying exponentially into the band gap [2]. States themselves are realized by such exponentially unlikely configurations of substitutional atoms that create the potential for containing the electronic level with a given energy in the band gap.

Formation of solid solution leads to overlapping of energy bands of basic materials, which in turn causes the complex nature of the Fermi level. Accordingly, the analysis of impurity scattering can not make in standard relaxation time approximation. Therefore, calculations of dominant scattering mechanisms were performed using a variational procedure. For correct calculation should take into account the specificity of modified material in the transition from binary compounds into solid solutions. The lattice constant formed by solid solution determined by Vegard's law, band gap, which in first approximation is linear, defined by generalization of experimental data, and the deformation constant, which is most sensitive to the atoms replacing some other method determined by [3].

*This work is partially financed by State Fund of Fundamental Researches of State Agency for Science, Innovation and Information of Ukraine (State registration № 0110U007674).*

1. P.N. Gorley, V.A. Shenderovsky. Variation Approach in Kinetic Theory. Naukova Dumka, Kyiv. 296 p. (1992).
2. S.D. Baranovsky, A.L. Efros. Blurring the edges of the bands in solid solutions // Semiconductor physics (USSR), – 1978. – V.12, N.II. – P. 2233-2237.
3. L.A. Faljkovski. Optical properties of grafene and IV-VI semiconductors // UFN. – 2008. – V. 178, №9. – 923.

## **Galvanomagnetic properties of PbSe<Cl> films**

Ol'khovskaya S.I., Sipatov A.Yu., Rogacheva E.I.

*National Technical University "Kharkiv Polytechnic Institute", Kharkiv, Ukraine*

PbSe is known as one of the promising thermoelectric materials. However, for its effective using high charge carrier concentrations ( $\sim 10^{19} \text{ cm}^{-3}$ ) are need. By now the number of studies on properties of degenerate electronic gas in PbSe thin films is limited.

The goal of the present work is to determine the possibility of PbSe<Cl> thin films preparation with a high electron concentration by thermal evaporation of PbSe crystals doped with chlorine and study their galvanomagnetic properties.

PbSe crystals doped with 2 mol% PbCl<sub>2</sub> were prepared by the method of direct melting of elements in evacuated quartz ampoules; PbSe<Cl> film with thickness 210 nm was obtained by thermal evaporation of the crystal in vacuum and following deposition on substrates (001) KCl. The film was covered with a protective layer Al<sub>2</sub>O<sub>3</sub>. The electrical conductivity  $\sigma$  and Hall coefficient  $R_H$  were measured by the method of the direct current and constant magnetic field in the temperature range 80-300 K. The error in the measurement of  $R_H$  and  $\sigma$  did not exceed 5%.

It is established that thermal evaporation of PbSe<Cl> crystal in vacuum makes it possible to obtain *n*-type films with high charge carrier concentration ( $8 \cdot 10^{20} \text{ cm}^{-3}$ ). It is shown that with increasing temperature electron concentrations in crystal and films PbSe<Cl> practically do not change, which is typical for degenerate semiconductors. It is established that the dominating scattering mechanism in PbSe<Cl> films is scattering by acoustic phonons.

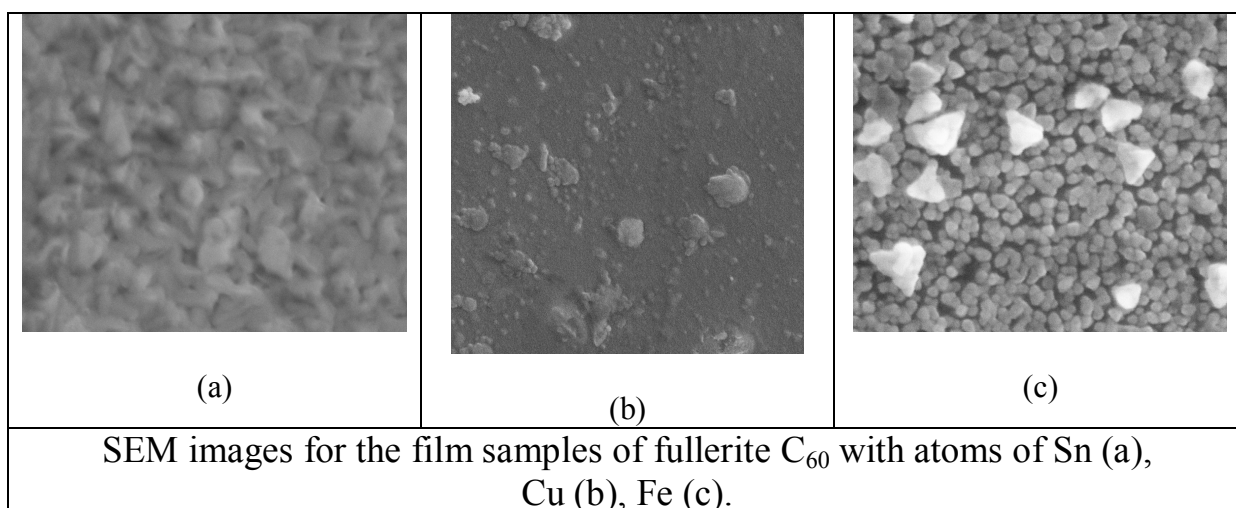
## Structure and vibration properties of C<sub>60</sub> with metals

Pavlenko O., Dmytrenko O., Kulish M., Brusentsov V., Rybiy V.,  
Tkach V., Korniyenko M., Strilchuk V.

*Kyiv National Taras Shevchenko University, Kyiv, Ukraine*

When fullerites are doped with the alkali metals, their mechanical, electronic, magnetic and optical properties are changed. The ability to control such induced changes is vital to progress in material science. In the work is studied doping of fullerites with Sn, Fe, Cu on the structural and vibration properties of C<sub>60</sub> fullerites.

The films were prepared by vacuum sublimation and deposition of fullerite powder of C<sub>60</sub> and metal atoms of Sn, Cu, Fe on the substrates. For investigation of Raman spectra was applied Horiba Jobin Yvon T64000 spectrometer (Ar laser, 514.5 nm), for study of morphology SEM Zeiss 60, for the changes was applied XRD method (Cu<sub>Kα</sub>).



It can be seen from the figures that crystallites of C<sub>60</sub> with metal crystallites are formed. Grain boundaries of the crystallites are smeared that can be explained by diffusion of the metal atoms into fullerites and that is confirmed by phase analysis. This can explain the shift and appearance of new vibration bands in the Raman spectra, especially for the samples with Sn, and appearance of new diffraction maximums on XRD patterns. The changes are possible due to donor-acceptor interaction and formation of chemical bonds between fullerenes and metal atoms on the interfaces of the crystallites. Possibility of formation of such complexes is proved by theoretical calculations. The possibility of formation of such complexes is confirmed by theoretical modeling.

## **Mechanical descriptions of nanoscale tapes are with the structure of zinc-blende**

Peleshchak R.M., Mats'ko M.B., Odrehivs'ka O.O.

*Ivan Franko Drohobych State Pedagogical Universiti, Drohobych, Ukraine*

Intensive development of nanotechnology for the last years brought to necessity of building adequate analytical models which help to describe physical-mechanical properties nanoobjects. (2D, 1D, 0D-nano). In majority existent models of this kind is accepted that the main mechanical characteristics nanoobjects coincide with their values obtained from macroscopic experiments. As results of micro-and macro experiments meaning modules of elasticity in volumetric materials do not coincide with the corresponding values to nanoobjects. [1]. One method of determining the elastic properties nanoobjects is research of microrelief, formed at stretching the sample, which has ultra-thin layers [2]. Mismatch modules of resiliency in by volume single-crystals and nanosystems concerned, on one hand with the specifics of the internal structure of the material, on the other is caused by discreteness on nanometer level.

In this paper the investigated dependence of the Poisson ratio and modulus Young nanodimensional tapes with zinc blende structure in the crystallographic planes is ((100) (110) (111)) depending on the number of monolayers. This work is the development and continuation of [3]. To investigate the influence of scale factor on the mechanical properties of the material examined nano two-dimensional monocrystalline material. Interaction between atoms is paired and considered only with close neighbors.

Set that size and shape of nanocrystals provide additional anisotropy in its mechanical characteristics. For nano fabric which containing  $N = 10$  monolayers of atoms, Young's modulus (to longitudinal direction) is increased as compared the to macroscopic parameters on 11%, and the coefficient of Poisson (to transversal direction) diminishes on 7% and 9% in crystallography planes (100) and (111) accordingly. When  $N = 100$  deviation parameter is 1%. For ultra-thin films ( $N=2$ ) module cabin Boy(to longitudinal direction) in two times exceeds the macroscopic value.

1. J.J. Kim, H.A. Marzouk, C.C. Eloi, J.D. Robertson. // J. Appl.Phys. – 1995 – V.78, №1 – P. 245.
2. С.Л. Баженов, А.Л. Волынський, Е.Е. Воронина, Н.Ф. Бакеев. // ДАН – 1999 – V.367, №1 – P. 75.
3. А.М.Кривцов, Н.Ф. Морозов // ДАН – 2001 – V.381, №3 – P.825.

## **Radiation modification of polyethylene composites of multi-walled carbon nanotubes under irradiation**

Pinchuk-Rugal' T.M.<sup>1</sup>, Nechyporenko O.S.<sup>1</sup>, Dmytrenko O.P.<sup>1</sup>, Kulish M.P.<sup>1</sup>,  
 Grabovskyy Yu.E.<sup>1</sup>, Zabolotnyy M. A.<sup>1</sup>, Mamunya E.P.<sup>2</sup>, Levchenko V.V.<sup>2</sup>,  
 Strelchuk V.V.<sup>3</sup>, Shlapatska V.V.<sup>4</sup>, Rugal' O.G.<sup>1</sup>.

<sup>1</sup>*Kyiv National Shevchenko University, Kyiv, Ukraine*

<sup>2</sup>*Institute of Macromolecular Chemistry NAS of Ukraine, Kyiv, Ukraine*

<sup>3</sup>*Institute of Semiconductor Physics NAS of Ukraine, Kyiv, Ukraine*

<sup>4</sup>*Pisarghevskiy Institute of Physical Chemistry of NAS of Ukraine, Kyiv, Ukraine*

Multi-walled carbon nanotubes are generally used for produce of polymer composites whereas they have high elastic properties and durability parameters. Such characteristics have only nanotubes with small concentration of structure defects. Moreover sencibilization of durability properties of composites is possible only at sufficient conjugation nanotude surface with polymer molecules.

In this work were observed crystal structure, vibrational spectra, micro hardness, resistivity, and luminescence of low-density polyethylene composites with nanotubes content of from 0, 1, 2,0 wt.% under high-energy electron irradiation ( $E_e = 1.8\text{MeV}$ ) and absorption dose 5 MRad.

It is shown the changes of optical and electrical properties of composites under irradiation. These changes in the spectral dependence of the Raman and photoluminescence, indicate a change in the vibrational and electronic structure of the composites as a result of doping carbon nanotubes and irradiation. Such changes are caused not only by conjugation of nanotubes with the polymer chains, and crosslinking of the macromolecules and the individual layers of nanotubes.

## Optimization of topological parameters of cold cathode based on ordered array of (9,9) carbon nanotubes with open ends

Pozdnyakov D, Borzdov A, Borzdov V

*Belarusian State University, Minsk, Belarus*

The topological parameters of cold cathode based on the array of (9,9) metallic single-wall armchair carbon nanotubes with open ends have been optimized for the case of room temperature. It was supposed that the nanotubes were placed on substrate with the metallic type of conductivity in square grid-type order.

In the first stage the height of nanotubes  $H$  has been optimized. Their height must be as large as possible on the one hand [1, 2]. On the other hand the strong electromechanical interaction takes place between very long nanotubes [3]. The interaction destroys the order [3]. It is ascertained by means of a number of estimations that the optimum height of (9,9) nanotubes  $H_{opt}$  amounts to 200 nm.

In the second stage the distance between the nanotubes  $S$  has been optimized. The optimization procedure is based on search of maximum of ratio of electric current density to electric field strength far from the cathode [1, 2]. Current density is calculated during a numerical solution of the Schrodinger equation after solving the Poisson equation. It is ascertained that the optimum distance between the nanotubes  $S_{opt}$  is equal to 500 nm. At that the cathode current density varies slightly for  $S$  in the range of values from 400 to 600 nm.

The obtained result confirms the estimations of Refs. [1, 2]. According to the estimations  $S_{opt}/H$  is in the range of values from 2 to 3.5.

1. Chen G. et al. Screening effects on field emission from arrays of (5,5) carbon nanotubes: quantum-mechanical simulations // *Phys. Rev. B.* – 2007 V.76, №19, – P. 195412-195417.
2. D. Kim, J. E. Bouree, S. Y. Kim. Numerical study on the field emission properties of aligned carbon nanotubes using the hybrid field enhancement scheme // *Appl. Phys. A.* – 2006 – V.83, P. 111–114.
3. N. Sinha et al. Electromechanical interactions in a carbon nanotube based thin film field emitting diode // *Nanotechnology*, – 2008 – V.19, №2. – P. 025701-1–12.

## Thermodynamics of native point defects in crystals of compounds $A^{IV}B^{VI}$

Prokopiv V.V.

*Vasyl Stefanyk PreCarpathian National University, Ivano-Frankivsk, Ukraine*

The basic electrical and photovoltaic properties of Lead Chalcogenides are defined by their point defects. Therefore an important task of material science is determinate the defect concentration, and establishing their influence on the crystal parameters. The method of thermodynamic potentials for calculation of crystals Lead Chalcogenides defect structure is proposed in this paper.

Equilibrium concentration of point defects in crystal by annealing two-temperature annealing determine from condition of equilibrium in the heterogeneous system at given pressure  $P$  and temperature  $T$ , which is the equality the chemical potentials of each component in all phases of system:

$$\mu_i^s = \mu_i^g, \quad \text{or} \quad dG_i^s / dN_i^s = dG_i^g / dN_i^g,$$

where  $G^s, N^s, G^g, N^g$  – Gibbs thermodynamic potentials and the concentration of particles in the crystal and gas, respectively,  $i - M, N$ .

Gibbs energy of crystal determine as:

$$G = U_0 + \sum (H + F_{vib})[D] + nE_C - pE_V - T(S_n + S_p + S_k)$$

where  $H$  – enthalpy of neutral defect formation,  $F_{vib}$  – free vibration energy of defect,  $[D]$  – defect concentration  $D$ ,  $n$  and  $p$  – electrons and holes concentration,  $E_C, E_V$  – energy of conductive band and valence band,  $S_k$  – configurational entropy,  $S_n$  and  $S_p$  – entropy of electron in the conductive band and entropy of holes in the valence band.

Chemical potential of defect was determined by differentiation of Gibbs energy on defect concentration.

$$\mu_{D_i}^s = H_i - kT \ln \left( \frac{J - \sum [D]}{[D_i]} \right) + \left[ n \left( \frac{E_C}{kT} - \ln \left( \frac{N_C - n}{n} \right) \right) + p \left( \frac{E_V}{kT} + \ln \left( \frac{N_V - p}{p} \right) \right) \right] \times \\ \times \frac{kT \cdot Z_i}{\sqrt{(\sum Z[D])^2 + 4N_C N_V \exp(-E_g / kT)}}$$

So, was receive a system of equations  $\pm \mu_{D_i}^s = \mu_i^g$  for finding of equilibrium concentration of defects.

Concentration of point defects was determined for  $V_M, V_N, M_i, N_i$ . Each of these defects can be has the three charge state: neutral, one, or double charged. So, we have system of twelve variables and solving that can receive depends of Hall concentration of the charge carriers and atomic defects from technology factors of two-temperature annealing (annealing temperature  $T$ , partial vapor pressure of component  $P$ ).

## Features of Phase Diagrams of Equilibrium and Imperfect Subsystem are a Cadmium, Lead and Tin Tellurides

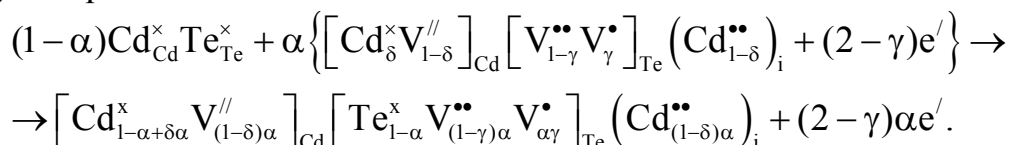
Prokopiv V.V. (Jr.)

*Vasyl Stefanyk PreCarpathion National University, Ivano-Frankivsk, Ukraine*

Cadmium, lead and tin tellurides belongs to compounds with noticeable deviation from stoichiometric. The change of composition within the homogenous area is conditioned of lattice defects, which determine by type of conductivity, concentration and carriers mobility, energy of radiate transitions and other electric and optical properties.

The area of existence of CdTe compound is asymmetric. For temperatures more small than 1000 K greater part of compound's homogenous area loafs surplus of Cd, and for temperatures more high 1000 K – displaced in the side of Te.

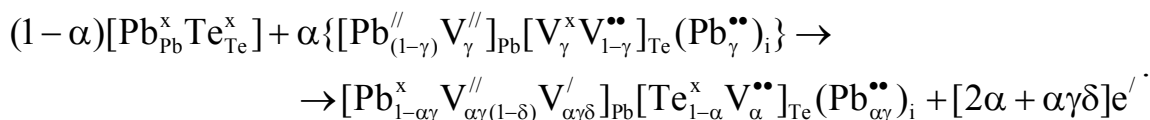
Crystal-quasichemical formula of n-CdTe:



For p-CdTe a crystal-quasichemical formula will be written down an analogical method.

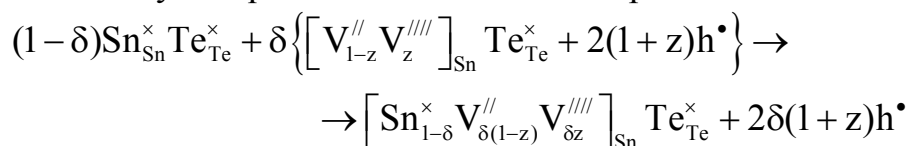
The analysis of Pb-Te phase diagram specifies in the presence of once compound of PbTe, which smelts congruent at temperature 1190 K. Maximum size of homogenous area of lead telluride is observed at temperature 1133 K and consist  $1,3 \cdot 10^{19}$  and  $6,3 \cdot 10^{18} \text{ cm}^{-3}$  for the superstoichiometrical atoms of tellurium and lead accordingly.

Crystal-quasichemical formula of n-PbTe (surplus of lead is within the homogenous area) taking into account disproportionation vacancies in cationic sublattice will be next:



Crystal-quasichemical presentation of unstoichiometrical p-PbTe is like set (surplus of tellurium is within the homogenous area).

In the Sn-Te system present one compound of SnTe that melt congruently at 1063 K. Area telluride lies the homogenous of tin fully on the side of tellurium surplus in relation to stoichiometrical composition and has maximal slowness from  $50.1 \pm 0.1$  to  $50.9 \pm 0.1\%$  of atomic maintenance of tellurium at 873 K. Crystal-quasichemical formula of p-SnTe will be written as follows:



## Constants of Equilibrium of The Quasichemical Reactions of Defects Creation in CdTe

Pysklynets U.M.

*Ivano-Frankivsk National Medical University, Ivano-Frankivsk, Ukraine*

The method of quasichemical reactions of defect formation is mostly used for prediction of material electric and physical characteristics. One of the most important problems is determination of equilibrium constants for quasichemical reactions. Equilibrium constants have been mainly determined by experimental method, which may lead to inaccuracy, especially when material contains some dominant defects with similar concentrations.

The current study represents a theoretical calculation of equilibrium constants for quasichemical defect formation reactions in CdTe, using the method of thermodynamic potentials [1]. It has been found analytical expressions to calculate equilibrium constants for reactions formation 8 point defect types in CdTe:  $V_{Cd}$ ,  $V_{Te}$ ,  $Cd_i$ ,  $Te_i$ . Each of these defects may be in once or doubly charged state.

The nature of point defects in the domain of p-n-transition has been investigated by the method of quasichemical reactions of defect formation with use of theoretically calculated, but not empirically determined, equilibrium constants for reactions of defect formation. Dependences of electron concentrations, holes and intrinsic point defects in undoped cadmium CdTe upon two-temperature annealing process variables have been formulated. Technological conditions for changing of dominant type free charge carriers in the material have been determined. Dependence of cadmium vapor pressure of thermodynamic p-n-transition upon annealing temperature has been calculated. It has been found satisfactory agreement of received results with previously published data. That proves acceptability of developed model.

Model for calculation of point defect structure and dependence of point defects concentration on selection of their parameters have been analyzed. The main advantage of usage of theoretically calculated constants is that parameters of point defects taken into calculation (energies of formation and ionization) are not model. It allows better understanding of the factors, which affect processes of defect formation, and more effective management in preparation of crystals with given beforehand properties.

1. Прокопів В.В., Горічок І.В., Писклинець У.М. Константи рівноваги квазіхімічних реакцій дефектоутворення в CdTe // Український хімічний журнал. – 2009. – Т. 73, № 6. – С. 77-80.

## Crystal, electronic structures and properties of TiNiSn semiconductor

Romaka V.A.<sup>1,2</sup>, Stadnyk Yu.<sup>3</sup>, Budgerak S.<sup>1</sup>, Romaka L.<sup>3</sup>, Horyn A.<sup>3</sup>

<sup>1</sup>National University "Lvivska Politechnika", Lviv, Ukraine

<sup>2</sup>Ya. Pidstryhach Institute for Applied Problems of Mechanics and Mathematics  
National Academy of Sciences of Ukraine, Lviv, Ukraine

<sup>3</sup>Ivan Franko National University of Lviv, Lviv, Ukraine

The well known best thermoelectric materials on this time are the highly doped semiconductors and semimetals. To such objects, among other, belong compounds of MgAgAs structure type, in particular, TiNiSn, ZrNiSn and HfNiSn phases.

Our previous researches on processes of introduction to ZrNiSn compound of atoms of Rare Earth metals, transition 3*d*- and 4*d*-metals, and also 5*p*-elements allowed to establish the mechanism of including of impurity atoms in the crystal structure of ZrNiSn, which, in end-point, determines its physical properties. It turned out that the most influential factors are nature of impurity atoms and their concentrations, and also peculiarities of ZrNiSn crystal structure, related to its imperfectness.

The crystal structure of TiNiSn compound was established by both powder and single-crystal methods. Phase and chemical compositions of samples were tested by means of scanning electron microscopy and microprobe analysis. The electronic structure modeling of TiNiSn was carried out as using of different methods of calculation so various variants of atoms location in the structure of compound. Electrokinetic researches of TiNiSn phase were carried out on single-crystals and polycrystalline samples. Experimental investigations confirmed correctness of results on electronic structure calculations of TiNiSn, which specified in the presence of the band gap and on the location of Fermi level near-by the conduction band. Measurement of magnetic susceptibility of *n*-TiNiSn showed that a semiconductor was Pauli paramagnet, and the magnetic susceptibility values had small changes with a temperature, representing the changes of density of states at the Fermi level.

The investigations on *n*-TiNiSn allowed determining the mechanism of "a priori doping" of semiconductor by donor impurities as result of imperfectness of its crystal structure. It's caused by partial, up to 0,5 at. %, occupying of Ti position by the Ni atoms and generation the structural defects of donor nature. Except that, for example of TiNiSn compound the method of optimization of crystal structure model on the basis of electronic structure results and physical properties of semiconductor was presented. The results allowed having predictable process of the high doping of *n*-TiNiSn for the receipt of maximal values of thermoelectric power factor.

## Optical properties of As-Sb-S-I amorphous films

Rubish V.M.<sup>1</sup>, Gera E.V.<sup>1</sup>, Pop M.M.<sup>2</sup>, Kozusenok O.V.<sup>2</sup>, Maryan V.M.<sup>1</sup>, Tarnaj A.A.<sup>1</sup>, Shtets P.P.<sup>1</sup>, Kyrylenko V.K.<sup>1</sup>, Durkot M.O.<sup>1</sup>.

<sup>1</sup>*Uzhgorod Scientific-Technological Center of the Institute for Information Recording, NASU, Uzhgorod, Ukraine*

<sup>2</sup>*Uzhgorod National University, Uzhgorod, Ukraine*

In this work the results of studying the influence of laser irradiation on transmission spectra of the  $(As_2S_3)_{47}(SbSI)_{53}$  have been adduced.

Thin films ( $d=1-2 \mu m$ ) were deposited by vacuum thermal evaporation of  $(As_2S_3)_{47}(SbSI)_{53}$  glasses from quasiclosed effusive cells on cool silica substrates. A uniform thickness of layers was provided by planetary rotation of substrates. Light exposure of films was made using defocused radiation of a semiconductor laser ( $\lambda=0,53 \mu m$ ,  $P_r=7, 31$  and  $100$  mW). Investigation of transmission spectra of the films was carried out at room temperature in wavelength range  $450-750$  nm by means of “МДР-23” spectrometer. The spectral resolution was no worse than  $10^{-3}$  eV.

The investigations have shown that with exposure time growing, absorption edge of films is shifting into long wave region of spectrum (Fig.) confirming the decrease of their pseudoforbidden width ( $E_g$ ) (Table).  $E_g$  was determined by extrapolation of dependences  $(\alpha \cdot hv)^{1/2} \sim f(hv)$  up to  $\alpha=0$  ( $\alpha$  is absorption coefficient).

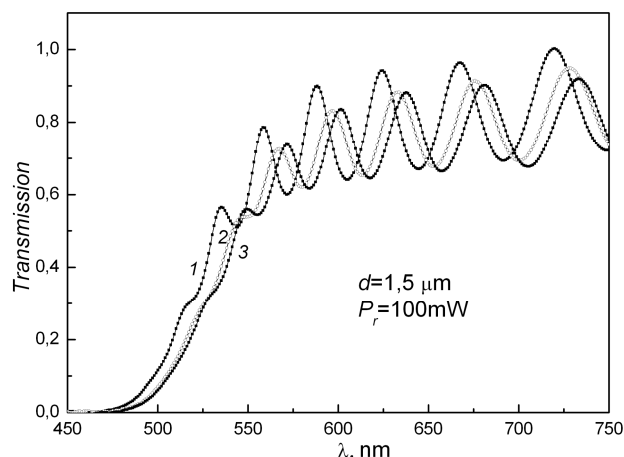


Fig. Dependences of transmission spectra as prepared  $(As_2S_3)_{47}(SbSI)_{53}$  films on exposure time: 1 – 0; 2 – 5; 3 – 20 s

Table

Values of  $E_g$  for  $(As_2S_3)_{47}(SbSI)_{53}$  films versus the exposure time

Parameter	Exposure time, s					
	0	5	10	20	40	90
$E_g$ , eV	2,250	2,216	2,204	2,196	2,192	2,190

The influence of film thickness and radiation power on the level of photoinduced changes of optical parameters of films is investigated.

## Formation of defects subsystem of films on the basis of IV-VI compounds

Saliy Ya.P.

*Vasyl Stefanyk Precarpathion National University, Ivano-Frankivsk*

The work is devoted to complex investigations of the kinetics of defects subsystem formation and electrical properties of films on the basis of IV-VI compounds. The kinetics of unstable crystal defects on the growth, annealing or by radiation influences is investigated both experimental, theoretical methods and the computer simulation of processes.

To study the structural and energetical parameters of the crystal and its defect subsystem by molecular – dynamics simulations it is necessary to define the interaction potentials and interacting structural particles. It is proposed the parameter  $K$  to determine the model of the potential – particle to investigate lead and tin chalcogenide crystals with the structure of NaCl. The influence of the central interatomic potential on formation of the stable structure: NaCl and BaF<sub>2</sub> have been investigated. The type of structures produced depends on the charge of ions.

The equilibrium concentrations of vacancies and interstitial metal atoms in PbSe films have been calculated as a function of the precipitation. on the basis of quasi-chemical reactions with a priori and posterior constants of the equilibrium of reactions and on the basis of electro-physical relations for the alone dominant singly charged defects. The band parameters of semiconductor films have been determined on the basis of experimental technological data. The crystal-chemical mechanisms of the atomic defects formation in PbTe thin films doped with In in the process of their growth from the vapour phase have been studied.

The spatial distribution of ionization and nuclear energy loss of  $\alpha$ -partical in IV-VI semiconductor are calculated. Effects on the temperature dependencies of electrical properties of n-type PbSe have been investigated. The carrier density in most cases increased due to the bombardment. Kinetic mechanism of electrical properties of p-type PbSe polycrystal films under  $\alpha$ -particle bombardment have been investigated. The carrier density  $p$  decreases and mobilities  $\mu^{-1}$  increases linear over  $\Phi^{1/2}$ ,  $\Phi$  is a dose of  $\alpha$ -particles. This behaviour are explained by a capture of interstitials on linear defects, that is dislocation and grain boundaries.

To define the characteristic relaxation time and the activation energy of migration processes of own unstable point defects in n - PbTe are used the approach of velocity quasi - chemical reactions theory and X-ray diffractometry data of isothermal annealing films on air. It is shown that the thickness distribution of the defect concentration and formation of the p-n -structure in isothermally vacuum-annealed thin PbS films of p-type can be explained both by the fast diffusion of sulphur interstitials, the low diffusions sulphur and lead vacancies and by the reactions between these defects.

A new model of the size effect description in thin polycrystalline semiconductor films was proposed to separate of the share of both one grain and grain surface electron scattering on size effect of. Simulation by cellular automata models of the epitaxial growth of films clusters and space correlations effects in the processes controlled by atom capture are considered. The influences of sink distribution upon the space distribution of immobile and mobile atoms and their capture rates have been studied.

## **Models of electrical conductivity diamond materials**

Samsonenko S.N., Samsonenko N.D.

*Donbass National Academy of Civil Engineering and Architecture,  
Makeyevka, Donetsk region, Ukraine*

Diamond is one of perspective materials of modern electronic technique. It possesses a wide spectrum of electronic properties which are caused by mainly structural defects. First of all them concern dislocation small-angle boundaries which general line is one-dimensional crystallography periodicity along axes of dislocations.

Because of a wide scatter of electric characteristics natural diamonds are not technological for application in the electronic technique.

Opening of methods of reception of synthetic diamonds at low pressures from methane-hydrogen of mix and at high pressures from a graphite or hydrocarbons stimulated interest to research of their electronic properties.

Electronic properties monocrystal homoepitaxial diamond films (HEDF), polycrystalline HEDF, polycrystalline diamond films (PDF) grown up on alien substrates and polycrystalline diamond compacts were investigated. It is established, that thin samples HEDF to 10  $\mu\text{m}$  are in the thickness monocrystal and have dislocation conductivity. Their specific resistance depends from density of the dislocations forming small-angle boundaries. Specific resistance of samples HEDF over 10  $\mu\text{m}$  does not depend in the thickness on density of dislocations. These samples are polycrystalline.

In them large-angle boundaries divide arbitrarily oriented mosaic crystallites with small-angle dislocation boundaries between mosaic blocks.

Dislocation conductivity is shown at their temperature researches electroconductivity. By us it is established, that in thin (4 ÷ 6  $\mu\text{m}$ ) texturing PDF grown up on alien substrates take place dislocation conductivity and hopping conductivity on large-angle to boundaries.

In polycrystalline diamond compacts which are formed at sintering of diamond particles under the big pressure, there is formation dislocation conductivity to sintering temperature  $\sim 2000^{\circ}\text{C}$ .

Thus, a basis of forming electronic properties of diamond materials is conditions of formation of diamond materials and a condition of their treatment.

## Thermodynamic theory of the phase separation in the non stoichiometric silicon oxide films

Sarikov A.V.

*V. Lashkarev Institute of Semiconductor Physics NAS Ukraine, Kiev, Ukraine*

Non stoichiometric silicon oxide films ( $\text{SiO}_x$ ,  $x < 2$ ) are perspective by their possible optoelectronic applications, which can be realized due to the phase separation in these films. Phase separation in non stoichiometric silicon oxide takes place at high temperatures and leads to the formation of amorphous or crystalline Si nano-inclusions capable of light emission, in the silicon oxide matrix.

The present work proposes a thermodynamic theory of phase separation process in the non stoichiometric silicon oxide films as a result of high temperature anneals. The expressions for the Gibbs free energy of the non stoichiometric silicon oxide as well as the silicon oxide in contact with the amorphous and the crystalline silicon phase are derived thermodynamically. The Gibbs free energy of amorphous Si / Si oxide and crystalline Si / Si oxide systems as a function of the relative concentration of separated silicon, the initial silicon oxide stoichiometry, and the temperature of anneals is studied. The phase separation process progresses itself toward the decrease of the Gibbs free energy of the systems under consideration down to the minimum value. The factors that promote and prevent the phase separation process in non stoichiometric silicon oxide films are investigated. The gain in the Gibbs free energy of the Si / Si oxide systems is obtained with the increase of the average oxidation degree (and thus the decrease of the penalty contribution to the Gibbs free energy) of Si–Si<sub>y</sub>O<sub>4–y</sub> complexes that build up the silicon oxide matrix. The phase separation in non stoichiometric silicon oxides is hindered by the configuration entropy resulted from the arrangement of oxygen atoms in the positions of Si–Si bonds of silicon oxide structure as well as by the silicon inclusions having the interfaces with silicon oxide surrounding. By minimization of the Gibbs free energy of systems under study, the equilibrium stoichiometries of silicon oxide as well as the solubility limits of silicon atoms in SiO<sub>2</sub> phase in contact with both amorphous and crystalline silicon are determined as functions of the initial silicon oxide stoichiometry and the annealing temperature. An especial attention is given to the strain appearing as a result of phase separation in non stoichiometric silicon oxide films. This strain refers to the factors preventing the phase separation in non stoichiometric silicon oxides and among all the factors has the maximum effect on the equilibrium state of the phase separated silicon oxide films. The account of strain contribution to the Gibbs free energy of Si / Si oxide systems has enabled to make a comprehensive description of the dependence of the equilibrium stoichiometry of phase separated silicon oxide films on the initial silicon oxide composition and the annealing temperature.

## Physical properties of $\text{CuInSe}_{2x}\text{S}_{2(1-x)}$ thin films

Shapoval P.<sup>1</sup>, Kusnezh V.<sup>2</sup>, Yatchyshyn J.<sup>1</sup>, Il'chuk G.<sup>2</sup>, Guminilovych R.<sup>1</sup>

<sup>1</sup>*Analytic Chemistry Department of Lviv Polytechnic National University, Lviv, Ukraine*

<sup>2</sup>*Physics Department of Lviv Polytechnic National University, Lviv, Ukraine*

The chemical bath deposition (CBD) of  $\text{CuInSe}_{2x}\text{S}_{2(1-x)}$  solid solution thin films is described. The technological conditions of chemical bath deposition and thermal annealing for  $\text{CuInSe}_{2x}\text{S}_{2(1-x)}$  semiconductor thin film fabrication were determined. The surface morphology, elemental composition and optical properties of films were investigated.

The film surface deposited at the Cu:In:Se = 1:1:3 volumetric ratio of the initial substances, at  $t = 60^{\circ}\text{C}$  changes from dendrites covered to densely packed by  $\text{CuInS}_{0,24}\text{Se}_{1,76} + \text{CuSe}$  crystallites with diameter 0.3-0.8 microns, with film bandgap  $E_g \approx 1.50$  eV. In case of  $t < 60^{\circ}\text{C}$  the film surface changes from packed by crystallites to covered by  $\text{CuInSe}_{2x}\text{S}_{2(1-x)}$  round lots, while  $E_g$  changes from 1.48 to 2.33 eV. The selenium was distributed in the film while the space between crystallites was filled with indium, and sulfur is evenly distributed over the samples area after annealing.

The surface of films obtained at the Cu:In:Se = 1:1:1.5 volumetric ratio of the initial substances at  $t = 60^{\circ}\text{C}$  changes from packed by crystallites to covered with blocks ( $E_g = 1.53$  eV). In case of  $t < 60^{\circ}\text{C}$  film surface changes from rarely covered by crystallites to rarely covered by dendrites.

Based on the bandgap value dependence on the selenium content in  $\text{CuInSe}_{2x}\text{S}_{2(1-x)}$  monocrystalline solid solution the empirical relationship  $E_g(\text{CuInSe}_{2x}\text{S}_{2(1-x)}) = 1,55 - x \cdot 0,52$ , where  $x$ - is atomic concentration of selenium, was derived. This dependence agrees with obtained results for different volumetric ratio of the initial substances of CBD  $\text{CuInSe}_{2x}\text{S}_{2(1-x)}$  semiconductor thin films.

## Size and temperature stability of liquid phase in Ge/Au layered film system

Sukhov R.V., Kryshtal A.P.

*V.N. Karazin Kharkiv National University, Svobody sq., 4, 61077, Kharkiv, Ukraine*

The eutectic melting is typical not only for highly refined systems, but also takes place at heating of an interface of two crystals forming eutectic system. Such melting at the temperature much lower than the melting temperature of both components is named “contact melting”. It is considered that the effect of the contact melting is not connected with the certain mass ratio of crystals contacting. At the same time recent theoretical works pointing to the possibility of the existence of the critical size in binary eutectic system below which the contact melting does not take place are known. Furthermore there is no common opinion about the mechanism of contact/eutectic melting. Therefore the aim of this work is the experimental study of size effects during contact melting in binary eutectic thin film systems.

The Ge/Au thin film system was chosen as the object under study. The components of this binary system form the “simple eutectic” phase diagram. The samples were prepared in high vacuum vessel by means of sequential thermal evaporation of the components from separate sources.

We revealed the critical thickness of contact melting in eutectic binary layered film systems Au-Ge by means of TEM and ED studies (i.e. the thickness of the first component film which is in contact with the thick film of the second component below which the formation of liquid phase does not take place at the eutectic temperature). The existence of critical thickness is in favour of the diffusion mechanism of contact melting phenomenon.

The dependence of the Ge-Au eutectic and freezing temperature on the thickness of film system of eutectic composition (0.3-60 nm) is determined by means of TEM studies. It is shown that the eutectic temperature and the degree of supercooling decrease with the reduction of film system thickness. Moreover, it was revealed that the formation of liquid phase in Au/Ge film system took place starting from ~120°C that is much lower than the eutectic point for bulk specimens.

The diagram describing the temperature and dimensional stability of the liquid phase in the eutectic binary film system Ge-Au is built. The obtained results are discussed in the framework of the diffusion mechanism of contact melting phenomenon and evolution of binary phase diagram with the reduction of the characteristic size of the components.

## Influence of technological parameters on characteristics of thin films

Suschenko O.N.<sup>1</sup>, Slusar T.V.<sup>1</sup>, Legkova G.V.<sup>1</sup>, Grebenshikov D.V.<sup>1</sup>,  
Gordienko S.O.<sup>2</sup>, Ermolenko V.M.<sup>3</sup>

<sup>1</sup>National Aviation University, Kiev

<sup>2</sup>Institute of Semiconductors Physics, NAS of Ukraine, Kiev

<sup>3</sup>G. V. Kurdyumov Institute of Institute of Metallophysics, NAS of Ukraine, Kiev

Thin (nanoscale) films have specific properties, which are uncharacteristic for macro objects. It determines actuality of research of thin-films in the field of nanotechnology.

Thin-films are extremely sensitive to physico-technological conditions. The primary purpose of this research is to examine influence of manufacturing conditions on characteristics of thin-films.

Thin-films of different thickness ( $37 \div 300$  nm) made of  $\text{Co}_2\text{CrGa}$  Heusler alloy and obtained by a flash-method on different substrates (glass, glassceramics, silicon, NaCl) have been researched in different technological conditions.

Electron probe microanalysis in the mode of secondary and reflected electrons revealed distinction of electronic images of thin-films deposited on different substrates (Fig.). It has been determined that technological parameters (type and temperature of the substrate) influence on the phase heterogeneity of the thin-films, and detected correlation between film thickness and size of phases.

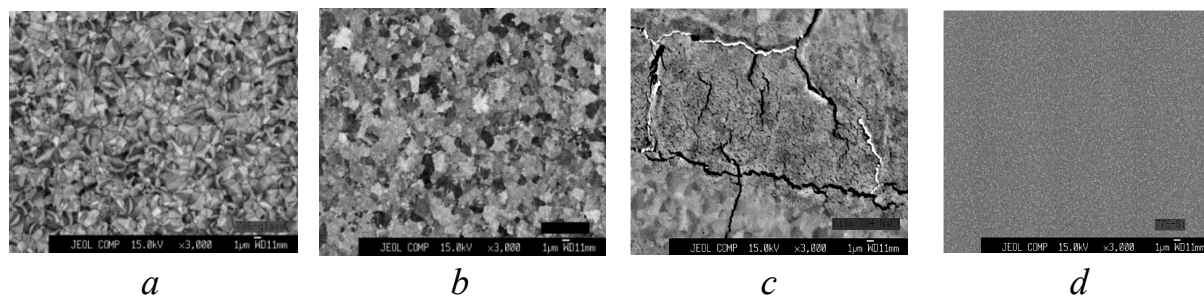


Fig.  $\text{Co}_2\text{CrGa}$  thin-film image in COMPO mode with increasing  $\times 3000$ :  
*a* – glass; *b* – glassceramics; *c* – Si; *d* – NaCl

A specific electrical resistance (SER) of the films has been determined by the two-probe method. The obtained value of SER is within the wide range: from  $16.3 \pm 0.4$  to  $64.6 \pm 0.3$  ( $\mu\Omega \cdot \text{m}$ ).

It has been established that the electrical characteristics are connected with thickness of the thin-films, as well as with presence (absence) of annealing, type and temperature of substrates.

It has been researched the temperature dependence of resistivity of thin-films and their magnetic behaviour. The results have been compared with the original bulk sample.

## Optical and operational properties of coatings based on complex fluorides and composites

Timukhin Ie.V.<sup>1</sup>, Zinchenko V.F.<sup>1</sup>, Mozkova O.V.<sup>2</sup>, Gorshtein B.A.<sup>2</sup>

<sup>1</sup>*A.V. Bogatsky Physico-Chemical Institute of NAS of Ukraine, Odesa, Ukraine*

<sup>2</sup>*State Enterprise for Special Instrument Making "Arsenal", Kyiv, Ukraine*

Fluorides of some metals are widely used in various branches of engineering, including film-forming materials to produce coatings with a low refractive index (from UV to mid-IR) in the interference optics. The significance of acid-base properties of inorganic compounds for the development and improvement of existing fluoride film-forming materials is discussed. Changes in the optical and operational properties of the coatings are due to the formation of complex compounds in the base material and the coating on its base, obtained by the thermal vacuum evaporation.

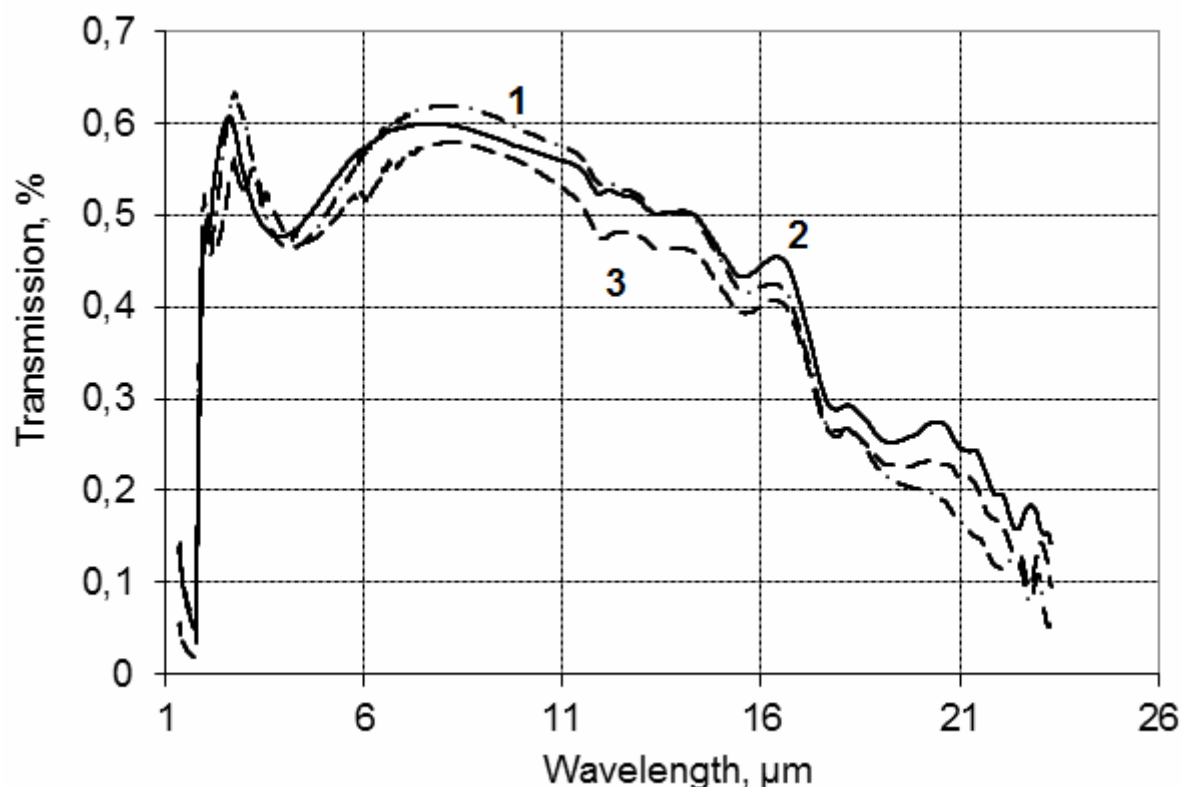


Figure - Spectral transmission characteristics in the infrared region of fluorides in thin-film coatings on the Ge substrates: 1 –  $\text{PbHfF}_6$ , 2 –  $\text{Ba}_2\text{MgF}_6$ , 3 –  $\text{YF}_3$

Being sufficiently enhanced, materials based on complex fluorides of magnesium, barium, hafnium and lead, differ significantly in their optical and operational characteristics (Figure, curves 1, 2) from those frequently used for infrared region (Figure, curve 3).

## Defect formation processes of Pb-Sn-Te thermoelectric material

Turovska L.V.

*Vasyl Stefanyk PreCarpathian National University, Ivano-Frankivsk, Ukraine*

IV-VI semiconductor compounds and their solid solutions are basic materials for thermoelectric energy converters which operate in the medium temperature area [1, 2]. Point defects and their complexes largely responsible for the physical and chemical properties of the material. At present there is no consensus about the nature of these defects and their charge states. Lead telluride has n-type conductivity with excess metal relative to stoichiometry and p-type conductivity with excess chalcogen [1].

The basis of the method of crystalquasichemical analysis is superposition of doping cluster formed on the basis of lead telluride antistructure, and the crystal formula of stoichiometric compound. Crystalquasichemical model of nonstoichiometric PbTe with a complex range of Frenkel defects ( $V_{Pb}^{2-}$ ,  $V_{Pb}^{-}$ ,  $V_{Te}^{2+}$ ,  $Pb_i^{2+}$ ,  $Te_i^0$ ), and based on them ternary systems have been offered. Dependences of concentration of point defects, electrons and holes, and the Hall concentration of current carriers on the size and nature of deviation from stoichiometry of n- and p-PbTe and solid solution composition have been calculated on the basis of the first developed crystalquasichemical formulas and equations of full electroneutrality. Thus hole conduction of lead telluride relates to a vacancy in cation sublattices  $V_{Pb}^{2-}$ ,  $V_{Pb}^{-}$ , and electronic – in anion sublattices  $V_{Te}^{2+}$  of lead telluride crystal structure. The influence of chemical composition and the deviation from stoichiometry on the side of tellurium on the ratio between doubly ( $V_M^{2-}$ ) and fourfold charged ( $V_M^{4-}$ ) cationic vacancies (dominant defects in this case) and thermoelectric properties of PbTe-SnTe solid solution have been specified. Complicated dependence of the spectrum of metal vacancies of  $Pb_{1-x}Sn_xTe$  solid solutions on the composition and size of deviation from stoichiometry on the side of tellurium significantly affects the entire range of thermoelectric properties of the material. In particular, considerable conductivity ( $\sigma$ ) is provided by high electrical activity of defects, which in our case associated with fourfold charged cationic vacancies  $V_M^{4-}$ .

Introduced crystalquasichemical approaches extend possibilities of scientific analysis of the defect subsystem in semiconductor crystals, and determine the technological aspects of managing their properties.

*This work to execute according department project (State registration № 0107U006768).*

1. Abrykosov N.Kh., Shalimova L.M. Semiconductors materials on the basis of  $A^{IV}B^{VI}$  compounds. – Science, Moscow. – 1975. – 196 p.
2. Ioffe A.F. Semiconductor thermoelements. – M.-H.: Publishing House of USSR Academy of Sciences. – 1960. – 346 p.

## Influence of Iron Impurities on Optical Properties of ZnSe:Fe Films and Layers

Vaksman Yu.F., Nitsuk Yu.A., Yatsun V.V.

*I.I. Mechnikov National University, Odessa, Ukraine*

During the last years, II-VI semiconductors doped with transition metal ions are actively investigated. It is conditioned by their wide application as active media and gates in lasers of medium infrared (IR) radiation range. Thus, most works are devoted to research of optical properties in the IR-region of spectrum. At the same time, to research of high-energy transitions in the transition elements ions was spared not enough attention. The purpose of this study is establishment of iron impurity influencing on optical absorption and luminescence of films and crystalline layers ZnSe in the visible region of spectrum.

For research ZnSe single crystals obtained by free growth method was used [1]. The crystals were doped via diffusion of impurity from metal powderlike Fe in He + Ar atmosphere at temperatures 1120-1320K during 10-30hours. ZnSe:Fe films were obtained by vacuum deposition on the warmed-up quartz substrates. Crushed ZnSe:Fe crystals with high iron concentration were used as a source.

Displacement of absorption edge ZnSe:Fe toward lower energies at increasing concentrations of doping impurities is established. It allowed to show that iron impurities concentrations in the explored films and layers was varied from  $10^{16}$  to  $10^{18}$  cm<sup>-3</sup>.

The structure of optical absorption and luminescence spectra in the spectral region 400-750nm is explored. The presence of identical lines in absorption and luminescence spectra of ZnSe:Fe films and layers is established. The luminescence excitation conditions for which it is possible to observe ZnSe:Fe blue-green emission was determined.

It is shown that spectral position of most absorption and emission lines does not depend on concentration of iron and temperature of measurements. It testifies to the presence of optical transitions within the limits of local center.

Comparison of optical absorption and luminescence spectra with results of calculations [2] of the Fe<sup>2+</sup> ions energy spectrum in the ZnSe crystals is executed. It allowed to identify optical transitions which predetermine the absorption and luminescence lines in ZnSe:Fe.

The results of researches allow to characterize high-energy optical transitions in the limits of the Fe<sup>2+</sup> ion in ZnSe:Fe films and layers.

1. Korostelin Yu.V., Kozlovsky V.I., Nasibov A.S., Shapkin P.V. Vapor growth and characterization of bulk ZnSe single crystals // J.Cryst.Growth. – 1996.–16 l. – P.51-59.
2. Zunger A. 3d-transition atom impurities in semiconductors // Solid State Physics.–1986.– 39. – P.276-474.

## Thermal conductivity measurement of $V_2VI_3$ thin films

Virt I.S.<sup>1,3</sup>, Rudyj I.O.<sup>2</sup>, Kurilo I.V.<sup>2</sup>, Lopatynskiy I.Ye.<sup>2</sup>, Dubov Yu.G.<sup>4</sup>

<sup>1</sup> *Drogobych State Pedagogical University, Drogobych, Ukraine*

<sup>2</sup> *National University "Lviv Polytechnic", Lviv, Ukraine*

<sup>3</sup> *University of Rzeszow, Institute of Physics, Rzeszow, Poland*

<sup>4</sup> *Ivan Franko National University of L'viv, Lviv, Ukraine*

Lead telluride and its alloys have been known to be the most efficient thermoelectric materials for power generation in the temperature range 300–800 K. Thin films based on  $Bi_2Te_3$  and  $Sb_2Te_3$  semiconductor compounds are also widespread enough materials for the thermoelectric devices due to their high coefficient of thermoelectric transformation  $Z$ . In particular,  $Bi_2Te_3$  presently is known as the best thermoelectric material. Because of the tendency of miniaturization of thermo-electric devices, it is necessary to study not only the properties of standard bulk materials but also their properties in thin films based on these alloys.

In the given work we studied thin films  $Bi_2Te_3$  and  $Sb_2Te_3$  deposited by YAG:Nd laser in a vacuum on warmed-up 200–300 °C substrates  $Al_2O_3$  and Si. The three omega method generally proceeds by applying an alternating current of frequency  $\omega$  through a metal heater line that has been directly deposited on an electrically insulating sample. This current heats the sample at a frequency of  $2\omega$  due to Joule heating, producing temperature oscillations also at a frequency of  $2\omega$  with an amplitude, say,  $\Delta T_{2\omega}$  and phase difference. Since the resistance of pure metals increases linearly with temperature, the temperature oscillations introduce resistance oscillations in the metal line at a frequency of  $2\omega$ . The resistance oscillations at  $2\omega$ , with the source current at frequency  $\omega$ , generate a small oscillating voltage signal across the metal line at  $3\omega$ . The amplitude of the  $3\omega$  voltage  $V_{3\omega}$  is given in terms of the voltage amplitude at the first harmonic,  $V_\omega$ , by  $V_{3\omega} = \frac{1}{2} I_0 R_0 \alpha \Delta T_{2\omega} = \frac{1}{2} V_\omega \alpha \Delta T_{2\omega}$ . In this work the voltages were measured using a lock-in amplifier UNIPAN which operates over a wide range of frequencies 1 Hz– $10^2$  kHz. The third harmonic voltages at a specified temperature were measured by performing a logarithmic frequency sweep typically from 50 Hz to 10 kHz. Finally, the thermal conductivity of the sample was evaluated by measuring the frequency dependence of the temperature rise. Comparison with known values of thermal conductivity measurements of  $Bi_2Te_3$ ,  $Bi_2Se_3$ ,  $Sb_2Te_3$  obtained on bulk materials at room temperature with thin films shows some difference, which is likely a result of differences in processing techniques.

## Thermoelectric properties of nanostructures compounds IV-VI

Yurchyshyn I.K.,

*Vasyl Stefanyk Precarpathian National University, Ivano-Frankivsk, Ukraine*

Development and research of low-dimensional thermoelectric materials can be combined in three different directions: the creation of quantum dots (QD), nanowires (NW) and quantum wells (QW) superlattices. Revealed that in such systems it have place physical phenomena that create additional opportunities for independent variation of Seebeck coefficient ( $S$ ), electro- ( $\sigma$ ) and thermal conductivity ( $\chi$ ) to increase the value of material thermoelectric figure of merit  $Z = S^2\sigma/\chi$ .

The paper presents an analysis of new approaches to improve thermoelectric parameters of nanostructures on the basis of compounds IV-VI.

Revealed that dimensionless thermoelectric figure of merit  $ZT$  of materials based on quantum dots superlattices PbTe/PbSnSe/PbTe reaches value  $ZT = 2$  at 300 K by a sharp decrease in lattice thermal conductivity of more than 4 times compared to the bulk material of the same composition [1].

Also, it was made calculations of kinetic parameters for nanowires superlattice, which had to occur in heterostructures, composed of different lead chalcogenides. In this case,  $ZT$  value reaches  $\sim 8$  (n-PbSe/PbTe) [2]. However, practically, such structures have not been created.

Theoretical analysis  $ZT$  of QWSL PbTe/Pb<sub>1-x</sub>Eu<sub>x</sub>Te allowed to receive its highest value  $ZT \approx 1.4$  for the QW thickness  $\sim 20$  Å with orientation (100) when carrier concentration  $n = 10^{19}$  cm<sup>-3</sup> and  $T = 300$  K [3].

Basing on the model of rectangular quantum well with infinitely high walls, the dependences of thermoelectric parameters on nanostructure thickness for lead chalcogenides (PbTe, PbSe, PbS) were studied. Shown that in such structures it have place nonmonotonous, oscillation dependence of Seebeck coefficient  $S$  on the nanostructure thickness. On basis of experimental oscillations period  $\Delta d_{\text{exp}}$  it was done the approximation of theoretical dependencies for Seebeck coefficient  $S$  with experimental data. This value  $\Delta d_{\text{exp}}$  defines the Fermi energy in respective structures.

*This work is partially financed by State Fund of Fundamental Researches of State Agency for Science, Innovation and Information of Ukraine (State registration № 0110U007676).*

1. Harman T.C., Walsh M.P., LaForge B.E., Turner G.W. Nanostructured thermoelectric materials // J. of Electronic Mater. – 2005. – V.34. – №5 – L19L22.
2. Yu-Ming Lin, M.S. Dresselhaus Thermoelectric properties of superlattice nanowires // Physical Review B – 2003 – V. 68 – 075304.
3. Casian A., Sur I., Scherrer H., Dashevsky Z. Thermoelectric properties of PbTe/PbEuTe quantum wells // Phys. Rev. B. – 2000 – V.61 – P. 15965-15974.

## Hyper sensibility of the dissipative structures and self-organizing processes in gradient non-crystalline materials based on glass-like Ge<sub>2</sub>S<sub>3</sub>

Yurcovitch N.V, Mar'yan M.I.

*Uzhgorod National University, Uzhgorod, Ukraine*

At considerable deviations of the system from the state of equilibrium or considerable external fields a determining role in forming of equipping with modern amenities, creation and storage of functional organization is played by synergetic effects and mechanisms of transformation energy. Approach to consideration of non-crystalline solids, which is based on the account of processes self-organization and formation of dissipative structures with the different level of the spatial-temporal ordering with modern amenities, is on the initial stage of development. A main place is occupied by tasks, related to development and receipt of non-crystalline semiconductor materials with structurally sensible properties and different level of necessity of the spatial or spatial-temporal (functional) ordering with modern amenities.

In this report theoretical and experimental researches of hyper sensibility of dissipative structures are presented consisting of non-crystalline semiconductors with the set division of concentration of modifier on the thickness of tape on the basis of glassy Ge<sub>2</sub>S<sub>3</sub>. The dynamics of running the number of particles is considered component of modifier of the system  $N_{\text{mod}}$  at the action of source  $G$  of atomic stream in the process of during time  $\tau_p$ . The atomic stream of particles changes in course of time after a certain law which can be varied (the exponential law of change is examined in this case):  $G = g_{\text{source}} \cdot \exp(-mz)$ , where  $g_{\text{source}}, m$  are constants of source of particles. Experimentally the atomic stream of modifier on the thickness of tape is described expression:

$$G_N = 3.513 \cdot 10^{22} \frac{a_1 P_e}{\sqrt{M_e T_e}} [cm^{-2} \cdot c^{-1}]. \quad (1)$$

Here  $P_e$  is pressure,  $a_1$  is coefficient evaporation,  $M_e$  is molecular weight,  $T_e$  is a temperature of evaporation. The technological parameters of receipt of the modified structures (speed of condensation, temperature of evaporation, thickness) are certain. This approach enables, being based on the unique physical principle, to describe forming of non-crystalline materials, their structure and features of co-operating with external factors at presence of self-organizing processes. Grounded possibility of receipt of hyper sensibility of dissipative structures of non-crystalline materials, got through the self-organizing processes, and development on the indicated phenomenon of new approach to forming of recordings environments, developments sensory devices.

## Electrochemical hydrogen sorption of carbon nanosize materials

Zhyllinski V. V.<sup>1</sup>, Drozdovich V. B.<sup>1</sup>, Zharski I. M.<sup>1</sup>, Zhdanok S.A.<sup>2</sup>

<sup>1</sup>*Belarussian State Technological University, Minsk, Belarus*

<sup>2</sup>*A. V. Lyekov Heat- and Mass Transfer Institute of National Academy of Sciences of Belarus, Minsk, Belarus*

One of the potential applications of hydrogen storage technology is high-power electrochemical accumulators which have high efficiency irrespective of their power. Furthermore, the quick charge of these accumulators can be made with use traditional power supplies or renewed sources of energy. The electrochemically reversible accumulation of hydrogen assumes to use new carbon nanosize materials which should have high sorption capacity by hydrogen [1].

The carbon nanosize materials (CNMs) were obtained by ultrasonic division of aqua dispersion of total carbon mass that had been synthesized by electro arc method from methane-air mix in A. V. Lyekov Heat and Mass Transfer Institute of NAS of Belarus. The investigated CNMs were obtained from aqua suspension of the carbon mass which had been stable in ultrasonic field. Such CNMs were black powder with bulk density up to  $0.2 \text{ g} \cdot \text{cm}^3$ , consisting of amorphous carbon (less than 30 %) and multiwall carbon nanotubes with diameter 10-40 nm and length 100-500 nm.

The part of CNMs was been activated by electrochemical reversible potentiastatic proceeding in concentrated sulphuric acid as result significant oxidation of CNMs[1]. The electrochemical hydrogen sorption capacity of initial and activated CNMs was investigated by discharge method of C, CNMs | 1 M  $\text{H}_2\text{SO}_4$  |  $\text{O}_2$ ,  $\text{PbO}_2$ , (Pb) at work on constant loading.

The hydrogen sorption capacity of CNMs achieved 0.3 wt. % of hydrogen for initial carbon material whereas capacity of activated CNMs was increased up 0.8 wt. % of hydrogen. It may be pointed out that the CNMs activated in concentrated sulphuric acid have more significant concentration of hydrogen-adsorption center (structure deficiency, inoculation of functional groups, implantation of heteroatoms) than that concentration in initial CNMs.

Moreover the activated CNMs had maximum charge-discharge currents in 1 M  $\text{H}_2\text{SO}_4$  which were reached  $1.5 \text{ A} \cdot \text{g}^{-1}$  that was more 3 times than the charge-discharge currents of the initial CNMs in 1 M  $\text{H}_2\text{SO}_4$ . It was pointed out to decrease of diffusion limitations of hydrogen transfer in deep structures of activated CNMs in spite of the introduction polar oxygen contented groups.

1. V.V. Zhyllinski, V.B. Drozdovich, S.A. Zhdanok, A.V. Krauklis Possibility of using activated CNM in electrochemical energy accumulation devices. *Electrochemical Technologies and Materials for XXI Century: Abstracts of 9th International Frumkin Symposium* Eds. A. Yu. Tsivadze, IPCE, Moscow. – 2010. – P. 145.

## Crystal model of point defects and physical and chemical properties of semiconductor crystals of ZnS

Zlomanov V.P.<sup>1</sup>, Freik N.D.<sup>2</sup>

<sup>1</sup>*M.V. Lomonosov Moscow State University, Moscow, Russia;*

<sup>2</sup>*Vasyl Stefanyk Precarpathian National University, Ivano-Frankivsk, Ukraine*

Zinc Sulphide is difficult for interpretation of the prevailing defects and their charge condition due to the peculiarities of the crystal structure and nonstoichiometry. Thus, in particular, the quantitative ratio between various types of defects that would allow to identify the dependence of physical-chemical properties on their concentration, is not found.

On the basis of the crystalquasichemical models has been made the analysis of defect subsystem and found out their influence on the physical-chemical characteristics of zinc sulphide. In contrast to ordinary simplified chemical formula ZnS, the obtained crystalquasichemical formula defines the range of point defects, which determine n-type of zinc sulfide crystals' conductivity, and therefore provides more complete information about its defective subsystem. Thus, in particular, for n-ZnS crystalloquasichemical formula will look like:

$$(Zn_{\gamma\alpha+1-\alpha}^{\times} V_{\alpha(1-\gamma)}^{//})_{Zn} (S_{(1-\alpha)}^{\times} V_{\alpha}^{\bullet\bullet})_S (Zn_{\alpha(1-\gamma)(1-\delta)}^{\bullet} Zn_{\alpha\delta(1-\gamma)}^{\bullet\bullet})_i + \alpha(\gamma + \delta - \delta\gamma + 1)e'$$

Here  $Zn_{Zn}^{\times}$ ,  $S_S^{\times}$  – zinc and sulfur in the knots of the crystal lattice,  $V_{Zn}^{//}$  – two-charged zinc vacancies,  $V_S^{\bullet}$  – one-charged sulfur vacancies,  $Zn_i^{\bullet}$  – one-charged internodal atoms of zinc,  $Zn_i^{\bullet\bullet}$  – two-charged internodal tellurium atoms,  $\alpha$  – molar part of the doping component,  $e'$  – electron concentration, “•”, “/”, “×” – positive, negative and neutral charges.

From the obtained crystalquasichemical formulas one can determine not only the prevailing types of the point defects, but also dependence of their concentration on the chemical composition - stoichiometry deviation values ( $\alpha$ ,  $\beta$ ), content of doping elements (Zn, S) accordingly. Thus, in particular, for n-ZnS crystals with sulfur vacancies' dominant defects ( $V_S^{\bullet\bullet}$ ) and interstitial atoms of zinc ( $Zn_i^{\bullet}$ ,  $Zn_i^{\bullet\bullet}$ ), with increasing deviation from stoichiometry ( $\alpha$ ), the augmentation of all types of point defects and charge carriers takes place.

The obtained two-dimensional diagrams “concentration of defects (charge carriers) - chemical composition” are determined by the technological factors (conditions of annealing), which provide obtainment of the crystals with preset properties.

1. Абрикосов Н.Х., Банкина В.Ф., Порецкая Л.В. // Полупроводниковые халькогениды и сплавы на их основе. – Наука, М. – 219 с. – 1975.
2. Межиловська Л.Й., Бабуцак Г.Я., Фреїк Н.Д., Шашко Н.В., І.Й. Перкатиюк. Кристалохімічні моделі точкових дефектів і фізико-хімічні властивості напівпровідникових кристалів ZnS // Фізика і хімія твердого тіла – 2008. –Т.9, №2. – С. 280-285.

**СЕКЦІЯ 3 (стендові доповіді)  
ФІЗИКО-ХІМІЧНІ ВЛАСТИВОСТІ ПЛІВОК  
ТА НАНОСТРУКТУР**

19 травня 2011 р.

**SESSION 3 (poster)  
NANOTECHNOLOGIES AND NANOMATERIALS,  
QUANTUM-SIZE STRUCTURES**

May, 19, 2011

## Molecular oxygen adsorption on $\text{Ge}_x\text{Si}_{1-x}/\text{Si}(001)$ surface

Afanasieva T., Grinchuck O., Koval I., Nakhodkin M.

*Taras Shevchenko National University of Kiev, Kiev, Ukraine*

The oxidation of SiGe alloys has been investigated for both fundamental and technological reason. It can be useful as the fabrication process for the gate oxide of SiGe channel metal-oxide field effect transistors (MOSFETs), which have higher carrier mobility than Si channel MOSFETs [1]. The first step of GeSi oxide formation is molecular oxygen adsorption on  $\text{Ge}_x\text{Si}_{1-x}/\text{Si}(001)$  surface. We consider molecular oxygen adsorption on perfect Ge, Si and mixed Si-Ge addimers of  $\text{Ge}_x\text{Si}_{1-x}/\text{Si}(001)$  surface.

Ab initio calculations were performed by using spin Restricted Open shell Hartree – Fock calculation (ROHF). The 3-21G(p, d) basis set was employed for Si, Ge, O and H atoms. The calculation was performed with GAMESS package [2].  $\text{O}_2\text{Ge}_2\text{Si}_{10}\text{H}_4/\text{O}_2\text{Ge}_2\text{Si}_{32}\text{H}_{32}$  ( (quantum mechanics)/(molecular mechanic)) cluster and SIMOMM (Surface Integrated Molecular Orbital Molecular Mechanic) [3] calculation scheme was used to investigate molecular oxygen adsorption on  $\text{Ge}_x\text{Si}_{1-x}/\text{Si}(001)$  interface. We perform optimization of two subsurface layer atoms, and O atoms position to establish oxygen molecular adsorption barrier.

The most chemical active part of  $\text{Ge}_x\text{Si}_{1-x}/\text{Si}(001)$  are addimers, due to their dangling bonds, therefore we consider molecular oxygen adsorption on perfect Si, Ge and mixed Si-Ge addimers of  $\text{Ge}_x\text{Si}_{1-x}/\text{Si}(001)$  interface. We find that there is no molecular oxygen adsorption barrier in case of perfect Si and mixed Si-Ge addimers of  $\text{Ge}_x\text{Si}_{1-x}/\text{Si}(001)$  surface. In case of perfect Ge addimers on Si(001) surface molecular oxygen adsorption barrier was 0.07 eV. This result is in agreement with experimental data [4].

Most energetic favorable spin state of  $\text{Ge}_x\text{Si}_{1-x}/\text{Si}(001)$  surface with adsorbed O molecule is singlet. While most energetic favorable spin state of  $\text{Ge}_x\text{Si}_{1-x}/\text{Si}(001)$  surface with oxygen molecule that haven't adsorbed yet is triplet. Hence we can conclude that molecular oxygen adsorption on  $\text{Ge}_x\text{Si}_{1-x}/\text{Si}(001)$  surface is accompanied by spin conversion from triplet to singlet state. Also we have to note that there is no energy barrier for such spin conversion.

1. LeGouse F.K., et al. // J. Appl. Phys. –1989.– 65.– P. 1724 .
2. Schmidt M.W., et al. // J. Comput. Chem. – 1993. – 14. – P. 1347.
3. Shoemaker J.R., et.al. // M. S. J. Phys. Chem. A – 1999. – 103. – P. 3245.
4. Fukuda T.T., et al. // Surf. Sci. –1997. –380. – P. 469-473.

## **Ab initio calculations of IR spectra in identification of stable and metastable structures of Bi addimer on the Si(001)2x1**

Afanasieva T.V., Koval I.F., Nakhodkin N.G.

*Taras Shevchenko National University of Kiev, Kiev, Ukraine*

The understanding of kinetics and energetics of adatoms and small clusters that diffuse over the Si(001) surface has broad implications for the development of microscopic models for epitaxial growth and for the fabrication of nanostructures such as quantum dots and nanowires. Recent STM study suggests that the stable sites for an isolated Bi dimer on Si(001) surface are the A and B-configuration [1]. The activation energy for A-B rotation has been estimated to be 0.87 eV [1]. The aim of this work is detailed study of stable and metastable structures of the Bi dimer using high level quantum chemistry calculation.

Density-functional theory (DFT) and multireference theory (CASSCF) calculations of vibrational spectra of the A, B stable and A/B metastable structures of Bi addimer on Si(001) surface were performed. CASSCF calculations were performed by using SIMOMM method.

The optimal pathways for A $\leftrightarrow$ B transformations through metastable A/B configuration have been found for each singlet and triplet potential energy surfaces (PESs) using B3LYP/SBK\*\* and CASSCF(10,10)/SBK\*\* methods. Configurations of A, B dimer were found to be not minima on triplet PES. Intermediate A/B configuration had been found minimum on triplet PES, only. A and B dimers are initially in their ground (singlet) electronic states. TS1 and TS2 configurations were found to be the transition states for singlet and triplet PESs, respectively. TS2 saddle point energy on triplet PES less than TS1 saddle point energy on singlet PES. So, during Bi dimer rotation on the Si(001) surface, intermediate A/B and TS configurations (saddle point region) have diradical character. The energy barrier for Bi dimer rotation has estimated to be 0.9 eV for A $\rightarrow$ B transformations, in good agreement with the STM data [1]. Calculated infrared spectra suggest the possibility to experimentally distinguish between A, B stable and metastable A/B structural configurations with different multiplicity.

1. Bulavenko S.Yu., et al. // Surf. Sci. – 2001. – 482-485. – P. 370.

## Growth and Characterization of Thermoelectric Lead Telluride

Ahiska R.<sup>2</sup>, Freik A.<sup>1</sup>, Gorichok I.<sup>1</sup>, Nykyruy L.<sup>1</sup>

<sup>1</sup>*Vasyl Stefanyk PreCarpathian National University, Ivano-Frankivsk, Ukraine*

<sup>2</sup>*Gazi University, Ankara, Turkey*

Lead telluride has been largely studied as thermoelectricity and thermoelectric materials due to various reasons. As regards to material science, to the fore come the issues of the search for new connections with high thermoelectric qualities, which appears to be a complicated task; or the development of special technological processes with the purpose of their improvement in materials which are already well-known and well-established in practice.

An excellent thermoelectric material exhibits a large dimensionless figure of merit, the so-called ZT value, defined by  $Z = S^2 / \rho k = S^2 \sigma / k$  where S is the Seebeck coefficient (thermal power),  $\sigma$  is the electrical conductivity, T is the absolute temperature, and k is the thermal conductivity.

We receive that materials which are synthesized from stoichiometric composition and lead-excess have the electronic conductivity, while the tellurium-excess materials have the hole conductivity. The absolute value of Seebeck coefficient for p-PbTe is significantly higher than (2-2.5 times) n-PbTe, also from the stoichiometric composition is higher than (1.2-1.5 times) the lead-excess material at 570 K. The differences in absolute values of Seebeck coefficient for n-PbTe and p-PbTe are determined by the peculiarities of the band structure and the transfer nature of the carriers (electrons or holes), as well as by their effective mass.

Depending of the Seebeck coefficient ( $\alpha$ ) with  $\Delta T$  is determined by the chemical composition of the samples. Thus, in the samples obtained by the synthesis of components of the stoichiometric composition, Seebeck coefficient proportionally changes with increasing  $\Delta T$  for all powder fractions. In case of the deviation from the stoichiometric composition, both lead-excess and tellurium-excess, properties appear which possess opposite characteristics. Such difference can be explained either by activation processes or by possible segregation of redundant components which are not detected by an X-ray method and accumulated at the grain boundaries. The temperature raise leads to increase in conductivity, which is the cause of the decrease in the S magnitude.

We receive, that value of Seebeck coefficient is significantly affected by the magnitude of powder fractions and compaction pressure. It should be noted that the maximum value of  $S_{\max}$  is obtained from the powder fractions 0.8-1.0 mm in size at pressures 0.75-1.0 GPa. Small fractions (i.e. 0.0-0.6 mm) and low pressures (i.e. 0.5 GPa) correspond to the lowest values of Seebeck coefficient. The decrease in the number of material particles and material porosity bring about decrease of Seebeck coefficient. Definitely first of them is more effective.

The obtained values of Seebeck coefficient of thermoelectric PbTe p-type are significantly greater than concerning electronic material. In this article also represents the models of the thermoelectric defect subsystem for n-PbTe and p-PbTe within the scope of crystallochemical formalism.

*This work is partially financed by State Fund of Fundamental Researches of State Agency for Science, Innovation and Information of Ukraine (State registration № 0110U007675).*

## Quantum-chemical study of H<sub>2</sub>O molecules adsorption on the graphene

Ananina Olga, Yanovsky Olexandr and Severina Olena

Zaporizhzhya National University, Zaporizhzhya, Ukraine

Graphite and its such a two-dimensional form as graphene, in particular, is of great interest today. Basically, this interest is caused by the unique physical and chemical properties of these materials.

The goal of this work is to study the H<sub>2</sub>O adsorption on a graphene layer. We examine the different orientation of the H<sub>2</sub>O molecule with respect to graphene surface: the H atoms (O-H bonds) pointing up, down and parallel to the graphene surface above three positions. We find that the binding energy differences are 16-22 meV with respect to the orientation.

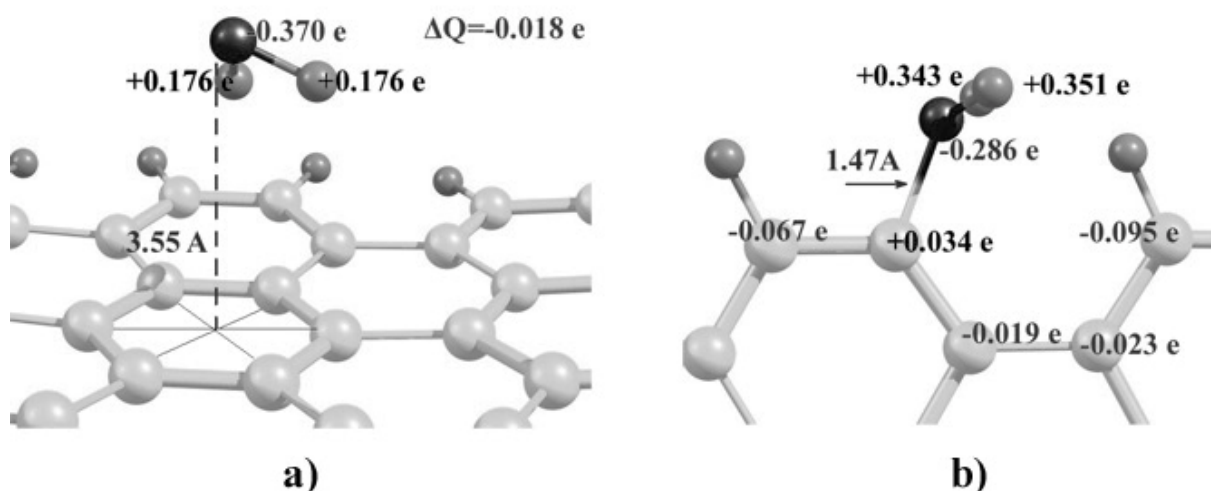


Fig. 1. H<sub>2</sub>O on graphene: a) H<sub>2</sub>O molecule above the surface; b) H<sub>2</sub>O chemisorption on the edge.

The most stable configuration shows on fig. 1. The H<sub>2</sub>O molecule is above the center of carbon hexagon. There is a small charge transfer from the surface to molecule of 0.018 e in this state. The adsorption (binding) energy for H<sub>2</sub>O molecule is 57.2 meV indicating a physisorption.

The adsorption energy (E), the charge transfer from the H<sub>2</sub>O to graphene, the distance of H<sub>2</sub>O from graphene surface (d) for two different geometries (fig. 1)

H <sub>2</sub> O	E, meV	ΔQ, e	d, Å
above the surface	57.2	-0.018	3.55
on the edge	1.41 eV	+0.412	1.47

The adsorption (binding) energy for H<sub>2</sub>O molecule on the edge (dangling-bond defect) is 1.41 eV indicating chemisorptions.

## **The concentration and field dependence of the corrosion of steel thin films in acidic medium under a constant magnetic field**

Andreeva A.F., Kasumov A.M., Vlasenko N.A., Goncharenko Y.V.

*Frantsevich Institute for Problems of Materials Science National Academy of Sciences of Ukraine, Kyiv, Ukraine*

The emergence in recent decades, a variety of mobile devices (phones, computers, cameras, etc.) has led to problems associated with their corrosion. Since these devices are fabricated using thin film technology, corrosion, primarily causes the damages of thin-film conductors and components. Features of the corrosion of such objects in mobile devices are: the dependence of corrosion parameters from the film thickness and the influence of the magnetic field generated by currents flowing in the conductors. In this work the corrosion of mild steel thin films ВСТ3СП in aqueous HCl solution under constant magnetic field was considered. The dependence of this process from a solution concentration and a magnetic field was studied.

It was found that at low solution concentration ( $C = 0.01\%$  vol.), when the corrosion process is close to the stationary, the magnitude and sign of the electrode potential of the films were close to the value of standard electrode potential of iron ( $V_{\text{Fe}}^{\circ}_{\text{reversive}} = -0.44$  v at the  $\text{Fe}^{2+}$  ion's participation in the corrosion process. At larger concentration up to  $C = 1\%$  vol. began the intensive interaction between the films and solution with a release of gas bubbles. In this case the potential's decrease up to  $V = -0.28$ v and corrosion current to 0 were observed. This decline may be caused by a breach of steady motion of ions in the electrolyte during stormy dissolution of the film and the release of gas bubbles.

When the magnetic field increases from 0.5 to 3 mT at solution concentration  $C = 0.01\%$  vol., the corrosion rate decreases by more than 2 times, that is useful to protect the mobile devices. The reducing of corrosion rate can be caused by the influence of the Lorentz force, which deflects the motion of the charges in the film and solution. At a further increasing of induction to 30 mT the growth of corrosion rate was observed. This is apparently due to increased magnetohydrodynamic flow, facilitated the transport of ions in the electrolyte.

## **Spin polarization of electrons in nanoscale films of magnetite Fe<sub>3</sub>O<sub>4</sub>**

Andreeva A.F., Kasumov A.M., Khrinovsky V.Z., Karavaeva V.M.

*Frantsevich Institute for Problems of Materials Science National Academy of Sciences of Ukraine, Kyiv, Ukraine*

Magnetite Fe<sub>3</sub>O<sub>4</sub> by combining a number of remarkable properties (100% - spin polarization of electrons at the Fermi level, high Curie temperature - 858 K, accessible technology in the manufacture of thin films) is a promising material for applications in spintronics. [1] However, these opportunities are limited by surface defects, reducing the polarization. [2]

In this paper, we consider the nanostructure Cu/Fe<sub>3</sub>O<sub>4</sub>/Y<sub>2</sub>O<sub>3</sub>/Fe<sub>3</sub>O<sub>4</sub>/Cu, consisting of polycrystalline Fe<sub>3</sub>O<sub>4</sub> semimetal layers and amorphous dielectric Y<sub>2</sub>O<sub>3</sub>, enclosed between the Cu - electrodes. A high polarization of electron spins in semimetal Fe<sub>3</sub>O<sub>4</sub> layers up to 95,7% was obtained at direct current operating, and up to 93,6% at alternative current. This is close to the maximum possible value of magnetite. A large value of spin polarization was obtained through the use of mutual screening of Cu - electrodes magnetic fields from each other.

The direct and inverse tunneling magnetoresistance effects were observed in this nanostructure at the work on dc and ac currents.

1. Šliwžiene K. Growth and investigation of magnetite thin films and heterostructures. // Summary of doctoral dissertation, Vilnius University, Vilnius, 2006.
2. De-Teresa J.M., Fert A., Contour J.P., Montaigne F., Seneor P. Role of metal-oxide interface in determining the spin polarization of magnetic tunnel junctions. // Science. – 1999. – V. 286, № 5439. – P. 507-509.

## Cathodoluminescence of thin oxide films for full-colored Flat Panel Displays (FPD)

Antonyuk V.G., Dovga I.V., Bordun I.O.

*Ivan Franko Lviv National University, Lviv, Ukraine*

Cathodoluminescence (CL) emission and excitation spectrums of thin oxide polycrystalline films  $Y_2O_3:Eu$ ,  $Zn_2SiO_4:Mn$ ,  $Y_2SiO_5:Ce$ ,  $Zn_2SiO_4:Ti$  were investigated. Films were achieved by radio-frequency (RF) ion-plasmas evaporation. Films thickness was 0.3 – 1.0  $\mu m$ .

$Y_2O_3:Eu$  films luminescence spectrum has narrow emission bands which were caused by intracenter transition between electron shells in border of activator ion.

Maximum wavelength of emission ( $\lambda_{max} = 613$  nm) corresponds to red light of radiation in optical range. CL spectrums of the other films makes wide emission band with maximums at 445 nm for  $Zn_2SiO_4:Ti$ , 390 nm for  $Y_2SiO_5:Ce$  and 525 nm for  $Zn_2SiO_4:Mn$ . It corresponds to blue ( $Zn_2SiO_4:Ti$ ,  $Y_2SiO_5:Ce$ ) and green ( $Zn_2SiO_4:Mn$ ) colors of emission. Achieved findings indicate fitness of this films for forming color displays, particularly for FPD.

CL intensity dependence of radiation dose was also investigated. Radiation dose was set by radiation time. Was determined that CL intensity dependence of radiation time has a good approximation as shown below [1]:

$$I = I_0 \exp(-\alpha C \sqrt{Et}),$$

where  $\alpha$  is a constant of ultraviolet optical absorption,  $C$  is a constant,  $E$  is an intensity of bombarding electron flux. Such approximation with  $U = 5$  keV and excite current density  $j = 25 \mu A/cm^2$  for  $Y_2O_3:Eu$  films indicates  $\alpha C \sqrt{E} = 9.63 \cdot 10^{-3} \text{ min}^{-1/2}$ , for  $Zn_2SiO_4:Mn$  films –  $5.4 \cdot 10^{-3} \text{ min}^{-1/2}$ , for  $Y_2SiO_5:Ce$  films –  $0.027 \text{ min}^{-1/2}$  and for  $Zn_2SiO_4:Ti$  –  $0.036 \text{ min}^{-1/2}$ .

Was determined that most stable to electron radiation effects  $Y_2O_3:Eu$  films up to 150 min and  $Zn_2SiO_4:Mn$  films after 150 min of irradiation with electron beam current  $50 \mu A$ .

1. W. Lehmann // J. Electrochem. Soc. – 1983. – №130. – P. 426-429.

## Quantum-chemical modeling of the oxidation process of ethylene glycol to glyoxal on nanocatalysts of the Cu group

Balabai R., Chernikova H.

*Krivoi Rog State Pedagogical University, Krivoi Rog, Ukraine*

Nanocatalysts are attractive objects for fundamental studies in the field of catalysis. The interconnected study of the structure of the catalytic active material, the chemisorptions phenomena, the kinetics and the mechanism of the catalytic processes is an obligatory stage to optimization of catalyst. Significantly, one can tailor the properties of nanocatalysts and thus improve their performance in a variety of applications by controlling their size, shape, composition, and porosity. Studies demonstrated the relationship between the catalytic activity and the particle morphology: that is, the more open the particle morphology is and the thinner the wall is, and the higher the catalytic activity will be than small solid nanoparticles.

In our research we used ab-initio calculations in the framework of the electron density functional theory and the pseudopotential on the author's program code to examine the electron structure of the reagents which participate in the process of the oxidation of ethylene glycol to glyoxal with the catalytic active centre (Cu, Ag or Au nanocage), the energetic profiles for the main routes of the conversion of ethylene glycol. On base of the conceptions about the mechanism of the syntheses of the glyoxal by the ethylene glycol oxidation on Cu (Ag or Au) this mechanism can be described by the definite set of reactions. The first reaction of this process is:  $(\text{CH}_2\text{OH})_2 + 2\text{Z} = \text{Z}_2((\text{CH}_2\text{OH})_2)$ , where Z – the active centre of the catalyst surface,  $\text{Z}_2((\text{CH}_2\text{OH})_2)$  – the two-centre adsorption of ethylene glycol. The atomic basis of the primitive tetragonal cell of the super lattice created the wall of the Cu nanocage and the adsorption molecules and/or intermediates. As a result of the calculation there is determined the energy of the ground state, the electron density distributions, as well as place on the Cu surface for the most preferred for the molecules adsorption (Fig. 1, 1 reaction).

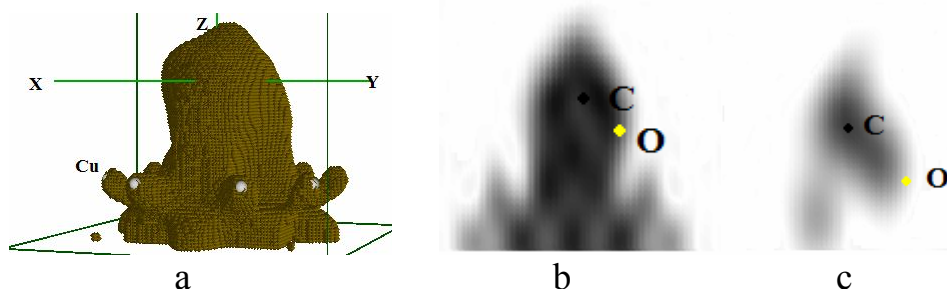


Fig. 1. The space valence electron density distribution for the atomic composite of the wall of Cu nanocage and the adsorption molecule of ethylene glycol (density from 0.6 to 0.7 from of the maximum value) (a); the (110) section of the space valence electron density distribution: (b) for atomic composite; (c) for single molecule of ethylene glycol.

## Electronic properties of strained CdTe and ZnTe layers in heterostructure

Balabai R., Pisklonov S.

*Krivoi Rog State Pedagogical University, Krivoi Rog, Ukraine*

The strained heterostructures CdTe/ZnTe (with continuous layers and layers of quantum dots) attracted significant attention the last ten years because of interesting physical characteristic and possibilities of their use in electronic devices [1]. The elastic strains, appearing because of unbalance of the lattice constants of CdTe ( $a = 6.48 \text{ \AA}$ ) and ZnTe ( $a = 6.1 \text{ \AA}$ ) (6.2%), cause shifts of the energy electronic states. The mechanism of the shaping of self-assembled semiconductors II-VI (for example, CdSe) quantum dots deposited on ZnSe was investigated on a series of samples grown by molecular beam epitaxy, with CdSe coverage from 0.5 to 2.6 monolayers in work [2]. Their results indicated a coexistence of 2D CdSe platelets and 3D islands showing that the platelets act as precursors for the formation of 3D islands.

In our research we used ab-initio calculations in the framework of the electron density functional theory and the pseudopotential on the author's program code to examine the evolution the electron structure of the compressed 2 monolayers (1 monolayer =  $3.05 \text{ \AA}$ ) CdTe film between the ZnTe layers on 4 monolayers, of the stretched 2 monolayers (1 monolayer =  $3.24 \text{ \AA}$ ) ZnTe film between the CdTe layers on 4 monolayers, of the assembled CdTe quantum dots in ZnTe matrices. The atomic basis of the primitive tetragonal cell of the super lattice consisted of the 10 monolayers of CdTe and ZnTe films. As a result of the calculation there is determined the energy of the ground state, the electron density distributions and electronic specters (Fig. 1).

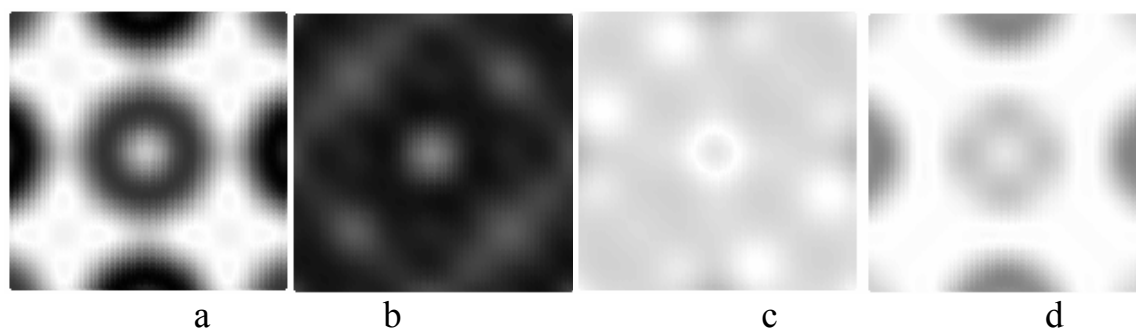


Fig. 1. The along heterostructures section of the space valence electron density distribution: (a) near Cd atom of no strained layer; (b) near Cd atom of compressed layer; (c) near Zn atom of no strained layer; (d) near Zn atom of stretched layer.

1. Кучеренко И.В. и др. // ФТТ. – 2009. – Т. 51, №. 11. – С. 2236.
1. Mackowski S. at all. // Phys. Rev. B. – 2004.– V. 69. – P. 205325.

**Kinetics of photo-induced transformations  
in amorphous As<sub>2</sub>S<sub>3</sub> thin films  
described in a framework of configuration-coordinate model**

Balitska V.O.<sup>1,2</sup>, Shpotyuk O.I.<sup>1</sup>

<sup>1</sup> *Scientific Research Company "Carat", Lviv, Ukraine*

<sup>2</sup> *Lviv State University of Vital Function Safety, Lviv, Ukraine*

The universal algorithm to describe complex effects of externally-induced influence in amorphous chalcogenide films (AChF) was developed. Within this algorithm, all possible defects states in AChF are characterized by energy connected with some geometric figures like to parabola or its different modifications with character configuration coordinate.

The first element of configuration-coordinate diagram (CCD), a so-called ground or initial state, represents itself as multi-well quasi-parabola, the deepest parabolic state corresponding to most stable atomic equilibrium within glass-forming network and can be satisfied owing to prolonged physical ageing. The second element of CCD state can be presented by single parabola with wide-stretched edges in accordance to strong electron-phonon coupling proper to covalent-bonded AChF networks. This state is single-well, despite a variety of external influences, which can be applied to AChF. Only vertical photoinduced Franck-Condon-type transitions are possible from ground state to metastable state and vice versa. The third element of CCD can be presented by parabola, which split to three quasi-parabola in accordance to different types of AChF defects, the first quasi-parabola corresponds to conjugate pair (CP) of under-coordinated defects known as IVAP (the intimate valence alternative pairs), while the second quasi-parabola corresponds to pairs of under-over-coordinated defects. The third elements of CCD corresponded to random defect pairs (alternatively, valence alternate pairs – VAP). Due to small potential barrier between excited and metastable states the glass matrix can relax from excited state in all metastable states.

As it follows from results of mathematical modeling, the stretched-exponential relaxation function is proper for all photoinduced kinetics in AChF films. This behavior tends towards single exponential in thinner films characterized by small structural dispersion (due to preference of *in-situ* photoinduced activation in the total balance of processes occurred). Within CCD, this photoinduced *in-situ* process corresponds to transition of carries from ground into excited state.

## Effect of cooling rate on mechanical properties and fine structure parameters of Pb-Sn-Ca alloys

Bashev V.F.<sup>1</sup>, Ivanov V.A.<sup>2</sup>, Litvin B.N.<sup>1</sup>, Sergeev G.A.<sup>1</sup>, Burdimova A.V.<sup>1</sup>  
Gudzenko V.N.<sup>1</sup>

<sup>1</sup>*Dnipropetrovsk National University name of O. Gonchara, Dnipropetrovsk, Ukraine;*

<sup>2</sup>*Institute of Transport Systems and Technologies NAS of Ukraine, Dnipropetrovsk, Ukraine*

In the lead-acid batteries high requirements are presented for mechanical properties of grids, which are designed to provide high performance batteries and reliability of their work. In the process of battery life grids are subjected to vibration and oscillating loads during charge-discharge of the active material in the grid cell. In this regard, battery grid must have high mechanical strength. There are two industrial Pb-Sn-Ca alloy compositions (wt.%): Pb-0.05Ca-1.1Sn - for positive grid and Pb-0.01Ca-0.3Sn – for negative grid which are rolled into strip with a thickness up to 750 microns. In the present work it was investigated the effect of cooling rate to improve the strength properties.

Three groups of samples were investigated: rolled industrial alloys casted with a cooling rate about 10 K/s; the cast alloy samples received by casting the melt to a form with a different cooling rate of about  $10^2$ ,  $10^5$  K/s and the samples with maximum cooling rate ( $\sim 10^6$  K/s) received during splat-cooling of melt between two rotating forming rolls (thickness of obtained films was about 100  $\mu\text{m}$ ). Changes in strength properties was estimated from the change in microhardness fully aged alloy samples PbCa0.05Sn1.1 and PbCa0.1Sn0.3, as well as the parameters of the fine-structure – the size of coherent scattering and the magnitude of microstresses.

As a result, in present investigations was found differences in the strength of rolled industrial samples (microhardness of PbCa0.05Sn1.1 alloy is on 18% higher than the microhardness of PbCa0.1Sn0.3 alloy). In samples of alloys, casted with a cooling rate of  $10^2$ - $10^6$  K/s was found significant increase of microhardness. Thus, samples of PbCa0.05Sn1.1 and PbCa0.1Sn0.3 alloys, casted with a cooling rate of about  $10^6$  K/s becomes the microhardness of 40% and 65% higher than similar rolled industrial samples respectively.

It was found differences in the dependences of alloys microhardness, which correlated well with the results of the fine structure parameters. The performance of changes in microhardness of PbCa0.1Sn0.3 alloy on the cooling rate suggests the possibility of beginning the alloy softening process caused by the decomposition of the supersaturated solid lead solution casted at the cooling rate of more than  $10^6$  K/s, with was confirmed by the changes in the level of microstresses.

The results shows a promising possibility of strength properties improving of industrial Pb-Sn-Ca alloys by increasing the cooling rate during crystallization.

## Investigation of electrophysical properties and magnetoresistance in three-layered film systems based on Al and Ni

Basov A.G.<sup>1</sup>, Dekhtyaruk L.V.<sup>2</sup>, Chornous A.M.<sup>1</sup>, Shkurdoda Yu.O.<sup>3</sup>

<sup>1</sup>*Sumy State University, Sumy, Ukraine*

<sup>2</sup>*Kharkiv State Technical University of Building and Architecture, Kharkiv, Ukraine*

<sup>3</sup>*Sumy State Pedagogical University, Sumy, Ukraine*

Using the modified model of Mayadas and Shatzkes [1], a general and asymptotic relations for the three-layer resistivity of polycrystalline metal films (sandwiches) was received. Based on the received relation, the dependence of resistivity of polycrystalline films on the thickness of the upper layer  $d_3$ , under the condition that the base layer thickness  $d_1$  and  $d_2$  layer remain unchanged, was theoretically analyzed.

It is shown that the size dependence of metal sandwiches resistance with polycrystalline structure is significantly different from similar expressions for homogeneous polycrystalline films.

In the small thickness of the covering layer the numeric value of the resistivity is determined by the nature of interaction of charge from the external boundaries and interfaces of conductor. With increasing thickness of the covering layer depends on  $\rho(d_3)$  there is a maximum, which is due to diffuse scattering of electrons sandwich boundaries, as with increasing of the mirror passage of charge carriers in adjacent layers of metal, maximum is degenerate resistivity monotonically is changing with increasing thickness of the sample.

The proposed model was conducted in the case of Ni/Al/Ni, the layers of which are monoblock in thickness. The thickness of the layer covering them ranged from 5 to 150 nm, and the base layer and layer thickness were 20 nm.

Depending on the experimental  $r(d_3)$  at the upper layer thickness  $d_3 < 30$  nm weakly expressed maximum is observed, which coincides qualitatively with the calculated curve.

Comparison of experimental and calculated values of resistivity of polycrystalline sandwich shows that they agree to within 20%

In all investigated samples based on Ni ( $d_{Ni} = 10-50$  nm) hysteresis of magnetoresistance of cyclical variations in magnetic field is observed. The positive longitudinal magnetoresistance effect (resistance increases with external magnetic field of application) is observed regardless of the thickness of layers in the samples, which is a sign of the anisotropic magnetoresistance.

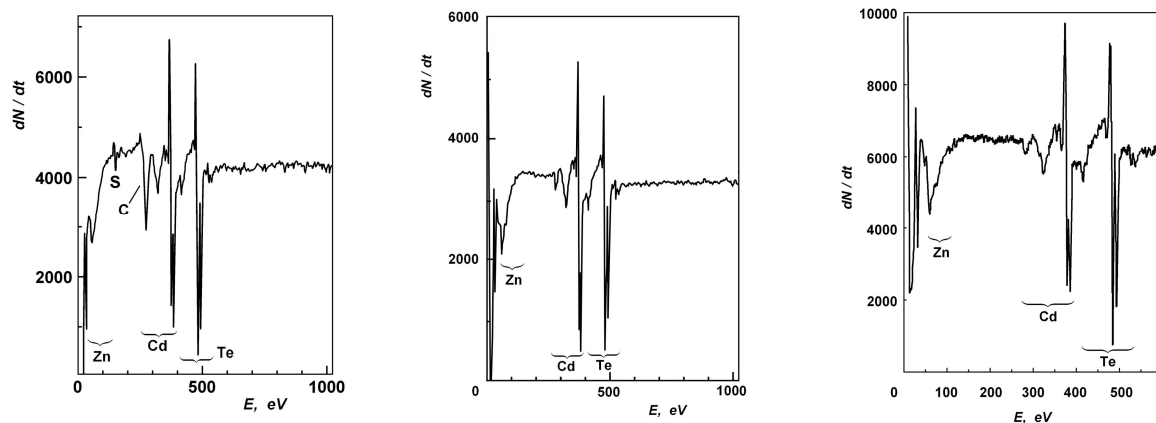
1. Mayadas A.F., Shatzkes M. Electrical-resistivity model for polycrystalline films: the case of arbitrary reflection at external surfaces // Phys. Rev. B. – 1970. – V. 1, №4. – P. 1382-1389.

## Auger spectroscopy of $\text{Cd}_{1-x}\text{Zn}_x\text{Te}$ LPE-grown epilayers

Beketov G.V., Rashkovetskyi L.V.

*V.E. Lashkaryov Institute of Semiconductor Physics, NAS of Ukraine, Kyiv, Ukraine*

Auger spectroscopic data of as-grown,  $\text{Ar}^+$  - sputtered and cleaved surfaces of  $\text{Cd}_{1-x}\text{Zn}_x\text{Te}$  ( $x < 0.15$ ) epitaxial layers are presented. The layers were grown using low-temperature ( $T = 500\text{-}600^\circ\text{C}$ ) liquid-phase epitaxy (LPE) from Te-rich melt on CdTe (111) substrates. Measurements were performed using JAMP-10S Auger spectrometer. Analysis depth was  $\sim 2$  nm, the probe diameter 1 to 10  $\mu\text{m}$ . Characteristic spectra are shown in figs a – c.



a – as-grown surface

b –  $\text{Ar}^+$ , 20 min

c – cleavage surface

Auger lines Zn MVV, Cd  $\text{M}_{45}\text{N}_{45}\text{N}_{45}$  (378, 386 eV), and Te  $\text{M}_4\text{N}_{45}\text{N}_{45}$  (484.5, 493.5 eV) were present in all spectra. For the as-grown surface, lines S LMM ( $\sim 150$  eV) and C KLL ( $\sim 270$  eV) were also observed, the last one being overlapped with the component of Cd Auger lines. The O KLL line ( $\sim 510$  eV), that normally should be seen on the samples without ion sputtering, possibly has been shaded by the Te 493.5 eV line.

After ion sputtering ( $\text{Ar}^+$ , 20 min), both S and C lines disappeared, indicating removal of surface contaminations.

Spectrum from the cleavage surfaces was essentially identical to the spectrum after ion sputtering, except the Zn MVV line shape. The difference possibly resulted from the change in the surface composition during ion sputtering. No lines of typical impurities (alkali metals, Fe, Si, Se) were observed, indicating high purity of the epilayers grown.

The absence of extrinsic and intrinsic defects has been confirmed by low-temperature ( $T = 5$  K) photoluminescence study, where only narrow peaks of bound excitons were observed, without any sign of the A-centers line.

## Quantum electron transport in ultra thin Cu films

Bihun R.I, Buchkovska M.V., Stasyuk Z.V.

*Ivan Franco Lviv national university, Lviv, Ukraine*

Properties of ultrathin slabs can essentially differ from properties concerning thick layers which are used in nowadays engineering. This difference first of all is caused by prevailing influence of the surface phenomena on ultrathin layer structure and electric parameters. The ultrathin electrically continuous metal film deposition on dielectric substrate surface is a problem of considerable difficulty due to the action of surface tension forces. The use of preliminarily deposited on a dielectric substrate surfactant underlayers of superficially active substances of a subatom thickness prevailing coagulation of metal condensates in other effective way of  $d_c$  decrease was in.

The residual resistivity  $\rho_{res}$  size dependences data of Cu film and Cu film deposited on Ge surfactant underlayers using the available quantum theories of size effects in metal films were investigated. It was found that the predictions of the model of Tesanovic [1], Trivedi-Ashcroft [2] and mSXW [3] have good agreement with experimental data. Those models allow as to predict the average amplitude of thin electrically continues metal film surface asperities in QSE region of charge transport. Those results have good agreement with our direct STM and AFM experimental data.

1. Tesanovic Z. // Solid State Phys. – 1987.– V.20, №6. – P. L829-L834.
2. Trivedi N., Ashcroft N.W. // Phys. Rev. B38. – 1988. – V.4, №17. – P. 12298-12309.
3. Fishman G., Calecki D. // Phys. Rev. Lett. – 1989. – V.62, №11. – P. 1302-1305.
4. Sheng L., Xing D.Y., Wang Z.D. // Phys. Rev. B. – 1995. – V.51, №11. – P. 7325-7328.

## **Size Effect in Optical Properties of Thin Metallic Au Films**

Bihun R.I., Stasyuk Z.V., Kravchenko O.E., Koltun N.S.

*Ivan Franco Lviv national university, Lviv, Ukraine*

Thin-film materials, in particular, metal films are used widely in modern technologies including electronics. The investigation of electrical and optical properties of ultrathin Ag, Au and Cu films are important for development of modern micro and nanoelectronics.

The influence of size effect on optical transmission and reflection spectra (200-2000 nm) of continuous Au films in 5-25 nm thickness range was investigated. The optical transmission and reflection were measured by double-beam spectrophotometer Shimadzu UV-3600. All measurements were carried out at room temperature. The gold films were deposited on cooled quartz optical glass at  $T = 100$  K at pressure of residual gasses  $P \leq 10^{-4}$  Pa. This thin metal film preparation technique allows produce the electrically continuous gold films up to 5 nm. The film thermostabilization was carried out by low-temperature annealing at  $T \leq 293$  K.

The anomalous behavior of transmission and reflection parameters were observed between 15-21 nm for Au film. The high frequency conductivity for visible optical spectra were calculated in the framework of classical size effect theories. The agreement between theoretical and experimental dependences were obtained [1,2].

1. Dryzek J., Czapla A. // *Phy. Rev. Letter.* – 1987.– V. 58, №7. – P. 721-724.
1. Fahsold G., Priebe A., Magg N. // *Thin Solid Films.* – 2003.– V. 428, – P. 107-110.

## Magnetoresistance and magnetothermo-power in $\text{Bi}_{1-x}\text{Sb}_x$ wires near the gapless state

Bodiul P., Moloshnik E., Popov I., Curoshu N.

*Institute of Electronic Engineering and Industrial Technologies, AS of Moldova*

As one of the interesting specific features of the transition of a substance into the gapless state, we should mention the increase in current carrier mobility, which is a characteristic that shows to what extent the carrier velocity in the electric field of a specified intensity varies. The theoretical analysis made by [1] shows that the disappearance of the energy gap between the bands,  $E_g$ , is accompanied by a significant increase in mobility; herein, the gapless state corresponds to the mobility maximum; while moving from the state with  $E_g = 0$  the current mobility decreases.

In present work was studied specific features of the thermopower and resistance as a function of temperature, magnetic field, and diameter of Bi-6at%Sb and Bi-8at%Sb wires near the gapless state. Glass-coated single-crystal wires with diameters (0.2-5  $\mu\text{m}$ ) were obtained by the liquid phase casting [2]. Fig. 1 shows the transverse field dependences residual magnetoresistance (a) and magnetothermopower (b) of a Bi-6%Sb wire at different temperatures.

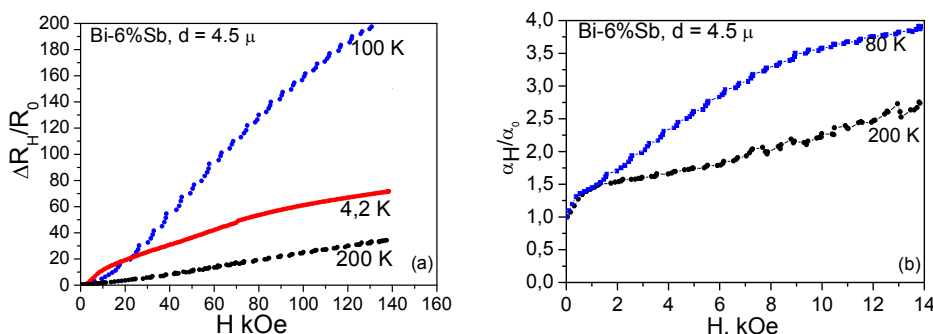


Fig. 1

At a temperature of  $\sim 100$  K a significant increase in the resistance  $R(H)$  (up to 20 000% at  $H = 14$  T) is observed. A shift toward lower ( $T < 80$  K) and higher ( $T > 140$  K) temperatures leads to the suppression of a giant increase in the magnetoresistance. In the range 90-100 K the thermopower increases by a factor of 4, achieving a value of 400-450  $\mu\text{V/K}$ . The effect is interpreted in terms of the substance transition into the gapless state.

This work was supported by SCOPES IZ73ZO \_ 127968 "Functional nano-wires" and Ukrainian project 10.820.05.08.UF.

1. Abrikosov A.A., Falkovskiy A.A. // Sov. Phys. JETP. – 1962. – V. 43, № 3, P. 1089.
2. D. Gitsu, L. Konopko, A. Nikolaeva, and T. Huber. // J. Applied Physics Letters. – 2005. – V. 86. – P. 10210.

## The morphology of non-percolated silver films

Bolesta I.M., Borodchuk A.V., Kushnir O.O.

*Ivan Franko National University of Lviv, Lviv, Ukraine*

Ultra-thin silver film were obtained by thermal evaporation of metal on glass substrates in vacuum of  $10^{-6}$  Torr. Mass thickness of films was controlled during deposition using a quartz resonator. In various manufacturing cycles were deposited films with different mass thickness  $d_m$ , in the range  $\sim 1-10$  nm, whose may be considered as metal-dielectric composites.

The topology of  $A_g$  was films studied with atomic-force microscope Solver PRO47 semicontact mode using a 100-micron scanner probes with radius  $\sim 10$  nm.

Fractal dimension of metal phase  $D_f$  was calculated by counting boxes method. The value of fractal dimension films determined averaging the corresponding quantities for at least four windows scanning with accuracy better than 3%. For the investigated range of thicknesses of mass fractal dimension is in the range 1.31..1.35 and linearly depends on the  $d_m$ .

To evaluate the geometry of the particles in a plane parallel to the substrate particles were determined by the length  $L$  - as the greatest distance between two elements of the image that corresponds to one cluster, and the equivalent diameter  $d = \sqrt{4S/\pi}$  - diameter of circle with area  $S$ , which corresponds to the square of the cluster. For values of  $L$  and  $S$  can be estimated width of the cluster  $l$ , considering it a form of elliptical, with the ratio  $l = 4S / \pi L$ .

The metal clusters with are formed in the first stages of growth of the films, are characterized by ellipsoidal shape. Dimensions of axes  $2a$  and  $2b$  were determined from the cut of the image with plane  $z = const$ , they coincide with the length  $L$  of the particle and width  $l$ , respectively. Averaged over ensemble of clusters the value of these parameters for films  $d_m=1.1$  nm is  $L = 46$  nm and  $l = 27$  nm. Size third axis of the ellipsoid coincides with the height of particles relative to the substrate and is  $2c = H = 30$  nm. Accordingly, the ratio between the axes  $a:b:c \approx 1:0.4:0.4$ , which indicates that the form of an ellipsoid is close to the ellipsoids of rotation.

Similar data set for films with mass thickness 2.2, 3.6, 4.3 and 5.7 nm. Obtained from AFM data form and size of metallic clusters correlate well with results of studies by other authors [1].

1. Vargas W.E., Azofeifa D.E., Clark N., Márquez X. Collective response of silver islands on a dielectric substrate when normally illuminated with electromagnetic radiation // Phys. D: Appl. Phys. – 2008. – 41. – 025309

## Optical characterization of the ultra-thin silver films

Bolesta I.M.<sup>1</sup>, Borodchuk A.V.<sup>1</sup>, Kushnir O.O.<sup>1</sup>, Kolych I.M.<sup>1</sup>,  
Karbovnyk I.D.<sup>1</sup>, Syworotka I.I.<sup>2</sup>

<sup>1</sup>*Ivan Franko Lviv National University, Lviv, Ukraine*

<sup>2</sup>*Scientific Research Company "CARAT", Lviv, Ukraine*

Silver is one of the most often used plasmonic materials which have gained interests of both experimentalists and theoreticians [1]. The properties of silver films, including the shape of clusters, the roughness, the minimum uniform thickness and optical losses are crucial for the achieving of good performance metamaterials and other Ag-based plasmonic devices.

The present work deals with the investigation of optical absorption spectra of ultra-thin silver films and their evolution depending on film mass thickness. Ultra-thin silver films were prepared by thermal evaporation of metal on glass substrates in vacuum of about  $10^{-6}$  Torr. The set of samples was obtained with Ag layer thickness varying from  $\sim 1$  nm to 20 nm.

AFM data shows that at the beginning of the deposition process, the metal forms small isolated particles and clusters composed of such particles on the substrate.

The optical studies revealed strong absorbance near the plasmon resonance wavelength of single particles and small clusters ( $\sim 480$  nm for Ag film with  $d \approx 1.1$  nm) and high transmittance for larger wavelengths.

Increasing of films mass thickness leads to the red shift of the absorbance band maxima and causes strong absorption in the long-wavelength range.

The evolution of Ag film absorbance spectra with the deposition of additional metal is due to the increasing number of non-spherical clusters and the formation of fractal clusters with complex morphology. These complex structures resonate in the broad spectral range extending from UV to near-IR and beyond.

For the films with  $d > 17$  nm the mentioned peak disappears and the absorption almost does not depend on the wavelength beyond the bulk metal plasma resonance range. Such behavior is related to percolation; therefore the percolation threshold for the investigated samples is nearly 17 nm.

For the silver films with the thickness only slightly above the threshold certain number of dielectric voids and localized metal clusters exist in the film, giving rise to the absorption band at  $\sim 390$  nm. With additional deposition of metal the voids and the isolated clusters disappear and the film eventually becomes completely homogeneous.

1. Kreibig U., Vollmer M. Optical properties of Metal clusters // Springer-Verlag, Berlin. – 1999. – P. 469.

## Cathodoluminescence of thin films based on $\text{ZnGa}_2\text{O}_4$

Bordun O.M., Bihday V.G., Kukharsky I.Yo

*Ivan Franko Lviv National University, Lviv, Ukraine*

Cathodoluminescence (CL) properties of  $\text{ZnGa}_2\text{O}_4$ ,  $\text{ZnGa}_2\text{O}_4:\text{Mn}$  and  $\text{ZnGa}_2\text{O}_4:\text{Cr}$  thin films have been investigated.

Based on X-ray diffraction analysis it has been ascertained that after heat treatment crystalline structure of films  $\text{ZnGa}_2\text{O}_4:\text{Mn}$  is considerably improved and meets space group  $Fd3m$  with crystal lattice parameter  $a = 8.32\text{-}8.33 \text{ \AA}$ . After thermal annealing of  $\text{ZnGa}_2\text{O}_4:\text{Cr}$  films in an atmosphere of argon at temperatures  $1000\text{-}1100^\circ\text{C}$  texture parameter decreases from  $\tau = 0.34$  to  $\tau = 0.29$ , and crystallite size accordingly increases from  $D = 218 \text{ \AA}$  to  $D = 706 \text{ \AA}$ , which also indicates improvement of the crystalline structure of  $\text{ZnGa}_2\text{O}_4:\text{Cr}$  films.

It has been investigated that the maximum range of CL of  $\text{ZnGa}_2\text{O}_4$  thin films has a maximum in the blue spectral region near  $420 \text{ nm}$ . CL of the  $\text{ZnGa}_2\text{O}_4:\text{Mn}$  films is characterized by a maximum at  $505 \text{ nm}$  with chromatic coefficients  $x = 0.133$ ,  $y = 0.635$ . This range is caused by transitions  ${}^4\text{T}_1 - {}^6\text{A}_1$  in  $\text{Mn}^{2+}$  ions, which replace Zn in the crystal lattice. Heat treatment on air at temperatures  $1000\text{-}1100^\circ\text{C}$  leads to increase CL intensity by 2-3 times, and in an atmosphere of argon in the same temperature region the intensity of CL increases by 20 times. Maximum spectrum of  $\text{ZnGa}_2\text{O}_4:\text{Cr}$  CL is observed in the red region  $700\text{-}720 \text{ nm}$  and is caused by R- and  $\text{T}_2 \rightarrow \text{A}_2$  transitions in  $\text{Cr}^{3+}$  ions. After heat treatment on air in temperature region  $1000\text{-}1100^\circ\text{C}$  CL intensity increases by 3 times, while after annealing in the argon atmosphere CL intensity increases by 100 times.

The CL intensity increase of  $\text{ZnGa}_2\text{O}_4:\text{Cr}$  and  $\text{ZnGa}_2\text{O}_4:\text{Mn}$  thin films after annealing in the inert anoxic atmosphere is explained on the basis of improvement of the crystal structure (texture) of  $\text{ZnGa}_2\text{O}_4:\text{Cr}$  and  $\text{ZnGa}_2\text{O}_4:\text{Mn}$  thin films and influence of the anoxic annealing conditions, which cause the maximum concentration of  $\text{Mn}^{2+}$  and  $\text{Cr}^{3+}$  luminescence centres.

## **The Influence of an Electric Field on Physicochemical Properties of Surface Layers of Lithium Niobate**

Borzanytsya D.V., Il'chenko V.V., Lushkin O.E.

*Taras Shevchenko National University of Kyiv, Kyiv, Ukraine*

Lithium niobate (LN) – transmission of optical and acoustic information and as transducer for novel sensors. Characteristics of the surface are very important that causes an importance of knowledge about possibility of controlled change of the surface under external influence.

An Auger-electron spectroscopy was used for experimental studies of changes of physicochemical properties of LN surface layers.

Surfaces of 128° Y-cut of LN (it is used for SAW-devices) and of negatively poled Z-cut of LN (because of the strongest influence of internal electric field on the physicochemical properties of the surface) were investigated. Target samples were prepared with cutting out of thick plates from the grown by the Chohralsky method monodomain deliberately not doped crystal of LN. External electric field with magnitudes  $\pm 1.5$  kV/cm (for Z-cut surface) and  $\pm 40$  kV/cm (for 128° Y-cut) were applied with an anode at distances of 1 mm and 3 mm respectively. Samples have been cleaned from surface contamination by heating. Researches were conducted in a vacuum chamber at a pressure that did not exceed  $10^{-8}$  Torr with sample's temperature from 300 K to 900 K.

The analysis of experimental results for the surface of 128° Y-cut of LN showed that there is a threshold value of applied field (near  $-40$  kV/cm), after which can be observed rapid long-term and short-term changes. At the same time for negatively poled z-cut of LN visible effect was even at magnitude of external field near 1.5 kV/cm. For both surfaces short-term changes includes the changing of the percentage of oxygen (or niobium – depends on surface) on the surface during the field influence with fast relaxation to the initial state after turning-off the external potential. For 128° Y-cut of LN, effect of negative potential is accompanied with increasing of pressure in the chamber from  $10^{-9}$  to  $10^{-8}$  Torr because of intensive evaporation of neutral (it confirmed with absence of the anode current) atoms and molecules. Finite time of changes testify achievement of electronic equilibrium. Impact to the surface of the negatively poled z-cut of LN is quite similar with corrections for surface features.

Received results can be partially explained with electron theory of evaporation [1].

1. Shnyukov V.F., Chaika G.E., Pikus G.Ya. Surface Composition of Binary Ionic Crystals: Correlation between Evaporation and Electronic Processes // Progress in Surface Science. – 1996. – Vol. 51, No. 3. – P. 175-231.

## Thermodynamics and crystal-chemistry of defect subsystem of PbTe crystals and Pb-Cr-Te solid solutions

Boychuk V.M., Turovska L.V., Mezhylovska L.Yo.

*Vasyl Stefanyk PreCarpathian National University, Ivano-Frankivsk, Ukraine*

Lead telluride has attracted attention primarily because of its wide using in infrared technology and thermoelectric devices [1]. It crystallizes in NaCl structure type ( $a = 6.461 \text{ \AA}$ ). It's characterized by a bilateral region of homogeneity and n- or p-type conductivity [2].

On the basis of the method of thermodynamic potentials and crystal-quasichemical formalism the calculation of concentrations of current carriers and point defects in lead telluride crystals depending on the parameters of the two-temperature annealing has been performed. The type of dominant own point defects, conditions of realization of thermodynamic n-p-conversion and influence of size of disproportionation of the charge states of cationic vacancies and interstitials lead on them have been determined.

Pb-Cr-Te solid solutions allow obtaining materials with unusual set of parameters. In paper the mechanisms of doping and the formation of PbTe-CrTe and PbTe-Cr<sub>3</sub>Te<sub>4</sub> solid solutions in Pb-Cr-Te system have been investigated.

For an explanation of the chromium donor effect quasichemical equations and crystal-quasichemical formulas for n- and p-Pb<sub>1-x</sub>Cr<sub>x</sub>Te subject to disordering in the cation sublattice have been offered, conditions of realization of p-n-transitions have been determined. Dependences of concentration of point defects and Hall concentration of current carriers on conditions of annealing and maintenance of tellurium have been calculated.

We have established that the main point defects in Pb<sub>1-x</sub>Cr<sub>x</sub>Te are chromium ions in cationic sublattice Cr<sub>Pb</sub><sup>+</sup> and Cr<sub>Pb</sub><sup>0</sup>, whose concentrations increase with the content of CrTe, and, moreover, if in n-Pb<sub>1-x</sub>Cr<sub>x</sub>Te interstitials lead Pb<sub>i</sub><sup>+</sup> are dominant point defects, then in p-Pb<sub>1-x</sub>Cr<sub>x</sub>Te cation vacancies V<sub>Pb</sub><sup>-</sup> are dominant point defects, which concentrations vary slightly with increase of the dopant content.

In n-PbTe-Cr<sub>3</sub>Te<sub>4</sub> solid solution doubly ionizing cation vacancies V<sub>Pb</sub><sup>2-</sup> and chromium ions in Pb places Cr<sub>Pb</sub><sup>+</sup> have significant impact on the concentration of current carriers, concentrations of these defects increase with increasing of Cr<sub>3</sub>Te<sub>4</sub> content. Significant growth in the concentration of dopant defects observed also for p-PbTe-Cr<sub>3</sub>Te<sub>4</sub>.

1. Shperun V.M., Freik D.M., Zapukhlyak R.I. Thermoelectricity of lead tellurides and its analogs. – Plai, Ivano-Frankivsk. – 2000. – 250 p.
2. Abrykosov N.Kh., Shalimova L.M. Semiconductors materials on the basis of A<sup>IV</sup>B<sup>VI</sup> compounds. – Science, Moscow. – 1975. – 196 p.

## ***Ab initio* simulation of nanoclusters in thin As-S films**

Boyko V.T., Shpotyuk O.I., Vakiv M.M.

*Scientific Research Company “Carat”, Lviv, Ukraine*

Computer *HyperChem* program was used to simulate structure of thin As-S films in wide range of concentrations (mean coordination numbers). The main idea was to start from simple, for example  $\text{AsS}_{3/2}$  pyramids, to more complicated clusters. Typical clusters, such as  $\text{As}_m\text{S}_n$  were examined.

After calculation procedure we have calculated total energy  $E_t$  of cluster including energy of hydrogen atoms  $E_{at}$ , used for saturation of dangling bonds. The energy of hydrogen atoms was used to calculate the formation energy of clusters:  $E_f = E_t - E_{at}$ . Then, we obtained the average formation energy as  $E_{av}^f = E_f/N$ , where  $N$  is total number of atoms in cluster without hydrogen.

The performed calculations showed that corner-shared  $\text{AsS}_{3/2}$  structural blocks with  $Z = 2.4$  in  $\text{As}_m\text{S}_n$  network are more energetically favorable, than edge-shared ones. Thus, a glassy network in the case of As-S glasses should be formed by corner-shared  $\text{AsS}_{3/2}$ . It was modeling more structural complicated clusters from  $Z = 2.40$  to 2.18 in frame of chain crossing model. The observed in MDSC peculiarities by P. Boolchand [1] correspond to calculated variations in cluster energy within  $Z = 2.225...2.29$ .

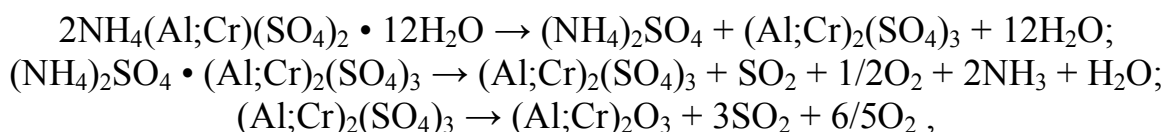
2. Boolchand P., Chen P., Vempati U. Intermediate phases, structural variance and network demixing in chalcogenides: the unusual case of group V sulfides // *J. Non-Cryst. Sol.* – 2009. – 355. – P. 1773-1785.

## Obtainment of Nano-Scale Ruby Particles of $\text{Al}_{2-x}\text{Cr}_x\text{O}_3$ Composition

Bukatyuk V.V., Tatarchuk T.R.

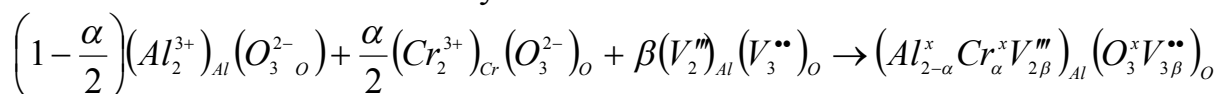
*Vasyl Stefanyk Precarpathian National University, Ivano-Frankivsk, Ukraine*

To date a growing attention is paid to the problems of obtainment of ultra-fine ruby powders with certain Cr contents, high optical purity and homogeneity, since these powders are applied in fiber optics as a duct amplifier incorporated into the organic polymeric matrix. In the present investigation the chemical method of dissolution of ammonium and ammonium chromic alums was used:



that allowed an accurate control of the final Cr content in ruby and provided sufficient homogeneity and purity levels.

The quasi-chemical lattice model was applied to explain the interaction mechanisms and the nature of defects in  $\text{Al}_2\text{O}_3\text{--Cr}_2\text{O}_3$  system. For the superposition of chemical lattice with ruby anti-structure  $(V_2^m)_{Al}(V_3^{\bullet\bullet})_O$  the intrinsic stoichiometric Schottky defects were taken into account.



The quasi-chemical lattice composition gives new information concerning the nature and concentration of point defects which affect the reactivity, magnetic and optical properties of samples synthesized. Apparently, vacancies in the Al sub-lattice  $V_{Al}^m$  are active donor centers, while vacancies in the O sub-lattice  $V_O^{\bullet\bullet}$  are acceptor centers.

The process of fine powder attainment consisted in: synthesis of initial products, milling, homogenization, and sintering at 1470 K. The solid solution  $\text{Al}_2\text{O}_3\text{--Cr}_2\text{O}_3$  powders with 2, 4, 8 % Cr contents were obtained. The phase composition of these materials was controlled with X-ray analysis at DRON-3M diffractometer under  $\text{CuK}\alpha$  radiation.

The powders were controlled both with light microscopy and MALVERN MASTERSIZER HYDRO 2000MU laser analyzer, and their size exceeded 100  $\mu\text{m}$ . Nevertheless, application of an ultrasonic disperser allowed to crash particle conglomerates, after that the real curve for particle size distribution was obtained. The final powder sizes varied from hundreds nanometers to 100  $\mu\text{m}$ , and the peak of the curve was observed at 15  $\mu\text{m}$ . The study showed that the obtainment of 10-300 nm sized powders is quite realizable, and more careful mechanical milling is needed for this.

## **Polymeric thin films of DAST nanocrystals for photonic applications: technology and properties**

Burunkova J.A., Denisyuk I.Yu., Minozhenko O.A.

*Saint-Petersburg State University of Information Technologies, Mechanics and Optics,  
Saint-Petersburg Russia*

Development of telecommunication systems, as well as optical processing of microwave signal systems is determined by the formation and investigation of new photonic elements. Organic nonlinear optical (NLO) materials have been intensely investigated due to their potentially high nonlinearities, rapid response in electro-optic applications and low dielectric constant in comparison with inorganic NLO materials. Electro-optic polymers and molecular crystals are the most commonly used organic materials.

Development of fundamentally new materials, which offers much better characteristics in compared to electro-optical polymers and which are more processable than molecular crystals, is based on completely different principles.

New material is thin-film nanocomposite consisting of oriented molecular nanocrystals with high hyperpolarizability, injected to the polymer matrix in high concentrations.

The purpose of this paper is the creation of technology for such materials based on DAST (trans-4'-(dimethylamino)-N-methyl-4-stilbazolium tosylate) nanocrystals and studying its properties. We proposed method and conditions for obtaining nanocrystalline polymer films using a mixture of polymer and DAST solutions.

Investigation of nanocrystalline polymer films technology includes the following parameters: different polymer matrix, ratio of solvents, annealing and orientation.

Obtaining DAST nanocrystals of red crystalline form is confirmed by absorption and luminescence spectra and SHG in polymer films.

## **Influence of annealing on transformation submonolayer coverage of chromium and titanium on Si(001) surface**

Butariev K.A., Koval I.P., Len Yu.A., Nakhodkin M.G.

*Kiev Taras Shevchenko National University, Kiev, Ukraine*

Transition metal silicides reveal many attractive properties for microelectronic applications due to the good compatibility with the conventional silicon technology. Indeed, silicides are used as ohmic contacts or interconnections in complementary metal oxide semiconductor (CMOS) transistors. One of the most interesting and well investigated compounds is the chromium and titanium disilicide.

Chromium disilicide ( $\text{CrSi}_2$ ) is a narrow-band semiconductor ( $E_g = 0.35\text{eV}$ ). Because of their fine crystal structure,  $\text{CrSi}_2$  nanoislands may exhibit the size effect, which causes quantization of energy levels and an effective expansion of the energy gap. Eventually, the indirect fundamental transition in  $\text{CrSi}_2$  may even change to direct. Therefore, one can expect a change in the optical, electronic, and thermoelectric properties both of individual  $\text{CrSi}_2$  nanocrystallites and of their aggregates in the semiconductor matrix.

Titanium silicides formed at the interface between Ti thin film and Si single crystal substrate have received much attention. This is due to their formation of low resistivity and high thermal stability contacts to silicon, as applied in ultra large scale integration (ULSI) devices and CMOS technologies.

Exposition of Ti thin film in oxygen atmosphere lead to formation titanium oxides.  $\text{TiO}_2$  is one of the most promising semiconductors for applications in microelectronic devices, sensors, photocatalysis, optical coatings, energy production and storage. Due to chemical and thermal stability titanium dioxide can be used as a protective coating.

In this article the structure of Si(001) surface covered by the pre-adsorbed of Ti and Cr at room temperature after annealing at temperatures which are characteristic for silicide phases formation was studied. The oxidation of Ti/Si(001) and Cr/Si(001) systems was compared.

It was found, that after annealing thin ( $\sim 3\text{nm}$ ) films of Cr and Ti on Si(001) at temperature  $\sim 450^\circ\text{C}$  formed island structure. The distributions of characteristic sizes of islands have maximums at 1250 nm and 150, 350, 800 nm for Cr and Ti films, respectively. Furthermore, it was determined that islands' composition after annealing Cr films was  $\text{CrSi}_2$ .

Submonolayer coverage of Ti or Cr play a role of catalytic agent for oxidation of Si(001) substrate. Catalytic properties of submonolayer Ti films are considerably worse in comparison with the Cr films.

This work was supported by the Ministry of Education and Science of Ukraine (grant № M/90-2010).

## The influence of nanodispersed titanium dioxide hydration degree on specific capacity of lithium power sources with cathodes on its base

Chelyadyn V.L., Kotsyubynsky V.O.

*Vasyl Stefanyk Precarpathion National University, Ivano-Frankivsk, Ukraine*

Nanoparticles of titanium dioxide with various hydration degrees were obtained by controlled hydrolysis of  $TiCl_4$  by hydrochloric acid. It was found out that the synthesis conditions (pH level and temperature of reaction medium, type and content of additional precursors) affect on the nucleation rate and determine the phase state and morphology of  $TiO_2$  nanoparticles.

Obtained materials were tested as a base component of cathode composition of model lithium power sources (LPS). Comparative analysis of characteristic parameters (specific capacity  $C$  and the energy  $W$ ) LPS with cathodes based on titanium oxide and titanium hydroxide obtained under different conditions of synthesis was carried out. Discharge of model LPS were realized in galvanostatic conditions, discharged current was 10  $\mu$ A. Maximal specific capacity (up to 900 mA·h/g) is fixed for LPS with cathodes on the base of X-ray amorphous oxide-hydroxide titanium  $TiO_2 \cdot 1.2 H_2O$ , for which mass loss at annealing up to 500°C is 21%. Multistage character of LPS discharge process is observed by the methods of potentiometry and impedance spectroscopy. Obtained data reflect the process of lithium ions intercalation in the material particles and the course of by-reactions on the surface of cathode material. The presence of surface hydroxyl and carboxyl groups and bound in the pores of the material molecules of  $H_2O$  is fixed by the method of infrared spectroscopy. Presence of the hydroxyl groups and protons in the electrolyte causes the formation of  $LiOH$ ,  $Li_2O$  and  $Li_2CO_3$  phases islands on the cathode material surface on the initial stage of discharge process. Simultaneously the diffusion of  $Li^+$  ions in crystal regions of the matrix material  $TiO_2 \cdot 1.2 H_2O$  takes place. Water in the electrolyte initiates the destruction of  $BF_4^-$  complexes. Molecules of  $HF$  are forming in the reaction of fluoride ions with protons. Nucleus of  $LiF$  is formed as the result of  $HF$  interaction with lithium-containing phases on the surface of the cathode. Thus, part of the  $Li^+$  ions which are transferred through the electrolyte takes part in the formation of passivate layer on the cathode surface. Similar mechanism of current formation is implemented for the cathode material on the base of anatase  $TiO_2$  with the water and hydroxyl groups content about 10 mass. %. In this case the value of the specific capacity of 540 mAh/g is reached. After dehydration of this material by calcination at the temperature of 600°C specific capacity about 360 mA·h/g is fixed which corresponds to the formation of intercalation compound  $LiTiO_2$ . Thus, the specific capacity linearly increases with hydration degree of  $TiO_2$ , which together with morphological and phase parameters affects on the specific energy characteristics of model LPS.

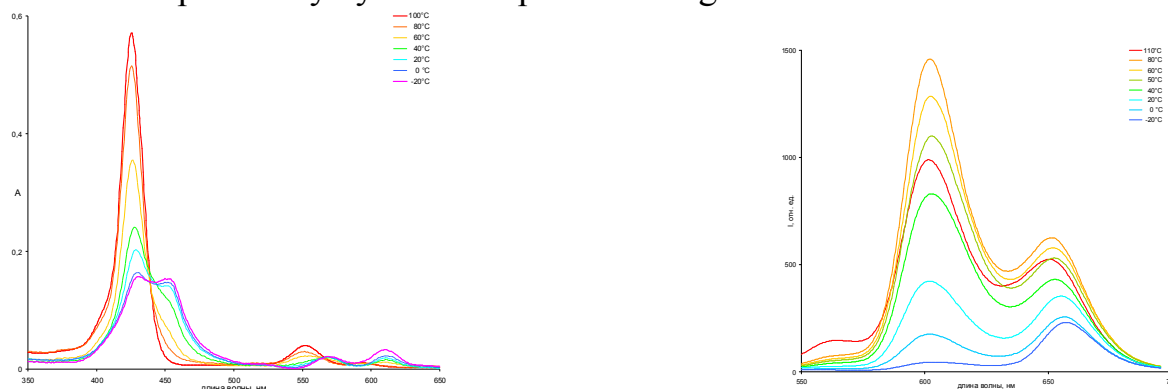
*The work is supported by CRDF / USAID (UKX2-9200-IF-08) and the Ministry of Education and Science of Ukraine (M/130-2009).*

## Thermochromic behavior of nanoparticles based on aluminum (III) crown-substituted porphyrin in toluene solution

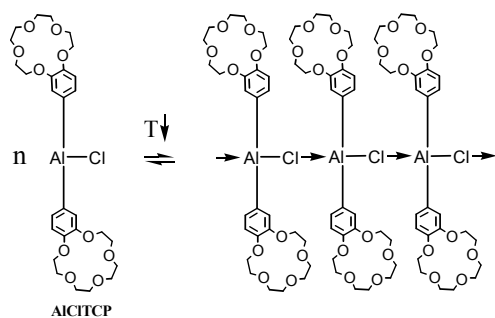
Chernyadyev A.Yu., Plachev Yu.A., Vysotsky V.V. and Tsivadze A.Yu.

*Institute of Physical chemistry and Electrochemistry RAS, Moscow, Russia*

Aluminum(III) porphyrins are of interest due to high quantum yield of fluorescence as compared of free base porphyrins, as catalyst of polymerization of epoxides and reduction of carbonyl compounds by alcohols. New crown-substituted aluminum(III) porphyrin was synthesized. It was found that saturated toluene solution of this compound manifests thermochromic behavior. Warmed solution is purple, cold solution (room temperature) is green. The solution was explored by methods of electronic absorption spectroscopy(EAS), luminescence spectroscopy and dynamic dispersion of light. Solution at room temperature is found to be stable in time colloid system with middle diameter of nanoparticles  $\sim 300$  nm. Solution of aluminum(III) porphyrin warmed to  $110^{\circ}\text{C}$  is molecular solution as probed by dynamic dispersion of light.



Changes of EAS(left picture) and luminescence spectra(right picture) with change of solution's temperature are shown on the figure. Colloid solution manifests weak absorption as compared of molecular solution and weak luminescence in red region, molecular solution manifests strong luminescence. We proposed the chemical mechanism of such process. Dramatic change of solution's optical properties with change of temperature probably can be explained by formation of oligomeric forms of aluminum (III) porphyrin (Scheme).



Colloid solution of aluminum(III) porphyrin is promising thermochromic material due to high contrast of color's change and very low concentration of active component in the solution ( $\sim 1 \times 10^{-6}$  M/L)

*The work was supported by Russian Academy of Science (Program №6) and Grant of RF President (MK-571.2011.3).*

## Mechanisms of growth, topology and properties of nanostructures based on lead telluride

Chobanuk V.M., Lishchynskyy I.M., Bachuk V.V. Krynytskiy O.

*Vasyl Stepanyk Precarpatian National University, Ivano-Frankivsk, Ukraine*

The analysis vapor-phase methods - hot wall, getting nanostructures based on lead chalcogenides. Attention is paid to the mechanisms of nucleation, growth and characteristics of self-organization of nanostructures.

Narrow-gap semiconductor IV-VI is the object of study for a long time as an interesting model in terms of objects and their practical use as optoelectronic devices for medium and far infrared light spectrum.

As for nanostructures semiconductors IV-VI, the traditional methods are vapor phase methods.

In work the results of some studies of growth mechanisms of nanostructures IV-VI compounds obtained by hot wall and open evaporation.

Analysis of results investigation surface morphology of PbTe nanostructures on mica muscovite chips (0001) shows that there is some regularity in the formation of epitaxial nanostructures depending on the temperature of growth and their thickness. In particular, low deposition temperature  $T_s = 353$  K promote the formation of nanocrystals with prevalence rates of growth in the tangential direction to the substrate surface. This indicates that their linear dimensions in the substrate plane in azimuth (0,2-1,4) mkm far outweigh size in normal direction - height nanocrystals 100 nm. Rising growth temperatures to  $T_s=(380-408)$  K leads to a more homogeneous of the nanocrystals as the shape, and with linear dimensions in the azimuth direction and normal to the substrate surface. Although the linear dimensions of crystals in the plane of the substrate (0,1-0,7) mkm precipitation for these conditions greatly exceed their height (100-350) nm.

Further significant increases deposition temperature to  $T_s = 633$  K leads to growth of well-formed crystals of diameter (0,2-0,8) mkm and height (100-400) nm of some "giants" of (1,6-1,8) mkm in basis and up to (300-1200) nm.

Thus, the nature of growth of nanocrystals on mica is characteristic for the mechanism of epitaxy *Volmer-Weber*. Three-dimensional crystals arise with little jaded when the layer is extremely tenuous, which is typical for weak adhesion, which determines expressed relationship of the crystal-condensate with the substrate. After the formation (sintering) a continuous layer of nanocrystals raise new centers of origin. Formation of tetrahedrons of inclination to the substrate surface edges also has power base - reducing the surface energy limits. This is due to the fact that their surface is "covered" ion of rows with dense that do not have electric charge (characteristic directions  $\langle 100 \rangle$  in the crystal with structure of the type NaCl). Crystal boundaries are well described by a model Brandon.

## New thermoelectric materials on the based semiconductors nanostructure

Chobanyuk V.M., Lysyuk Yu.V.

*Vasyl Stepanyuk Precarpatian National University, Ivano-Frankivsk, Ukraine*

Condensed Matter Research found that it is possible significantly to increase the value of the material thermoelectric figure of merit  $Z$  in them [1]. The paper presents an analysis of new approaches to improve the thermoelectric parameters of nanostructures on the basis of compounds IV-VI.

Found that thermoelectric figure of merit for materials based on superlattices of quantum dots reaches a value  $ZT = 2$  at 300 K by a sharp decrease lattice thermal conductivity of more than 4 times compared to the bulk material of the same composition [2].

The optimal parameters of the segment length and orientation for superlattice nanowires based on lead chalcogenides is evaluated [3].

Oscillation character for thickness dependence of kinetic parameters of quantum wells superlattices suggests that this behavior is caused by quantum size effects associated with movement confinement of the main carrier [f.e. 4]. Defining the period of oscillations has allowed to get energy parameters of appropriate nanostructures for future calculations of  $Z$  component and select the appropriate technological modes for obtaining materials with predicted properties.

We studied samples of p-PbTe on polyamide and p-SnTe on mica. Results of atomic force microscopy show a clear island structure for both p-PbTe and p-SnTe nanostructures. It is due to Volmer-Weber growth mechanism on dielectric substrates for lead chalcogenides. The thickness dependencies of kinetic parameters in this structures have been explained by the quantum-size nature due to confinement of carrier movement in the quantum well, formed by the substrate and oxidative layer on the surface of structure.

Note, that calculations of  $Z$  and  $S^2\sigma$  in systems with quantum wells and wires have shown that they are influenced by changes in the electronic density of states due to dimension decrease. Indeed, as shown in, using the density of states in low-dimensional systems, we can achieve a substantial increase in the asymmetry of the density of states and, consequently, the growth of thermopower by changing the position of Fermi level with respect to these features.

1. M.S. Dresselhaus, G. Chen, M.I. Tang, R. Yang, H. Lee: New directions for low-dimensional thermoelectric materials. *Adv. Mater.* **19**, 1 (2007).
2. Sur I., Casian A., and Baladin A. Electronic thermal conductivity and thermoelectric figure of merit of n-type PbTe/PbEuTe quantum wells // *Phys. Rev. B.* - 2004. - V.69. – 035306.
3. Yu-Ming Lin, M.S. Dresselhaus Thermoelectric properties of superlattice nanowires // *Physical Review B* – 2003 – V. 68 – 075304.
4. Rogacheva E.I., Nashchekina O.N., Vekhov Y.O., Dresselhaus M.S., Cronin S.B., Effect of thickness on the thermoelectric properties of PbS thin films // *Thin Solid Films.* – 2003 – №423. - P. 115–118.

## Influence of annealing on optical parameters of $\text{Cu}_6\text{PS}_5\text{I}$ amorphous thin films

Chomolyak A.A.<sup>1</sup>, Kranjčec M.<sup>2</sup>, Studenyak I.P.<sup>1</sup>, Vorohta M.<sup>3</sup>, Matolin V.<sup>3</sup>

<sup>1</sup>*Uzhhorod National University, Uzhhorod, Ukraine*

<sup>2</sup>*University of Zagreb, Varaždin, Croatia*

<sup>3</sup>*Charles University, Prague, Czech Republic*

$\text{Cu}_6\text{PS}_5\text{I}$  compound belongs to argyrodite family and is known as a superionic conductor. The thin films were deposited onto silicate glass substrates by non-reactive radio frequency magnetron sputtering. The film growth rate was 3 nm/min, the film thickness was 0.5-0.6  $\mu\text{m}$ . The deposition was carried out at room temperature in Ar atmosphere. The structure of the deposited films was analyzed by X-ray diffraction; the diffraction spectra showed the films to be amorphous. Annealing was performed in vacuum for 1 h at temperatures of 50 and 100°C.

Optical transmission spectra  $T(\lambda)$  of  $\text{Cu}_6\text{PS}_5\text{I}$  thin films were studied in the interval of temperatures 77-300 K by an MDR-3 grating monochromator, a UTREX cryostat was used for low-temperature studies. From the temperature studies of interference transmission spectra, the spectral dependences of absorption coefficient as well as dispersion dependences of refractive index were derived. It is shown that the optical absorption edge spectra in the range of their exponential behavior in amorphous  $\text{Cu}_6\text{PS}_5\text{I}$  thin films are described by Urbach rule. It is shown that annealing leads to decreasing of optical pseudogap  $E_g^*$  and increasing of Urbach energy  $E_U$ . The temperature behavior of the Urbach absorption edge is explained by electron-phonon interaction which is strong in amorphous  $\text{Cu}_6\text{PS}_5\text{I}$  thin films. In thin films under investigation the electron-phonon interaction intensifies with annealing temperature increase while the energy of effective phonon - enlarges.

An essential characteristic of the absorption edge spectra of the  $\text{Cu}_6\text{PS}_5\text{I}$  thin films is a lengthy Urbach tail which results in the Urbach energy  $E_U$  being more than by an order of magnitude higher than that in the crystal. It should be noted that the relative value of the contribution of static structural disordering into the as-deposited film Urbach energy equals of 86% from value  $E_U$ . Static structural disordering in  $\text{Cu}_6\text{PS}_5\text{I}$  thin film appears due to (i) the absence of long-range order in the atomic arrangement and chemical bond breakdown; (ii) lower density of the atomic structure packing due to the presence of pores; (iii) the transition from the three-dimensional bulk structure to the two-dimensional planar structure. It is shown that with annealing temperature increase the contribution of static structural disordering into  $E_U$  increases and in annealed to 100°C thin films it equals 89%.

## **The nanocompositions on Van-der-Waals surface of InSe single crystal**

Dmitriev A.I. Fedorchenko D.A.

*I.M. Frantsevich Institute for Problems of Material Science, National Academy of Sciences  
of Ukraine, Kyiv, Ukraine*

The morphology of Van-der-Waals surface (VdWs) for InSe layered single crystal at different kinds of its treatment was researched by methods of scanning tunnel microscopy. It was supposed that the VdWs prepared by adhesive tape oxidized in an open air as a result of hemosorbition of acid agents by broken In and Se bonds. The kinds of Volt-Ampere characteristics allow to affirm, that the composition of natural oxides present the mixture of  $\text{In}_2\text{O}_3$  and wide-gap selenium oxides.

The tunnel microscope scanning of InSe surface, prepared by sliding and further exposure on an air during 2 min reveals the surface ordering in the form of a corrugation of a complicated profile with fine structure. The latter reflects the redistribution of charge density after hemosorbition of gas molecules from air and surface relaxation to the state with minimal energy.

The atomic resolution is observed on the VdWs (0001) for InSe single crystal, prepared by sliding in oxygenless media. The surface corrugation is absent. Point defects disturb a periodic crystal potential. This perturbation has dimensions up to four lattice periods and looks like shaded area.

The method of the growth oxide nanostructures  $\text{In}_2\text{O}_3$  on crystal surface of layered semiconductor InSe with a help of probe of atomic force microscope as the nanoindenter is offered. The probe ability to operate in gaseous as well as in liquid medias essentially widens the possibilities of the method.

## **Tuning of surface plasmon resonance in ultrathin gold films by post-growth thermal processing**

Dmitruk N.L., Kondratenko O.S., Kotova N.V., Romanyuk V.R.

*Institute for Physics of Semiconductors NAS of Ukraine, Kyiv, Ukraine*

Thin semitransparent continuous (solid) and island (nanoparticles) metal films are important element of devices based on surface plasmon polaritons excitations. Stability of films, optical and other parameters strongly depend on film fabrication technology and post-fabrication treatment. In this work we report our results of systematic study of transformation of ultrathin metal (gold) films morphology induced by thermal annealing and effect of these changes on surface plasmon resonance characteristics (spectral position, bandwidth etc.).

Gold films with thickness from 8 to 80 nm were thermally evaporated in vacuum on the glass substrates kept at room temperature. Structure and morphology of films were examined with TEM and AFM techniques. Optical parameters of thin gold films were determined from transmittance/reflectance spectroscopy of *p*- and *s*-polarized light ( $\lambda=350-1100$  nm) at various angles of incidence, by monochromatic ( $\lambda=632.8$  nm) ellipsometry in standard reflection mode and in the Kretschmann geometry of attenuated total reflection (ATR).

Vacuum annealing of these ultrathin films caused in both morphology and optical behavior modifications (especially in the region of surface plasmon resonance excitation). Our investigations have shown that film morphology change induced by thermal annealing depends strongly on film thickness. Relations between optical parameters and annealing temperatures are considered in respect to structural changes in polycrystalline gold nanofilms. Optical behavior of produced metal films has been described by Bruggeman effective medium approximation taking into account the particles shape effect (anisotropy). The optimal annealing conditions for obtaining the maximal quality coefficient of plasmon resonance  $\gamma=|\text{Re } \varepsilon / \text{Im } \varepsilon|^2$  in metal nanoparticles have been ascertained.

The considered processes might be crucial for thin film optical properties determination and need to be taken into account for the choice of adequate structure model. Besides that, post-fabrication thermal annealing enables a wide modification of ultrathin metal films morphology and surface plasmon resonance parameters, offering new possibilities for surface enhancing metal substrates design.

These results are very important for many applications in polaritonic optoelectronics, photovoltaics and surface plasmon resonance sensors.

## Structure and properties of the modified polyethylene films

Domantsevych N.I.<sup>1</sup>, Aksimentyeva O.I.<sup>2</sup>, Martynjuk M.M.<sup>1</sup>

<sup>1</sup>*Lviv Commercial Academy, Lviv, Ukraine;*

<sup>2</sup>*Ivan Franko Lviv National University, Lviv, Ukraine*

The application of inhibited polymer films for long protection of metal production is restricted by lowering the barrier and protective properties of the films, their accelerated destruction. The using amine inhibitors in polymer films improves the protective properties during the initial stage of saving, nevertheless can result to activation of destruction processes, which decrease a period of film exploitation till to 5 years.

The aim of present research was study influence of modifying components on the structure and physical-chemical properties of the films, including the gas transport processes across the films.

As polymer matrix a polyethylene of high-pressure (PEHP) was used. The components, which applied for modification of material were amine inhibitors of corrosion such as – Dicyclohexylamine benzoate (DCHAB) and Cyclohexylamine benzoate (CHAB) and plasticizers – Dioctyl phthalate, Dioctyl sebate, Di-2 –ethylhexyl phthalate. Samples of the films were fabricated on a laboratory extruder. The inhibitors brought into polymer matrix during the stage of bloating near zone of film exit hose near the shaping head. The additional supplementary of a plasticizer into polymer composition reduced processing temperature and simplified overlapping between inhibitors and polymer substance.

Obtaining results show mediocre barrier properties of unmodified polyethylene. The films contained an inhibitor of corrosion in the composition are characterized by reduced index of permeability. It has been found that more active structure changes in protective films are proceed during initial 3 years of atmospheric ageing. In the inhibitor contained films an increasing in initial crystallinity of polymer matrix leads to the growth of defects between amorphous and crystalline phases. In result an index of oxygen permeability is increasing. At addition of the inhibitors the processes of surface passivation and displacement of the oxygen inside the packet may proceed. In presence of the plasticizers the permeability index also decreased. Such tendency to reduction of diffusion coefficient value is characteristic for all polymer films with plasticizer additions during the time of exploitation.

By electron microscopy investigations there are confirmed that in inhibited films without plasticizer an active process of crystallization at film ageing during more than 5 years. Thus, destruction of coating, the crack and pores initiation occurs along the demarcation line between amorphous and crystalline phase. Two typical cracks of destruction are detected during of the initial stages.

## Formation of Nanostructured Oxides of Alkaline Earth Metals on Scandium Oxide

Dudko A.O., Il'chenko V.V., Lushkin O.E.

*Taras Shevchenko Kyiv University, Kyiv, Ukraine*

The researches of thermoemitters are relevant because nowadays they are the main element in the microwave devices used in space communications. The best parameters of these devices are achieved when using exactly Sc MDE. However, to date there is no clear theory for explanation of the mechanism of the emission for such emitters. Despite the fact that already received a lot of experimental results there is a series of questions which need to find the answer. One of them is the possible dependence of the emission possibility of the emitters from its structure (needle-shaped formation of the active substance or thick layers of this substance on tungsten beans) and the composition of the emitting surfaces. So investigation of formation of nanostructures of alkaline earth metals on scandium oxide and development of a model of crystal grow on its surface is relevant.

The researches were carried out in ultra high vacuum chamber at a pressure that does not exceed  $6.8 \cdot 10^{-7}$  Pa. There was an Auger analyzer type cylindrical mirror to analyze the composition of the surface. As a substrate compressed mixture of tungsten powder with submicron grains of  $Sc_2O_3$  powder was selected. Activated  $2.4BaO \times 0.6CaO \times Al_2O_3$  MDE was used as a source of Ba, BaO and Ca components.

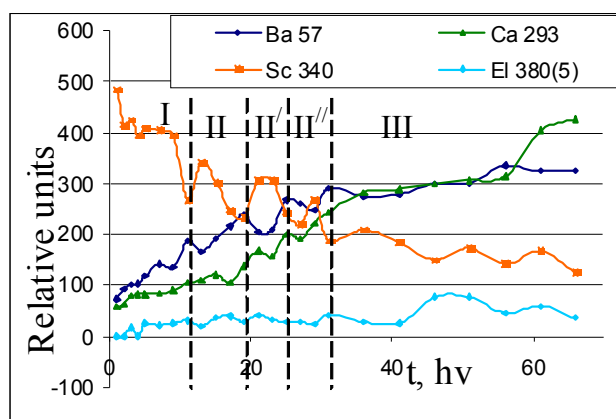


Fig. 1

Time dependence of Auger peak amplitudes of the active substance during MDE sputtering the surface  $Sc_2O_3$ .

Ba-component adsorbs with a Stranski-Krastanov mechanism and Ca-component adsorbs with a Volmer-Weber mechanism. Grow of Ba-islands and increase of Ca-cone volume depends on a ratio between their volume and surface diffusion coefficients.

The experiment showed that scandium oxide surface loosening by barium atoms take place in first minutes of adsorbate sputtering. Our studies also confirmed the main role of calcium oxide molecules for the formation of crystallites on the basis of oxides of alkaline earth metals.

Binding energy of scandium oxide with Ba- and Ca-components differs: Ba-component has bigger thermal stability than Ca-component.

It helps to build a model of complicated structure grow on a scandium oxide surface in which Ba-

## **Size effects melting of the condensed metal films**

Dukarov S.V., Sukhov V.N., Churilov I.G.

*V.N. Karazin Kharkiv National University, Kharkiv, Ukraine*

Phase transitions in condensed films differ from transitions in bulk material or in isolated microparticles. This is because of the substrate and considerable number of the defects present in condensed films. Investigated melting of the continuous pure metal (Sn, Bi, Pb) more than 200 nm thick and multilayer binary (Bi-Sn, Sn-Pb) films formed by alternated layers about 20 nm thick. Films was created by vacuum deposition to carbon substrate with the following creation of the temperature gradient on substrate. That was observed that above the meting temperature film formed by islets of the spherical shape that is typical for liquid state. Continuous polycrystalline film observed at temperature below melting point. In intermediate section film structure changing from flowed crystalline particles to maze structure while temperature decreases. Phase transitions in condensed films differ from transitions in bulk material or in isolated microparticles. This is because of the substrate and considerable number of the defects present in condensed films. Liquid phase in this transition section observed at temperature essentially below equilibrium melting point.

We explain this phenomenon as result of the significant contribution of the grain boundary energy or phase boundary energy into total energy of the system in melting process. In the melting process boundaries dissipating freed boundary energy that stimulates further melting. Forming of the supercooled liquid and following crystallization explains presence on the substrate at the temperatures below melting point of the flowed crystalline particles.

The results suggest that internal size effect associated with the large quantity of the grain borders lead to local occurrence of liquid phase below equilibrium melting temperature.

## Monomolecular films and reactivity of diacyl diperoxides

Dutka V., Opaynich I., Dutka Yu., Kovalskyi Ya.<sup>1</sup>

*Ivan Franko Lviv National University, Lviv, Ukraine*

<sup>1</sup>*Lviv Polytechnic National University, Lviv, Ukraine*

Organic diperoxides (DP) have in molecules the polar O-O-groups and non-polar hydrophobic hydrocarbon radicals. Biphyllic nature of molecules of DP does them able to be concentrated on boundary of phase's division. Adsorption of peroxides on liquid or solid surfaces substantially influences on reactionary ability of O-O-groups and on the polymeric reactions and modification processes on surface.

Surface pressure of diacylic diperoxides monolayers on water-air phase interface was studied. Investigation the monomolecular layers of organic peroxides at the liquid-gas interface gives possibility to estimate the reactivity initiators of radical processes in heterogeneous polymerizations and modification processes on surface. The studied objects were monomolecular films of DP, which are formed from different solvents on the surface of water: diacetyl diperoxiadipinate (DP 2-4), dicapronil diperoxiadipinate (DP 6-4), dicaproyl diperoxiadipinate (DP 10-4) and dicaproyl diperoxiphtalate (DP 10-P). Investigated DP were characterized by different length of both ended hydrocarbon radicals and by a size and nature to the radical which is between O-O-groups. Got results it is specified on that polar O-O-groups are on boundary of phase's division, and hydrocarbon radicals can be situated both on boundary of phase's division and oriented sideways gas phase. The obtained results show that on the water surface all DP form the condensed monolayer. A molecule area in monolayer depends on a solvent from which the monomolecular films are formed. At the compression of DP 10-4 and DP 10-P layers it is observed quasi-isobar effect which specifies on forcing of long hydrocarbon radicals out of plane of phase's division.

The thermal decomposition rates constants in the different solvents for DP and the corresponding values of the area occupied by its molecule in monolayer were founded. Optimized structures of DP and numerical values of the investigated peroxides areas were calculated by the quantum-chemical RM1 and PM3 methods. The results of quantum-chemical calculations are well responsible for the numerical values of DP areas.

The adsorptions of DP are studied on dispersible mineral oxides. It is shown that adsorption of investigated DP carries physical character and well described by Langmuier equation.

## Obtaining and oxidation of NiSi and NiSi<sub>2</sub> films on single-crystal silicon

Dvorina L.A., Dranenko A.S., Koshelev M.V.

*Frantsevich Institute for Problems of Materials Science of NASU,  
Kyiv, Ukraine*

Due to the limits of TiSi<sub>2</sub> and CoSi<sub>2</sub> for their application in future generation IC devices, NiSi has been attracting more and more interests in recent years. NiSi has a orthorhombic MnP structure, which belongs to the space group of Pnma. While there are six stable phases present in the Ni–Si system at room temperature (e.g., Ni<sub>3</sub>Si, Ni<sub>31</sub>Si<sub>12</sub>, Ni<sub>2</sub>Si, Ni<sub>3</sub>Si<sub>2</sub>, NiSi, and NiSi<sub>2</sub>), only NiSi has a low resistivity that is comparable to those of TiSi<sub>2</sub> and CoSi<sub>2</sub>.

In this work the phase formation and thermal oxidation stability of NiSi and NiSi<sub>2</sub> thin films on n-type Si(111) substrates have been investigated.

The objects of study were thin-film layers of Ni (200nm) on crystalline Si substrates with orientation (111) doped with phosphorus. Thin-film system Ni/Si obtained by electron-beam deposition in vacuum of  $2 \cdot 10^{-4}$  Pa. Deposition rate was 0.3 nm / sec. After deposition the samples were annealed in a furnace with oil-free vacuum pumping  $1.33 \cdot 10^{-3}$  Pa in the temperature range 470-1270 K. Phase identification was performed in a “Elektronohraf EMR-100” (Ukraine) using reflection electron diffraction method. The thermogravimetric analysis (TGA) was performed in a “Derivatograph Q-1500D” (Hungary) thermoanalytical instrument. The sample was heated in a platinum crucible in static air atmosphere at a rate of 5 K/min.

The values of interplanar distances were compared with tabulated values. In the initial state in thin-film system Ni (200 nm)/ Si (111) with a layer of "natural" oxide SiO<sub>2</sub> (~10 nm) was present nickel phase. At annealing temperature 770 K a number of nickel phase remains after annealing the system. Further increase in annealing temperature to 970 K leads to formation of Ni<sub>2</sub>Si and NiSi. Remaining phases of nickel is not observed. This means that the reaction was throughout the volume of metal film. Nickel disilicide NiSi<sub>2</sub> formed at a temperature of 1270 K.

According to data TGA, non-isothermal oxidation of single-crystal silicon substrate and nickel silicide films can be concluded that the oxidation of the films and the associated increase in weight begins at about 100 degrees higher than the oxidation of a silicon substrate. As the temperature rises (up to 1270 K), the rate of oxidation increases and weight gain for the films is much smaller (approximately 2.5 times) than the silicon substrate at the same temperature. It was established that the thermal oxidation resistance of nickel silicide films on n-type Si (111) increases when changing stoichiometry composition of the films in the direction from NiSi to NiSi<sub>2</sub>.

## Thermoelectric properties of laminate structures in the PbTe-Cd (Zn) Te, PbTe-Bi(Sb)<sub>2</sub>Te<sub>3</sub>

Dykun N.I.

*Vasyl Stepanyuk Precarpatian National University, Ivano-Frankivsk, Ukraine*

The results of investigation of thermoelectric properties of polycrystalline structures PbBi<sub>4</sub>Te<sub>7</sub> and PbSb<sub>2</sub>Te<sub>4</sub> is given.

Basic thermoelectric parameters were determined – thermo.-e.m.f. coefficient ( $\alpha$ ), electrical conductivity ( $\sigma$ ), thermal conductivity ( $k$ ), thermoelectric power ( $\alpha 2\sigma$ ), figure of merit ( $Z = \alpha 2\sigma/k$ ) and thermal figure of merit, - of synthesized PbBi<sub>4</sub>Te<sub>7</sub> and PbSb<sub>2</sub>Te<sub>4</sub> connections both stoichiometry and compositions with the tellurium surplus by 1at.%. It is shown that polycrystal material has the better thermoelectric performances than monocrystals of corresponding compositions.

Some datas from the results of investigation of termoelectric properties of compounds is given on the table.

Comparative datas of thermoelectric parameters of monocrystals and polycrystal samples PbBi<sub>4</sub>Te<sub>7</sub> and PbSb<sub>2</sub>Te<sub>4</sub> at 300K.

Parameters	PbSb <sub>2</sub> Te <sub>4</sub>	PbBi <sub>4</sub> Te <sub>7</sub>
Monocrystals		
$\alpha, \text{mkV}^{-1}$	26	-18
$\sigma \cdot 10^{-3}, \text{Om}^{-1} \text{cm}^{-1}$	2.35	3.36
$k \cdot 10^3, \text{Wt cm}^{-1} \text{K}^{-1}$	29.1	41.5
Polycrystal stoichiometry		
$\alpha, \text{mkV}^{-1}$	42	-32
$\sigma \cdot 10^{-3}, \text{Om}^{-1} \text{cm}^{-1}$	2.12	3.08
$k \cdot 10^3, \text{Wt cm}^{-1} \text{K}^{-1}$	19.2	28.3
Polycrystal with the tellurium surplus		
$\alpha, \text{mkV}^{-1}$	38	-35
$\sigma \cdot 10^{-3}, \text{Om}^{-1} \text{cm}^{-1}$	2.04	3.81
$k \cdot 10^3, \text{Wt cm}^{-1} \text{K}^{-1}$	13.6	21.7

It should be noted that in the polycrystal materials the thermal conductivity is less, and thermo.-e.m.f. coefficient is greater then for monocrystals. Because polycrystal is characterized by a large number of grain boundaries of the chaotic structure, which creates additional areas for the scattering of phonons. The tellurium surplus, due to considerable chaotic cationic sublattice via the formation of defects antystructure TeBi + (Te<sub>Sb</sub> +) and Te<sub>Pb</sub> + leads to substantial reduction of lattice thermal conductivity component, that is causing the increase in the value of thermoelectric figure of merit.

In addition, on the value of lattice thermal conductivity influence the fluctuations of atomic masses and tensions, which arising from mixed depending position in the crystal structures of complex compounds.

For n-PbBi<sub>4</sub>Te<sub>7</sub> the tellurium surplus is donor, so there is some increase in electrical conductivity by increasing the concentration of electrons. At the same time for p-PbSb<sub>2</sub>Te<sub>4</sub>, for the same activity of tellurium (Te<sub>Pb +</sub>, Te<sub>Sb +</sub>), there is a decrease in carrier concentration and, accordingly, electrical conductivity. The main energetic thermoelectric characteristics  $\alpha^2\sigma$ ,  $Z$  і  $ZT$  investigated polycrystal materials is rise with increasing temperature. This is due to the dominant influence of the thermo-e.m.f. coefficient, which increases with little reduction of electrical conductivity, especially thermal conductivity.

Improvement of thermoelectric parameters associated with decrease thermal conductivity and increase the thermo-e.m.f. coefficient due to structural chaotic at grain boundaries and high concentration of point defects.

*This work is partially financed by State Fund of Fundamental Researches of State Agency for Science, Innovation and Information of Ukraine (State registration № 0110U007676).*

1. Д.М. Фреїк, Н.І. Дикун, В.М. Бойчук, Р.І. Запукляк. Термоелектричні властивості шаруватих структур у системах PbTe-Bi(Sb)<sub>2</sub>Te<sub>3</sub> // Фізика і хімія твердого тіла. – 2009. – 10(4). – С. 872-876.

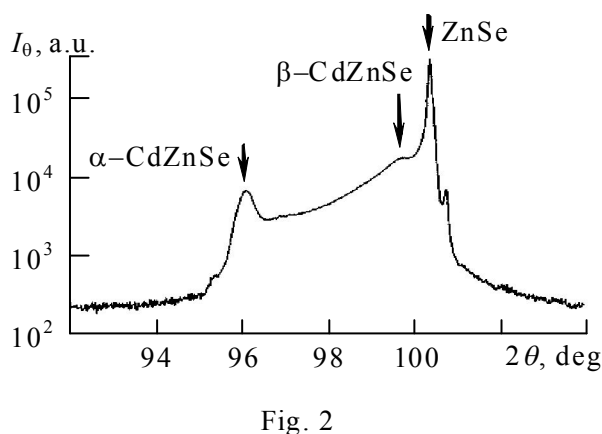
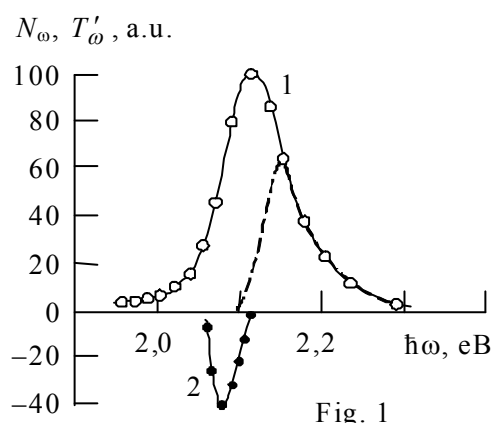
## Optical and structural properties isovalent-substituted CdSe layers

Dynowska E.<sup>2</sup>, Makhniy V.P.<sup>1</sup>, Melnyk V.V.<sup>1</sup>, Khusnutdinov S.V.<sup>2</sup>

<sup>1</sup>*Yu. Fedkovich Chernivtsi National University, Chernivtsi, Ukraine*

<sup>2</sup>*Institute of Physics, Polish Academy of Sciences, Warsaw, Poland*

Despite the fact the cadmium selenide can have a cubic ( $\beta$ ) and hexagonal ( $\alpha$ ) structure overwhelming part of research is devoted to the  $\alpha$ -CdSe. This is because of the bulk crystals and epitaxials of cubic modification are unstable in time. Even at the room temperature they can gradually transform into hexagonal modification. Only the  $\beta$ -CdSe layers, obtained by isovalent substitution at temperature synthesis  $T_a \approx 800^\circ\text{C}$  are the exceptions. They are characterized by effective edge luminescence with maximum  $\hbar\omega_m \approx 2.0$  eV, close to the band gap  $E_g$  of this compound at 300 K. Further investigation showed that, in contrast to the isovalent-substituted  $\alpha$ -CdSe layers, raise of the synthesis temperature of  $\beta$ -CdSe layers to  $T_a \approx 900^\circ\text{C}$  leads to a shift of  $\hbar\omega_m$  to the high-energy region, curve 1 in Fig. 1. At the time increases also the value of  $E_g$ , which corresponds



to the "negative peak" in the spectrum of  $\lambda$ -modulated transmission  $T'_\omega$ , curve 2 in Fig. 1. Near to  $E_g$  the value on the axis of energy cuts dashed curve  $N_\omega$ , which is calculated according to the known formula for interband recombination. Based on the optical spectra research it should be admitted that the raise of the synthesis temperature leads not to the formation of the binary CdSe compound but to the CdZnSe solid solution. This is confirmed by the X-diffractogram (Fig. 2) where both peaks of the basic substrate (ZnSe) and a layer of solid solutions CdZnSe as hexagonal so and cubic modifications are. Thus, variation of synthesis conditions of isovalent-doped cadmium selenide layers on zinc selenide substrates, allows changing of their physical properties. A question of practical use of research objects is discussed.

## CdTe films structure

Evmenova A.Z.<sup>1</sup>, Odarych V.A., Sizov F.F.<sup>1</sup>, Vuichyk M.V.<sup>1</sup>

<sup>1</sup>*V. Lashkaryov Institute of Semiconductor Physics, NAS of Ukraine, Kyiv, Ukraine*

<sup>2</sup>*Taras Shevchenko Kyiv National University, Kyiv, Ukraine*

Semiconductor CdTe films are used in different branches of micro- and optoelectronics. Knowledge of the film optical constants and its thickness, film thickness proportional distribution in area extent, film radiation and chemical durability are necessary for the film devices construction.

In published works it was shown that surface structure and values of film optical parameters considerable depends on methods and conditions of film deposition. Particularly it was found out that CdTe film refractive index is always smaller then refractive index of massive single-crystal CdTe. This fact is explained by the film porosity and deviation from the stoichiometric composition. The aim of this investigation was to study the dynamic of spectra changes of CdTe film optical parameters with the deposition time increasing and with correspondent thickness increasing; try to correlate feature of film optical parameters behavior with its inhomogeneity.

Thin CdTe films were obtained at the vacuum “hat-wall” epitaxy device. Si single-crystal plates were used as substrates. Films were deposited during fixed time: 6, 10 and 14 minutes. Under these circumstances we obtained three samples with different interference color through the area that obviously marked on the different thickness of each point of the film. Morphological and X-ray studying of such films obtained at the same devise showed that films have a polycrystalline structure.

Ellipsometric parameters of CdTe films were measured at the  $\lambda = 632.8$  nm; refractive and absorptive indexes and film thickness were calculated. Dependence of refractive and absorptive indexes on volume fraction of the matter in the film were obtained by Maxwell-Garnett approximation. It was detected that film optical parameters depend on film thickness, it could be explained by different volume fraction of the base matter in the film. Consequently deviation of CdTe film optical parameters from the bulk CdTe optical parameters could be explained by the porous structure of the film. Volume fraction of the base matter in the film is 85%. Volume fraction of the filling compound is approximately equal, but its refractive index increases from 1 (films with small time of evaporation) to 2 (films with time of evaporation 14 minutes). Films, those were exposure over a long period more then 1 year at the open air, have such values of optical parameters which corresponds to cavities in films; they are filled with relatively strong absorptive matter, may be with compound of oxide and suboxide matter.

## Low temperature magnetic states of the nano phase segregated CMR compound $(\text{Nd}_{0.9}\text{Y}_{0.1})_{2/3}\text{Ca}_{1/3}\text{MnO}_3$

Fertman E., Beznosov A., Desnenko V., Dolya S.

*Institute for Low Temperature Physics and Engineering NASU, Kharkov, Ukraine*

Insulating perovskite  $(\text{Nd}_{0.9}\text{Y}_{0.1})_{2/3}\text{Ca}_{1/3}\text{MnO}_3$  is a colossal magnetoresistance compound which possesses phase segregated state at low temperatures: nanoclusters of two antiferromagnetic (AF) phases and the ferromagnetic (FM) one coexist below 60 K [1]. Here we have studied low temperature magnetic properties of the compound.

Initial susceptibility curve  $\chi''(T)$  displays maximum at  $T_f = 50$  K which shifts upwards with increasing frequency, which is a distinct feature of magnetic glass state. This maximum corresponding to the cusp of ZFC magnetization curve (Fig. 1, inset) has been taken as a spin-glass freezing temperature. Rate of the frequency shift of the  $T_f$ , estimated as  $\partial \ln T_f / \partial \ln \omega \approx 0.017$ , is in a agreement with analogous estimations, made for other spin-glass systems. Strongly divergent ZFC and FC static magnetizations are evident of the glass behavior of the system as well. External magnetic field up to 1 kOe suppresses the glassy state, shifting the freezing temperature to the low temperature range.

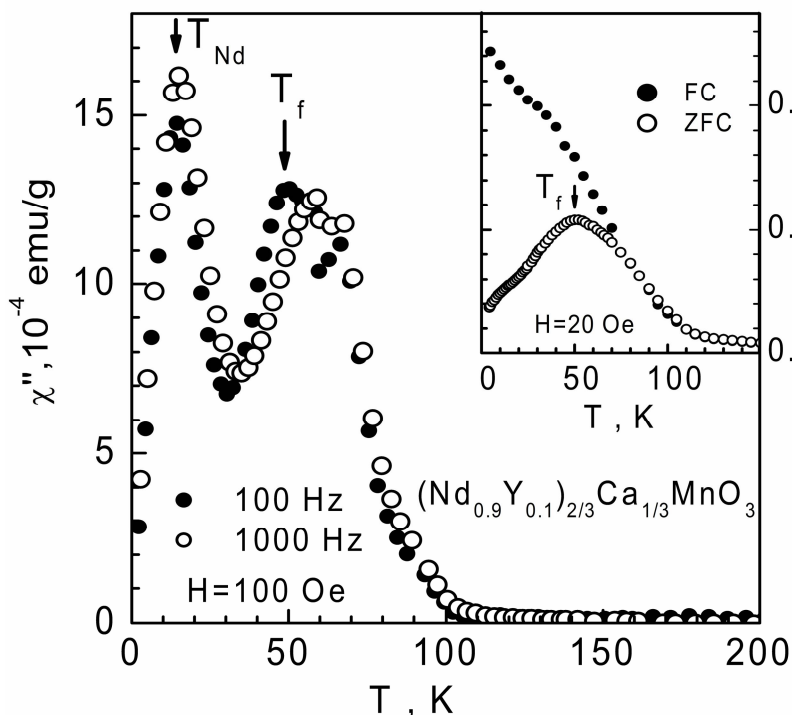


Fig. 1. Ac susceptibility  $\chi''(T)$  at different frequencies. Inset: ZFC and FC magnetization in magnetic field  $H = 20$  Oe. The low temperature maximum of  $\chi''(T)$  curve  $T_{\text{Nd}} = 15$  K, independent on the frequency, corresponds to the magnetic ordering of Nd magnetic subsystem.

The data obtained permit to conclude that nano phase segregated state of the compound  $(\text{Nd}_{0.9}\text{Y}_{0.1})_{2/3}\text{Ca}_{1/3}\text{MnO}_3$  leads to its glassy magnetic behavior.

1. A. Feher *et al* Analysis of the low temperature magnetic contributions to the specific heat of  $(\text{Nd}_x\text{Y}_{1-x})_{2/3}\text{Ca}_{1/3}\text{MnO}_3$  ( $x = 0, 0.1$ ) // J Low Temp Phys. – 2011. – V. 162, Iss. 5. – P. 529-535.

## Thermodynamics of crystal defects in cadmium and lead telluride

Freik D.M., Gorichok I.V., Parashchuk T.O.,  
Makovushun V.I., Bardashevskaya S.D.

*Preคาร์pathion National University named after V. Stefanyk, Ivano-Frankivsk, Ukraine*

Semiconductor Group  $A^{II}B^{VI}$   $A^{IV}B^{VI}$  are basic materials for a creation of wide class of optoelectronic device structures. These materials attract special attention of cadmium and lead telluride, it is caused by the peculiarities of their physical and chemical properties and relatively straightforward and sufficiently studied the technology of their synthesis. In last years, the promising research activities of the above mentioned materials are quantum heterostructures in the system  $A^{IV}B^{VI}/A^{II}B^{VI}$ , and thermoelectric materials which based on solid solutions  $A^{II} - B^{IV} - B^{VI}$ .

Despite the significant progress made in this direction, some problems that relating each material particular, need supplementary research. First of all it concerns the influence of technological parameters two-temperature annealing on the formation of defect structures and the effect of point defects on the physical and chemical properties of cadmium telluride and lead.

Using the method that based on minimizing the thermodynamic potential of "crystal-pair as a function of concentration of defects in this work were calculated equilibrium concentration of point defects free charge carriers and the degree of deviation from stoichiometry of CdTe, PbTe, it depend of technological factors two-temperature annealing (annealing temperature T and vapor pressure of component). At the calculation used a model that takes into account practically all possible types of own point defects:  $V_A$ ,  $V_B$ ,  $A_i$ ,  $B_i$ ,  $B_A$ ,  $A_B$ , each of which may be in three charge states (neutral, one or twofold charged). The concentration of point defects were determined directly from the system of equations, which describe the equilibrium in two-phase two-component system of crystal - pair:

$$\pm\mu_{D_i}^s = \mu_i^g$$

where  $\mu_{D_i}^s$  – chemical potential of the defect and i - component (i = A, B),  $\mu_i^g$  – chemical potential of i-component in the pair. The chemical potential of the defects determined by the differentiation of Gibbs energy of the crystal of concentrations of defects.

In the investigation resulted it was identified the dominant types of defects in material with metal or chalcogen excess. Theoretically calculated the concentrations of free carriers and the degree of deviation from stoichiometry of CdTe, PbTe satisfactory agreement with experimental data in a wide range of vapor pressure components and annealing temperature T.

*This work is partially financed by State Fund of Fundamental Researches of State Agency for Science, Innovation and Information of Ukraine (State registration № 0110U007675).*

## Features investigated the influence of Bi, Sb on the kinetic parameters of compounds IV-VI semiconductor crystals

Freik D.M., Dzumedzey R.O., Mateik G.D.<sup>1</sup>, Gevak T.P., Kotyk M.V.

*Vasyl Stefanyk Precarpathian National University, Ivano-Frankivsk, Ukraine*

<sup>1</sup>*Ivano-Frankivsk National Technical University of Oil and Gas, Ivano-Frankivsk, Ukraine*

Lead Telluride is a basic material for a thermionic energy converters, photodetectors, and radial structures of the middle and far infrared spectrum. Impurities periodic table group V (Sb, Bi) differently affect the energy spectrum of electrons in PbTe, which is associated with amphoteric properties. Exchange of electrons between the band and impurity levels leads to momentum scattering of charge carriers. This causes a change in carrier mobility, which is especially noticeable when the Fermi level lies within the peak density of states of impurity levels. For the analysis of these processes is appropriate variational procedure.

The research, based on a variational principle defined temperature and concentration dependences of charge carrier mobility for crystal PbTe, doped with Bismut.

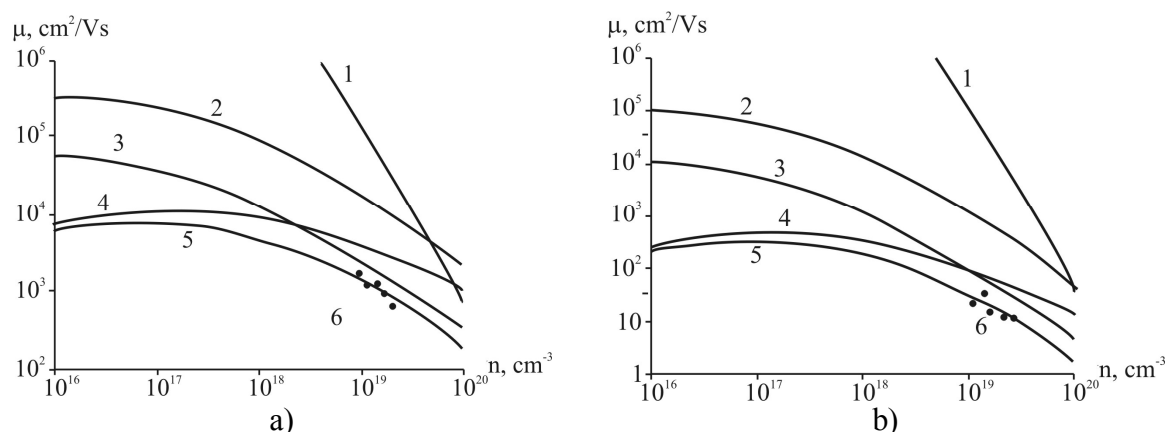


Fig. 1. Concentration dependence of charge carrier mobility for PbTe:Bi impurity concentration 0.25 at%. Bi, taking into account the scattering of carriers on short-range potential vacancies (1), acoustic phonons (2), impurity potential (3), optical phonons (4), 5 - total scattering taking into account (1) - (4) and 6 - experimental data. Temperature, K: 77 (a) and 300 (b).

Concentration dependence of charge carrier mobility (Fig. 1) indicate that with increasing temperature impurity scattering on the atoms cease to be exclusively dominant (observed at lower temperatures). When approaching to room temperature scattering on optical phonons has a commensurate contribution to the overall mobility of carriers. This is due to the fact that most impurity atoms are ionized and the Fermi level stabilizes.

*Work partially funded by State Committee of Science and Notice of Ukraine (state registration number 0110U007675).*

## **Changing kinetic parameters of IV-VI thin films during their holding in air**

Freik D.M., Dzundza B.S., Kostjuk O.B., Letsyn R.B.,  
Arsenych I.I., Gatala I.B.

*Vasyl Stefanyk PreCarpathian National University, Ivano-Frankivsk, Ukraine*

Lead chalcogenides thin films – promising materials for creating detectors and radiation sources in the infrared light spectrum as well as thermoelectric materials in high temperatures (500-700 K). It was found that their properties are defined by the technological factors of the growing process, and conditions of their subsequent operation.

In the research the changes in kinetic parameters of lead telluride films of different thickness at long holding time in the air are examined.

Films for research were received from the vapor phase by open evaporation in vacuum on polyamide tape substrates. Measurements of electrical parameters of films was in air at room temperature in stationary magnetic fields. For each sample series of measurements over time for about one year were carried out.

The received dependences of conductivity and the Hall coefficient for PbTe film on the thickness show that while increasing of film thickness regardless of time of air exposure conductivity increases with access to the full when thickness of about 0.8 microns. For aged in air for several days' films while thickness reducing the Hall coefficient also decreases, the concentration of p-type carriers increases, due to the acceptor influence of adsorbed oxygen and formation of concentrated of p-type carriers layer on the surface. At long holding time in air (about 1 year) with decreasing of film thickness  $R_H$  increases and concentration of current carriers decreases respectively, which indicates a small rate of diffusion of oxygen deep into the surface and subsequent diffusion of lead to surface which compensates the acceptor influence of oxygen.

For the quantitative assessment of the conductivity of the near-surface layer of the films its appropriate to analyze electrical properties by Petrits' two-layer model, which allowed to determine the dependence of the surface layer thickness on the air exposure time and average speed of oxidation at each stage.

In the initial stages of exposure oxidation rate is significant, but in the sequel it sharply decreases, and during the first day it becomes negligible. This fact also indicates the difference of oxidation mechanisms at an early stage and during prolonged exposure in the air.

*This work is partially financed by NAS of Ukraine (State registration № 0110U006281) and Ministry of education and science, youth and sport of ukraine (State registration № 0110U001766).*

## Mechanisms of formation and defect subsystem of solid solutions based on zinc chalcogenides

Freik D.M., Gurgula G.Y., Freik N.D., Vadyuk M.P., Vintonyak T.P., Zinyuk R.R.

*Vasyl Stefanyk Precarpathian National University*

Sulfide and selenide Zn are the perspective materials which have broad application in manufacturing of the optical elements that operate in the visible and infrared wavelengths [1]. Significantly less are studied their solid solutions  $ZnSe_xS_{1-x}$  ( $0 < x < 1$ ). The interest regarding obtainment and research of the properties of sulfa-selenides Zn is determined by the possibility of variation of their properties with changing composition, which is important for creation of electroluminescence diodes in the yellow-green zone of the optical spectrum.

We proposed crystalquasichemical formulas, which determine the defective subsystem of solid solutions based on ZnSe and ZnS. For example, for a solid solution on the basis of n-ZnSe + n-ZnS the formula will look like:

$$\left( Zn_{(1-\alpha_1+\alpha_1\gamma_1)x+(1-\alpha_2+\alpha_2\gamma_2)(1-x)}^{x''} V_{\alpha_2(1-\gamma_2)(1-x)}^{''} \right)_{Zn} \left( V_{Zn}^{''} V_{Se}^{\bullet} \right)_{\alpha_1(1-\gamma_1)x}^{\bullet}$$

$$\left( Se_{(1-\alpha_1)x}^x S_{(1-\alpha_2)(1-x)}^x V_{\alpha_1\gamma_1 x}^{\bullet} V_{\alpha_2(1-x)}^{''} \right)_A$$

$$\left( Zn_{\alpha_1(1-\gamma_1)(1-\delta_1)x+\alpha_2(1-\gamma_2)(1-\delta_2)(1-x)}^{\bullet} Zn_{\alpha_1(1-\gamma_1)\delta_1 x+\alpha_2(1-\gamma_2)\delta_2(1-x)}^{''} \right)_i +$$

$$+(\alpha_1(1+\gamma_1+\delta_1-\gamma_1\delta_1)x+\alpha_2(1+\gamma_2+\delta_2-\gamma_2\delta_2)(1-x))e' + \alpha_1 x h^{\bullet}$$

Where  $Zn_{Zn}^x$ ,  $S_A^x$ ,  $Se_A^x$  – zinc, sulfur and selenium in the knots of the crystal lattice,  $V_{Zn}^{''}$  – two-charged zinc vacancies,  $V_S^{\bullet}$  – one-charged sulfur vacancy,  $V_{Se}^{''}$  – two-charged selenium vacancies,  $Zn_i^{\bullet}$  – one-charged internodal atom of zinc,  $Zn_i^{''}$  – two-charged internodal atoms of zinc,  $\alpha_1$  – atomic fraction of Zn in the crystals of ZnSe,  $\alpha_2$  – atomic fraction Zn in ZnS crystals,  $\gamma_1$  and  $\gamma_2$  – fraction of substituted zinc vacancies in the cation sublattice ( $Zn_{Zn}^{''}$ ) ( $0 \leq \gamma \leq 1$ ),  $\delta_1$  i  $\delta_2$  – fraction of the two-charged internodal zinc ( $0 \leq \delta \leq 1$ ),  $e'$  – concentration of the electrons, “ $\bullet$ ”, “ $''$ ”, “ $x$ ” – positive, negative and neutral charges.

The obtained dependences of concentrations of defects ( $N_D$ ) and free current carriers ( $n_H$ ) of solid solution composition ( $x$ ), confirm, that for the compositions  $0 < x < 0,5$  dominate the same point defects as in ZnS, and for compositions  $0,7 < x < 1$  prevail the defects which are inherent for ZnSe. For  $ZnSe_xS_{1-x}$  crystals in the composition zone  $0,5 < x < 0,7$  one can observe the defects typical for ZnS, as well as for ZnSe.

*This work to execute according department project (State registration № 0107U006768).*

1. Морозова Н.К., Кузнецов В.А., Рыжиков В.Д. и др. *Седенид цинка. Получение и оптические свойства.* – М. Наука. – 1992. – 96 с.

## **Topology of thin films and nanostructures II-VI, IV-VI received vapor phase methods**

Freik D.M., Sokolov O.L., Bilina I.S., Nesteruk O.R.

*Vasyl Stefanyk Precarpathian National University, Ivano-Frankivsk, Ukraine*

Narrow-gap semiconductor IV-VI is the object of study for a long time as an interesting model in terms of objects and their practical use as optoelectronic devices for medium and far infrared optical spectrum.

In work the results of some studies by atomic force microscopy growth mechanisms of nanostructures IV-VI compounds obtained by hot wall and open evaporation.

*Hot-wall method.* Introduction of heat shield between the evaporator and the substrate holder contributes to the fact that not only direct but also reflected molecules condense on the substrates. Thus thermal screen plays the role of surface sources, resulting in significantly increased rate of condensation at constant temperature evaporation.

Some results of surface morphology of PbTe nanostructures on mica chips (0001) make it possible to establish some regularities in the formation of epitaxial nanostructures, depending on growth temperature and thickness. In particular, low deposition temperature  $T_s = 353$  K contribute to the formation of nanocrystals with prevalence rates of growth in the tangential direction to the substrate surface. Rising temperatures increase to  $T_s = (380-408)$  K leads to a more homogeneous nanocrystals as in form and with linear dimensions in the azimuth direction and normal to the substrate surface. Further dramatic increases deposition to  $T_s = 633$  K leads to growth against a background of well-formed crystals of diameter (0,2-0,8) mkm and height (100-400) nm of some "giants" of (1,6-1,8) microns in basis and up to (300-1200) nm.

*Open evaporation in a vacuum.* The possibilities of formation of PbTe nanostructures open evaporation in a vacuum deposition on a pair of single crystals of silicon oxide film PbTe/SiO<sub>2</sub>-Si. The temperature of deposition (substrate) varied within  $T_s = (320-570)$  K. The temperature of the evaporation batch advanced synthesized compounds PbTe survive constant and was spelling  $T_e = (970 \pm 10)$  K. The thickness of condensate (10-40) nm asked at the time of deposition speed  $(1-2) \cdot 10^{-2}$  nms<sup>-1</sup>.

On the basis of two-and three dimensional images of their topological features can be seen that for given conditions of deposition of nanostructures are formed as separate entities columnar foundation that statistically evenly cover the surface of the substrate. The sizes of these nanostructures, to some extent, depend on technological factors of a (temperature, deposition time) and change from ten to several tens of nanometers. Thus with increasing lateral dimensions of nanostructures their height linearly increases.

Analogous research presented for nanostructures based on CdTe.

*This work is partially financed by Ministry of education and science, youth and sport of Ukraine (State registration № 0110U001766).*

## Nonstoichiometry and crystal-chemistry of defects in lead chalcogenides crystals

Freik D.M., Turovska L.V., Andriishyn I., Pokryshka O.Ya, Hrubyak O.B.

*Vasyl Stefanyk PreCarpathian National University, Ivano-Frankivsk, Ukraine*

The type and concentration of current carries for the area of impurity conduction is determined by own points defects of crystal lattice in IV–VI semiconductors where impurity content does not exceed a background value [1].

Lead chalcogenides have conductivity of n-type at surplus of lead in relation to the stoichiometric composition and conductivity of p-type at surplus of chalcogen. In the case of lead telluride the maximal values of concentration of current carriers are:  $1.5 \cdot 10^{19} \text{ cm}^{-3}$  of electrons at 993 K and  $5 \cdot 10^{18} \text{ cm}^{-3}$  of holes at 1053 K [1, 2].

In present work crystalquasichemical formulae are represented for n- and p-PbTe crystals with the complex spectrum of point defects in cation sublattice. The mechanisms of self-doping n-PbTe by tellurium and p-PbTe by lead have been analysed and the terms of realization of n-p and p-n-conversion have been determined respectively.

Analysis of computational results of defect concentration have showed that in the case of n-PbTe Hall concentration ( $n_H$ ), concentrations of current carriers (n) and concentration of singly and doubly-charged cation vacancies ( $V_{Pb}^-, V_{Pb}^{2-}$ ), interstitials lead ( $Pb_i^{2+}$ ); doubly-charged anionic vacancies ( $V_{Te}^{2+}$ ) vary insignificantly according to increase of superstoichiometric lead.

With increase of quantity of disproportionation of the charge state of cation vacancies the concentration of interstitials lead, singly and doubly-charged vacancies of lead increase. Concentrations of other defects remain virtually unchanged.

With increase of quantity of interstitials lead the concentrations of cation vacancies increase. Hall concentration, concentrations of current carriers and anionic vacancies change insignificant. Concentrations of interstitials lead, singly and doubly-charged vacancies of lead are much less than concentrations of current carriers and vacancies of tellurium.

Analogical analysis has been made for p-PbTe.

*This work to execute according department project (State registration № 0107U006768).*

1. Ravich Yu.I., Efimova B.A., Smirnov I.A. Methods of investigation of semiconductors in the application to lead chalcogenides PbTe, PbSe, PbS. – M. Science, 1968. – 84 p.
2. Abrikosov N.Kh., Shelimova L.Ye. Semiconductor materials based on  $A^{IV}B^{VI}$  compounds. – M. Science, 1975. – 196 p.

## **Modeling of thickness dependences of thermoelectric parameters for compounds IV-VI**

Freik D.M., Wojcik V., Yurchyshyn I.K., Nadraga O.R.

*Vasyl Stefanyk Precarpathian National University, Ivano-Frankivsk, Ukraine*

Thickness dependences of kinetic parameters of quantum wells (QW) based on IV-VI compounds show non-monotonic oscillatory behavior that is associated with size quantization due to carrier movement restrictions in one direction [1-3].

In work on basis of theoretical model of rectangular quantum well with infinitely high barriers the dependences of thermoelectric parameters on nanostructures thickness of lead chalcogenides (PbTe, PbSe, PbS) are investigated. Shown that in such structures it has place nonmonotonous, oscillation shange of Seebeck coefficient  $S$  with well thickness. Basing on the oscillations period  $\Delta d_{\text{exp}}$  the approximation of theoretical  $d$ -dependencies of Seebeck coefficient  $S$  with experimental was carried out and determined the Fermi energy in the respective structures.

Revealed that thickness dependence of the Seebeck coefficient  $S$ , based on model of QW with infinitely high walls, is characterized by breaks with some period.

Mismatch between the theoretical and experimental oscillation amplitudes of Seebeck coefficient  $d$ -dependencies explained by the simplified model of quantum well.

Shown that values  $\Delta d_{\text{exp}}$  of oscillations period are equal to QW thickness  $d_{\text{min}}$ , when the bottom of lowest subband coincides with the Fermi energy  $E_F$ . This thickness  $d_{\text{min}}$  was explained like the minimum QW thickness, when quantum size effects are the main factor, that determines the nonmonotonous behaviour in thickness dependencies of thermoelectric parameters of the relevant structures.

*This work is partially financed by State Fund of Fundamental Researches of State Agency for Science, Innovation and Information of Ukraine (State registration № 0110U007676).*

1. Rogacheva E.I., Nashchekina O.N., Vekhov Y.O., Dresselhaus M.S., Cronin S.B., Effect of thickness on the thermoelectric properties of PbS thin films // *Thin Solid Films*. – 2003. – № 423. – P. 115-118.
2. Rogacheva E.I., Tavrina T.V., Nashchekina O.N., Grigorov S.N., Nasedkin K.A., Quantum size effects in PbSe quantum wells // *Applied Physics Letters*. – 2002. – V. 80, № 15. – P. 2690-2692.
3. Rogacheva E.I., Nashchekina O.N., Grigorov S.N., Dresselhaus M.S., Cronin S.B., Oscillatory behaviour of the transport properties in PbTe quantum wells // *Institute of Physics Publishing. Nanotechnology*. – 2003. – №14. – P. 53-59.

## Influence of strong inclined anisotropy on the phase states of ultrathin magnetic films

Fridman Yu.A., Gorelikov G.A., Klevets Ph.N.

*V.I. Vernadskiy Taurida national university, Simferopol, Ukraine*

The terms like  $S_i \beta_{ij} S_j$  determining the single-ion anisotropy (SA) energy can be separated in the spin Hamiltonian of the magnetic dielectrics at microscopic description. It is of interest to investigate the spin-1 magnetically ordered crystal when the non-zero components of SA are not only  $\beta_{zz}$ , but also  $\beta_{zx} = \beta_{xz}$ . The most interesting situation is when the constants of SA exceed the constant of exchange interaction. Such a model describes the inclined anisotropy in the ZOY-plane with the easy-axis of magnetization making the angle  $\varphi_0$  with the OZ-axis. This model quite adequately describes the SA energy of the disoriented films. The Hamiltonian of the magnetic investigated has the following form:

$$\mathcal{H} = -\frac{1}{2} \sum_{f, f'} [J(f - f') \delta_{ij} + V^{ij}(f - f')] S_f^i S_{f'}^j + \frac{\beta_{zz}}{2} \sum_f (S_f^z)^2 - \frac{\beta_{zx}}{2} \sum_f (S_f^x S_f^z + S_f^z S_f^x),$$

where  $J(f - f')$  is the constant of bilinear exchange interaction;  $f$  is the number of a crystal site;  $S_f^i$  is the  $i$ th component of the spin operator on the  $f$ th site;  $\beta_{zz} > 0$  is the constant of the in-plane SA;  $\beta_{zx} > 0$  is the constant of the easy-axis SA;  $V^{ij}$  are the components of the magnetic dipole interaction tensor. The further evaluations will be carried out in the low-temperature limit ( $T = 0$ ) when the properties of strong SA are exhibited most evidently.

As our investigations have shown the ferromagnetic phase realizes at weak anisotropy. In this phase the magnetic moment is oriented in the ZOY-plane (FM<sub>ZX</sub>-phase), and the equilibrium angle is determined by the SA constants ( $\text{tg } 2\varphi_0 \sim \beta_{zx} / \beta_{zz}$ ). If the constants of the SA anisotropy exceed the constant of the exchange interaction, then the quadrupolar phase realizes in the system. The average value of the spin per one site equals zero in this phase, but there is spontaneous breaking of the continual symmetry related with the non-trivial quadrupolar averages. Besides, we have investigated the possibility of the domain phase realization.

## Trapping and delocalization of charge carriers in CdI<sub>2</sub>-PbI<sub>2</sub> crystal system

Galchynsky O.V.<sup>1</sup>, Gloskovska N.V.<sup>2</sup>, Yarytska L.I.<sup>3</sup>

<sup>1</sup>*Lviv Medical Institute, Lviv, Ukraine*

<sup>2</sup>*Bogolyubov Institute for Theoretical Physics, Kyiv, Ukraine*

<sup>3</sup>*Lviv State University of Vital Activity Safety, Lviv, Ukraine*

Isomorphic cadmium and lead iodide layered crystals exhibit different stable polytypic modifications – 4H and 2H, respectively. Recent electron-force microscopy investigations have shown that in CdI<sub>2</sub>-PbI<sub>2</sub> crystal system lead iodide impurity incorporates into CdI<sub>2</sub> lattice in the form of 4H polytype nanoparticles.

In the present work we study the trapping centers of CdI<sub>2</sub>-PbI<sub>2</sub> in the temperature range 80-305 K. Analysis of spectral sensitivity of CdI<sub>2</sub>-PbI<sub>2</sub> photoelectret state in the range 3-4 eV allowed us to define five temperature intervals with specific mechanisms of charge carrier delocalization:

1. at the lowest considered temperature direct band-to-band excitation of CdI<sub>2</sub> lattice prevail;
2. at the temperatures from 120 to 140 K transitions to indirect exciton band of CdI<sub>2</sub> dominate;
3. in the range 140-240 K the main contribution is made by high-energy PbI<sub>2</sub> cationic excitons;
4. in the interval 240-280 K indirect band-to-band transitions in CdI<sub>2</sub> are effective;
5. beyond 290 K delocalization mechanism is associated with linear structure defects of the crystal system and, possibly, electron transitions from the lower PbI<sub>2</sub> valence sub-band to the conductivity band.

Two pairs of trapping centers with different polarity were detected by combined method of thermo- and photostimulated depolarization of photoelectret state generated in CdI<sub>2</sub>-PbI<sub>2</sub> crystal at 80 K. Characteristics of these centers were compared with those of the trapping sites in PbI<sub>2</sub> crystals. This enabled us to identify CdI<sub>2</sub>-PbI<sub>2</sub> electron traps as Pb<sup>+</sup>-centers in 2H and 4H PbI<sub>2</sub> polytypes.

## Crystal-chemistry of point defects and their complexes and thermoelectric properties of solid solutions

Galuschak M.O.<sup>1</sup>, Boryk V.V.<sup>2</sup>, Tkachuk A.I.<sup>1,2</sup>

<sup>1</sup>*Ivano-Frankivsk National Technical University Oil and Gas;*

<sup>2</sup>*Vasyl Stefanyk Precarpatian National University, Ivano-Frankivsk, Ukraine*

On the basis of unique crystal-chemistry approaches which consider a complex spectrum of point defects in PbTe ( $V_{Pb}^{2-}$ ,  $V_{Pb}^{-}$ ,  $V_{Te}^{2+}$ ,  $Pb_i^{2+}$ ,  $Te_i^0$ )  $V_{Sn(Ge)}^{2-}$ ,  $V_{Sn(Ge)}^{4-}$ ), in p-SnTe (GeTe), disproportionation charge conditions of M (Ga, In, Tl) impurities of in Plumbum Telluride crystals according to doping mechanisms of n-and p-PbTe: M for the first time are explained, formation of solid solutions in systems n-and p-PbTe-MTe ( $M_2Te_3$ ) and their influence on physical and chemical properties of a material.

It is shown, that dominant doping of M(Ga, In, Tl) plumbum telluride it is necessary to consider as mechanisms replacement cation vacancies in crystals p-PbTe  $\langle Te \rangle$ : M, or completion cation sublattice, in n-PbTe  $\langle Te \rangle$ : M from the account of size disproportionation charge conditions of an impurity and their concentration N. Under conditions of realization thermodynamic n-p-(PbTe  $\langle Pb \rangle$ : Tl) and p-n-(PbTe  $\langle Te \rangle$ : In) transitions the certain value disproportionation charge conditions of impurity Z, which make  $Z = 0.56$  ( $N_{Tl^{1+}} = 1.7 \cdot 10^{19} \text{ cm}^{-3}$ ,  $N_{Tl^{3+}} = 1.3 \cdot 10^{19} \text{ cm}^{-3}$ ) and  $Z = 0.37$  ( $N_{In^{1+}} = 1.1 \cdot 10^{19} \text{ cm}^{-3}$ ,  $N_{In^{3+}} = 1.9 \cdot 10^{19} \text{ cm}^{-3}$ ) accordingly. Thus with increase in size of an initial deviation from stoichiometry on the side tellurium in basic matrix PbTe the size disproportionation ions impurity decreases.

For the first time are offered the crystal-quasichemical formulas, calculations and experimental researches dependences concentration of point defects, free carriers and Hall's concentration of charge from value of a deviation from stoichiometry and structure in n-PbTe  $\langle Pb \rangle$ : Mn(Cr), p-PbTe  $\langle Te \rangle$ : Mn(Cr), PbTe-MnTe ( $MnTe_2$ , CrTe,  $Cr_3Te_4$ ), on the basis of which established defect subsystem and nature of doping and formations of solid solutions also conditions of realization thermodynamic p-n-transition are certain.

It is established that by the basic physical and chemical and technological directions of thermoelectric parameters of materials optimization of on the basis of PbTe, SnTe, GeTe, there is a reduction of size of heat conductivity ( $\chi$ ), growth of electric conductivity ( $\sigma$ ) and activity of dot defects and maintenance of noncentral accommodation ions of impurity in solid solutions which opens prospect of their use in devices of alternative energy sources and refrigerating modules.

## On the possibility of using lithium-iron spinels replaced by titanium as a cathode material of chemical power sources

Gasuyk I.M., Grabko T.V.

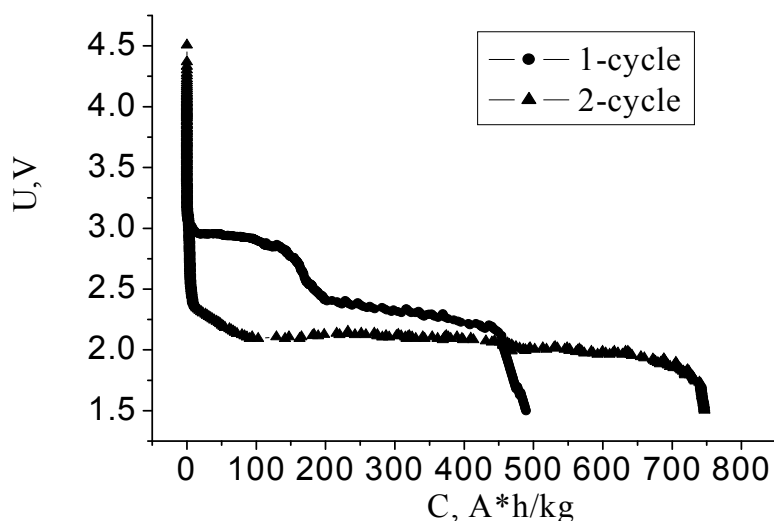
*Vasul Stefanyk Precarpatian National University, Ivano-Frankivsk, Ukraine*

The search of new, cheap, environmentally safe cathode materials that have a stable structure and characteristics for a large number of charging-discharging cycles is one of the main problems of lithium storage devices technology. The use of natural and synthetic minerals, such as  $\text{MoO}_3$ ,  $\text{SO}_2$ ,  $\text{SOCl}_2$ , and  $\text{LiNiO}_2$ , and lithium manganese spinel  $\text{LiMn}_2\text{O}_4$  is the most appropriate way for solving this problem. The main drawbacks of these materials are first of all negative cycle and reproducibility of compositions and structural characteristics which are determined by using of synthesis methods.

The mentioned problem is being solved by using a cathode active material as a lithium-iron spinel replaced by titanium ions  $\text{Li}_{0,63}\text{Fe}_{2,26}\text{Ti}_{0,11}\text{O}_4$  the material was received by solid-phase synthesis of mixtures of powders like  $\text{Fe}_2\text{O}_3$ ,  $\text{TiO}_2$  (rutile) and  $\text{LiCO}_3$ , taken in appropriate stoichiometric ratios. Final sintering was carried out at the temperature of 1473 K followed by quenching in water.

X-ray analysis of synthesized samples showed the monophasic structure of obtained spinel structure.

As a result of electrochemical studies it was shown that the specific value for the electrochemical capacitance of the first discharge cycle is 453 A·h/kg. Discharge curve of the second cycle has smoother monotonically decreasing



character and the intercalation peaks seen in the first charge-discharge cycle is gradually reduced until their disappearance. Capacity of the second cycle is characterized by higher values of 746 A·h/kg compared with the first one, that is gained due to an optional "attracting" of the matrix lithium ions in the processes of

electrochemical intercalation.

These samples obtained by ceramic method have high values of specific capacity, thus making such materials having prospects for use as a cathode of lithium electrochemical power sources.

## The study of $(\text{As}_2\text{S}_3)_{100-x}(\text{Sn}_2\text{P}_2\text{S}_6)_x$ glasses crystallization

Gasynets S.M.<sup>1</sup>, Solomon A.M.<sup>2</sup>, Azhniuk Yu.M.<sup>2</sup>, Yasinko T.I.<sup>1</sup>,  
Guranich O.G.<sup>1</sup>, Shpyrko G.N.<sup>1</sup>, Gomonnai A.V.<sup>2</sup>, Rubish V.M.<sup>1</sup>

<sup>1</sup>*Uzhgorod Scientific-Technological Center of the Institute for  
Information Recording, NASU, Uzhgorod Ukraine*

<sup>2</sup>*Institute of Electron Physics, NASU, Uzhgorod, Ukraine*

$\text{Sn}_2\text{P}_2\text{S}_6$  (tin hypothiodiphosphate) is well-known ferroelectric-semiconductor. Data about obtaining it in the form of glass are missing. In turn, glassy  $\text{As}_2\text{S}_3$  is obtained without any special difficulties. So, it was expected that introducing  $\text{As}_2\text{S}_3$  into  $\text{Sn}_2\text{P}_2\text{S}_6$  would considerably increase glass forming ability of mixed melts  $(\text{As}_2\text{S}_3)_{100-x}(\text{Sn}_2\text{P}_2\text{S}_6)_x$  and thus broaden the range of materials in which crystalline inclusions with ferroelectric properties in a glassy matrix can be obtained. In the present report the results of investigation of crystallization processes in  $(\text{As}_2\text{S}_3)_{100-x}(\text{Sn}_2\text{P}_2\text{S}_6)_x$  ( $0 \leq x \leq 40$ ) glassy alloys are given.

Glassy alloys were prepared by vacuum melting method of corresponding mixture of components in quartz ampoules. The homogenization temperature and time of melts were 940-1100 K and 36-48 hours, respectively. Cooling of melts was carried out in the air ( $0 \leq x \leq 10$ ) and into cold water.

Typical temperatures of heat effects  $T_g$ ,  $T_c$ ,  $T_m$  were determined by differential-thermal method at heating rates 3 and 6 K/min. Investigations of X-ray diffraction patterns of glassy, crystallized and crystalline materials were carried out on DRON-3 X-ray apparatus ( $\lambda = 1.5418\text{\AA}$ ). Raman spectra were investigated with help the of DFS-24 spectrometer on the  $\lambda = 0.63 \mu\text{m}$ . Dielectric permittivity  $\varepsilon$  and tangent of dielectric loss angle  $\text{tg } \delta$  of glasses and glass ceramics were measured at the frequency of 1.0 MHz and the measuring fields of 1.0 and 0.1 V/cm in the temperature range 80-600 K. The dielectric permittivity was measured within the accuracy of  $\pm 3\%$ ,  $\text{tg } \delta$  – within  $\pm 10\%$ .

It was established that all investigated glasses have a nanoheterogeneous structure. Glassy matrix is formed by only binary structural groups with heteropolar and homopolar bonds.

It has been found that in glasses with  $20 \leq x \leq 40$  in the conditions of continuous heating in the range  $T_g$ - $T_c$  crystallization with predominant mechanism of stable phase  $\text{Sn}_2\text{P}_2\text{S}_6$  separation is taking place. The mechanism of formation of crystalline inclusions of  $\text{Sn}_2\text{P}_2\text{S}_6$  in glassy matrix is discussed.

Formations in the glass matrix at heating nanosized crystals of tin hypothiodiphosphate and their growth are accompanied by anomalies on the  $\varepsilon(T)$  and  $\text{tg } \delta(T)$  dependences. Glass crystallization is accompanied by sharp increase of  $\varepsilon$  and  $\text{tg } \delta$ .

The effect of heat and time related treatment regimes on structure and dielectric properties of crystallized  $(\text{As}_2\text{S}_3)_{100-x}(\text{Sn}_2\text{P}_2\text{S}_6)_x$  glasses was determined.

## **Ab-initio study of atomic adsorption on graphene**

Gorbenko V.I.

*Classical Private University, Zaporizhzhya, Ukraine*

The graphite monolayer named as graphene has attracted interest due to the possible application in new carbon-based nanoelectronics [1,2]. Therefore the understanding of chemical interaction of various chemical species of particles with graphene is both scientifically and technologically important. The main aim of this work was to define the preferred adsorption sites for various atoms and to obtain the geometry characteristics of these.

Ab-initio calculations have been performed by using GAMESS package [3] on computers cluster of National Technical University “KPI”. The adsorption of following atomic species on graphene was simulated: H, Be, C, N, O, F, Na, Mg, Al, Si, P, S, Cl, K, Zn, Ga, Ge, As, Se, Br. The 88 carbon atoms in the hexagonal cells and 36 hydrogen atoms at the cluster perimeter have been included in the model of graphene sheet. Before simulation of atoms adsorption the model of graphene sheet was geometric optimized.

The performed calculations showed three sites of possible adsorption centers: over middle of the C-C bond (bridge), over single C-atom and over center of hexagonal cell. The type of the site of adsorption center is sensitive to the atomic species of adsorbate. The accordance between the atomic species and the site of its adsorption has been established.

The binding of adsorbate atom to graphene atoms leads to a reconstruction of graphene sheet. More significant changes of atomic structure occur in the adcenter and smaller changes are in second circle from the site of adsorption. The adsorption of atoms both over single C-atom and over C-C bond shows a weakening of shorter C-C bond in adcenter.

The analysis of both the changes of molecular orbitals and the energy characteristics of species adsorption has been performed.

1. Geim A.K., Novoselov K.S. The rise of graphene // *Nature Materials*. – 2007. – 6. – P. 183-191.
2. Chen Zh., Lin Yu-Ming, Rooks M.J. and Avouris Ph. Graphene Nano-Ribbon Electronics // *Physica E: Low-dimensional Systems and Nanostructures*. – 2007. – Vol. 40/2. – P. 228-232.
3. Gordon M.S., Schmidt M.W. Advances in electronic structure theory: GAMESS a decade later // in "Theory and Applications of Computational Chemistry: the first forty years" by ed. C.E. Dykstra, G. Frenking, K.S. Kim, G.E. Scuseria. – 2005. – Elsevier, Amsterdam. – P. 1167-1189.

## **Dendrite Ni self-similar structures received by electrodeposition in the external magnetic field**

Gorobets S., Gorobets O., Dvoynenko O., Cherednychenko D., Lebeda G.

*National technical university of Ukraine "KPI", Kyiv, Ukraine*

The functional surfaces of ferromagnetic materials or their alloys with the ramified structure come into the considerable notice of researchers through their potential possibilities. Such surfaces are perspective for creation of high-gradient ferromagnetic attachments for magnetic separation [1]. Separate elements of the ramified structures with size of 500  $\mu\text{m}$  it is possible to use such as implants in medicine [2].

The surfaces of attachments and implants with numerous sharp edges in the external magnetic field generate the high-gradient magnetic fields and serve as the focus of fascination of low magnetic liposome's, magnetic marked bio objects, ions of heavy metals, radionuclide's and so on [3].

For effective work elements of functional surfaces must be with equal size with target objects. Therefore an important task is a control of the sizes and forms of separate elements of structures.

One of the simplest by the technical methods of receiving the ramified dendrite systems is a method of electrodeposition.

In the work was investigated the influence of magnetic field and previous magnetizing of lining-wire on the sizes of dendrite structures which was formed on lining at the electrodeposition of nickel.

It was shown that an applying of magnetic-field during an electrodeposition, and also change of magnetic properties of lining substantially influence on the structure of the besieged layers of nickel. At the use of such ramified structures as high-gradient ferromagnetic attachments considerably change their descriptions such as dirt capacity, consumption of materials, characteristic sizes of separate elements of attachment, and consequently and efficiency of separation of working liquids and exception of special target objects.

1. Friedman G., Yellen B. Magnetic separation, manipulation and assembly of solid phase in fluids.// *Current Opinion in Colloid & Interface Science*. 2005. – V. 10, № 3-4. – P. 158-166.
2. Misael O. Aviles, D. Ebner, James A. Ritter In vitro study of magnetic particle seeding for implant-assisted-magnetic drug targeting: Seed and magnetic drug carrier particle capture // *Journal of Magnetism and Magnetic Materials*. – 2009. – V. 321.– P. 1586-1590.
3. Laura A.Worl, Dennis D.Padilla, F.Coyne Prenger , Dallas D. Hill, Thomas L. Tolt High-gradient Magnetic Separation (HGMS) Plays an Important Role in Radioactive Waste Remediation // *The Actinide Research Quarterly. Nuclear Materials Technology Division*.– 1999.– P. 1-3.

## **High gradient ferromagnetic matrix in the form of self alike dendritic Ni nanostructures parameters research**

Gorobets S.V., Dvoynenko O.K., Mykhailenko N.O.

*National Technical University of Ukraine "Kyiv Polytechnic Institute", Kyiv, Ukraine*

Current level of nanotechnology allows to create unique tools for medicine and biotechnology of purification and separation of liquid media (blood, bone marrow, water, etc.) due to the magnetically operated sorbents and magnetic separators using [1]. Today it is safe to say that the future of medicine and biotechnology is closely related to the use of nanomaterials and nanotechnology methods. The nanobiotechnology is a research direction that integrates the achievement of nano- and biotechnology. High-gradient ferromagnetic matrixes (HGFM) are used for effective removing of magnetically labeled micro- and nanoobjects by magnetic separators. The magnetic separators with HGFM with branched structure of the surface are used for this.

The economically sound and simple methods of producing of HGFM was suggested by the method of the plating of the nickel dendrites in external magnetic field on the steel net and on the plate received by the method of the magnetically operated corrosion [2, 3].

After the self alike dendritic Ni nanostructures HGFM receiving their parameters were determined. For future application in the magnetic separators various filtration characteristics as contaminant capacity and filterability was tested. Also there were determined different technological parameters for the most effective working media purification. As we were working with different magnetically operated bioobjects it was important to determine their magnetic properties as magnetic susceptibility.

HGFM, received by methods referred above, have small materials consumptions, high contaminant capacity, small hydrodynamic resistance and are able to provide with high fineness of the cleaning of working media in biology and medicine.

1. Направленный транспорт лекарственных средств с помощью липосом / Т.Т. Березов, Н.В. Яглова, Т.Б. Дмитриева, Ю.А. Жирков, В.П. Чехонин // Вестн. Рос. акад. мед. наук. – 2004. – № 3. – С. 42-46.
2. Preparation of high-gradient ferromagnetic matrices for magnetic filters (separators) with fractal surface structure by magnetoelectrolysis / Gorobets S.V., Gorobets O.Yu., Bylo O.N., Potyomkin M.M. // Journal of Functional Materials –2009. – Vol. 16, № 3. – P. 347-350
3. Очищення стічних вод від іонів купрум (II) магнітокерованим біосорбентом за допомогою високоградієнтних ферромагнітних насадок / Горобець С.В., Горобець О.Ю., Двойненко О.К. Михайленко Н.О. // Наукові вісті НТУУ "КПІ", – 2010 – 3. – С. 21-25.

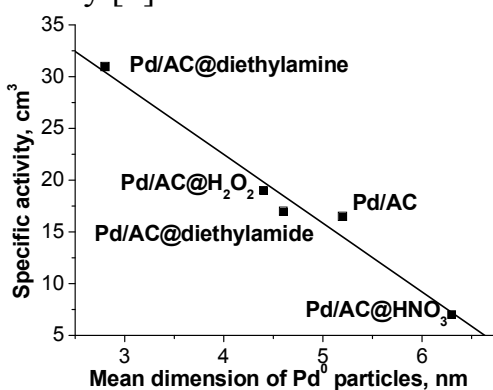
## The surface functionalization of activated carbon carries for nano-scale Pd catalysts

Grischenko L., Bezugla T., Zaderko O., Radkevich V., Diyuk V.

*National Taras Shevchenko University, Kyiv, Ukraine*

The remarkable properties of nano-scale catalysts are caused by special structure of such fine formations. The creation of nano-scale catalytic systems for heterogeneous process such as hydrogenation, partial oxidation, dehydrogenation and others is the scientific and production problem.

Activated carbons (AC) possess an advantage over other carriers for catalysts due to unique adsorptive and chemical properties. As it was shown early [1] the size of Pd<sup>0</sup> active centers effects strongly on the catalytic activity of



heterogeneous AC/Pd catalysts with different pre-treatment (Figure). As it was ascertained the most active samples in model reaction of hydrogen oxidation were the ones modified with diethylamine.

An increased surface concentration of basic N-containing groups inhibits aggregation of Pd clusters resulting in an increased metal dispersion. Moreover, the treatment of the AC surface with CCl<sub>4</sub> and N-containing compounds lowers the hydrophilic properties of the carrier. So amination of the carbon surface is a perspective method for creation of nano-sized Pd catalysts.

The work was aimed to develop the methods and techniques for AC surface layer modification with N-containing groups trough the forerunning halogenations of substrates that makes possible to obtain the precursors for further substitution. The bromination of AC samples was carried out using solution of Br<sub>2</sub> / KBr or the liquid bromine. The chlorination was carried out at 450 °C with CCl<sub>4</sub> vapor. As it was shown such techniques ensure the insertion into AC surface layer the active halogen (0.5-1.0 mmol/g) that can be substituted by diethylamine, ethanolamine, sulfolanyl ethylenediamine, piperazine, ethylenediamine. The developed methods lead to obtaining AC basic derivatives with 0.5 mmol/g N-containing groups. They were appeared to be thermally stable: the maxima of basic centers desorption are in the range of 250-350 °C in dependence of the nature of N-containing groups.

1. Radkevich V., Senko T., Wilson K., Grischenko L., Zaderko A., Diyuk V. The influence of surface functionalization of activated carbon on palladium dispersion and catalytic activity in hydrogen oxidation // *Appl. Catal.* – 2008. – A 335. – P. 241-251.

## **Modification of nanocrystalline of wares from amorphous metallic alloys**

Hertsyk O.M.<sup>1</sup>, Bojchyshyn L.M.<sup>1</sup>, Kovbuz M.O.<sup>1</sup>, Pandiak N.L.<sup>2</sup>

<sup>1</sup>*Ivan Franko National University of Lviv, Lviv, Ukraine*

<sup>2</sup>*Ukrainian National Forestry University, Lviv, Ukraine*

One of the methods to get amorphous metallic alloys (AMA) from fusions is them ultrafast cooling by a flowspinning on a massive metallic drum and receipt amorphous alloy as a ribbon of the different measuring. By the grinding of annealed ribbons get alloys as powder. To such wares from amorphous metallic alloys characteristic high mechanical, magnetic and anticorrosive properties. However the local or complete heating of amorphous material in the process of forming of good assists heterogeneous crystallization and causes the loss of many physical descriptions. In such case it is actual to search methods of their renewal.

By the diffractometry (ДРОН-3) and cyclic voltammetry (Jaisse Potentiostat/Galvanostat IMP 88PC-R) methods were investigated the influence of heat treatment (670 K) and permanent magnetic field of 360 kA/m on a structure and electrochemical properties of AMA  $\text{Fe}_{92.7}\text{Ni}_{1.19}\text{Mo}_{0.97}\text{Nb}_{0.94}\text{Si}_{1.14}\text{B}_{3.06}$  and  $\text{Co}_{86.85}\text{Fe}_{3.58}\text{Mn}_{3.51}\text{Si}_{2.82}\text{B}_{3.24}$ .

In case of both samples heat treatment results in the increase of values of currents of corrosion and change of potential in a cathode field, and on diffractograms, for example  $\text{Co}_{86.85}\text{Fe}_{3.58}\text{Mn}_{3.51}\text{Si}_{2.82}\text{B}_{3.24}$  after a 24 sentinel annealing appears sharp peak, at  $S \approx$  of  $31.3 \text{ nm}^{-1}$ . Structural changes in the alloy, which is predefined by a thermal action, related to the relaxation processes, which is accompanied by the removal of remaining tensions and diminishing of surplus free volume.

By the cyclic voltammetry method it was set, that the exposition of the investigated samples in the magnetic field of 360 kA/m during 1440 min proceeds in anticorrosive descriptions of samples of amorphous alloys. In addition, influence of magnetic field results in strengthening of diffusion of metallic particles, what the nanostructural state of alloys and physical descriptions peculiar to pre-product recommence as a result of .

Obviously as a result of action of magnetic field clusters are formed, for example  $\alpha$ -Co. Directions of magnetized in these clusters are determined by the external magnetic field in which samples are placed after annealing, and in the real terms amorphous materials which yield to heat treatment during forming of wares.

Thus, operating of magnetic field on amorphous alloys on the basis of iron and cobalt, in which by heat treatment were broken primary structural descriptions, proceeds them to the initial state.

## Charge transport in the nanosystems based on conducting polymers

Horbenko Y.Yu., Konopelnyk O.I., Aksimentyeva O.I.,  
Demchenko P.Yu., Pavlyk M.R.

*Ivan Franko Lviv National University, Lviv, Ukraine*

Nanosystems based on conducting polymers doped by semiconductor or magnetic nanoparticles are promising materials for memory devices, organic displays, and sensors. The charge transport in these systems is realized by non-linear topological excitations created in polymer chains - solitons in trans-polyacetylene, polarons and bipolarons in conjugated polyarenes – polyaniline and others [1, 2]. We studied the temperature dependence of conductivity and structure of conjugated polyarenes doped by both acid dopants (toluene sulfonic acid /TSA/, sulfuric acid /SA/) and nanoparticles – carbon nanotubes (CNT), fullerene (C<sub>60</sub>), silica (SiO<sub>2</sub>) etc, in the temperature interval of 273-393 K.

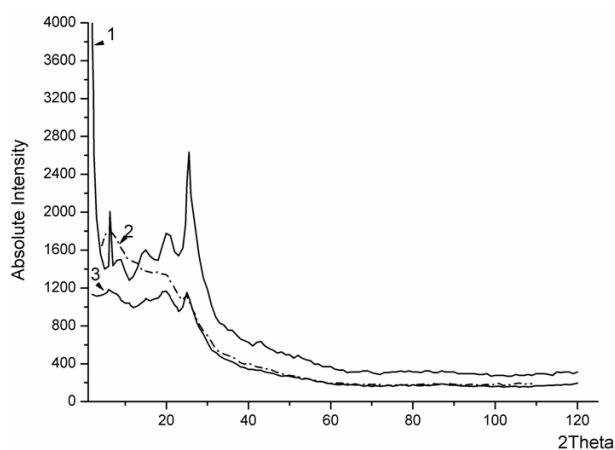


Fig.1. X-ray patterns of PANI-CNT(1), PANI-TSA (2) and PANI-SA (3) nanosystems.

Charge transport in low-dimensional polymer nanosystems may be considered in the frame of “domain” or “granular” model of conductivity. According to these performances in polymer there are existed the ordered areas (domain or crystallites) with high conductivity. Charge transport between these domains occurs by hopping mechanism across the low-conductive amorphous shells, which create the energetic barrier to conductivity. It may be expected that inside crystalline domains the significant inter-chain overlapping of wave function by all domain volume take a place.

1. Aksimentyeva O., Konopelnyk O. et al. Interaction of components and conductivity in polyaniline-PMMA nanocomposites // *Rev. Adv. Mater. Sci.* – 2010. – V. 23. – P. 30-34.
2. Aksimentyeva O.I., Konopelnyk O.I. Structure of near-order in conducting polyaniline films // *Molec. Cryst. Liq. Cryst.* – 2005. – V.427. – P. 127-137.

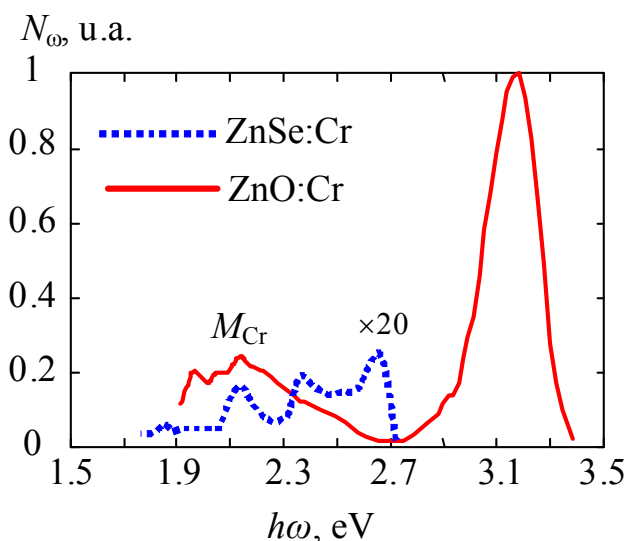
## ZnO:Cr heterolayers luminescence

Horley V.V.<sup>1</sup>, Kinzerska O.V.<sup>1</sup>, Melnyk V.V.<sup>1</sup>, Tkachenko I.V.<sup>2</sup>

<sup>1</sup>*Yuri Fedkovych Chernivtsi National University, Chernivtsi, Ukraine*

<sup>2</sup>*Chernivtsi Trade Economics Institut, KNTEU, Chernivtsi, Ukraine*

Raised in recent years, interest in ZnO due to the rapid development of shortwave optoelectronics, spintronics and solar energy. To meet the needs of the latest first of all need bulk crystals or thin films ZnO with magnetic impurities, the method of creation of which paid significant attention. Prospective in this aspect may be isovalent replacement technology that allows to produce semiconductor materials with new unique properties. In particular, ZnO heterolayers with effective UV radiation at 300 K were synthesized on zinc chalcogenides single crystal substrates by this method. This work is dedicated to research of ZnO heterolayers basic luminescent properties with Cr magnetic impurity. Layers of zinc oxide were created by annealing pre-doped with chromium vapor single crystal plates of ZnSe in the air, and luminescence was excited by N<sub>2</sub>-laser with  $\lambda_m \approx 0.337$  microns. As seen from the figure luminescence spectrum  $N_\omega$  of basic substrates ZnSe:Cr contains edge band centered  $\hbar\omega_m \approx 2.6$  eV, and compared with it by intensity, several low-energy



bands. The first band with maximum at  $\hbar\omega_m \approx 2.4$  eV due to transitions involving singly charged zinc vacancies, and the band from the  $M_{Cr}$  with maximum at  $\hbar\omega_m \approx 2.1$  eV – internally transitions in the chromium ion. Proof of the latter is that  $M_{Cr}$ -band is present also in the ZnO:Cr layers luminescence spectra. Slight changes in its main maximum energy position is caused by the proximity of dielectric constant values of ZnSe and ZnO. Since the ZnO:Cr heterolayers luminescence efficiency  $\eta$  is much

higher than  $\eta$  of ZnSe: Cr samples, then  $M_{Cr}$ -band of first looks structured, which is a consequence of transitions with the participation of split levels in the Cr ion. We note that in the ZnO: Cr layers spectra dominates the UV band with energy maximum at  $\hbar\omega_m \approx 3.2$  eV, the characteristic for pure ZnSe bands with the maxima at 2.4 and 2.6 eV, are missing. Practical use possibilities of the research objects are discussed.

## About the Dependence of Barrier Height on Dioxide Film Thickness in SnO<sub>2</sub>(Pt) – p-Si Heterojunction

Il'chenko V., Kravchenko O., Teslenko S.

*Taras Shevchenko Kyiv University, Kyiv, Ukraine*

Heterojunction based on tin dioxide films and silicon, are interesting structures for building gas sensors, that's why the investigation of its electro-physical characteristics took place.

The investigated experimental structures were made by spray pyrolysis from solution on p-type silicon wafers. Were received samples with tin dioxide film thickness 4, 7, 10, 15, 20 and 30 nm. Current - voltage characteristics ( $C-V$ ) were measured in voltage range  $-1.5 \div 1.5$  V,  $C-V$  analysis carried out in the approximation of over-barrier current transport mechanism. For semiconductors charge transfer can be described by thermionic over-barrier emission for majority carriers.

The barrier height decreases with increases of the thickness of the film from 4 to 15 nm (Fig. 1) and gets out on saturation.

As atomic-force microscopy studies have shown tin dioxide films have discontinuous structure. When they are nanoscale they may grow with mechanism of Stranskoho - Krastanova. With increasing of film thickness islets dimensions increases, until they begin to merge with each other. The mean surface roughness (as follows from the results of atomic force microscopy) decreases until becoming constant value on film thickness at about 20 nm.

Accordingly to the reduction of mean surface roughness, adsorption-active surface area of metal dioxide film decreases. This reduces the number of traps on the surface of SnO<sub>2</sub>, which arise as a result of oxygen adsorption on oxygen vacancies. Presumably, this dependence of film morphology explains the dependence of heterojunction barrier height on the thickness of metal dioxide film.

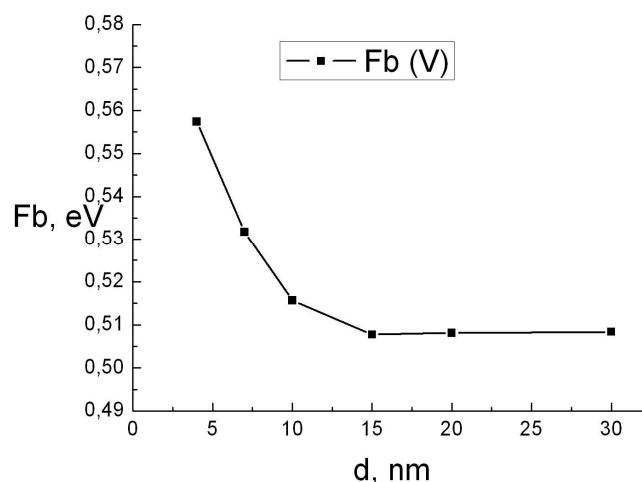


Fig. 1. Dependence of barrier height on the thickness of metal dioxide film.

## **The CdS thin films fabrication and properties**

Il'chuk G., Kusnezh V., Shapoval P., Petrus' R., Guminilovych R.

*Lviv Polytechnic National University, Lviv, Ukraine*

The Chemical Surface Deposition (CSD) of CdS ultra thin films (from 30 to 100 nm) from aqueous solutions on glass, ITO coated glass and single crystal wafer CdTe substrates is described. Three different cadmium sources: cadmium sulfate, cadmium chloride, cadmium iodide have been used. The effect of cadmium sources on the film growth rate, film thickness, optical properties as well as composition, crystalline structure, and surface morphology was investigated.

In CSD, a solution at ambient temperature containing the desired reactants is applied to pretreated surface. Multidepositions were used to obtain thicker films for further characterizations and investigate film thickness dependence on depositions. The thiourea was used as sulfur precursor. Ammonia was used as complexing agent. The substrate temperature was kept constant during the entire deposition process. Heterogeneous nucleation is favored over homogeneous precipitation by thermally-enhanced reactivity at the warmer growth surface, resulting in a high fraction of cadmium product in the film and heteroepitaxial film growth on the oriented substrate. Heat loss from the solution to the ambient helps maintain favorable conditions for heterogeneous film growth in the time frame needed for film deposition.

The film growth rate and bandgap were found to be sensitive to the Cd source used. The films were highly stoichiometric when cadmium iodide was used. The highest thickness obtained was in the case of CdSO<sub>4</sub>, and the lowest thickness in the CdI<sub>2</sub> case. Thickness of CSD film was measured after each successive deposition by elipsometer. We verified that the obtained thickness increased linearly with the number of deposition for up to 4 depositions for CdCl<sub>2</sub> and CdSO<sub>4</sub> salts. Regardless of the Cd salt used, all films were polycrystalline with a main (111) reflection and weaker (220) peaks that confirms the cubic nature of investigated films.

## Electrical Properties of Anisotypical Heterojunctions of ZnO/p-Cd<sub>1-x</sub>Zn<sub>x</sub>Te

Ilashchuk M.I., Orletsky I.G., Parfenyuk O.A., Gavaleshko N.M.

*Yuri Fedkovych Chernivtsi National University, Chernivtsi, Ukraine*

There presented the results of electrical properties research of anisotypical ZnO/p-Cd<sub>1-x</sub>Zn<sub>x</sub>Te heterojunctions, obtained by pulverization with following pyrolyse of thin-filmed ZnO on monocrystal Cd<sub>1-x</sub>Zn<sub>x</sub>Te (x = 0.04) substrate.

Crystal for substrates grown by Bridgman method at low cadmium vapour pressure in ampule ( $P_{Cd} \approx 0.02$  atm), had p-type conductivity and resistivity of  $\rho = 7.7 \cdot 10^2$  Ohm·cm at T = 295 K. Zink oxide films deposition has been done on the surfaces of singlecrystal Cd<sub>1-x</sub>Zn<sub>x</sub>Te plates, chemically polished in 2% bromine solution in methanol.

Analysis of VAC in received structures has been made, taking into consideration essential amount of surface defects  $N_S$  (evaluated  $N_S \approx 2.4 \cdot 10^{14}$  cm<sup>-3</sup>) in the interface boundary of semiconductors due to their lattice constants discrepancy. With such concentration they can be capture or recombination centers and have to influent essentially on the mechanism of current transition through the heterojunction, that is experimentally confirmed. In direct bias region of  $3 kT/e < U < 0.4$  eV coefficient of unideality A is more than 2 and changes from 3.2 to 2.4 when temperature changes from 293 to 343 K that gives evidence that capture centers as well as recombination centers participate in direct current formation. At  $U > 0.4$  V  $\lg I(U) = f(U)$  dependence becomes slower and can be explained by tunneling of charge carriers through the potential barrier.

Reverse current on voltage dependence is described by  $I(U) \sim U^m$  law. In small voltage region of  $U < 0.4$  V the quantity of m, determined from the direct part of curves equaled to  $m \approx 1.0$ . This means that electric leak upon the surface is the dominant behaviour for change carriers transition. When  $U > 0.4$  V,  $m \approx 2.0$ , that can be conditioned by the release of change carriers from capture centers because of electric field action.

Volt-farade characteristics of researched ZnO/p-Cd<sub>1-x</sub>Zn<sub>x</sub>Te heterojunction were obtained at different frequencies of measured signal, and can be explained in the frames of rectification structures with high serial resistance  $R_0$  model. The latter one is confirmed by the value of  $R_0 = 6.2 \cdot 10^3$  Ohm at T = 292 K, determined from the direct branches of VAC in their linear parts region. One can suppose that a big value of  $R_0$  is caused by oxide film, formed on the Cd<sub>1-x</sub>Zn<sub>x</sub>Te surface because of heating of substrates during structure formation process.

## **Influence of Low-Temperature Annealing on the Properties of Near-Surface Layer of CdTe, Doped with Vanadium**

Ilashchuk M.I., Orletsky I.G., Parfenyuk O.A., Gavaleshko N.M.

*Yuri Fedkovych Chernivtsi National University, Chernivtsi, Ukraine*

The purpose of this work was the research of changes in near-surface layers of semiinsulating CdTe:V, doped with V impurity after heating in the air at low temperatures ( $T \leq 503$  K). Temperature dependences of electroconductivity and Hall coefficient in wide temperature interval ( $503 \text{ K} > T > 298 \text{ K}$ ) with increase and decrease of temperature have been studied.

All the crystals were semiinsulating of n-type conductivity. For the researched samples a noncoincidence of  $\lg \rho = f(10^3/T)$  and  $\lg R_H = f(10^3/T)$  experimental curves for two directions of measurements is characteristic. After heating the crystals have become more low-resistance. Annealing of the materials was fulfilled at  $T \geq 465$  K.

As the results of thermal treatment volume and surface sample properties can change. To determine which of these processes is dominant, there was carried out the investigation of conductivity temperature dependence in crystals heated to 503 K, a surface layer of  $\sim 300 \mu\text{m}$  from which has been polished away. Increase of resistance in surface-polished away sample indicates that at  $T \geq 465$  K the surface of cadmium telluride essentially changes. A near-surface low-resistance layer with hole-type conductivity has been formed.

The formation of low-resistance near-surface p-layer on the semiinsulating n-type material is also confirmed by time dependences of  $R_H$  and  $\rho$  changes at 503 K. For  $\sim 50$  minutes resistance has decreased 2.7 times and Hall coefficient – 4.3 times. More rapid decrease of  $R_H$  is explained by the increase of holes amount because when conductivity is mixed,  $R_H$  value depends on the correlation between the concentrations of charge carriers. The increase of holes quantity in our case results in diminishing of  $R_H$  coefficient.

Formation of low-resistance p-type layer on the surface of the investigated crystals is caused by evaporation of Cd atoms from the surface at  $T \geq 465$  K. Near-surface layer is enriched by cadmium vacancies ( $V_{\text{Cd}}$ ) that provide p-type conduction. Our results correlate well with data of work [1], where a sharp increasing peak, connected with  $V_{\text{Cd}}$  at  $T > 453$  K was revealed in photoluminescence of semiinsulating CdTe research.

1. Корбутяк Д.В., Крилюк С.Г., Крюченко Ю.В., Вахняк Н.Д. Особливості фотолюмінесценції компенсованих монокристалів CdTe:Cl (огляд) // Оптоелектроніка и полупроводникова техніка. – 2002. – Вып. 37. – С. 23-40.



## Melting temperature of the nanocluster embedded in rigid matrix

Ivlev G.D.<sup>1</sup>, Gatskevich E.I.<sup>1</sup>, Malevich V.L.<sup>1</sup>,  
Zinovyev V.A.<sup>2</sup>, Dvurechenskii A.V.<sup>2</sup>

<sup>1</sup>*Institute of Physics of NASB, Minsk, Belarus*

<sup>2</sup>*Institute of Semiconductors Physics, Novosibirsk, Russia*

It is well known that the melting temperature  $T_m$  of free nanocluster is lowered with size decrease in comparison with bulk melting temperature. The different situation takes place for nanoclusters embedded in rigid matrix. Along with nanocluster size the conditions at nanocluster - matrix interface will be made an impact on melting temperature. The embedded nanoclusters can melt below or above melting temperature of bulk material depending on the interface structure.

In this work the dependence of the melting temperature of embedded nanocluster on size, shape, and mechanical stresses has been studied. Our consideration was carried out by the example of Ge nanoclusters embedded in solid Si matrix. The hut and dome nanoclusters are studied. The validity of the thermodynamical description of temperatures and phase transitions in Ge nanoclusters are discussed.

We used two theoretical approaches for the description of size dependence of  $T_m$ . In the first approach  $T_m$  is determined by the entropy of thermal crystal vibrations. The entropy depends on nanocrystal size, shape and nanocrystal – matrix interface properties. The dependence of  $T_m$  for two different shapes of nanocrystals on size was obtained. In the second approach it is assumed that  $T_m$  is proportional to nanocluster cohesion energy. In the frame of the first approach we obtained that the increase in melting temperature up to ~85 K for hut cluster and ~45 K for dome cluster with the decrease of base size up to 5 nm, for the case of the second approach these values are ~50 K and ~35 K respectively.

The embedded nanocluster are in stressed state due to lattice mismatch. The influence of lattice mismatch pressure can be estimated on the basis of Clausius-Clapeyron equation. Under the solid – liquid phase transition the Ge specific volume decreases about 5%. It indicates that  $T_m$  decreases with pressure increase. We obtained that the pressure due to lattice mismatch results in decrease in  $T_m$  on 90 K.

Thus according to our calculation melting temperature of Ge nanoclusters embedded in Si matrix slightly changes because of the impacts of nanocluster size and mechanical stresses on  $T_m$  compensate each other.

*This work was particularly supported by BRFFI (project No. F09SO-015) and RFFI (project No. 08-02-00121-a).*

## Photoluminescence and infrared radiation of Ge/Si heterostructures with quantum dots at nanosecond laser exposure

Ivlev G.D.<sup>1</sup>, Gatskevich E.I.<sup>1</sup>,  
Smagina Zh.V.<sup>2</sup>, Dvurechenskii A.V.<sup>2</sup>, Nikiforov A.I.<sup>2</sup>

<sup>1</sup>*Institute of Physics of NASB, Minsk, Belarus*

<sup>2</sup>*Institute of Semiconductors Physics, Novosibirsk, Russia*

Laser-induced processes in Ge/Si heterostructures with Ge quantum dots (QDs) have been studied. The samples were grown by molecular beam epitaxy and include 5 layers of QDs interchangeable with 5 nm Si nanolayers. The systems with QDs were covered by 150 nm i-Si layers. The samples were irradiated by the ruby laser pulses with duration 80 ns (FWHM) at the energy density  $W$  varied from 0.8 to 3.2 J/cm<sup>2</sup> in the spot of 4 mm in diameter at  $W$  inhomogeneity less than  $\pm 5\%$ . The same experiments with Si single crystals were carried out for comparison. Near infrared (IR) radiation of the laser heated area was detected in 0.9 - 1.2  $\mu\text{m}$  spectral region by means of a pyrometric sensor with a multiplier phototube as IR-detector. Also, a probe radiation flux ( $\lambda = 0.53 \mu\text{m}$ ) reflected from the laser-heated zone was detected by another photomultiplier that allowed to observe the laser-induced melting of the sample surface. The output signals of the radiation detectors were simultaneously recorded by two-beam oscilloscope. Under the experimental conditions the surface melting of the samples is reached if  $W > 1 \text{ J/cm}^2$ . IR-radiation signals recorded at  $W = 0.8\text{-}1.0 \text{ J/cm}^2$  follow the form and duration of the laser acting pulse. IR-radiation intensity culminates to the moment of the laser power peak. This radiation is laser-stimulated recombination luminescence (RL) of Si, at that its intensity is well above the same of thermal IR-radiation (TR) emitted by the heated layer.

At larger values of  $W$  in the dynamics of detected radiation the quenching of RL takes place at premelting stage and then TR of arising liquid phase is recorded. Under  $W = 2.6$  and  $3.2 \text{ J/cm}^2$  well-defined maximum of TR intensity is observed at the moment of the attainment of molten surface peak temperature  $T_p$  which is equal to 1950 K and 2100 K, correspondingly, as it follows from the measurement results at the effective wavelength  $\lambda_e = 1.04 \mu\text{m}$  in this case. Obtained data on  $T_p$  as a function of  $W$  agree with similar measurements, carried out at  $\lambda_e = 0.53$  and  $0.86 \mu\text{m}$ . The dynamics of IR-radiation at the stage of solidification of the molten layers is qualitatively the same in comparison with dynamics of visible thermal radiation of Si. The presence of QDs leads to the decreasing of solidification temperature of molted Si layer in comparison with Si single crystal.

*This work was particularly supported by BRFFI (project No. F09SO-015) and RFFI (project No. 08-02-00121-a).*

## **The near-IR light absorption in 2D macroporous silicon structures with SiO<sub>2</sub> nanocoatings**

Karachevtseva L., Goltviansky Yu., Konin K., Lytvynenko O.,  
Parshin K., Tsybrii Z.

*V. Lashkaryov Institute of Semiconductor Physics of NASU Kyiv, Ukraine*

We investigated the near-IR light absorption oscillations in 2D macroporous silicon structures with SiO<sub>2</sub> nanocoatings 70÷800 nm thick, taking into account the electro-optical effect within the strong electric field approximation.

We observed the oscillating structure in the absorption spectra of macroporous silicon structures with SiO<sub>2</sub> nanocoatings of 70÷800 nm thickness. The amplitude of oscillations is maximal in the spectral ranges of surface level absorption. This process is a result of the resonance electron scattering on impurity states. The macroporous silicon structures with thick SiO<sub>2</sub> nanocoatings have high potential of heterojunction between the silicon matrix and nanocoating. Therefore, the onset of giant oscillations can be attributed to the electro-optical processes in strong electric field. The electric field intensity in the surface heterojunction area  $F_s$  is determined by the oscillation period in the macroporous silicon structures and is equal to  $(2\div3)\cdot 10^4$  V/cm.

The Wannier–Stark ladder is not destroyed by impurities, if the intervals between the transitions due to scattering from impurity atoms with lifetime  $\tau$  are bigger than the period of electron oscillations in external field,  $T_B$ . The inequality  $\tau/T_B > 1$  holds in the whole spectral regions considered for macroporous silicon structures with SiO<sub>2</sub> nanocoatings, taking into account that the surface impurity concentration  $N_i$  for macroporous silicon structures is less than  $5 \times 10^{11} \text{ cm}^{-2}$ .

The oscillation period and electric field intensity in the macroporous silicon structures with SiO<sub>2</sub> nanocoatings fluctuate about a constant value at low photon energies and become quadratic in photon energy depending on the geometrical sizes of silicon matrix and SiO<sub>2</sub> nanocoatings. The relevant electric field intensity growth corresponds to the quasi-guided mode formation in the silicon matrix (minimal distance between the macropores) and in the silicon column. Thus, the spectral curves for the oscillation period and electric field intensity in macroporous silicon structures with SiO<sub>2</sub> nanocoatings have a constant section and growing one due to the quasi-guided mode formation. The electron transitions from the  $v$ -band to empty acceptor surface levels and free electron motion are realized due to additional change of local electric field as a result of grazing light incidence and quasi-guided mode formation.

## On the models of normal indentation size effect in application to chalcogenide vitreous semiconductors

Kavetsky T.S., Tsmots V.M., Matlak O.S.

*Drohobych Ivan Franko State Pedagogical University, Drohobych, Ukraine*

In this work the models of normal indentation size effect used usually for crystalline materials are considered in application to non-crystalline materials on the example of chalcogenide vitreous semiconductors.

It is well known that the apparent microhardness of solids depends on the applied indentation test load. This phenomenon is known as the indentation size effect (ISE) [1]. The ‘normal ISE’ usually involves a decrease in the apparent microhardness with increasing test load. In contrast to the normal ISE, an increase in the apparent microhardness with increasing test load is also known, and the phenomenon is called as ‘reverse ISE’. The nature of normal ISE and especially reverse ISE still remains poorly understood for crystalline solids and to our knowledge these phenomena are practically unknown yet for non-crystalline solids like amorphous chalcogenides. In order to describe the normal ISE behaviour of materials, several models have been proposed in the literature such as Meyer’s law, Hays-Kendall approach, elastic/plastic deformation (EPD) model, proportional specimen resistance (PSR) model [1].

The goal of the present work is three-fold: (1) to describe the normal ISE within the above models in application to chalcogenide vitreous semiconductors on the example of  $\text{As}_2\text{Se}_3$  glasses doped by rare-earth elements (Nd, Sm, Ho, Er) system using Vickers microhardness data [2], (2) to compare the parameters obtained within the models for the non-crystalline materials studied with ones reported in the literature for some crystalline cobalt-based alloys [1], and (3) to establish the differences (if any) in the models for explanation of normal ISE in the glassy and crystalline alloys. The results obtained show that the above models are not fully satisfied and the PSR model written in the new form [2] as  $H = H_0(1 + d_0/d)$ , where  $H_0$  is the load-independent hardness of a sample and the parameter  $d_0$  is a constant related to elastic and plastic deformation of the sample, should be used in the case of glassy chalcogenides.

1. Sangwal K., Surowska B., Blaziak P. Analysis of indentation size effect in the microhardness measurement of some cobalt-based alloys // *Mat. Chem. Phys.* – 2002. – V. 77. – P. 511-520.
2. Kavetsky T., Borc J., Sangwal K., Tsmots V. Indentation size effect and Vickers microhardness measurement of metal-modified arsenic chalcogenide glasses // *J. Optoelectron. Adv. Mater.* – 2010. – V. 12, N. 10. – P. 2082-2091.

## Radiation impact on the concentration of magnetic ordered clusters and paramagnetic centres per clusters in chalcogenide glasses

Kavetsky T.S., Tsmots V.M., Pankiv L.I.

*Drohobych Ivan Franko State Pedagogical University, Drohobych, Ukraine*

In this work the results of investigation of impact of  $^{60}\text{Co}$   $\gamma$ -irradiation on the concentration of magnetic ordered clusters and paramagnetic centres per clusters in  $\text{As}_2\text{S}_3$  and  $\text{Ge}_{28.125}\text{As}_{6.25}\text{S}_{65.625}$  chalcogenide glasses are reported and discussed.

The most important property of chalcogenides as a part of the big family of the glasses is the disorder. The structure is composed by frozen of the melt and during the preparation the bonds created could be not satisfied or regularly formed. Thus some of the bonds are “dangling” or “broken”. The dangling bonds or paramagnetic centres should form magnetic nanoclusters in the material which can be evaluated within Langevin model [1]. The purpose of this work is the investigation of impact of  $^{60}\text{Co}$   $\gamma$ -irradiation on the concentration of magnetic ordered clusters and paramagnetic centres per clusters using magnetic susceptibility measurements by Faraday method at the temperatures of 77 and 293 K in  $\text{As}_2\text{S}_3$  and  $\text{Ge}_{28.125}\text{As}_{6.25}\text{S}_{65.625}$  chalcogenide glasses. The concentrations of magnetic nanoclusters  $N_{\text{cl}}$  and paramagnetic centres per clusters  $N_0$  are evaluated and analyzed for the glasses studied in the non-irradiated and  $\gamma$ -irradiated states. A correlation between radiation-induced changes in the magnetic susceptibility data for  $\text{As}_2\text{S}_3$  and  $\text{Ge}_{28.125}\text{As}_{6.25}\text{S}_{65.625}$  alloys reported in this study with radiation-induced changes in the electron spin resonance data for  $\text{As}_2\text{S}_3$  [2,3] and  $\text{Ge}_x\text{S}_{1-x}$  glasses [4,5] is found out.

1. Tsmots V.M., Litovchenko P.G., Pavlovska N.T., Pavlovskyy Yu.V., Ostrovskyy I.P. Research and modeling of magnetic susceptibility of Si and  $\text{Si}_{0.95}\text{Ge}_{0.05}$  whiskers, *Semiconductors*. – 2010. – V. 44, N. 5. – P. 623-627.
2. Shpotyuk O.I., Matkovskii A.O. Radiation-stimulated processes in vitreous arsenic trisulphide // *J. Non-Cryst. Solids*. – 1994. – V. 176. – P. 45-50.
3. Shpotyuk O.I., Matkovskii A.O. Radiation-optical properties of vitreous  $\text{As}_2\text{S}_3$  // *Opto-Electron. Rev.* – 1994. – V. 2, N. 4. – P. 100-103.
4. Zhilinskaya E.A., Lazukin V.N., Valeev N.Kh., Oblasov A.K.  $\text{Ge}_x\text{S}_{1-x}$  glasses. Defects, density and structure // *J. Non-Cryst. Solids*. – 1990. – V. 124. – P. 48-62.
5. Zhilinskaya E.A., Valeev N.Kh., Oblasov A.K.  $\text{Ge}_x\text{S}_{1-x}$  glasses. II. Synthesis conditions and defect formation // *J. Non-Cryst. Solids*. – 1992. – V. 146. – P. 285-293.

## Size phenomena in condensed systems

Kharun L.T.

*Vasyl Stepanyuk Precarpatian National University, Ivano-Frankivsk, Ukraine*

Among the size effects in condensed systems distinguish classical, internal and quantum size effects.

Dimensions condensate significantly affect its electronic properties. The size leads to changes in the energy band structure and charge transfer characteristics. Theoretical and experimental studies show that the kinetic parameters of the sample limited size parameters differ from the bulk material. In the case of the classical size effect is due to the fact that the contribution of surface scattering of carriers in the resulting relaxation time depends on the sample thickness  $d$ .

Thin films mainly consist of small crystallites sizes are substantially smaller than the size of crystallites in bulk polycrystals. Intercrystalline boundaries are additional lenses carriers. Consequently, and provided that the linear dimensions of crystallites  $D$  is comparable with the mean free path length of carriers  $\lambda$  ( $\lambda \sim D$ ), kinetic parameters of films depend on the dimensions of crystallites  $D$ . This phenomenon was called the internal size effect.

If the film thickness  $d$  and crystalline size  $D$  are commensurate with the de Broglie wavelength for carriers, then the sample is quasi momentum quantization components of the electron, which is transverse to the sample surface. The relevant components of the quasi momentum states form a discrete system, which leads to the oscillating dependence of kinetic, electrical and thermodynamic parameters of a sample of its size. And during these oscillations  $\Delta d$  equal to half the de Broglie wavelength ( $\lambda_D/2$ ). The last phenomenon has been called quantum size effect (QSE). In the review article [1] the historical perspective shows theoretical and experimental study of QSE in condensed systems.

1. Фреїк Д.М., Харун Л.Т., Добровольська А.М., Лисюк Ю.В. Квантово-розмірні ефекти у конденсованих системах. Науково-історичні аспекти // Фізика і хімія твердого тіла. – 2011. – Т.12, №1. – С. 9-26.

## **Degradation of structure and physical properties of AIVBVI compounds films under the influence of external factors**

Klanichka Yu.V., Mezhylovska L.Yo., Klanichka V.M., Zukowski P.

*Vasyl Stefanyk PreCarpathian National University, Ivano-Frankivsk, Ukraine*

The regularity of reformation of chemical and phase compositions, real structure both as-grown films of lead chalcogenides and tin telluride and those influenced by thermal effect in atmospheric oxygen and vacuum is determined.

The heterogeneity in their thickness is found. It is demonstrated that degradation processes are determined by the condition of condensate crystal structure, temperature and annealing time. Within the limits of the average free path of charge carriers, drift barrier and Petric model of double layers kinetic parameters of films with different structure (monocrystal, polycrystal) are calculated and it is determined their dependence upon thickness.

It is demonstrated that due to the dispersion of charge carriers on grain boundary the average length of free run of the charge carriers in polycrystal films is vastly less than in monocrystal and depends significantly upon temperature. The electrical parameters of near-surface layers and the value of energetic barriers are determined.

The research was conducted as to the dependence of electrical parameters of polycrystal films of lead chalcogenides with different thickness  $d=(20-250)\text{nm}$  from the oxygen pressure  $P_{O_2}=10^{-4}-10^4\text{ Pa}$ . There are two different mechanisms of oxygen acceptor interaction with the thin films surface which are connected with replacement of chalcogenide in anionic interlattice and rootage main matrix between nodes. It is also proposed their crystal-chemical models.

It is determined the degradation processes at isochronous and isothermal annealing of lead chalcogenides, tin telluride of different structure, type of conductivity, initial carrier concentration in the open air and explained by introphase and phase processes with oxygen involvement.

It is demonstrated that the complicated character of electric parameters change at vacuum annealing kept in the open air films is caused by the oxygen and chalcogenide desorption and demonstration of their own conductivity.

## **Influence of surface layers on electrical properties semiconductor structures in Petrits' model**

Klanichka Y.V., Yavorskiy Ya.S., Klanichka V.M., Yavorskiy R.S.

*Vasyl Stefanyk PreCarpathian National University, Ivano-Frankivsk, Ukraine*

There were explored oxidising processes in thin films of PbTe by their long-term exposure on air. With using of Petrits model, was measured dependence of surface layer thickness from time of exposure. It was shown that at the initial stages are dominating processes of adsorption of oxygen on a surface, and its diffusion in depth of a film, which further become inappreciable and is compensated by lead diffusion to a surface.

Films for investigation were obtained from a vapour phase with method of open vaporization was carried out in vacuum on polyamide substrates. Measurement of electrical parameters of films was carried out on air with room temperature in constant magnetic fields. It was carried out a series of measurements through certain time throughout approximately one year for each sample. Also there were obtained dependences of specific conductance and Hall coefficient for lead chalcogenide films from a thickness. For films PbTe witch were exposed on air about several days with decreasing of a thickness the Hall coefficient also decreases. Concentration of p-type carriers grows, what is related to acceptor activity of adsorbed oxygen and formation on a surface enriched on carriers p-type layer. At the long-term exposition on air (about 1 year) with decreasing of a thickness of a film, concentration of carriers becomes lower that shows on small velocity of diffusion of oxygen in depth of a surface and the further diffusion of lead to a surface which compensates acceptor influence of oxygen.

For a quantitative evaluation of surface layer conductivity in films the analysis of electrical properties is expedient to carry out with two-layer Petrits model. The model allowed to determine dependence of a thickness of a surface layer from exposure time on air and average velocity of an oxidising at each stage.

At the initial stages of exposition, velocity of oxidising is considerable, further it becomes lower sharply, and throughout the first days becomes small. It also shows on difference of mechanisms of oxidizing processes on early stage and during the long-term exposure on air.

*The work is partially financed by NAS Ukraine (the state registration № 0110U006281) and State Fund of Fundamental Researches of Ukraine State Committee of Science Information (the state registration № 0110U007674).*

## Pulse plating of zinc oxide nanowires

Klochko N.P.<sup>1</sup>, Khrypunov G.S.<sup>1</sup>, Volkova N.D.<sup>2</sup>, Kopach V.R.<sup>1</sup>,  
Lyubov V.M.<sup>1</sup>, Klepikova K.S.<sup>1</sup>, Kopach A.V.<sup>1</sup>

<sup>1</sup>National Technical University “Kharkiv Polytechnic Institute”, Kharkiv, Ukraine

<sup>2</sup>National Aerospace University “Kharkiv Aviation Institute”, Kharkiv, Ukraine

ZnO nanostructures are promising semiconductor materials in gas sensors and dye-sensitized solar cells (DSSC) due to their chemical stability and optimal photochemical properties. Recently, ZnO nanowires were successfully grown via a variety of methods including sol-gel and hydrothermal methods, chemical vapor deposition and electrodeposition. Effects of electrolyte formula, deposition temperature and time and even gravitation on structure and properties of the electrodeposited ZnO nanowire arrays are studied extensively. Nevertheless, there are only rare attempts to employ a pulsed potential technique for ZnO electrodeposition. Purpose of this work is study of influence of the different pulse plating regimes on ZnO structure and optical properties in order to reveal means for obtaining of one-dimensional (1D) zinc oxide nanostructures and for optimization of ZnO nanowire structures.

ZnO arrays were electrodeposited on fluorine doped tin oxide (FTO) covered glass cathodes in aqueous electrolyte contained Zn(NO<sub>3</sub>)<sub>2</sub> and NaNO<sub>3</sub> in three-electrode cell with platinum counter-electrode and saturated Ag/AgCl reference electrode. Electrodeposition of each ZnO sample was carried out during 1 hour at 70°C under pulse plating regimes with rectangular impulses of cathode potential, which were supported by potentiostat PI-50-1.1. Phase composition and structure of the deposited films were determined by XRD-method using an X-ray diffractometer DRON-4M with CoK $\alpha$  radiation according to  $\theta$ - $2\theta$ - scheme. Preferable orientations, average crystalline sizes and lattice strains of the electrodeposited ZnO arrays were researched by analytical treatment of the X-ray diffractions. Surface morphology of ZnO array has been shown by scanning electron microscopy. Transmittance spectra of ZnO layers were measured by double beam spectrophotometer SF-46.

We searched for pulse plating regimes for the obtaining of ZnO arrays with strong (002) preferable orientation on the basis of investigation of electrochemical processes on cathode during ZnO deposition and by means of variation of frequency, on-off time ratio and potentials of impulses as such as ZnO nanowires that grow along c-axis in direction perpendicular to the substrate are results of the preferential growth in the (001) plane. As a result of our investigations we have demonstrated for the first time successful growth of 1D ZnO nanostructures by pulse plating without using of templates. The novel electrodeposition technique gives possibilities for the manufacture of ZnO nanowires suitable for DSSC and gas sensors.

## Magnetoresistive properties of multilayers based on Fe/Cu and Fe/Pd

Kondrahova D.M., Synashenko O.V., Protsenko I.Yu., Tkach L.V.  
Odnodvoret O.P.

*Sumy State University, Sumy, Ukraine*

The aim of this work is the experimental study of magnetoresistive effect (MRE) of multilayer film systems based on Fe/Cu and Fe/Pd fragments and its correlation with the structural-phase state. The investigations were done in high vacuum ( $p = 10^{-6}$ - $10^{-7}$  Pa), the thicknesses of several layers were controlled in situ by quartz resonator method. MRE measurements were done in CIP(current-in-plane) geometry with two- and four-point contact scheme using in three geometries relative to the external magnetic field (from 0 to  $0.3 \div 1$  T) – longitudinal, transverse and perpendicular. The value of MRE was determined by correlation  $\Delta R/R_s = (R(B) - R_s)/R_s$ , where  $R_s$  – the resistance in saturation field.

The multilayers based on Fe/Cu and Fe/Pd with perpendicular magnetic anisotropy [1] have the wide distribution in memory devices with big recording density of information [2]. It is known that the MRE is depended from different factors as number of fragments  $n$ , geometries and temperature [3]. In Fe/Cu film system the anisotropy of  $R(B)$  is observed, which appeared in negative MRE in longitudinal and positive MRE – in transverse geometries ( $\Delta R/R_s \cong 0.05\%$ ). This regularity is typical for samples with atomic concentration of Fe atoms  $c_{Fe} > 50\%$ . For smaller values of  $c_{Fe}$  the anisotropy is vanished and MRE is increased ( $\Delta R/R_s \cong 0.2\%$ ), which point to the presence of GMR effect in Fe/Cu multilayers. The structural-phase state investigations in Fe/Cu system with thin layers point to formation of solid solution based on FCC or BCC lattice in contrast to our early investigations [4] of two-layer system, where the individuality of layers was observed. The investigations of magnetoresistive effect in systems  $[Pd(1.1)/Fe(0.9)]_n/S$  ( $n = 3, 5, 10$ ) indicate the growth of magnetoresistance values from 0.05 to 0.27 % with  $n$  increasing in all geometries.

*This work is done in frame of the theme № 0109U001387.*

1. Shima H., Oikawa K., Fujita A. et al. Lattice axial ratio and large uniaxial magnetocrystalline anisotropy in L10-type FePd single crystals prepared under compressive stress // *Phys. Rev. B.* – 2004. – V. 70. – P. 224408.
2. Daughton I.M. GMR applications // *J. Magn. Mater.* –1999. – V. 192. – P. 334–342.
3. Parkin S.S. Giant magnetoresistance in magnetic nanostructures // *Annu. Rev. Sci.* – 1995. – V. 25. – P. 357-388.
4. Проценко С.І., Чешко І.В., Великодний Д.В. та ін. Структурно-фазовий стан, стабільність інтерфейсів та електрофізичні властивості двошарових плівкових систем // *Успехи физ. мет.* – 2007. – Т. 8, № 4. – С. 247-278.

## Ab initio calculations and Raman spectra of As<sub>2</sub>S<sub>3</sub>, Sb<sub>2</sub>S<sub>3</sub> and Bi<sub>2</sub>S<sub>3</sub> films

Kondrat O.<sup>1</sup>, Popovich N.<sup>1</sup>, Holomb R.<sup>1</sup>, Mitsa V.<sup>1</sup>, Petrachenkov O.<sup>1</sup>, Veres M.<sup>2</sup>

<sup>1</sup>*Uzhhorod National University, Uzhhorod, Ukraine*

<sup>2</sup>*Research Institute for Solid State Physics and Optics of the Hungarian Academy of Sciences, Budapest, Hungary*

Theoretical and experimental investigations in the last years shown that two- and three-components chalcogenide glassy semiconductors (ChGS) continuous media are formed in a considerably wider variety of basic structural units than their crystal analogs. The majorities are combined into the middle-range ordering grouping (clusters) with different geometry, depending on concentration of additives and producing technology. To understand the dependence of optical absorption on glass/film internal structure we combined the spectroscopic studies of ChGS binary systems with *ab initio* quantum-mechanical calculations of the vibrational spectra and electronic structure of different clusters

The aim of this work is comparative analysis of the calculated and experimental spectra of As<sub>2</sub>S<sub>3</sub>, Bi<sub>2</sub>S<sub>3</sub> and Sb<sub>2</sub>S<sub>3</sub>.

The non-crystalline As(Bi, Sb)<sub>2</sub>S<sub>3</sub> films of different thickness were obtained by discrete thermal evaporation on glassy and silica substrates. This method give a possibility to easy vary the evaporation velocity, temperature of evaporator, number of samples of different thickness at one cycle of deposition.

The Raman spectra of films were measured using Renishaw System 1000 spectrometer. A diode laser with wavelength  $\lambda_{\text{ex}} = 785$  nm (photon energy  $E_{\text{ex}} = 1.58$  eV) was used as excitation source.

The structural fragments of As(Bi,Sb)<sub>2</sub>S<sub>3</sub> crystals were used for cluster modeling and ab initio calculations. The calculations of these structures are useful to understand the differences in optimal geometry, electronic structure and Raman spectra of the clusters compare with the corresponding crystals.

The optimal geometry and vibrational properties of As(Bi,Sb)<sub>n</sub>S<sub>m</sub> clusters were calculated by ab initio using quantum-mechanic program GAMESS (US). A DFT method with hybrid B3LYP functional were used for optimize the cluster structures and Raman spectra calculations. The Stuttgart RLC ECP basis set (for heavy atoms) and the standard Poples' 3 - 21G basis set (for saturating hydrogens) were used.

The Raman spectra of these samples were interpreted using the results of ab initio calculations.

## Optical properties of $\text{Cd}_{1-x}\text{Mn}_x\text{Te}$ films

Kosyak V.V.<sup>1</sup>, Opanasyuk A.S.<sup>1</sup>, Bukivskij P.M.<sup>2</sup>, Gnatenko Yu.P.<sup>2</sup>

<sup>1</sup>*Sumy State University, Sumy, Ukraine*

<sup>2</sup>*Institute of physics NAS of Ukraine, Kyiv, Ukraine*

It is known that  $\text{Cd}_{1-x}\text{Mn}_x\text{Te}$  semimagnetic semiconductors are perspective materials for modern magneto-optical devices [1]. Recently this material is also used as alternative to  $\text{Cd}_{1-x}\text{Zn}_x\text{Te}$  solid solutions for radiation detector applications [1, 2]. It should be noted that  $\text{Cd}_{1-x}\text{Mn}_x\text{Te}$  semiconductor films remain insufficiently investigated, that due to difficulty obtaining them, as pressure solution components differ significantly from each other.

In this work the investigations of optical characteristics of  $\text{Cd}_{1-x}\text{Mn}_x\text{Te}$  films were carried out with aim to determine an influence of growth conditions on chemical composition and optical quality of  $\text{Cd}_{1-x}\text{Mn}_x\text{Te}$  films deposited by close-spaced vacuum sublimation technique.

$\text{Cd}_{1-x}\text{Mn}_x\text{Te}$  films were deposited on cleaned glass substrates using a VUP-5M vacuum equipment at the residual gas pressure about  $5 \cdot 10^{-3}$  Pa.  $\text{Cd}_{1-x}\text{Mn}_x\text{Te}$  solid solution with manganese concentration of 30% was used as a mixture. Substrate temperature was  $T_s = (623-798)$  K, temperature of evaporator was varied in the range of  $T_e = (943-1123)$  K.

Measurement of optical characteristics was performed with spectrophotometer SF-26 in the wavelength region  $\lambda$  from 700 to 1000 nm. As a result, the spectral dependencies of refraction  $R(\lambda)$  and transmission  $T(\lambda)$  coefficients were obtained. The photoluminescence spectra were measured using an SDL-1 grating spectrometer equipped with liquid-helium cryostat provided by temperature regulation “UTREKS” system in the range from 780 to 900 nm. An LGN-404 argon laser was used for excitation by the  $\lambda = 488$  nm line.

Low-temperature photoluminescence investigations of  $\text{Cd}_{1-x}\text{Mn}_x\text{Te}$  films indicate that the formation of solid solutions leads to a significant improvement of their optical quality. It can be explained by the “healing” of the point defects namely cadmium vacancies. This studies also allowed us to determine a manganese concentration in the films as well as the optimal growth conditions to obtain the thin films of high optical quality.

It was found that the band gap energies of obtained films equal to  $E_g = (1.46-1.57)$  eV that corresponds to manganese concentration in films of  $x = 0.02-0.04$ .

1. A. Mycielski, L. Kowalczyk, R.R. Galazka, et al. Applications of II–VI semimagnetic semiconductor s// J. Alloy. Comp. – 2006. – V.423. – P. 163-168.
2. A. Owens, A. Peacock. Compound semiconductor radiation detectors // Nucl. Instrum. Methods. – 2004. – V. 531. – P. 18-37.

## Electrochemical Intercalation of $\text{Li}^+$ in the Dehydrated Anatase Synthesized by the Method of $\text{TiCl}_4$ Hydrolysis

Kotsyubynsky V.O.<sup>1</sup>, Chelyadyn V.L.<sup>1</sup>, Myronyuk I.F.<sup>1</sup>, Ilnytskyy R.V.<sup>1</sup>,  
Mokliak V.V.<sup>2</sup>, Dmytruk V.V.<sup>1</sup>

<sup>1</sup>*Vasyl Stefanyk Precarpathian National University, Ivano-Frankivsk, Ukraine*

<sup>2</sup>*A general research laboratory of physics of magnetic films of G.V. Kurdyumov Institute for Metal Physics, N.A.S. Ukraine and Vasyl Stefanyk Precarpathian National University, Ivano-Frankivsk, Ukraine*

Ultra-dispersed  $\text{TiO}_2$  was synthesized by the method of titanium tetrachloride hydrolysis ( $\text{TiCl}_4$ ) by hydrochloric acid ( $\text{HCl}$ ).  $\text{TiCl}_4$  was cooled to 273 K and after that the  $\text{HCl}$  solution was added. Condensation process was stimulated by the sodium carbonate solution, then the sol was aging at room temperature. Structure, morphology and dispersion of nanoparticles was determined by flow rate of condensation processes, pH and temperature of reaction medium. According to the X-ray analysis data monophase anatase was created. Electron microscopic researches showed similar to spherical morphology of particles with linear dimensions at the range 40-300 nm. For the case of obtained material using as a base of cathode composition of model lithium power sources the specific capacity value was reached  $372 \text{ mA} \cdot \text{h} \cdot \text{g}^{-1}$  (the galvanostatic discharging up to 1.5 V). Obtained value is in about 10% higher than the theoretically predicted maximum. It was explained by the fact that despite the dehydration of material its surface contains the adsorbed water (IR spectroscopy data). Molecules of  $\text{H}_2\text{O}$  dissociate in the electrolyte (1M solution of  $\text{LiBF}_4$  in  $\gamma$ -butyrolactone). Positively charged complexes [ $\text{Li} - \gamma$ -butyrolactone] near the cathode interact with protons, which caused the destruction of dissolver molecules and forming of  $\text{HF}$  molecules. Note that at the first  $\text{LiOH}$  and  $\text{Li}_2\text{O}$  as prepared phases at the cathode surface are created. Surface layer of  $\text{LiF}$  phase as a result of their interaction with  $\text{HF}$  are formed. Thus, part of the lithium ions, which are transferred through the electrolyte, take part in the formation of passivated layer on the cathode surface. All these processes take place with the simultaneously  $\text{Li}^+$  intercalation in the titania. It was found that lithium ions during intercalation processes occupy the host positions in the near-surface area of titania particles with the forming of two zones – subsurface lithium enriched and internal one. At the intercalation degree of lithium ion per formula units of titania about  $x = 0.6$  the electrode covered by  $\text{LiF}$  film with the ionic type of conductivity. Intercalation of  $\text{Li}^+$  in the cathode continues to  $x \leq 0.8$ . The final blocking on the  $\text{TiO}_2$  particles surface is happening at  $x \geq 1.0$  with the charge transferring through two interface. In the range of intercalation degree  $0 < x \leq 0.8$  a sharp decline of the lithium ions diffusion coefficient ( $D_{\text{Li}}$ ) in the anatase structure is observed with the  $D_{\text{Li}}$  values changing within the range  $10^{-9}$ - $10^{-11} \text{ cm}^2 \cdot \text{s}^{-1}$  (impedance spectroscopy data).

*The work is supported by CRDF / USAID (UKX2-9200-IF-08) and the Ministry of Education and Science of Ukraine (M/130-2009).*

## Photovoltaic cells based on nonodispersed titania sensitized by anthocyanine dyes

Kotsyubynsky V.O.<sup>1</sup>, Mokliak V.V.<sup>2</sup>, Kolkovskyy P.I.<sup>1</sup>, Grubyak A.<sup>1</sup>

<sup>1</sup>*Vasyl Stefanyk Precarpathian National University, Ivano-Frankivsk, Ukraine;*

<sup>2</sup>*A General Research Laboratory of Physics of Magnetic Films of G.V. Kurdyumov Institute for Metal Physics, N.A.S. Ukraine and of Vasyl Stefanyk Precarpathian National University, Ivano-Frankivsk, Ukraine*

The complex of works aimed at constructing and testing models of photoelectrochemical energy sources based on nonodispersed titania sensitized by anthocyanine dyes is carried out. The phenomena of electronic and ionic transport in photovoltaic cells (PVC) is researched. Several series of PVC are constructed using synthesized and commercial ultrafine titania. All stages of the process of forming an electrode are worked out, such as deposition of colloidal solution on the glass substrate coated with  $SnO_2: Sb$ , multistage heat treatment, dye sensitization, sealing the cell. Anthocyanine dyes based on extracts of *Vaccinium myrtillus* L. and *Hibiscus sabdariffa* are obtained and tested as photosensitizers. The complex optical spectroscopic researches of the obtained materials, both original and sensitized dyes of different types, are carried out. A number of electrolytes based on  $\gamma$ -butyrolactone and acetonitrile are tested. It was found that optimal operating characteristics of PVC are achieved using electrolyte based on  $LiI$  and  $I_2$  solution in the  $\gamma$ -butyrolactone with the addition of  $LiBF_4$ . The model that explains the influence of lithium ions intercalated in titanium dioxide on the value of photocurrent is suggested. It was found out that the fill factor for the current-voltage characteristics of the constructed models is between 0.45-0.57, while coefficient of efficiency is 0.2-0.5 %. There is a linear dependency between the size of short-circuit current and geometric area of the frontal electrode. The value of photocurrent was 1.5-2.5 mA/cm<sup>2</sup> at internal resistance of PVC 0.15-0.20 Ohm. For a model based on  $TiO_2$  Degussa P25, sensitized by *Vaccinium myrtillus* L. extract with the electrolyte 0.5M  $LiI$  + +0.05M  $I_2$ +1M  $LiBF_4$  in  $\gamma$ -butyrolactone coefficient of efficiency is 0.51 % at the filling factor of 0.57. All tests are carried out at the simulated illumination with optical power 1000 W/m<sup>2</sup>. Diffusion coefficient  $D_c$  of electrons in the film is 0.0016 cm<sup>2</sup>/s (data of photoelectrons lifetime measurement). For the initial phase of illumination at the implementation stage 0.001 mol of lithium ions per 1 mol of  $TiO_2$  diffusion coefficient of  $Li^+$  ions is about  $4.5 \cdot 10^{-11}$  m<sup>2</sup>·s<sup>-1</sup> (impedance spectroscopy data). The obtained results are important for developing a conceptual approach to solving of global problem – the development of new materials with adapted for use in photoelectrochemical energy sources structural and morphological characteristics and optimization of all components of photovoltaic systems to increase coefficient of efficiency with the use of safe and low cost materials and technologies.

*The work is supported by CRDF/USAID (UKX2-9200-IF-08) and the Ministry of Education and Science of Ukraine (M/130-2009).*

## Ab Initio Study of Gas Adsorption on ZnO Nanotubes

Kovalenko M.V., Bovgyra O.V., Kapustianyk V.B.

*Ivan Franko National University of Lviv, Lviv, Ukraine*

Gas sensors have attracted intensive research interest due to the demand of sensitive, fast response, and stable sensors for industry, environmental monitoring, biomedicine, etc. ZnO was the first metal oxide used in semiconductor gas sensing devices. In the last years, there appeared many publications on the ZnO nanostructures or thin film based gas sensors using various synthesis methods, sputtering, pulse laser deposition, chemical vapor deposition, chemical solution deposition, molecular beam epitaxy etc [1]. The extremely high surface-to-volume ratio and hollow structure of nanomaterials is ideal for the adsorption of gas molecules. Therefore, gas sensors based on nanostructures, such as ZnO nanotubes (NTs), nanorods, nanoflowers, and nanohelices, have been investigated widely. To reveal the mechanism of these sensors models based on experimental phenomena were established, in which the importance of charge transfer were accentuated.

In this work, we present a density functional theory (DFT) study of the adsorption of various gas molecules ( $H_2$ ,  $O_2$ ,  $H_2O$ ,  $CO$ ,  $NH_3$ , and  $CH_3OH$ ) on a ZnO NTs without or with vacancies. We determine their exact orientation on the NT wall and their preferential binding site by calculating their binding energy. Their charge transfer to the NT wall is investigated in order to determine the donor or acceptor character of the molecular adsorbates. Particular attention is paid to understanding the modification of electronic structures of ZnO NTs by the gas-molecule adsorbates. The nanotubes considered here are armchair (4, 4) and zigzag (8, 0).

The relativistic all-electron DFT calculations and the full geometry optimizations on the single-walled (4, 4) and (8, 0) ZnO NTs with and without gas molecules were performed using the generalized gradient approximation with revised Perdew, Burke and Ernzerhof functional for the exchange-correlation energy. The electronic wave functions were expanded in a double-numeric polarized basis set. Charge transfers are calculated based on the Mulliken population analysis.

The optimized geometry, binding energies for the ZnO NT/molecule system are similar to those obtained by other theoretical studies and experimental data;  $O_2$  and  $H_2$  are physisorbed on ZnO NTs with weak binding and little charge transfer;  $CO$ ,  $NH_3$ , and  $CH_3OH$  are molecularly chemisorbed. With the oxygen vacancy defects, the binding interaction between gas molecules and the ZnO nanotube becomes stronger.

1. Eranna G., Joshi B.C., Runthala D.P., Gupta R.P. Oxide materials for development of integrated gas sensors – a comprehensive review // Crit. Rev. Sol. State Mater. Sci. – 2004. – 29. – P. 111-188.

## Photoinduced bleaching of GeS<sub>2</sub> chalcogenide glass amorphous films

Kozak M.I., Studenyak I.P., Loya V.Yu.<sup>1</sup>, I.I.Makauz, Fedelesh V.I., Solomon A.M.<sup>1</sup>, Zhikharyev V.M., Krafchik S.S.<sup>1</sup>, Krasilinets V.M.<sup>1</sup>

*Uzhhorod National University, Uzhhorod, Ukraine*

<sup>1</sup>*Institute of Electron Physics, Ukr. Nat. Acad. Sci., Uzhhorod, Ukraine*

Among chalcogenide glasses there are two compounds transparent in the visible optical range – red As<sub>2</sub>S<sub>3</sub> glass and yellow GeS<sub>2</sub> glass. It is interesting that in these glasses photoinduced changes of optical parameters are of opposite character. In As<sub>2</sub>S<sub>3</sub> under illumination with light with the energy  $h\nu \approx E_g^{\text{opt}}$  optical pseudogap decreases, exhibiting a so-called red shift of the absorption edge or photodarkening, with a corresponding increase of the refractive index. In GeS<sub>2</sub>, on the contrary, photoinduced bleaching is observed with the refractive index decrease.

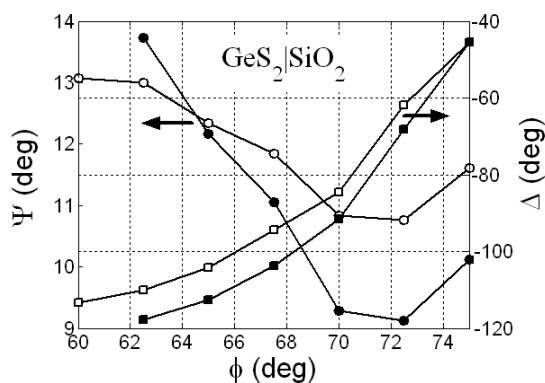


Fig. 1. Dependence of ellipsometric angles on the incidence angle before and after illumination (open and dark circles, respectively).

substrates of silicon and fused quartz, based on ellipsometry studies. The measurements were performed using a LEF-3M-1 ellipsometer equipped with a He-Ne laser (wavelength 6328 Å), the illumination was performed by a quasimonochromatic light source (2 mW/cm<sup>2</sup>) with the maximum of intensity at the wavelength 465 nm. Figure 1 shows changes in the dependences of ellipsometric angles  $\Psi$  and  $\Delta$  on the incidence angle  $\phi$  of the laser beam caused by 60 min illumination. The calculations, performed in the model of an anisotropic uniaxial medium, have shown the refractive index to decrease by 0.01÷0.05, after illumination during 30-45 min the anisotropy sign can change to the opposite.

Since, contrary to As<sub>2</sub>S<sub>3</sub>, GeS<sub>2</sub> glass is unstable and spontaneously crystallises within a short time, thermally evaporated films of this glass crystallise especially rapidly (as shown here, within several days), there is not enough data available in the literature to confirm or reject photoinduced bleaching in films of this glass. Here we confirm the photoinduced bleaching in  $\sim 1.5 \mu\text{m}$  GeS<sub>2</sub> films evaporated at 10<sup>-5</sup> Torr onto

## The conductivity and structure of ultrathin lead and manganese films

Kozak M.M., Kravchenko O.E., Penyukh B.R.

*Ivan Franko National University of Lviv, Ukraine*

Structural and electrical properties of thin (1-40 nm) Pb and Mn films have been studied in the temperature range 78-300 K. The Pb and Mn films were deposited onto glass or NaCl substrate (pure or precovered by the subnanometer thick Cr layers) at a rate of 0.1 to 0.2 nm/min by thermal evaporation. Thin films thickness was monitored by applying a quartz-crystal oscillator. The sample thickness increased by additional deposition on the same film.

Electron-microscopic (TEM and REM) and electron-diffraction investigations of films gave the following results. Metal layers more than 5-8 nm thick were polycrystalline and continuous, they had a crystal lattice similar to that of bulk metal. The average linear crystalline size  $D$  in the plane parallel to substrate did not depend on the film thickness ( $D = 6-10$  nm for Mn films to  $D = 45$  nm for Pb films).

The experiment showed that resistivity and temperature coefficient of resistivity  $\beta$  possessed a size-dependence. The experimental results for  $\rho$  were interpreted in the framework of heterogeneous cross section polycrystalline film model size-effect theories. The electron transport parameters for thin films were calculated. The average amplitude of surface asperities  $h$  was estimated from the results of electrical measurements and shows a good agreement with STM data. It was shown that subnanometer thick Cr layers (mass thickness less than 0.3-1 nm) hastened Mn and Pb films metallization.

## Optical diagnostics of physical-chemical properties and changes in NiO/Al<sub>2</sub>O<sub>3</sub> nanocomposite at different exposures

Kudanovich A.M.<sup>1</sup>, Khairullina A.Ya.<sup>1</sup>, Parchomenko I.N.<sup>1</sup>,  
Filimonenko D.S.<sup>1</sup>, Vorobyova T.N.<sup>2</sup>

<sup>1</sup>*Institute of Physics, National Academy of Sciences of Belarus, Minsk, Belarus,*

<sup>2</sup>*Research Institute for Physical Chemical Problems of Belarusian State University, Minsk, Belarus*

Measurements of optical characteristics of samples in a wide spectral region from 325 nanometers up to 10 micrometers have been carried out with the purpose of interpretation of the processes occurring at influence on a surface of nanostructured NiO/Al<sub>2</sub>O<sub>3</sub>-composites various physical and chemical factors (exposure by gases, heating, pumping out), at parallel influence of laser radiation. For calculations of absorption spectra on factors diffusion reflections and transmittances in UV and visible areas of a spectrum we offer the formula which is approximately taking into account dispersion by structure and a luminescence [1]. Authors revealed selective sensitivity to carbon monoxide and methane of NiO/Al<sub>2</sub>O<sub>3</sub>-composites at room temperature.

Absorption spectra of NiO/Al<sub>2</sub>O<sub>3</sub>-composite strongly change in the field of 340-345 nanometers at influence carbon monoxide. The increase in absorption factor at 345 nanometers can be explained by formation of a carbon included layer [2]. Displacement of an absorption maximum of a composite in long-wave area at influence of gas and heating can be connected with increase in the size of the particles of composite. In transmittance spectra of composites the minimum is observed at 2345 cm<sup>-1</sup>. This band can be related to antisymmetric valent fluctuation of CO<sub>2</sub> molecule [3] that testifies to oxidation of carbon monoxide. In this case gas is in chemisorbtion condition since this band after pumping does not decrease. Of great interest are the absorption bands 2858 cm<sup>-1</sup>, 2924 cm<sup>-1</sup> and 2957 cm<sup>-1</sup> caused by carbon [3]. Pumping out after exposure of gas appreciably strengthens these bands, that, apparently, is connected to masking action of carbon oxide. It is necessary to note, that the band of 1570 cm<sup>-1</sup> increases at influence of carbon monoxide co while a band at 1530 cm<sup>-1</sup> practically do not change. The absorption bands of in the mentioned above frequencies are shown and on a pure substrate (γ-Al<sub>2</sub>O<sub>3</sub>) that testifies to formation of carbon compounds also on aluminium oxide.

1. Khairullina A.Ya., Olshanskaya T.V., Kudanovich A.M., Filimonenko D.S. // J. Appl. Spec. – 2010. – 77. – P. 760-767.
2. Kratschmer, K. Fostiropoulos, Donald R. Huffman // Chem. Phys. Let. – 1990. - Vol. 170 (2-3). - P.167-170.
3. IR-spectroscopy in chemistry of oxide surface / A.A. Davydov - Nivosibirsk: Nauka. – 1984. – 243 p.

## **Research on behaviour peculiarities of a dislocation-impurity subsystem in the thin near-surface Be layers**

Kurek E.I., Oliynych-Lysyuk A.V., Raransky M.D.

*Yu. Fedkovich Chernivtsi National University, Chernivtsi, Ukraine*

It is well known that weak external magnetic fields ( $B < 1$  T) can cause in diamagnetic materials an abnormal (10-100%) change of their physical (plastic inclusive) properties. This phenomenon got the name of a magnetoplastic effect. At the present stage of interpretation of its nature it is considered that magnetoplastic effect is not related to direct action of magnetic field on crystal dislocations, since the magnitude of magnetic field corresponding to this magnetic induction is much less than the energy of thermal fluctuations ( $\sim kT$ ) and the energy of crystal lattice barriers. The magnetic field effect occurs indirectly through spin “bridging” of defects that take part in plastic deformation. Therefore, experimental and theoretical studies of magnetoplastic effect became the basis for a new division of physics of strength – spin micromechanics that emerged at the interface of physics of plasticity and spin chemistry. Moreover, with a better insight to the physical nature of magnetoplastic effect, it came to be more frequently used as a powerful tool for studying the structure and properties of spin subsystem of defects that take part in the process of plastic deformation [1].

In this paper, the effect of a weak ( $B \sim 0.03$  T) constant magnetic field on the elastic and nonelastic characteristics of thin near-surface layers of condensed magnesium thermal beryllium was studied with a view to establish the behaviour peculiarities of its dislocation-impurity structure. Studies were conducted at different temperatures and deformation degrees prior to and after the magnetic field action, as well as immediately during the magnetic field action.

The main results of studies are as follows:

- a) considerable change of nonelastic characteristics was established under the magnetic field effect in the range of 20 – 400°C both on heating and cooling;
- b) relative change  $(\Delta Q^{-1} / Q^{-1})_{T=const}$  in a magnetic field has increased more than a factor of 12, and the magnetic field aftereffect was observed for 5 days;
- c) magnetic field in situ had a pronounced effect on temperature hysteresis of shear modulus ( $G_{ef}$ ), and magnetic aftereffect resulted in the inversion of temperature hysteresis of modulus  $G_{ef}$ .

1. Morgunov R.V. Spin micromechanics in physics of plasticity // *Uspekhi Fizicheskikh Nauk.* – 2004. – V.174, № 2. – P. 131-153.

## Microhardness of helium implanted monocrystalline materials with a garnet structure

Kurovets V.V., Yaremiy S.I.

*Vasyl Stefanyk Precarpathion National University, Ivano-Frankivsk, Ukraine*

Synthetic garnets are widely used as materials for microwave devices and magnetic storage materials in bubble memory devices. Knowledge of mechanic parameters of this materials is very important not only for machining such crystals, but also for the device fabrication and expluatation.

The aim of our work was to study the microhardness of single crystals  $Gd_3Ga_5O_{12}$  and epitaxial  $Y_3Fe_5O_{12}$  films in dependence of the helium implantation dose. Microhardness measurements were made on the (111) face of the origin and helium implanted ( $E = 100$  keV,  $D = 1 \cdot 10^{15} \text{ cm}^{-2} \div 1 \cdot 10^{16} \text{ cm}^{-2}$ ) monocrystalline materials.

The Vicker's microhardness  $H_V$  was calculated from the formula  $H_V = 1854,4 \cdot P/d^2$ ,

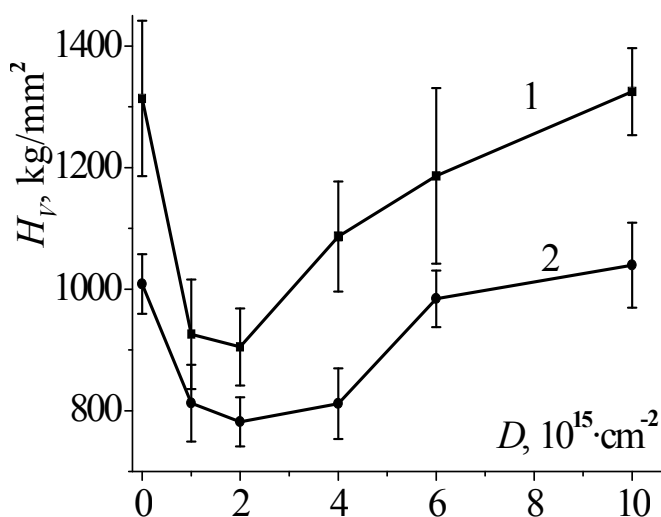


Fig. 1. Microhardness  $H_V$  as function of dose for helium implanted single crystals  $Gd_3Ga_5O_{12}$  (1) and epitaxial films  $Y_3Fe_5O_{12}$  (2).

where  $P$  is the load in g and  $d$  the length of the diagonal of the impression measured in  $\mu\text{m}$ ;  $H_V$  is in units of  $\text{kg/mm}^2$ . Indentations were made at 50 g load.

Microhardness decreasing (fig. 1) at the implantation dose  $1 \cdot 10^{15} - 2 \cdot 10^{15} \text{ cm}^{-2}$  for both series of samples is explained by defects presence under irradiation and broken atom boards in crystal structure.

Beginning from the implantation doses  $> 2 \cdot 10^{15} \text{ cm}^{-2}$  crystalline structure disordering grows and the processes of defects association in complexes are intensifies. When implantation layer amorphisation takes plase there is the microhardness increasing, which is explained by the presence of amorphous areas in ion-implanted layer and blocking by them dislocation mechanism of crystal destruction.

This work has been funded by the CRDF/USAID (UKX 2-9200-IF-08) and the Ministry of Education and Science of Ukraine (M/130-2009).

## **Structure and Electrico-Physical Properties of Complex Compounds On Ge Basis**

Lepikh Y.I.

*Odesa Mechnikov National University, Odesa, Ukraine*

In order to improve the performance of micro-and nanoelectronics, reducing their size and cost, as well as the new devices creation intensive research of new functional materials are widely carried out.

Complex compounds (CC), including complex compounds of germanium (CCGe) are of particular interest for micro-and nanoelectronics, optical, acoustics and other areas of functional electronics.

One of the main advantages of these compounds is that CCGe (IV) with organic molecules possesses a good combination of physical and chemical properties and electric physical parameters (EPhP).

In this case, the EPhP and physico-chemical properties of CCGe can be relatively easily modified by introducing appropriate impurities into their structure, which form salts with ions of other metals and organic cations.

We investigated the structure and electrical properties of the complex of germanium with oxietylenediphosphonic acid ( $H_4Oedph$ ).

CCGe is a supramolecular assembly, where the structural units are combined by the branched system of hydrogen bonds.

Germanium is one of the hexanuclear complex anion, hydrogen ions are located in the outer sphere complex, and the water molecules perform the bridging function: connect the complex molecules in layers, and layers, in its turn, with each other.

The current-voltage characteristics (CVC) of pure CCGe film with oxietylenediphosphonic acid, and the film of the same substance in a stock solution which hydrofluoride ammonium  $NH_4^+ HF$  was added to, as well as the temperature dependence of the current flowing through the CCGe film with adding ammonium hydrofluoride at heating and cooling regimes has been measured.

CCGe film samples resistance exceeded  $1 \cdot 10^{10} \Omega \cdot cm$ .

When added to a solution the ammonium hydrofluoride  $NH_4F- HF$  the decrease in resistivity of the samples to a value less than  $1-10 \Omega \cdot cm$  was observed.

The mechanisms of charge transport in supramolecular structure of the CCGe have been researched.

## Thermodynamic and structural investigations of As<sub>2</sub>S<sub>3</sub>-based glasses with additions of Ag and/or I

Lishchynskyy I., Klanichka V., Varvaruk V.

*Vasyl Stefanyk Precarpathian National University, Ivano-Frankivsk, Ukraine*

Amorphous chalcogenides based on As, S, Se and Te are of high interest due to their unique properties such as electric switching, optical phase change recording, superionic conducting or high infrared transmittance. Technologies based on chalcogenide glasses are successfully applied, for example, in the phase change optical recording (DVD technology) or optical telecommunication.

The amorphous nature of the As-S, As-S-I, As-S-Ag and As-S-AgI alloys was verified by X-ray diffraction using an X-ray diffractometer SEIFERT XRD 3000 PTS. Absence of any sharp peak in XRD patterns of a glassy alloy confirms the glassy nature of As-S, As-S-Ag and As-S-AgI samples.

The thermal properties of the amorphous alloys were investigated using a differential scanning calorimeter NETZSCH DSC 404 (temperature accuracy ±1.0 K). Temperature calibration of the device was performed using melting temperatures of high purity In, Sn, Bi, Pb, Al, and Cu samples. DSC measurements were performed under argon atmosphere.

Glass transition temperatures decrease with the increase of silver content for glassy (As<sub>2</sub>S<sub>3</sub>)<sub>100-x</sub>Ag<sub>x</sub> ( $x = 0, 4, 8, 12$  and  $x = 5, 15, 25, 35$ ) system. This can be explained by the low free crystallization energy of Ag (48 kcal/mol). Kawaguchi et al [1] have suggested that the of T<sub>g</sub> to lower temperatures is associated with an increase in the looseness of the network structure.

In glassy (As<sub>2</sub>S<sub>3</sub>)<sub>100-x</sub>(AgI)<sub>x</sub> system the glass transition temperatures slightly increases with the increase of x. The endothermic peaks for glassy (As<sub>2</sub>S<sub>3</sub>)<sub>100-x</sub>(AgI)<sub>x</sub> at  $x = 25, 30, 35, 40$  agree with the β-α phase transition in silver iodide. Up to 147°C, AgI exists in the β-phase, which has a wurtzite structure. Above 147°C, AgI undergoes a transition to the α-phase, which has a body-centered cubic structure [2].

The activation energy of glass transition,  $E_a$ , for the As-S, As-S-Ag and As-S-AgI alloys was estimated with Kissinger's formula [3]:

$$\ln(T_g^2/\alpha) = E_a/RT_g + \text{const}$$

where  $\alpha$  is the heating rate,  $R$  the gas constant,  $T_g$  glass transition temperature.

The experimental data obtained during the research visit of the at Institute of Physics, Chemnitz University of Technology.

1. Kawaguchi T., Maruno S., Elliott S.R. // J. Non-Cryst. Solids. – 1997. – 211 – P. 187-195
2. Binner J.G.P., Dimitrakis G., Price D.M., Reading M. and Vaidhyanathan B. // J. Therm. Anal. Cal. – 2006. – 84 – P. 409.
3. Kissinger H.E. // Anal. Chem. – 1957. – 29 – P. 1702.

## Observation of crystallization of $(As_{0.4}Te_{0.6})_{100-x}Ag_x$ ( $x = 0, 5, 15$ at. %) glasses

Lishchynskyy I., Varvaruk V., Dolibsky M.

*Vasyl Stefanyk Precarpathian National University, Ivano-Frankivsk, Ukraine*

Chalcogenide glasses with Ag impurities are attractive materials for fundamental studies of their structure and properties [1]. Scientific and applied interest in amorphous chalcogenide-based As-S doped Ag occurs through a combination of their semiconducting properties of As-S and ion conductivity impurities Ag. They have already applied and are promising for applications in optics and optoelectronics [1,2]. Low free energy of crystallization of Ag (48 kcal/mol) and some peculiar doping effect switching chalcogenide glasses, explains the success of their application in devices for optical and electrical recording of information [2].

The activation energy of crystallization ( $E_C$ ) has been determined by using approaches of Augis-Bennett, Kissinger, and Matusita-Sakka (Table 1,2,3). Relation between the pre-exponential factor  $K_0$  of the crystallization rate and the activation energy of crystallization  $E_C$  in the present has been obtained. This indicates the presence of compensation effect for the non-isothermal crystallization process in the glasses studied.

Table 1

The activation energy for glass transition and crystallization constants  
for compounds  $(As_{0.4}Te_{0.6})_{100-x}Ag_x$  by using approaches of Augis–Bennett

x	$E_C$ , kJ/mol	$K_0$ , min <sup>-1</sup>	$K_{00}$ , min <sup>-1</sup>	$K_0=K_{00}\exp(E_C/RT_C)$	$R^2$
0	191±17	4.26·10 <sup>20</sup>	5.37·10 <sup>-4</sup>	4.76·10 <sup>20</sup>	0.988
5	146±18	1.79·10 <sup>15</sup>	5.37·10 <sup>-4</sup>	1.09·10 <sup>15</sup>	0.972
15	133±8	1.73·10 <sup>13</sup>	5.37·10 <sup>-4</sup>	2.55·10 <sup>13</sup>	0.994

Table 2

The activation energy of  
crystallization  $(As_{0.4}Te_{0.6})_{100-x}Ag_x$  by  
using approaches of Kissinger

x	$E_C$ , kJ/mol	$R^2$
0	187±15	0.994
5	142±18	0.971
15	128±7	0.987

Table 3

The activation energy of  
crystallization  $(As_{0.4}Te_{0.6})_{100-x}Ag_x$  by  
using approaches of Matusita–Sakka

x	$E_C$ , kJ/mol	$R^2$
0	195±15	0.988
5	150±17	0.974
15	137±7	0.994

1. Венгер Е.Ф., Мельничук А.В., Стронский А.В. Фотостимулированные процессы в халькогенидных стеклообразных полупроводниках и их практическое применение. – 2007. – 284 с.
2. Yamada N., *MRS Bull.* – 1996. – 21, 48.

## SEM, HSEM examination of surface palladium nanoparticles

Lisnyak V.V.<sup>1</sup>, Yatsimirsky V.K.<sup>1</sup>, Safonova V.V.<sup>1</sup>,  
Stratiychuk D.A.<sup>2</sup>, Boldyreva O.Yu.<sup>1</sup>

<sup>1</sup>*Kyiv Taras Shevchenko National University, Kyiv, Ukraine*

<sup>2</sup>*V.N. Bakul Institute for Superhard Materials, Kyiv, Ukraine*

Metal nanoparticles with spatial dimensions belonging to the nano-scale ( $10^{-9}$  m) range can catalyze a multitude of chemical transformations in particular oxidizing of pollutants or converting chemical energy to electricity [1]. Nanoscaled objects fill the gap between bulk matter and individual atoms. High surface area which realizes due to significant concentration of ratios of surface metal atoms in the objects makes the nanoparticles ideal candidates to be used in the composite catalysts as a key component [2]. Morphology, chemical compositions of nanoobjects, the nanoparticle size are parameters of high interest for scientists in order to achieve a better understanding of origin of high catalytic activity. The catalytic activity of double diphosphates of Mo(III)  $M^I Mo^{III} P_2 O_7$ ,  $M^I = Na, K, Rb, Cs$ , and systems on their basis with supported metallic Pd, obtained by the method of impregnation, is studied in the reaction of  $H_2$  oxidation. It is shown that the systems possess higher activity in the reaction of  $H_2$  oxidation, when traditional 0.5 % mass Pd/ $Al_2 O_3$  catalyst with the same content of palladium and close value of specific surface. The near-surface layer of Pd catalysts was characterized by low and high resolution scanning electron microscopy (SEM and HSEM) and EDX/WDX microanalysis. EDX/WDX mapping were provided in addition to the conventional SEM image a meaningful picture of the element distribution of a surface. The acquisition times of 12 h was taken for a satisfactory resolution and noise performance to found the metallic Pd particles. Also transmission electron microscopy studies were performed to confirm the EDX/WDX mapping results. It was shown that the most active catalysts are characterized the least values of average dimension of the Pd metal crystallites.

1. Astruc D. Nanoparticles and Catalysis – Weinheim: Wiley-VCH. - 2007. – 663 p.
2. Toshima N. Metal nanoparticles for catalysis. In: Liz-Marzan L.M., Kamat P.V. (Eds.) // Nanoscale materials – London: Kluwer, 2003. – P. 76-96.

## The mobility of the paramagnetic probe in the polyurethane films with various content of neodymium (3+) complex

Lobko E.V., Kozak N.V., Klepko V.V.

*Institute of Macromolecular Chemistry of NAS of Ukraine, Kyiv, Ukraine*

It was investigated the mobility of the nitroxyl paramagnetic probe 4-amino-2,2,6,6-tetramethylpiperidine-1-oxyl (TEMPO) in the cross-linked polyurethane films (CPU), which modified by of neodymium (3+) acetylacetonate (0.5; 1; 3; 5 %wg.). On the Figure the typical spectra of the electronic spin resonance of TEMPO in polymer matrixes (at the temperature is 20°C) are presented.



The spectra have three components with the noticeable intensity increasing of the central components and components in the high fields.

The mobility of the TEMPO in the polyurethane matrix with various percentage of neodymium (3+) acetylacetonate was estimated on the value of the correlation time of the probe rotation, which determined as:

$$\tau = 6.65 \Delta H_{(+1)} \left( \sqrt{I_{(+1)} / I_{(-1)}} - 1 \right) 10^{-10} \text{ c,}$$

where  $H_0$ ,  $H_{(+1)}$  – the width of the central spectrum components and components in the low field, accordingly;  $I_0$ ,  $I_{(+1)}$ ,  $I_{(-1)}$  – the intensity of the central component of the spectrum and the component in the low and high field, accordingly.

The correlation time of the probe rotation ( $\tau$ ) in the cross-linked polyurethane matrix are resulted in the Table.

System	$\tau * 10^{-10}$ , c
CPU-0	15
CPU-0.5%Nd	18
CPU-1%Nd	21
CPU-3%Nd	25
CPU-5%Nd	25

Evidently, that the increase of the modifier quantity (the complex of neodymium (3+)) in the polyurethane matrix results to the increase of the  $\tau$ , that is to the decreasing of the mobility of the paramagnetic probe in the matrixes. That is indicate on the increase of the polymer matrix density, as a result of the formation of the additional co-ordination net at the growth of modifier quantity.

## Conductivity of nanocrystalline alloy CoNi films

Loboda V.B., Kravchenko V.O., Shkurdoda Yu.O., Kolomiets V.M.

*A.S. Makarenko Sumy State Pedagogical University, Sumy, Ukraine*

The electrophysical properties of nanocrystalline metal films differ significantly from the properties of solid films and massive materials. In particular, they tend to be exponentially dependent on temperature resistance and, accordingly, – on the negative thermal coefficient of resistance (TCR), which indicates the nature of the activation conductivity of such films. For these samples, the temperature dependence of resistivity can be represented by the well-known relation:

$$\rho(T) = \rho_0(1 + \beta T) + C \exp(E_a / (kT)),$$

where the item  $\rho_0(1 + \beta T)$  represents the involvement of the common resistance metal dependence on the temperature,  $C_{\text{exp}}(E_a / (kT))$  – the involvement of some thermally activated process. For not solid (irregular) films the involvement of the first item can be neglected, which provides with the opportunity to determine conductivity activation energy  $E_a$ .

In the process of the first cycle of thermal stabilization while heating the samples of all thicknesses, irreversible resistance reduction (ten times and more) is observed. Hereafter (II-III cycles) the dependences  $\rho(T)$  recur. For the

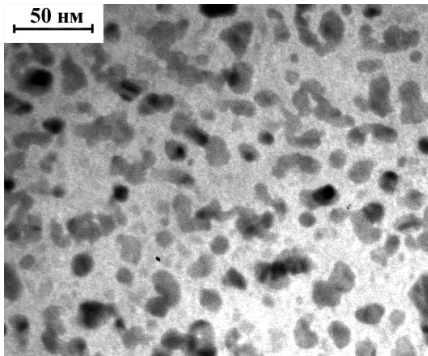


Fig. 1 Microstructure of  $\text{Co}_{30}\text{Ni}_{70}$  ( $d = 9 \text{ nm}$ ) alloy films

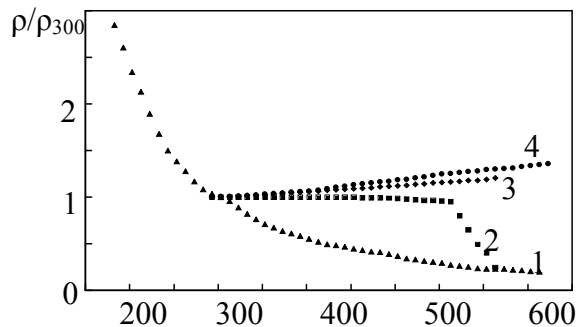


Fig. 2 Dependence of resistivity transferred  $\rho/\rho_{300\text{K}}$  on temperature for films CoNi: 1 –  $d = 10 \text{ nm}$ , 2 –  $d = 18 \text{ nm}$ , 3 –  $d = 22 \text{ nm}$ , 4 –  $d = 31 \text{ nm}$ .

samples with  $d < 10 - 12 \text{ nm}$  there is a transition from irregular to labyrinth (Figure 1) structure. These films are characterized by clearly expressed exponential dependence of resistance on temperature with activation energy of conductivity of  $0.1 - 0.06 \text{ eB}$  (Fig. 2, dependence 1). Film thickness increase entails activation energy decrease, and when the thickness is over  $25 \text{ nm}$  exponential dependence is not observed (Fig. 2, dependences 3 and 4). Energy magnitude does not depend on the concentration of alloy components and correlates with literature data for pure metals. For the transitional thickness range  $d \sim 20 \text{ nm}$  (Fig. 2, dependence 2) the TCR value is approximate to zero, and in the process of the consequent thickness increasing, the TCR changes to positive (dependences 3 and 4).

## The effect of giant magnetoresistance in three-layer nanocrystalline films Fe/Ag/Co

Loboda V.B.<sup>1</sup>, Kolomiets V.M.<sup>1</sup>, Shkurdoda Yu.O.<sup>1</sup>,  
Saltykova A.I.<sup>1</sup>, Dekhtyaruk L.V.<sup>2</sup>

<sup>1</sup>Sumy State Pedagogical University named after A.S. Makarenko, Sumy, Ukraine

<sup>2</sup>Kharkiv State Technical University of Building and Architecture, Kharkiv, Ukraine

The presence of the Ag nonmagnetic interlayer (spacer) between the Fe and Co magnetic layers leads to the antiferromagnetic ordering of local magnetization vectors in the three-layer Fe/Ag/Co film. Experimental studies of the effect of magnetoresistance in unannealed and annealed samples have shown that the phenomenon of giant magnetoresistance (GMR) with a value ranging from 0.4 % to 1 % at room temperature is observed in the unannealed sandwiches with the interlayer thickness  $d_{\text{Ag}} = 5 - 20$  nm. The above-mentioned effect is caused by the asymmetric scattering of charge carriers with different spin polarization at grain boundaries. When the spacer Ag thickness  $d_{\text{Ag}} < 5$  nm the GMR is not observed which is conditioned by the presence of “bridges” over the nonmagnetic interlayer leading to the appearance of a ferromagnetic bond between the layers and, as a result, to the breach of their antiparallel configuration. If the interlayer thickness  $d_{\text{Ag}}$  is  $\sim 8$  nm the magnetoresistance reaches its peak value. Further increasing of the nonmagnetic interlayer to  $d_{\text{Ag}} > 10$  nm decreases the amplitude of the above-mentioned effect. On the one hand, it is conditioned by the current bypass in the nonmagnetic interlayer with a high conductivity. On the other hand, this phenomenon is caused by the weakening of the exchange bond between the ferromagnetic layers which is instantiated by the presence of a magnetoresistant hysteresis loop and by the small values of saturation fields ( $H_S < 20$  kA/m).

Annealing of the sandwiches at 400 K in a magnetic field with intensity of 8 kA/m decreases the GMR value (in 1.2 - 2 times) for all the films.

Further annealing at 550 K enhances the GMR amplitude of the films with the nonmagnetic layer thickness ranging from 10 nm to 20 nm. Ulterior decreasing of the GMR amplitude and the appearance of magnetoresistant anisotropy are observed in the films with  $d_{\text{Ag}} < 10$  nm which is conditioned by the breaking of the initial magnetic order in magnetic layers. The recrystallization processes, the interdiffusion of Ag, Fe and Co and a small value of the interlayer Ag thickness ( $d_{\text{Ag}} = 3 - 15$  nm) cause the breach of the nonmagnetic layer continuity which leads to the disappearance of the spin-dependent electron scattering.

Further annealing at 700 K only enhances the value of anisotropic magnetoresistance which is mainly conditioned by the increase of the crystal size in the film plane.

## Optimization of Technology and Simulation of Physical Processes in Thin Films II-VI and IV-VI and Structures on Their Base

Lopyanko M.A.

*Vasyl Stefanyk PreCarpathian National University, Ivano-Frankivsk, Ukraine*

In paper study the effects of operational technology factors of growing from a vapor phase on physical properties of thin films of monochalcogenide of lead, tin, and solid solutions on their bases:  $\text{PbSe}_{1-x}\text{Te}_x$ ,  $\text{Pb}_x\text{Sn}_{1-x}\text{Te}$ ,  $(\text{SnSe})_{1-x}(\text{PbTe})_x$ ,  $(\text{SnTe})_{1-x}(\text{PbSe})_x$  by the method of hot-wall [1,2]. Are offered both the technological diagrams are constructed and technology is optimized, which one ensure growth of thin film materials with beforehand parameters.

The physico-chemical models of process of II-VI and IV-VI films growth from a vapor phase is offered. On the base of the generative-recombination mechanisms of radiation defect formation the dosed dependence of concentrations of charge carriers in acting epilayers are explained at an exposure by alpha-particles.

Modeled diffusion-recombination mechanisms of isochronal and isothermal annealing of the own atomic defects in binary compounds. The influence the both of internal (the concentration of charge carriers, diffusion activation energy) and external (steps on the temperature and in time) process of annealing parameters on the change of defect concentration. Comparing the experimental data with calculation results determined activation energy of annealing of defects in films of lead chalcogenides.

The general rules of physical properties change of the solid solutions epitaxial films. Shown that thin films of  $\text{PbSe}_{1-x}\text{Te}_x$  ( $0.0 < x < 1.0$ ),  $(\text{SnTe})_{1-x}(\text{PbSe})_x$  and  $\text{Pb}_x\text{Sn}_{1-x}\text{Te}$  ( $0.0 < x < 0.1$ ) at 420-580 K have electronic type of conductivity. Increasing of deposition temperature leads to the conversion of type of conductivity and electron concentration further growth. Epitaxial films  $(\text{SnTe})_{1-x}(\text{PbSe})_x$  and  $\text{Pb}_x\text{Sn}_{1-x}\text{Te}$  of  $0.2 < x < 1.0$  have only p-type of conductivity.

Increasing deposition temperature reduces the concentration of holes and increase of their Hall mobility.

Films of the solid solutions  $(\text{SnSe})_{1-x}(\text{PbTe})_x$  and  $\text{Pb}_x\text{Sn}_{1-x}\text{Se}$  of the phase compositions for  $0.0 < x < 0.4$  are mono-phases. When  $0.0 < x < 0.1$ , depending on the temperature of deposition, the film can have as n-, and p-type of conductivity, and at  $0.1 < x < 0.4$  – only p-type of conductivity.

1. D.M. Freik, M.O. Galushchak, L.Y. Mezhylovska. Physica and technology of thin films. Lviv: Lviv University. – 1988. – 152 p.
2. L.S. Palatnik, V.K. Sorokin. The bases of films semiconductor material science. M.: Energiya. – 1973. – 294 p.

## **Structure and physical properties of films of lead chalcogenides obtained from gas-dynamic stream of steam.**

Lopyanko M.A., Nykyruy R.I., Mateik G.D.

*Vasyl Stefanyk PreCarpathian National University, Ivano-Frankivsk, Ukraine*

Based on the calculations of gas-dynamic stream parameters of lead chalcogenides steam in the case of expenditures in a cylindrical chamber of the technological factors of thin films and nanostructures growing in order to receive condensate from preset properties: structural perfection, type of conductivity, carriers concentration, and optical performance.

The structure, thermoelectric and spectral characteristics obtained by vapor methods (gas-dynamic stream, “hot wall”) the self-organized nanostructures and thin films of lead chalcogenides with different topology on monocrystalline (chips (0001) mica-muscovite), amorphous (polyamide film PM-1, polished glass) substrates, oxide gel films of SiO<sub>2</sub>, GeO<sub>2</sub>, HfO<sub>2</sub> on single crystals of quartz and on substrate of the silicon oxide film of SiO<sub>2</sub>. Determined that the formation of such structures is the mechanism Volmer-Weber.

There oscillation nature of the profiles of lead chalcogenides nanostructures kinetic parameters caused by quantum size effects. Shown that these effects are determined by topological features of nanostructures, and nature of their self-organization.

Detected and the peculiarities of optical properties (absorption spectra, absorption and reflection) of IV-VI nanostructures are defined as natural of condensate, and its topological features. In particular, we show that PbTe nanostructures on the polished glass characterized spectrally selective relaxation of visible radiation and the topology of PbTe nanostructures on oxide gel films of SiO<sub>2</sub>, GeO<sub>2</sub> and HfO<sub>2</sub> is defined as the deposition temperature and size of substrate thermal conductivity.

## Magnetic composite films based on $\text{La}_{0.7}\text{Sr}_{0.3}\text{MnO}_3/\text{ZrO}_2$ nanopowders

Lubenets V.A.<sup>1</sup>, Lyubchanskii I.L.<sup>1,2</sup>, Gorban O.A.<sup>2</sup>, Burkhovetskii V.V.<sup>2</sup>,  
Dvornikov E.A.<sup>2</sup>, Volkova G.K.<sup>2</sup>, Danilenko I.A.<sup>2</sup>, Konstantinova T.E.<sup>2</sup>

<sup>1</sup>*Donetsk National University, Donetsk, Ukraine*

<sup>2</sup>*Donetsk Physicotechnical Institute named after A.A. Galkin,  
National Academy of Sciences of Ukraine, Donetsk, Ukraine*

Ceramic composite films based on  $\text{ZrO}_2$  and  $\text{La}_{0.7}\text{Sr}_{0.3}\text{MnO}_3$  nanopowders prepared by Tape Casting were investigated. The influence of amount of LSMO on morphology, phase structure and magnetic properties has been studied.

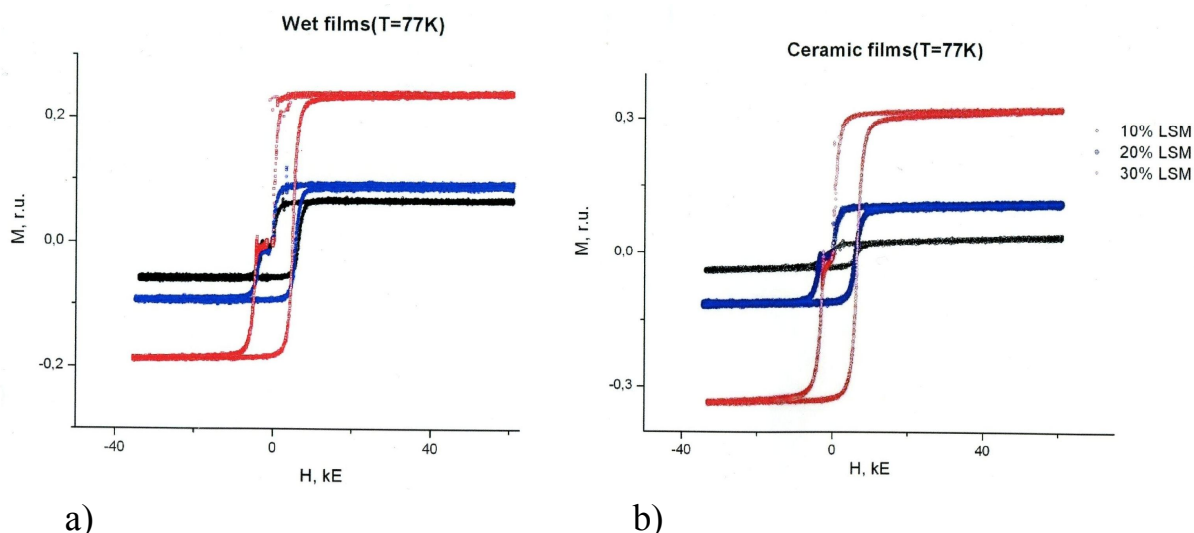
Magnetic composites based on manganite  $\text{La}_{0.7}\text{Sr}_{0.3}\text{MnO}_3$  (LSMO) are perspective materials for optoelectronics and microelectronics thanks to large magnetoresistance and frequency dependence of the hysteresis loop form.

In this work it was investigated ceramic composite films based on LSMO nanopowders, which are a diamagnetic matrix from zirconia of a tetragonal phase with included ferromagnetic phase of the LSMO.

Using scanning electron microscopy method the films structure with different concentration of the ferromagnetic phase – 10%, 20% and 30% were investigated. Phase structure has been estimated by X-ray analysis method. For diamagnetic matrix creating it was used  $\text{ZrO}_2$ -3 mol. %  $\text{Y}_2\text{O}_3$  nanopowders of a tetragonal phase, as a matrix filler were used LSMO nanopowders. Magnetic properties have been estimated by pulse magnetometer.

It has been shown that Tape Casting technology allows creating magnetic nanocomposites in the form of micron thick films [1]. The structure of the received composite films by Tape Casting technology without polymer removing represents linked by polymer globules, consist of  $\text{ZrO}_2$  nanoparticles and homogeneously distributed LSMO nanoparticles (size of 12 nm and 50 nm) there. Thermal treatment of this materials (at  $T = 1270^\circ\text{C}$ ) leads to ceramic composites formation. It has been shown that in the sintered state structure consist of the sintered grains of the  $\text{ZrO}_2$  (average size 200 nm), LSMO grain size depends of the concentration of the ferromagnetic nanopowder input in the diamagnetic matrix and varies from 0.1 mkm to 5 mkm. Size concentration increases proportional to the LSMO contene.

It has been studied magnetization curves of the investigation samples. On the pic. 1 shown magnetization curves of the wet and sintered films at the liquid nitrogen temperature.



Picture 1. Magnetization curves of the composite films (wet films – a), ceramic films, sintered at  $T = 1270^{\circ}\text{C}$  – b)) at the liquid nitrogen temperature.

As we can see from the picture, magnetization increases with the LSMO concentration increasing.

It has been shown possibility of the film elements creating based on the  $\text{ZrO}_2$  and LSMO nanopowders, that can be used as the structure elements of the one dimensional photonic crystals [2].

1. Gorban' O.A., Lubenets V.A., Lyubchanskii I.L., Burkhovetskii V.V., Danilenko I.A. and Konstantinova T.E. Zirconium dioxide nanoparticles as a new model material for nanophotonics: Self-organization effects // High Energy Chemistry. – 2009. – Vol. 43. Number 7. – pp. 566-569.
2. John D. Joannopoulos, Steven G. Johnson, Joshua N. Winn, Robert D. Meade Photonic Crystals Molding the Flow of Light // Princeton University Press. – 2008.

## Structure and electrical conductivity of amorphous films of the GaSb-GeTe system

Lutsyk N.Yu.

*Ivan Franko Lviv National University, Lviv, Ukraine*

Structure of thin amorphous films GaSb-GeTe system was studied by methods of electronography and transmission electron microscopy. The films with thickness approximately 50 nm were prepared using a method of flash vacuum evaporation.

As electronography investigations have indicated, the films of all investigated compositions of the GaSb-Ge system obtained at room temperature were amorphous. A continuous decrease of the averaged area at the first coordination maximum determined from the radial distribution curve (from 2.77 units for a-GaSb to 2.44 for a-GeTe), as well as a linear change of the nearest interatom distance ( from 0.272 nm for a-GaSb to 0.255 nm for a-GeTe) with increasing the GeTe concentration, witnesses about the formation in the films of the system investigated the “alloyed” structure. In the amorphous films of GaSb, the threefold coordination is observed in the distribution of the nearest neighbors. The atoms of Ge are surrounded, on the average, by two atoms of Ge with a distance 0.244 nm and two atoms of Te with a distance 0.259 nm, the atoms of Te are surrounded by two atoms of Te with a distance 0.259 nm in the amorphous films of GeTe. The values of valence angles estimated by the first and second interatom distances are equal  $102^\circ$  and  $109^\circ$  for GaSb and GeTe, respectively.

Electrical conductivity of GaSb films at temperatures above the room temperature is determined by an activation mechanism of conductivity with energy of activation 0.32 eV, and at low temperatures it becomes hopping conductivity in localized states around Fermi level. The density of localized states at Fermi level is near  $4 \cdot 10^{18} \text{ cm}^{-3} \text{ eV}^{-1}$ . With an increase of the GeTe concentration in the films, the density of localized states at the Fermi level decreases and the activation conductivity becomes dominated one with an increase of the activation energy up to 0.38 eV.

With a growth of the GeTe concentration, the conductivity of the amorphous films sharply decreases measured at room temperatures.

## Production of nanocrystalline bcc-phase in the Ce<sub>79</sub>Ag<sub>21</sub> alloy

Lysenko A.B., Kalinina T.V., Kosinskaya O.L., Zagorulko I.V.

*Dniprodzerzhynsk State Technical University, Dniprodzerzhynsk, Ukraine*

The peculiarities of structural transformations of a rapid-quenched amorphous foils of Ce<sub>79</sub>Ag<sub>21</sub> alloy being heated were analysed combining the methods of measurements of the specific resistivity, thermal and X-ray diffraction analysis. It is shown, that transition of truly amorphous samples in structurally stable state is carried out in two stages. At the first stage there is a polymorphic crystallisation of a metastable bcc-phase with average size of grains ~8 nm that at higher temperatures experiences single-phase dissolving for mixture of fcc  $\gamma$ -modification Ce and equiatomic compound CeAg with lattice CsCl. Each stage of the structural transformations is accompanied by inconvertible decrease of the specific electroresistance (SER) and an exotherm effect with heat generation maximas at the temperatures 398 and 493 K. Crystallization of amorphous foils causes also a change of temperature coefficient SER sign from negative to opposite.

By the processing of isothermal curves of specific electroresistance was determined an activation energy of crystallization process of the bcc-phase ( $128.4 \cdot 10^3$  J/mol) and empirical relationship of SER from an annealing time  $\tau$ .

$$\rho(T) = \rho_m + (\rho_a + \rho_m) \exp(-\alpha\tau), \quad ((1))$$

where  $\rho_a$ ,  $\rho_m$  - accordingly, SER of an explored alloy in the amorphous state and after bcc-phase crystallization;

$$\alpha = 7.3 \cdot 10^{13} \exp\left(-\frac{15443}{T}\right), \text{ s}^{-1};$$

$T$  – annealing temperature.

The mechanism of forming the nanocrystalline bcc-phase is suggested. According to it the crystallization centres are homogeneouslu nucleated and reach their finite sizes  $L$  in a very short time at the expense of cooperative diffusionless atoms displacements on small distances, then the growth processes are stopped. Within the limits of the suggested model the analytical kinetic equation accorded with the experimental data is derived:

$$x(\tau) = 1 - \exp\left(-\frac{\pi}{6} L^3 \cdot I \cdot \tau\right), \quad ((2))$$

where  $x$  – a fraction of a crystallized volume;  $I$  – a generation rate of nucleus of the bcc- phase.

## Gap appearance in the distorted multilayer graphene

Lytovchenko V.G., Strikha M.V., Klui M.I.

*V.E. Lashkariov Institute of Semiconductor Physics, NAS Ukraine, Kyiv, Ukraine*

The crystalline carbon exists in two allotropic forms:  $sp^3$  (the diamond – dielectric with extremely strong lattice) and  $sp^2$  (the fragile semimetal graphite). Within recent years the mixed  $sp^2/sp^3$  forms, like amorphous carbon, and the diamond-like carbon films (DCF), with the essential fraction of the hybridized  $sp^3$  carbon atoms, and (possibly) with the great number of hydrogen atoms, were studied intensively. For the different conditions of fabrication these films can be either totally amorphous, or they can contain the diamond crystallites.

The intensive development of the graphene physics had given the additional impact for these studies. It is well known, that the construction of graphene-based field transistor meets the principal obstacles. The zero gap in graphene yields, that it hardly possible to get the essential modification of conductivity, necessary for the creation of the open and closed states in binary logics, under any gate voltage. Therefore the aim is to induce the gap of such an energy width to make the thermally excited carriers under room temperature to make a small input into conductivity in graphene.

From these point of view the study of ultrathin (containing few graphene mono-layers only) carbon films can be very fruitful. The presence of Dirac massless fermions in ultrathin graphite was proved by the examination using the photoemission methods with the angle separation, by the scanning tunneling spectroscopy, and by infrared reflection. The previous theoretical estimations predict the appearance of the gap in the thin distorted graphite films.

We have demonstrated both theoretically and experimentally [1]: the substitution of the metallic properties of the distorted thin graphite films by semiconductor ones occur. The theoretical analysis for the band structures with the damaged  $sp^2$  groups, carried in the LCAO approximation, demonstrates the appearance of the gap, proportional to the lattice distortion. It is necessary to note, that the effect occurs not in the amorphous carbon only, but also in the thin (up to 100 nm thick) monocrystalline graphite (or multilayer graphene) films.

Quantitatively the gap can be described by the angle of the shift of one graphene monolayer in ideal graphite relatively to other. Therefore the lattice distortion can be used for the engineering of the new class of the carbon semiconductors (especially for the fabrication of the field transistors).

1. Lytovchenko V.G., Strikha M.V., Klui M.I. // Ukrainian Journal of Physics. – 2011. – 56. – 175.

## Lanthanide sulfofluorides as alloying additives to film-forming materials MgF<sub>2</sub> and ZnS

Magunov I.P.<sup>1</sup>, Zinchenko V.F.<sup>1</sup>, Stoyanova I.V.<sup>1</sup>, Timukhin Ie.V.<sup>1</sup>,  
Stamikosto O.V.<sup>1</sup>, Mazur O.S.<sup>2</sup>, Kryvda M.Yu.<sup>2</sup>

<sup>1</sup>*A.V. Bogatsky Physico-Chemical Institute of the NAS of Ukraine, Odesa, Ukraine*

<sup>2</sup>*Odesa National Polytechnic University, Odesa, Ukraine*

Film-forming materials (FFM) on the basis of magnesium fluoride MgF<sub>2</sub> (a material with low refractive index) and zinc sulfide ZnS (a material with high refractive index) are applied often together in interference optics [1]. The basic lacks of both materials are similar, it's presence in their structure of oxygen compounds which strongly (essentially) worsen optical and operational characteristics of thin-film coatings of optical articles (mechanical durability, adhesion to a substrate, optical homogeneity etc.).

Synthesis of lanthanide (RE) sulfofluorides has been reported earlier [2]. Synthesis of the composite materials with alloying additive was carried out in high-temperature tube furnace RHTC 80-450, Nabertherm, Germany; inert (Ar) high purity medium was used.

Remove of oxygen compounds (MgO, ZnO) in FFM or essential reduction of their negative influence was carried out by means of alloying additives of RE sulfofluorides (LnSF, where Ln- La, Sm, Tm). The interactions most likely should be described by the following equations:



Ln<sub>2</sub>O<sub>2</sub>S, LnOF, MgS are low-volatile compounds and they don't introduce themselves into thin-film coatings.

Efficiency of alloying action of RE sulfofluorides increases in La-Sm-Tm series, which is connected with strengthening of distinction in the acid-base properties MgO, ZnO from one hand and LnSF additives –from another. Thin-film coatings base on the composites of MgF<sub>2</sub>-LnSF and ZnS-LnSF exhibits the improved properties (index of dispersion ≤ 0.1%, high mechanical durability and optical uniformity).

1. Окатов М.А., Антонов Э.А., Байгожин А. и др. Справочник технолога-оптика // Под ред. Окатова М.А. – 2-е изд., перераб.и доп. – 2004. – СПб.: Политехника. – С. 491-492.
2. Зінченко В.Ф., Єрємін О.Г., Єфрюшина Н.П., Стамікосто О.В. // Деклараційний патент України на винахід, №36744А, Бюл.№3, 2001.

## Plasma Resonance in Granular Films of the Al-In Alloy

Makarovsky N.A., Letyago L.M.

*V.S. Karazin Kharkiv National University, Kharkiv, Ukraine*

A plasma resonance occurs in granular films of noble metals. In the visible part of the spectrum absorption bands appear that are absent in the solid films of these metals. Only a single band of plasma resonance is always excited in granular films of noble metals deposited on fused silica or glass substrates. It is fundamentally possible to affect the phenomenon of resonant absorption of light by granular films by varying the dielectric permittivity of the ambient medium, filling factor and mutual distribution of islands. The nature of the island material plays the main role in the location of the absorption band. Therefore one can expect to control the location of the absorption band by varying the relative amounts of the quantities of metals in the film.

Composite Al-In films have a single strong of plasma absorption that is due to the light absorption by free electrons in metal granules and dipole-dipole interaction between the granules, and therefore it is called a plasma resonance band. The metals were fused in a molybdenum boat in high vacuum and then deposited by evaporation on fused silica substrates heated to 300<sup>0</sup>C. Granular film samples were obtained from pure Al, pure In and Al-In alloy of a given concentration. By means of spectrophotometric measurements it was shown, that plasma resonance band position of the alloy granular film is defined by the alloy concentration concerning to the same band positions of pure component granular films. The conclusion on the island structure of the films under study may be drawn from a similarity with the Au-Al granular films [1], possessing a similar condensation mechanism, as well as on the ground of electron microscopic studies. The shape of metallic islands of the Al-In alloy is close to a spherical one and the granules are located sufficiently close to each other. Twin boundaries are clearly observed in some granules indicating their single-crystal structure.

1. Летьаго Л.М., Макаровський Н.А. Плазменний резонанс в гранулярних плівках сплавів системи Au-Al // Вісник ХНУ, серія "Фізика". – 2006. – Т. 9, № 739. – С. 138-140.

## Comparative studies of colloidal nanoparticles and nanocomposites

Makoviy V.V., Savchuk A.I., Stolyarchuk I.D., Tkachuk P.M., Savchuk O.A.

*Chernivtsi National University, Chernivtsi, Ukraine*

In the past two decades semiconductor nanocrystals, nanoparticles, or quantum dots have attracted much attention because their optical and electronic properties can be controlled by their size. The observed peaks in absorption and photoluminescence spectra of such nanostructures are shifted to shorter wavelengths just by changing their size. For this reason semiconductor nanocrystals open a wide range of potential applications such as biological sensors, solar cells, and light-emitting devices. However, the synthesis of nanoparticles in aqueous phase with tuned nanocrystalline size and narrow size distribution still remains challenge task. Optical spectroscopy provides a unique way to learn about both polymer/nanoparticles colloidal solutions and appropriate composites. In this work, we focus our attention on optical and magneto-optical studies of  $\text{Cd}_{1-x}\text{Mn}_x\text{S}$  nanocrystals in form of colloidal nanoparticles and nanocomposite films.

The synthesis of  $\text{Cd}_{1-x}\text{Mn}_x\text{S}$  nanoparticles with  $x < 0.03$  was realized in the system  $\text{CdCl}_2\text{-MnCl}_2\text{-Na}_2\text{S-H}_2\text{O}$ -surfactant (or polymer) at room temperature. Nanoparticles with various properties were obtained by varying either the pH value, or the surfactant concentration and the  $[\text{CdCl}_2]:[\text{Na}_2\text{S}]$ ,  $[\text{CdCl}_2]:[\text{MnCl}_2]$  molar ratios. In order to keep the system in the focusing regime (the formation of nearly monodisperse nanocrystals) for a long time, it was possible to perform additional injections of precursors during the growth, effectively keeping the concentration of free species in a solution above a critical threshold. The films of the polyvinylalcohol (PVA)/  $\text{Cd}_{1-x}\text{Mn}_x\text{S}$  nanoparticles composites were formed by adsorptive dessication method. For this purpose the colloid solution was transferred to glass Petri dishes which were placed in a pressure-tight vessel that contained an absorbent.

Transmission electron microscopy (TEM) analysis was used in order to confirm the nanocrystallinity of the grown samples, estimate shape and determine the average size of nanoparticles. In order to estimate surface morphology of composite PVA/  $\text{Cd}_{1-x}\text{Mn}_x\text{S}$  nanoparticle films the atomic force microscopy (AFM) analysis was performed. Optical absorption and Faraday rotation measurements were carried out at room temperature.

The AFM images show the regular fluctuation profile of the studied films due to the dispersed nanoparticles. The maximum height fluctuation is about 20 nm and the root-mean-square surface roughness is about 4 nm. The observed energy shift of exciton structure in colloidal and nanocomposite film samples suggests of quantum confinement effect due to changing of nanoparticle size. The revealed transformation of the Faraday rotation spectra is discussed.

## Electron scattering on the short-range potential of the crystal defects in GaN

Malyk O.P., Kenyo G.V.

*Lviv Polytechnic National University, Lviv, Ukraine*

Usually the charge carrier scattering models in GaN are considered in relaxation time approximation or using the variational principle. However, these models have essential shortcoming – they are long-range which contradict special relativity. From the other side in [1-3] the short range models of electron scattering were proposed for  $A^{II}B^{VI}$  semiconductors in which the above mentioned shortcomings were absent. The purpose of the present work is to use this approach for description of the electron scattering in GaN.

For the charge carrier scattering on the nonpolar optical and acoustic phonons, neutral defects, disorder and static strain potential the interaction radius of the short-range potential is limited by one unit cell. For the charge carrier scattering on the ionized impurity, polar optical and piezoelectric (piezoacoustic and piezooptic) phonons the interaction radius of the short-range potential is founded in a form  $R = \gamma b$  ( $b$  – lattice constant,  $\gamma$  – the respective adjusting parameters).

To calculate the conductivity tensor components the method of a precise solution of the stationary Boltzmann equation was used [4]. The temperature dependences of the electron mobility in the range 80 – 500 K in GaN films (the thickness of the films  $\sim 2 \div 4.5 \mu\text{m}$ ) are calculated. The influence of the different scattering mechanisms on the charge carrier mobility is considered. A good agreement between theory and experiment in all investigated temperature range is established. The scattering parameters  $\gamma$  for different scattering modes are determined.

1. Malyk O.P. // Materials Science & Engineering – 2006. – B V.129. – P. 161-171.
2. Malyk O.P. // Phys. Status Solidi (c) – 2009. – V.6 – P. 86-89.
3. Malyk O.P. // Physica B:Condensed Matter – 2009. – V.404. – P. 5022-5024.
4. Malyk O.P. // WSEAS Trans. Math. – 2004. – V.3. – P. 354-357.

## The cyclic voltammetry of nanodispersed tin dioxide

Mandzyuk V.I., Myroniuk I.F., Chelyadyn V.L.

*Vasyl Stefanyk Precarpathian National University, Ivano-Frankivsk, Ukraine*

The possibility of application of that or other material as an electrode (first of all, anode) for lithium power sources depends on many factors, one of which is its ability to accept and return the lithium ions in the process of discharge and charge. In a recent year the attention of researchers is concentrated on the application of tin dioxide for the indicated aims [1,2], which is called to replace graphite used in industrial production of power sources.

For research of tin dioxide the materials got at different technological conditions were chosen: standards 1 and 2 – liquid-phase method, standard 3 – gas-phase method.

For identification of electrochemical processes, which take place in the Li | 1M LiBF<sub>4</sub> (GBL) | SnO<sub>2</sub> system at its cycling, cyclic voltamograms were got

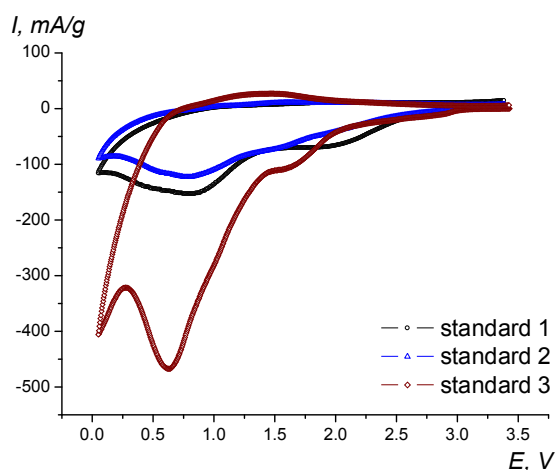
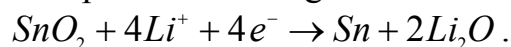
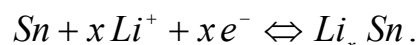


Fig. CV-curves for SnO<sub>2</sub> at first cycle.

(figure). At the first cycle on the discharge branch of all materials a peak at potential 0.83; 0.78 and 0.63 V is identified, which it is possible to ascribe to forming of Li<sub>2</sub>O phase according to reaction:



Metallic tin interacts with the lithium ions with formation of Li<sub>x</sub>Sn intermetallic compounds at lower potentials in accordance to reaction:



It is significant that there is enough large area at the first discharge cycle in the voltage range of 2.9 ÷ 1.7 V, which it is possible to ascribe to forming of solid electrolyte interface on the surface of electrode material.

*This work has been funded by the CRDF/USAID (UKX 2-9200-IF-08) and the Ministry of Education and Science of Ukraine (M/130-2009).*

1. Kim J.Y., King D.E., Kumta P.N., Blobgren G.E. Chemical synthesis of tin oxide-based materials for Li-ion battery anodes influence of process parameters on the electrochemical behaviour // *The Journal of Electrochemical Society*. – 2000. – V.147. – P. 4411-4420.
2. Park M.-S., Wang G.-X., Kang Y.-M., Wexler D., Dou S.-X., Liu H.-K. Preparation and electrochemical properties of SnO<sub>2</sub> nanowires for application in lithium-ion batteries // *Angew. Chem. Ed.* – 2007. – V.46. – P. 750-753.

## Anthracite as electrode material for lithium power sources

Mandzyuk V.I.<sup>1</sup>, Nagirna N.I.<sup>1</sup>, Povazhnyi V.A.<sup>2</sup>, Golovko L.V.<sup>2</sup>, Rachiyy B.I.<sup>1</sup>

<sup>1</sup>*Vasyl Stefanyk Precarpathian National University, Ivano-Frankivsk, Ukraine*

<sup>2</sup>*Institute of Bioorganic Chemistry of National Academy of Science of Ukraine, Kyiv, Ukraine*

Among a wide range of coals, anthracite is interesting for its abundance, low cost, high carbon content, non-graphitizable nature, microporous structure and high density [1, 2]. Easy handling and simple material preparation make the anthracite attractive as a candidate for cathodes of lithium power sources.

Six standards of nanoporous carbon obtained from natural Donets anthracite (Ukraine) by steam and gas activation method in boiling bed at temperature of 1100-1200 K.

The isotherms of nitrogen adsorption were got using automotive device KELVIN-1042 (KOSTECH MICROANALYTICAL).

Electrochemical introduction of lithium ions was carried out in two-electrode glass cells with separated cathode and anode space in galvanostatic regime (current density was 40  $\mu\text{A}/\text{cm}^2$ , voltage interval was 3.4  $\div$  0.05 V) using TIONiT P2.00-xx charge / discharge stand.

As follows from received results (table), the value of specific capacity of the explored materials correlates with the size of specific surface and total pores volume. The effect of micropores volume is less significant.

Table

The structure-adsorption and energy characteristics of nanoporous carbon obtained from anthracite

Standard	Specific surface, $\text{m}^2/\text{g}$	Total pores volume, $\text{cm}^3/\text{g}$	Micropores volume, $\text{cm}^3/\text{g}$	Specific capacity, $\text{mA}\cdot\text{h}/\text{g}$
A-1	450	0.26	0.20	940
A-2	680	0.34	0.18	979
A-3	880	0.49	0.23	1193
A-4	940	0.50	0.25	1150
A-5	980	0.55	0.17	1157
A-6	990	0.59	0.17	1440

This work has been funded by the CRDF/USAID (UKX 2-9200-IF-08) and the Ministry of Education and Science of Ukraine (M/130-2009)

1. Bessant G.A.R., Walker P.L. Activation of anthracite: Using carbon dioxide versus air // Carbon. – 1994. – V.32, №6, – P. 1171-1176.
2. Povazhnyy V.A., Golovko L.V. The catalyst carrier of vinyl acetate synthesis on activated anthracite base of Donetsk deposits // Catalysis and Petrochemistry. – 2010. – V.18. – P. 67-71.

## Crystal-chemistry defects in bromine doped crystals of cadmium telluride

Mezhylovska L.Yo., Koznyk A.P., Koznyk V.P., Korzhenevskyj O.Y.

*Vasyl Stefanyk Precarpathion National University, Ivano-Frankivsk, Ukraine*

Semiconductor group A<sup>II</sup>B<sup>VI</sup> are the basic materials for building optoelectronic device structures that function in a wide range of optical spectrum. Cadmium telluride, thanks especially a complex of physical and chemical properties, occupies a significant place among these compounds. The band gap CdTe ( $E_g = 1.6$  eV at 0 K) determines the efficiency of its use for solar cells, and a high radiation resistance allows the creation of uncooled detectors of X- and  $\gamma$ -radiation, that operate at room temperature.

Despite the long research, the problem of defect creation in undoped and doped crystals CdTe is actual today.

In this Work was investigated the defect structure of Undoped and doped cadmium telluride crystals of bromine using crystal-chemical model, that account all possible types of their own ( $V_{Cd}$ ,  $Cd_i$ ,  $V_{Te}$ ,  $Te_i$ , each of which may be in three charge states: 0,  $\pm 1$ ,  $\pm 2$ ) and impurities point defects and their complexes.

Based on the proposed model compensation of donor impurities in the crystals of cadmium telluride, which takes into account the possibility of formation of impurity precipitates, it is calculated concentration prevailing point defects and free carriers. It is determined the constants of the quasi-chemical reactions of substitution defects and their complexes with own point defects. Using the electrochemical and thermodynamic parameters of halogen atoms and atoms of the matrix (cadmium and tellurium) it is determined enthalpies of the complexes of halogen atoms with the cadmium vacancy.

It is determined the factors that limit the electrical action of halogen impurities. Based on the experimental data and thermodynamic modeling of the defect structure in doped crystals of cadmium telluride, it is found that as a result of low impurity compensation bromine and high values of mobility given materials contain significant concentration of electrons and can be used in photovoltaic structures.

## **Features of heat transfer in porous silicon films**

Monastyrskii L.S.<sup>1</sup>, Pavlyk M.R.<sup>1</sup>, Vaskiv A.P.<sup>1</sup>, Yarytska L.I.<sup>2</sup>

<sup>1</sup>*Ivan Franko Lviv National University, Lviv, Ukraine*

<sup>2</sup>*Lviv State University of Vital Activity Safety, Lviv, Ukraine*

The work describes the process of heat transfer in spatial heterogeneous structures based on porous silicon films. Using mathematical modeling methods it makes possible get possibility to forecast results of experimental investigation, implementing which connected with big labor input.

It was studied problem of nonstationary heat transfer in heterostructure of film porous silicon - silicon wafer after pulsed laser and electron-ray heating. It is shown, that temperature of heterostructure surface linear increase during pulse time and exponent monotonously drop during 8-10 pulse period. It was observed features in temperature dependences of cooling-down structures after pulsed laser radiation of classical film superlattice of porous silicon with different degree of porosity of layers. Such features are connected with difference of thermo-physics parameters of superlattice layers with different degree of porosity. It was achieved maximum temperature not only the surface, but inside the porous silicon samples after electron-ray heating.

It was study 2D problem of stationary dependence of heat transfer in a model, which considers porous silicon as matrix of vertical rods. It was shown, that zones of low temperature and gradient temperature place in separate rods during heating.

Analyzing head transfer process in films of nanoporous silicon it is necessary to take to account low size effects that is we have taken into not only conductive component and ballistic component of heat transfer. It was shown, that role of ballistic component of heat transfer increases when thickness of porous silicon film decreases. For calculation it was used numerical methods such as difference schemes and finite elements method.

## **Electron-microscopy investigations of nanoporous carbon**

Morushko O.V., Budzulyak I.M., Rachiy B.I., Yablon L.S.

*Vasyl Stefanyk PreCarpathian National University, Ivano-Frankivsk, Ukraine*

Nanoporous carbon which is used in the devices of energy accumulation (supercapacitors) should correspond to the certain conditions of structure and developed surface. For this material pore size distribution, together with the value of developed surface, is one of the most important parameters which determines specific capacitance characteristics of certain supercapacitors, whereas the access of electrolyte to the pores is substantially depends from the microstructure of carbon material.

To find out the peculiarities of developed surface structure we have carried out the comparative analysis of this surface after its thermal, chemical and laser treatment on the basis of electron-microscopy investigations.

It was found out that additional thermal treatment causes the appearance of additional microcracks in the carbon particles. At the same time capacitance of the corresponding supercapacitors sharply increases that testifies the fact that such microcracks open the closed pores, which results in the increasing of working surface.

Original nanoporous carbon is characterized by the presence of circle or oval transport pores which usually are filled by the fragments of carbon. Laser irradiation of nanoporous carbon, doped by Cr, results in the appearance of doped areas in surface, which can testify about nonequal distribution of Cr in the near-surface layer with the formation of absorbing centre. On the irradiated areas of doped nanoporous carbon Chrome distribution becomes almost equal, that follows from elementwise analysis of free chosen points of surface. At the same time pores are cleaned from the mentioned fragments, probably because of their evaporation at the laser heating.

In the nanoporous carbon doped by manganese at the mentioned conditions of irradiation melting is absent that can be explained by different manganese distribution in the near-surface layer. It should be mentioned that although Cr and Mn have high density of electron state near Fermi level, their state in the structure of carbon is different that results from the differences in the behavior of electrochemical capacitor systems formed on the base of nanoporous carbon irradiated by laser.

So, analysis of electron-microscopy investigations of nanoporous carbon developed surface and its elementwise composition in the single points adds and proves the data about the structure of pore systems, obtained by the methods of porometry and X-ray low-angle scattering [1].

1. Ткачевський В.В. Приповрехневі зміни в поруватому вуглецевому матеріалі, ініційовані лазерним опроміненням / В.В. Ткачевський, М.В. Беркешук, Б.І. Рачій, О.М. Трохименко, А.К. Мельник, Т.Л. Яценко // Наносистеми, наноматеріали, нанотехнології. – 2009. – Т.7, №2. – С. 345-358.

## Radiation-induced effects in non-crystalline GeSe(S) films

Mykolaychuk O.G.<sup>1</sup>, Romanyuk R.R.<sup>2</sup>, Balyts'ka V.O.<sup>3</sup>

<sup>1</sup>*Ivan Franko Lviv National University, Lviv, Ukraine*

<sup>2</sup>*Western Scientific Centre, Lviv, Ukraine*

<sup>3</sup>*Lviv State University of Vital Activity Safety, Lviv, Ukraine*

The complex investigations in respect to make clear the physical features of localized states forming in mobility gap GeSe(S) of amorphous films, caused by high-energy electromagnetic irradiation, were carried out. The thin films under investigation (thickness near 0.3-1.2  $\mu\text{m}$ ) were obtained using the method of discrete evaporation of fine-dispersive mixture on surface in vacuum ( $10^{-4}$  Pa) from fresh cleave NaCl, glass-ceramics and quarts at 293-450 K.

The temperature region of GeSe(S) amorphous structure existence was determined. The peculiarities of low order of amorphous thin films in dependences of technology preparation and influences of gamma-irradiation were studied. The topology and micro-local features of disordered structure GeSe(S) films formation process were established using the method of analysis of experimental scattering curves as well as model interpretation of radial distribution function of atomic density. It was established that  $\gamma$ -irradiation (1.25 MeV) with dose  $10^4$ - $10^5$  Gy causes the changes of electro-physical properties of GeSe amorphous films, in particular, the decrease of specific resistance and appearance of jump mechanism of conductivity on localized states near Fermi level. The gamma-irradiation of GeSe films caused low-energetic shift of their fundamental optical absorption edge and increasing of refraction index, while the energy gap and steepness of Urbach edge were decreased. It was established, the form and position of main diffusion maximum, studied by X-ray method, does not change after  $\gamma$ -irradiation. It was shown that crystalline processes in irradiated amorphous condensates become more denominated in comparison with non-irradiated ones. Low-energy irradiation (non-focus electron beam with energy  $35 \cdot 10^3$  eV) stimulated the more ordering structure GeSe(S) films with amorphous phase conservation, because leads to increasing the mobility gap and decreasing of electro-conductivity of films. The amorphous GeS films show the stability to influence of electron irradiation. It was shown that direction of physical properties changes in GeSe(S) films can leads to disordered processes as well as to decreasing of structures defects. Radiation-induced changes of physical properties in amorphous GeSe(S) thin film are explained in the framework of radiation defect-formation processes as results of destruction-polymerization transformations.

The main topological reactions of radiation defects centres formation were proposed as well as the model of energy gap transformation under irradiation with provision for peculiarities reconstruction spectra of localized states.

## Atomic structure and morphology of SnO<sub>2</sub> nanoparticles prepared by pyrogenic and liquid-phase methods

Myronyuk L.I., Kotsyubynsky V.O., Chelyadyn V.L.

*Vasyl Stefanyk Precarpathian National University, Ivano-Frankivsk, Ukraine*

Tin dioxide in the form of dispersed particles or film material is widely used in various branches of science and technology. SnO<sub>2</sub> films is used as a transparent contact electrode material, for gases sensors, catalyst for fuel cell and electrode material in lithium power sources. Nanodispersed SnO<sub>2</sub> is typically obtained by chemical conversion of tin-containing substances. The purpose of this study was to examine the influence of obtaining method on the crystal structure, morphology and surface condition of SnO<sub>2</sub> nanoparticles. The material obtained by the interaction of SnCl<sub>4</sub> or SnCl<sub>4</sub>·5H<sub>2</sub>O with NaOH solution is a hydrated product with the average size of coherent scattering areas about (1 ? 4) nm. This result corresponds to electron microscopy data (fig., a) Tin dioxide nanoparticles obtained by pyrogenic method based on process of SnCl<sub>4</sub> sintering in hydrogen-air flame does not contain adsorpted forms of water. High activity of the SnO<sub>2</sub> particles surface and peculiarities of the pyrogenic synthesis conditions result in the sintering and growth of material particles, whose size

accordingly to direct observation (fig.,b) was 120 -180 nm. Size effects were found that are connected with the influence of Laplace pressure on the tin dioxide particles. Countering of the convergence of Sn<sup>4+</sup> ions weakens their connection with O<sup>2-</sup> ions. Reducing of the symmetry for the nanoparticles due to the hydration of their surface leads to the disappearance in the IR spectras of SnO<sub>2</sub> bands at 541 and 424 cm<sup>-1</sup> which are caused by twice degenerated Sn-O vibrations E<sub>u</sub> modes and the formation of new bands at 569-573 cm<sup>-1</sup>. The presence of ozonid groupings ≡ SnO<sub>2</sub>H and ≡ SnO<sub>3</sub>H on the tin dioxide surface is caused by oxidation of Sn<sup>2+</sup> to Sn<sup>4+</sup>, adsorption of oxygen and their conversion in O<sub>2</sub><sup>-</sup> and O<sub>2</sub><sup>2-</sup> and the formation with water anions HO<sub>2</sub><sup>-</sup> and HO<sub>3</sub><sup>-</sup>.

*The work is supported by CRDF/USAID (UKX2-9200-IF-08) and the Ministry of Education and Science of Ukraine (M/130-2009).*

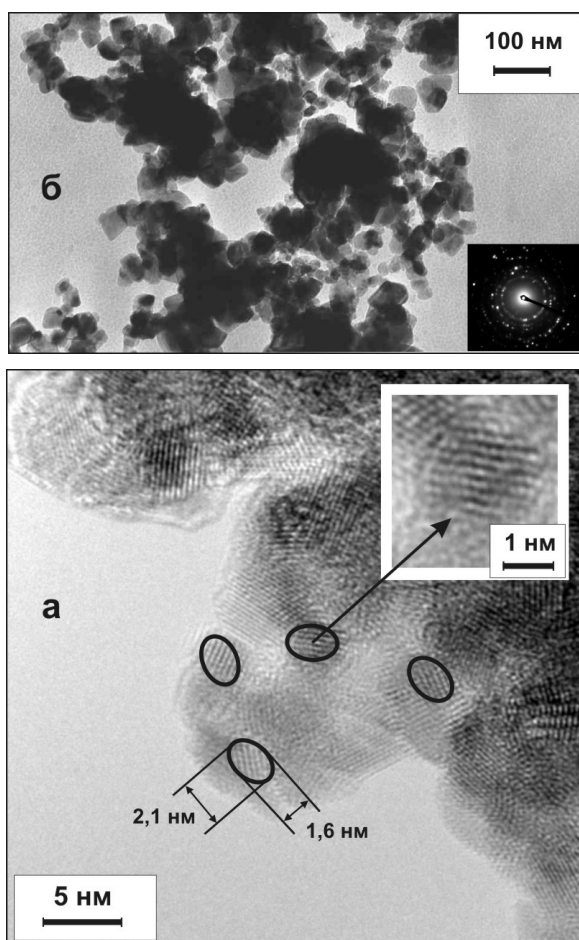


Fig. SnO<sub>2</sub> particles, obtained by liquid-phase (a) and pyrogenic (б) methods.

## Deposition and spectrometric studies of $(\text{Ga}_{0.1}\text{In}_{0.9})_2\text{Se}_3$ thin films

Nagy R.O.<sup>1</sup>, Kranjčec M.<sup>2</sup>, Hip I.<sup>3</sup>, Petrachenkov E.I.<sup>1</sup>,  
Suslikov L.M.<sup>1</sup>, Studenyak I.P.<sup>1</sup>

<sup>1</sup>*Uzhhorod National University, Uzhhorod, Ukraine*

<sup>2</sup>*University of Zagreb, Varaždin, Republic of Croatia*

<sup>3</sup>*University of Debrecen, Debrecen, Hungary*

$(\text{Ga}_x\text{In}_{1-x})_2\text{Se}_3$  semiconductor solid solutions in the compositional interval  $0.02 < x < 0.55$  crystallize in the defect wurtzite structure and possess hexagonal symmetry ( $P6_1$  or  $P6_5$  space group). They are characterized by high optical activity along the optical axis and are promising materials for acousto-optical modulators of laser light.

$(\text{Ga}_{0.1}\text{In}_{0.9})_2\text{Se}_3$  films were sputtered onto a quartz glass substrate by thermal evaporation, their thickness being  $1.99 \mu\text{m}$ . The structure of the deposited films was analyzed by X-ray diffraction; the diffraction spectra show the films to be amorphous. The composition of the layers was determined by EDX on Hitachi S4300 SEM. The transmission spectra  $T(\lambda)$  of the  $(\text{Ga}_{0.1}\text{In}_{0.9})_2\text{Se}_3$  thin film were studied by MDR-3 grating monochromator. For the low-temperature studies a UTREX cryostat was used. The refractive index was measured by a LEF-3M laser ellipsometer ( $\lambda = 632.8 \text{ nm}$ ).

From transmission spectra the absorption spectra of thin film were calculated; their analysis in the region of exponential behaviour of the optical absorption edge is performed. It is shown that the temperature behaviour of exponential parts of thin film absorption edge is described by the Urbach rule. The convergence point coordinates of the Urbach bundle are determined:  $E_0 = 2.252 \text{ eV}$  and  $\alpha_0 = 1.3 \times 10^5 \text{ cm}^{-1}$ . In  $(\text{Ga}_{0.1}\text{In}_{0.9})_2\text{Se}_3$  crystal  $E_0$  and  $\alpha_0$  values respectively equal  $2.252 \text{ eV}$  and  $1.8 \times 10^9 \text{ cm}^{-1}$  for the polarization  $\mathbf{E} \parallel c$ . In amorphous  $(\text{Ga}_{0.1}\text{In}_{0.9})_2\text{Se}_3$  thin film as well as in the single crystal absorption edge is formed by electron-phonon interaction (EPI), which is enhanced in the thin film in comparison with the single crystal. Thus, the EPI parameter equals  $\sigma_0 = 0.922$  for single crystal and  $\sigma_0 = 0.256$  for thin film.

Based the analysis of absorption edge spectra the optical pseudogap  $E_g^*$  ( $E_g^*$  is the absorption edge energy position at the fixed value of the absorption coefficient  $\alpha = 10^3 \text{ cm}^{-1}$ ) and Urbach energy  $E_U$  ( $E_U$  is the energy width of the exponential absorption edge) are determined; at temperature  $T = 300 \text{ K}$  they are respectively equal  $1.693 \text{ eV}$  and  $115.8 \text{ meV}$ . It should be noted that the optical pseudogap for the single crystal is  $E_g^* = 1.940 \text{ eV}$  and  $E_U = 30.9 \text{ meV}$  for the polarization  $\mathbf{E} \parallel c$ . The nonlinear decrease of  $E_g^*$  as well as the nonlinear increase of  $E_U$  with temperature are revealed. Both temperature dependences are well described in the framework of the Einstein model.

## Nanofacet structure of twin boundaries in polysilicon films

Nakhodkin N.G., Kulish N.P., Rodionova T.V.

*Taras Shevchenko Kyiv National University, Kyiv, Ukraine*

Polysilicon films are widely used as a material for solar cells. It is well known [1] that the electrical and optical properties of polysilicon films are dominated by grain boundary defects. It is therefore of particular interest to study grain boundary transformation in films, including twin boundaries in the interior of grains.

In this work, the grain boundary nanofaceting transitions of twin boundaries inside grains of polysilicon films under annealing has been investigated by transmission electron microscopy (TEM).

It has been shown that interior of some grains contains twin plates. Parallel elongated sides of the twin plates are formed by the coherent symmetric twin (STGB) and correspond to the plane  $(100)_{\text{CSL}}$  in the framework of simple coincidence site lattice (CSL). The width of twin plates increases with increase of annealing temperature. STGB are stable at all annealing temperatures. Tips of twin plates are characterized by nanofacet structure, which is temperature dependent.

Nanofacet type depends on annealing temperature ( $T_0$ ). TEM studies show that four types of nanofacet are observed in the twin tips of at  $T_0 = 1120^\circ\text{C}$ :  $(110)_{\text{CSL}}$ ,  $(120)_{\text{CSL}}$ ,  $(130)_{\text{CSL}}$ ,  $(210)_{\text{CSL}}$ . Between  $1120^\circ\text{C}$  and  $1150^\circ\text{C}$  both  $(120)_{\text{CSL}}$  and  $(210)_{\text{CSL}}$  facets disappear and  $(010)_{\text{CSL}}$  facet appears. The length of  $(130)_{\text{CSL}}$  facet increases from 100 nm to 30 nm. At  $T_0 = 1200^\circ\text{C}$  only  $(110)_{\text{CSL}}$  facet is present in the twin tip. Its normalized length (relative to the twin width) at  $1200^\circ\text{C}$  is three times smaller than at  $1120^\circ\text{C}$ . This indicates that the grain boundary faceting transition takes place between these temperatures at that one facet type exchange another one. Furthermore, at  $1120^\circ\text{C}$  some twin plates with curved (rough) tip are observed. With increasing temperature the transition of curved grain boundary into faceting grain boundary takes place. This transition was observed in Zn [2], while for the first time in Si.

1. Rath J.K. Low temperature polycrystalline silicon: a review on deposition, physical properties and solar cell applications // Solar Energy Materials and Solar Cells. – 2003. – V. 76, № 4. – P. 431-487.
2. Sursaeva V.G., Gornakova A.S., Yashnikov V.P., Straumal B.B. Motion of the faceted  $57^\circ [11 \bar{2}0]$  tilt grain boundary in zinc // J Mater Sci. – 2008. - V.43. – P. 3860-3866.

## Thermoelectric properties of Bi wires in a glass coating with the orientation of $C_3$ along the wire axis

Nikolaeva A.A.<sup>1,2</sup>, Konopko L.A.<sup>1,2</sup>, Tsurkan A.K.<sup>1</sup>, Botnary O.V.<sup>1</sup>

<sup>1</sup>*Institute of Electronic Engineering and Industrial Technologies, AS of Moldova*

<sup>2</sup>*International Laboratory of High Magnetic Fields and Low Temperatures, Wroclaw, Poland*

In bismuth, the direction of high electron mobility coincides with the low thermal conductivity. This fact makes Bi a promising thermoelectric material.

However, crystals of Bi with the orientation of  $C_3$  along the axis are easily cleaved along cleavage planes (111) perpendicular to  $C_3$ , which reduces the mechanical reliability of thermoelectric branches. One way to improve the mechanical strength can be the use of samples in the form of single-crystal "rods" a glass coating. It is known that, the preparation of single-crystal wires of Bi and  $Bi_{1-x}Sb_x$  in a glass coating by liquid phase casting gives wires with the (1011) orientation along the wire axis [1], i.e., the crystallographic  $C_3$  axis makes an angle of  $70^\circ$  with the wire axis.

For the first time, using the method of the horizontal zone recrystallization, we obtained glass-insulated single-crystal Bi wires with the orientation of  $C_3$  along the wire axis, which is confirmed by the study of angular rotation diagrams of transverse magnetoresistance and SdH oscillations. The effect of the transverse ( $H \perp \Delta T$ ) and longitudinal ( $H \parallel \Delta T$ ) (Fig. 1) magnetic fields on the thermopower and resistance is studied.

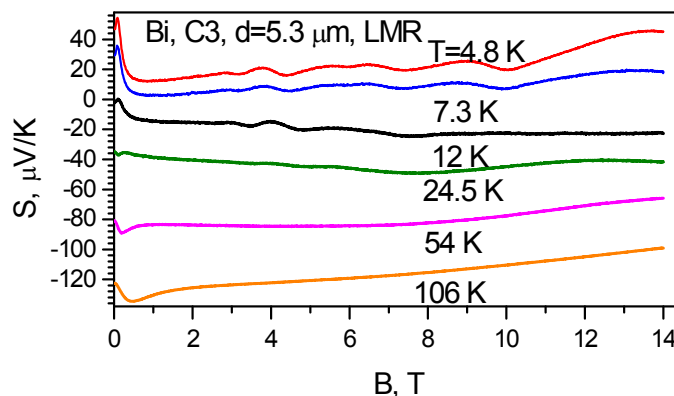


Fig. 4. Dependences of the magnetothermopower of a Bi wire with  $d = 5.3 \text{ mm}$  at different temperatures  $H \parallel \Delta T$  in magnetic fields up to 14 T.

It is shown that the maximum value of Powder factor ( $P.f. = \alpha^2 \sigma$ ) is reached in a region of 100-200 K and is  $3.4 \cdot 10^{-4} \text{ W/cm} \cdot \text{K}^2$  in a magnetic field of 0.4 T.

This work was supported by STCU grant № 5050.

1. Gitsu D., Konopko L., Nikolaeva A. and Huber T. Pressure dependent thermopower of individual Bi nanowires // *J. Applied Physics Letters* – 2005 – V.86, P. 10210.

## Futures of tensoresistive effect in film materials on the range of elastic and plastic deformation

Odnovorets L.V.

*Sumy State University, Sumy, Ukraine*

The unique electrical and mechanical properties of bulk and film nanocrystalline materials continue to attract the attention of researchers. Along with mechanical properties, of special interest is the mechanism of plastic deformation in these materials. Considering the general relationship for the longitudinal strain sensitivity coefficient averaged over the measured strain range:  $\gamma_l = \gamma_l^\rho + 1 + 2\mu$ , and assuming that the volume resistivity of the grains remains unchanged under grain-boundary slip (i.e.,  $\gamma_l^\rho \cong 0$ ), author [1] concludes that  $\gamma_l \cong 2$  at the plastic flow. In the above expression,  $\gamma_l^\rho = \frac{1}{\rho} \frac{\partial \rho}{\partial \varepsilon_l}$ ,  $\rho$  is the resistivity (superscript  $\rho$  means that  $\gamma_\rho$  is expressed through the resistivity), and  $\nu$  is Poisson's ratio (equal to 0.5 under plastic flow).

In film materials, the grain-boundary scattering of electrons makes a major contribution to the strain sensitivity coefficient: the value of  $\gamma_l$  reaches several unities. Apparently, this scattering mechanism causing a decrease in mean free path  $\lambda_0$  competes with its increase due to an increase in the grain size, with the result that  $\gamma_l^\rho < 0$  for the Cu and Mo wires and  $\gamma_l^\rho > 0$  for the Ni wire.

The aim of this work is gaining a deeper insight into the tensoresistive effect in single-layer Cr, Fe, Mo, Ni and Pd films and double-layer Fe/Cr, Cu/Cr, Ni/Cr and Pd/Fe films in the range of elastic and plastic deformation.

Single- and double-layer films (the layer thickness 10-80 nm) were obtained by thermal evaporation in a VUP-5M setup equipped with a specially designed automated vacuum condensation system. The films were deposited on a polystyrene substrate. The advantage of this substrate material over glass-fiber laminate, teflon, or dielectric-covered nickel foil, which were used earlier, is that it remains elastic up to a strain of 2%. Value  $\varepsilon_{lr}$  - deformation of transition indirectly determining, from the  $R$  versus  $\varepsilon_l$  curve. The tensoresistive properties were studied with an automated system [3] that made it possible to carry out many compression–extension cycles under static and dynamic conditions at a strain rate from 0 to 0.1%/s (Figure).

The crystal structure and phase composition were examined by transmission electron microscopy and electron diffraction. The phase composition of the Fe/Cr and Pd/Fe double-layer films corresponds to an  $\alpha$ -Fe–Cr bcc solid solution and an fcc Pd–Fe solid solution, while that of the Cu/Cr and Ni/Cr films corresponds to a Cr/Ni–bcc Cr + fcc Ni biplate and a Cr/Cu–bcc Cr + fcc Cu

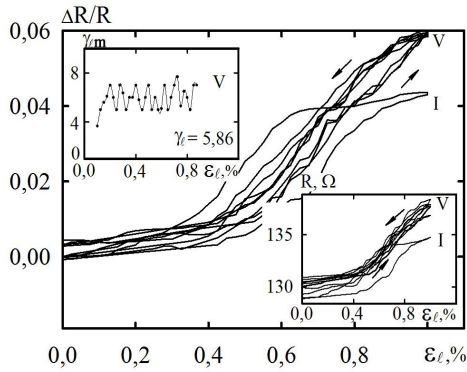


Fig.  $\Delta R/R$ ,  $R$ , and  $\gamma_{lm}$  vs. longitudinal strain  $\epsilon_l$  for the Pd(30)/Fe(15)/sub film systems (sub - substrate)

biplate. Table suggests that the plastic strain sensitivity is several times higher than the elastic strain sensitivity (see, for example, [4]). The size effect is observed for all three tensor resistive parameters, although the opposite trend in the size dependence of  $\epsilon_{lr}$  for the single-layer Fe films remains unclear.

Table. Strain sensitivity of the films in the elastic and plastic strain ranges

Film (thickness, nm)	$\epsilon_{lr}$ , %	Film (thickness, nm)	$\epsilon_{lr}$ , %
Cr(30)	0.20	Fe(20)/Cr(30)	0.40
Cr(75)	0.10	Fe(50)/Cr(30)	0.25
Ni (20)	0.20	Cr(20)/Ni(20)	0.40
Ni (40)	0.15	Cr(20)/Ni(40)	0.30
Pd (18)	0.52	Pd(30)/Fe(15)	0.57
Pd (100)	0.25	Pd(10)/Fe(20)	0.48

It is found that the processes of electron scattering at grain boundaries and in the volume of grains make a major contribution to the strain sensitivity of elastically and plastically strained film materials. Surface scattering is tangible only in the case of thin films. The plastic strain sensitivity of the films is several times higher than the sensitivity to elastic strain. The strain at which the elastic–plastic transition takes place depends on the film thickness and decreases monotonically with increasing thickness. It is demonstrated with Fe/Cr films, which represent a through-thickness homogeneous solid solution, that the grain-boundary scattering of electrons is equally effective under elastic and plastic strains, since the respective grain-boundary scattering coefficients (about 0.4) coincide within the experimental error. Electron scattering in the volume and at the boundaries of grains leads to a 30% decrease in the mean free path of electrons.

The author is grateful to Tkach O.P. for their participation in the experiments.

*Work performed under the theme № 0109U001387.*

1. Klokova N.P., Tenzoresistivnost (Mashinostroenie, Moscow, 1990).
2. Lasyuchenko O., Odnodvoretz L., Protsenko I. // Cryst. Res. Technol. – 2000. – V.35. – P. 329.
3. Protsenko S.I., Velykodnyi D.V., Kheraj V.A., Desai M.S., Panchal C.J., Protsenko I.Yu. // J. Mater. Sci. – 2009. – V. 44. – P. 4905.
4. Ткач О.П., Однедворець Л.В., Проценко С.І., Великодний Д.В., Тищенко К.В., Проценко І.Ю. // Ж. нано-електрон. фіз. – 2010. – V.2 – P. 51.

## The nature of the manganese luminescence centers in thin-film emitting devices

Omelchenko S.A., Plakhtiy E.G., Bulanyi M.F., Kovalenko A.V.,  
Khmelenko O.V., Gorban A.A.

*O. Gonchar Dnipropetrovsk National University, Dnipropetrovsk, Ukraine*

It is now widely used thin-film light-emitting devices based on ZnS-Mn. But despite this, on the question about the number and the nature of different manganese centers in these materials is still no definitive answer. That is why, the trying of exact identification of some elementary bands of manganese photoluminescence in ZnS crystals grown up from the melt is made in this report.

ESR researches has shown, that in such crystals there can be four types of nonequivalent  $Mn_{Zn}^{2+}$  centres [1]. In cubic areas of twin sphalerite, the centres with local  $T_d$  symmetry (sites of AN type) are placed. In areas of stacking faults and crystals with hexagonal structure the centres with local  $C_{3V}$  symmetry (sites of AS, PN and PS types) are placed. It possible also existence of luminescence  $Mn_i$  centres in tetrahedral or octahedral interstitial sites. Besides, some "hypothetical" sites, which are situated «near to dislocations» or «near with point defects clouds» are offered [2]. However, neither the quantity of the elemental emission bands, nor their connection with concrete type of Mn-centres, exactly have not been spotted till now. In this report is informing about some results of investigations, which was devoted the solution of this problem.

The grown from the melt, ZnS-Mn crystals, in which artificially was stabilised hexagonal structure(2H), were investigated. The structure of such crystals is depending from regime of thermal annealing. Possibility demonstrating of samples obtaining with any necessary relation of different types  $Mn_{Zn}^{2+}$  centres, was made. Magnitude of this relation was determined by ESR measurements. If each of these types of centres take part in formation of a common band of a luminescence, then by means of corresponding mathematical processing of spectroscopic lines probably their partitioning and the further exact identification. It main idea of our experiments which was realized here.

Besides, it was shown, that the manganese centres of sensitized luminescence, together with sensitizing centres are localised in atmospheres Cottrells around grown dislocations.

1. Берлов П.А., Буланый М.Ф., Омельченко С.А. Изменение структуры и локализации центров  $Mn^{2+}$  при деформации кристаллов сульфида цинка // Кристаллография. – 1998. – Т.43, № 3. – С. 457-462.
2. Борисенко Н.Д., Буланый М.Ф., Коджеспиров Ф.Ф., Полежаев Б.А. Свойства центров свечения в монокристаллах сульфида цинка с примесью марганца // ЖПС. – 1991.– Т.55, №3. – С. 452.

## **Formation and properties of anodic aluminum oxide, resulting in a complex electrolyte**

Ostapenco E.V., Mazurenko N.I.

*Institute of Physics, National Academy of Sciences of Belarus, Minsk, Belarus*

This paper presents results on the formation and investigation of the anodic alumina (AA), obtained in a complex electrolyte based on oxalic acid and citric acid.

Samples of AA were obtained by anodization of aluminum foil grade A99 in a complex electrolyte under galvanostatic conditions at current density  $7 \text{ mA/cm}^2$  and electrolyte temperature  $10 \text{ }^\circ\text{C}$ . Then, the samples of AA were annealed at different temperatures:  $900$ ,  $1000$  and  $1300 \text{ }^\circ\text{C}$ .

The main morphological parameters of the amorphous and annealed samples (cell diameter, pore diameter, surface roughness) were identified by atomic force microscopy (AFM) and scanning electron microscopy (SEM). Significant differences in surface morphology and cell size of anodic alumina annealed at  $900$  and  $1000 \text{ }^\circ\text{C}$  has not been established. Cells of AA annealed at a temperature of  $1300 \text{ }^\circ\text{C}$ , while maintaining size, are composed of particles of arbitrary shape. The sizes of these particles are different and have a significant variation in value. Established that the annealing temperature has no significant effect on the surface roughness value of the AA samples. It should also be noted that high-temperature processing of AA did not lead to violation of the integrity of the samples.

The samples of amorphous anodic alumina were subjected to differential thermal analysis. Significantly lower concentration of impurities as compared with the oxide formed in sulfuric and oxalic electrolytes was established for the AA obtained in the complex electrolyte.

The results of thermogravimetric analysis are confirmed by optical studies. For the amorphous and annealed samples of the AA the absorption and transmission spectra were recorded in the wavelength range from  $200 \text{ nm}$  to  $800 \text{ nm}$ , and infrared spectra. The IR spectra of original and annealed samples suggest a decrease in the number of impurities with increasing annealing temperature AOA. As follows from the results of the study, the dependence of the transmission and absorption of the samples on the annealing temperature is determined by the presence of anions of the electrolyte and the presence in the oxide structure of F-centers (oxygen vacancies) in different charge states.

## **The study of phase composition for diffusion zone after saturation the surface with both boron and carbon**

Philonenko N.Yu., Beryoza Ye.Yu., Baskevich A.S.

*Dnipropetrovsk State Medical Academy, Dnipropetrovsk, Ukraine*

Despite the wide applications of saturation the surface with boron, the question concerned with mechanism of structure formation in diffusion zone still remains undetermined. Thereby, in this paper we investigate the formation mechanism of multiphase inclusions in surface diffusion zone of low-carbon alloy after saturation with both boron and carbon.

The investigation was carried out for specimens of iron-base alloys with a carbon content of 0.25%. The alloys under examination previously had been isothermal annealed at the temperature of 950°C for five hours and then had been casehardened with boron in charcoal carburizer with boron carbide and activation dopant for four hours. For the research we used the following methods of analysis: X-ray, microspectrum, durametric and layer-by-layer spectrographic analysis.

Upon saturation the surface of previously annealed low-carbon alloy with both boron and carbon the boron-case layer of a depth of 1600-1700  $\mu\text{m}$  with a surface hardness index of 72-76 HRCe is forming. The research results show that the multiphase inclusions, obtained as a result of the saturation the surface of low-carbon alloy with both boron and carbon, demonstrate the same structure as the multiphase inclusions in the cast boron-bearing alloy. The multiphase inclusion consists of three phases: in the centre of inclusion there is boride  $\text{Fe}_2\text{B}$  surrounded by boron cementite  $\text{Fe}_3(\text{CB})$ , whilst outer shell represents the cubic boron carbide  $\text{Fe}_{23}(\text{CB})_6$ .

Formation of multiphase inclusions on the pearlite grain boundaries adversely affects on micromechanical properties of boron-case layer. To improve the mechanical properties of boron-case layer after casehardening with boron we used stoppage at the temperature of 1133-1173 K. Due to the stoppage within the temperature interval of 1133-1173 K the multiphase inclusions are dissolving and the formation of single-phase inclusions  $\text{Fe}_3(\text{CB})$  and  $\text{Fe}_2\text{B}$  takes place. The stoppage at the temperature of 1133-1173 K enables to obtain a boron-case layer which is homogeneous in structure and depth and is hardened with finely divided boron carbides. The result is 1.2-1.4 times increase in hardness and 1.2-1.4 times increase in its relative wear resistance. Besides, the frailty of the surface layer decreases.

## Nonstructure defects in cadmium telluride

Prokopiv V.V., Vanchuk V.B.

*Vasyl Stefanyk PreCarpathion National University, Ivano-Frankivsk, Ukraine*

Cadmium Telluride is widely used in transformers of solar energy, nuclear energy, and infrared nonlinear optics.

Electrical and optical properties of the crystal are determined mainly by its own defects. Despite the considerable number of papers, which studied the structure of point defects in CdTe, clearly remains uncertain on their dominant species.

The existing of anti-structure defects in CdTe crystals is actual task, which according to various authors can be both shallow and deep donor.

Aim of paper is to explain the electrical properties and temperature dependence of homogeneity area width of the cadmium telluride, using model of defect subsystem, which also vacancies and interstitial atoms of anions and cations ( $V_{Cd}$ ,  $V_{Te}$ ,  $Cd_i$ ,  $Te_i$ ) included anti-structure defects  $Te_{Cd}$ .

The equilibrium concentration of point defects in the crystal at two-temperature annealing was determined by minimizing of crystal-gas thermodynamic potential.

There was correctly explain results of electrical properties measurements of crystals in wide range of annealing temperature and additional pressure component at two-temperature annealing using of proposed model.

The anti-structure defect model significantly better reconcile the experimental and theoretical temperature dependence of the homogeneity compounds, compared with models that do not include these defects. According to calculations by this model, at temperatures below  $\approx 900$  K the major defects that cause the deviation from stoichiometry, is vacancy of cadmium  $V_{Cd}$  at the tellurium surplus and vacancy of tellurium  $V_{Te}$  at the cadmium surplus, and at higher temperatures – interstitial atoms of cadmium  $Cd_i$  at cadmium surplus and tellurium atoms in the Cadmium sublattice  $Te_{Cd}$ , and interstitial  $Te_i$  at tellurium surplus.

The compare of experimental and theoretical the temperature and pressure dependencies of free charge carriers concentration shows, that anti-structure defects are deep donors, and create the energy levels near the valence band.

*This work to execute according department project (State registration № 0107U006768).*

## Influence of Growth Conditions on Defect Subsystem in Lead Telluride Films

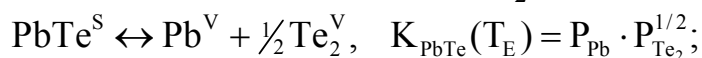
Prokopiv V.V. (Jr.), Dumenko N.V., Volochanska B.P., Pylyponyuk M.A.

*Vasyl Stefanyk PreCarpathian National University, Ivano-Frankivsk, Ukraine*

Lead Telluride is the perspective material for detectors and sources for IR optical emission spectrum and thermoelectric devices. Experimentally known, that when growing the lead telluride films from vapor phase by hot-wall method the change of tellurium partial vapor pressure  $P_{Te_2}$  of additional source of tellurium under low pressure of tellurium ( $P_{Te_2} < 10^{-3}$  Pa) does not affect on charge carriers and defects concentrations. Further, the same increase of tellurium partial vapor pressure at constant temperature of substrate temperature  $T_S$  and those of evaporation temperature  $T_E$  reduces the Hall's electron concentration  $n$ , and to conductivity type inversion from n- to p-type, and increase of holes concentration  $p$  [1].

In this paper the pressure dependencies of Hall's concentration could be explained that at low tellurium pressures  $P_{Te_2}$  of additional source the tellurium pressure in the system is determined by evaporation temperature.

Lead telluride dissociated with molecules  $Te_2$  formation at evaporation:



There is set the partial pressure  $P_{Te_2}$  in system that corresponds to congruential sublimation of lead telluride and describe of equation [2]:

$$\lg(P_{Te_2}, Pa)_{\min} = -\frac{10940 \pm 350}{T_E} + 10.26 \pm 0.38.$$

This pressure will influence on formation of defect subsystem of the growing films under low of tellurium pressure in additional source ( $P_{Te_2} < 10^{-3}$  Pa).

Was determined that the area expands with increasing of evaporation temperature for charge carriers and defects concentration that not dependent from partial vapor tellurium pressure  $P_{Te_2}$  of tellurium additional source.

1. Lopez-Otero A., Hoas L.D. // Thin Solid Films. – 1974. – V. 23. – № 1. – P. 1-6.
2. Zlomanov V.P., Novoselova A.V. P-T-x-diagrams of metal – chalcogen system state. – M.: Nauka, –1987. – 208 p.

## **Investigation of magnetic properties of films of Gd-Fe system**

Prysyazhnyuk V.I., Mykolaychuk J.G.

*Lviv National University, Lviv, Ukraine*

We conduct investigation of magnetic properties of films of  $GdFe_2$  and  $Gd_2Fe_{17}$  compounds. Films have been gained by a method of thermal evaporation on glassceramic substrates at room temperatures. The thickness of films – 1000-2000 Å.

Values of Curie temperature for massive and thin-film samples are determined. It is spotted that the Curie temperature of massive samples corresponds to references. At examination of thin-film samples Curie temperature reduction was observed. Such depression of Curie temperature speaks expansion of a crystalline lattice owing to formation of microdefect (films were is amorphous-crystal).

Temperature dependences of magnetic saturation for compounds and films of Gd-Fe system are determined. The given dependences characteristic for materials of such class. Magnetic saturation of films  $Gd_2Fe_{17}$  at room temperature makes 4.8  $\mu b$ . The given value gets to an interval 6.21-1.84  $\mu b$  for rhombic and hexagonal modification properly. It means that our films are an intermixture of these modifications.

## Parameters of radiation disordering process of epitaxial YIG films crystalline microstructure at implantation by oxygen ions

Pylypiv V.M., Grygoruk O.O.

*Vasyl Stefanyk Precarpathian National University, Ivano-Frankivsk, Ukraine*

Changes in the magnetic microstructure of surface layers epitaxial yttrium iron garnet films (YIG) after implantation by  $O^+$  ions with energy 90 keV were investigated by methods of electronic conversion Mossbauer spectroscopy and mathematical modeling of radiation defect formation process.

Amorphous clusters were considered as paramagnetic inclusions in the ferrymagnetic matrix, the  $c$  concentration of which depends on the ion fluence  $D$  as  $c(D) = A \cdot (1 - \exp[-\beta D])$  ( $\beta = N_0 \sigma_n V_0$ ,  $N_0$  – target ion concentration,  $\sigma_n$  – elastic defect formation section,  $V_0$  – the average volume of amorphous cluster,  $A$  – the multiplier), and it is directly proportional to the relative content

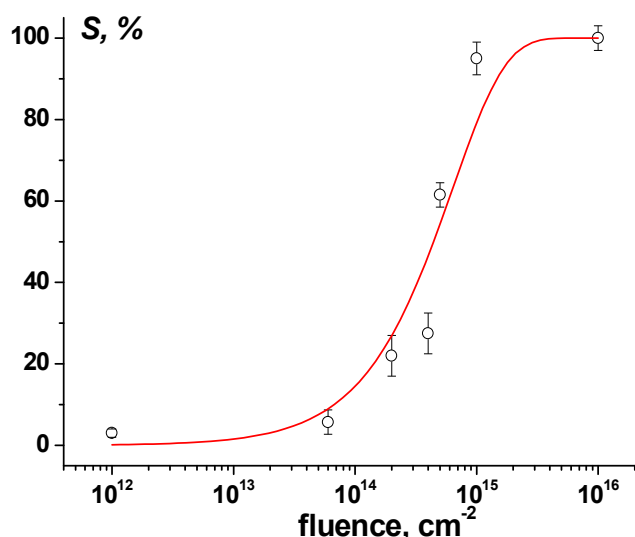


Fig. Relative content of doublet components of YIG films Mossbauer spectra vs  $O^+$  ions implantation fluence (points) and approximation function  $c(D)$

of doublet components of the Mossbauer spectrum  $S_D$ . Considering that the concentration of amorphous region formed during atom-atomic collisions is directly proportional to the relative content of doublet components of Mossbauer spectras, an average volume  $(8.2 \pm 1.0) \cdot 10^{-20} \text{ cm}^3$  of disordered clusters was determined, which corresponds to the linear size  $4.3 \pm 0.3 \text{ nm}$  (Fig.). Crystal microarea after cascade atom-atomic collisions consists of amorphous nuclear and defective crystalline zone. At low fluences ion tracks do not overlap and imperfection structure is minimal.

At fluences of  $D = (4 \div 6) \cdot 10^{14} \text{ cm}^{-2}$  a gradual accumulation of point defects begins with the following binding them in simple complexes that is displayed by increasing of  $c(D)$  changes rate for  $D = 10^{14} - 10^{15} \text{ cm}^{-2}$  range. The size of amorphous cluster grows, gaining the maximum value of  $5.5 \pm 0.5 \text{ nm}$  at  $D = 10^{15} \text{ cm}^{-2}$ . Further increase of fluence results in the emergence of defects complexes and amorphous regions formation which causes gradual overcoming of  $S(D)$  dependence on the plateau ( $D \geq 1 \cdot 10^{15} \text{ cm}^{-2}$ ). Analysis of the data shows that the amorphous cluster size for this range is  $3.5 \pm 0.5 \text{ nm}$ , that is explained by increase of the density of crystal disordering areas with the growth of implantation fluence.

## X-ray diffraction methods for dimensional measurement of nanocrystals – CdMnS, TiO<sub>2</sub>, fullerenes

Raransky M.D., Balazyuk V.N., Melnyk M.I., Kovalyuk Z.D.

*Yu. Fedkovich Chernivtsi National University, Chernivtsi, Ukraine*

With the advance in nanotechnologies and a wide application of nanocomposites, nanocrystals and semiconductor nanostructures, the problem of dimensional measurement of small crystals (10-100 nm) by nondestructive methods becomes extremely important. Atomic-force and tunneling scanning microscopy allow observing with a high space resolution ( $\Delta r \sim 0.1-10 \text{ \AA}$ ) only the surface relief [1]. Electron microscopy possesses high resolution (1-10  $\text{\AA}$ ). At the same time, artifacts arising in the manufacture of thin films do not enable unambiguous interpretation of a real structure.

In this paper, X-ray diffraction methods and computer simulation are used to perform phase and structural analysis of synthesized nanocomposites CdMnS, TiO<sub>2</sub> and fullerenes C<sub>60</sub>. X-ray diffraction spectra were obtained on the DRON-3M installation and recorded in the range of angles from 5 to 70 degrees in CuK<sub>α</sub> – radiation. With crystal dimensions 1-10<sup>2</sup> nm, one can observe smearing of diffraction maxima, the width of which  $\beta(\theta) = \frac{\int I(\theta) d\theta}{I(\theta)}$  is related

to nanocrystal dimension  $L$  by the Scherrer relation:

$$\beta(\theta) = \frac{K \cdot \lambda}{L \cdot \cos \theta} \quad (1)$$

where  $\theta$  is diffraction angle,  $\lambda$  is wavelength,  $K$  is coefficient that depends on diffraction geometry. However, with crystal dimensions 10<sup>3</sup> – 10<sup>5</sup> nm, the width of diffraction maxima  $\beta(\theta) \approx 10''$ . With further increase in crystal dimension  $L > 10^5$  nm, separate crystallite images can be seen on diffraction maxima (Fig.1), the number of which  $n_{hkl}$  on the Debye line equals

$$n_{hkl} = L \cdot V \cdot m \cdot P \cdot \cos \theta \quad (2)$$

where  $V$  is irradiated crystal volume,  $m$  takes into account X-ray divergence,  $P$  is repeatability factor.

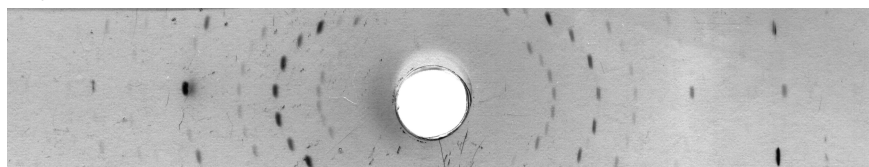


Fig. 1. Diffraction maxima of CdS, CuK<sub>α</sub> – radiation.

Physical properties of synthesized nanocrystals and nanocomposites are also analyzed.

1. Rashkovich L.N., Shustin O.A., Chernevich T.G. Fluctuations on the sides of dihydrophosphate kalium crystals // Solid State Physics. – 2000. – V.42, №10. – P. 1869-1873.

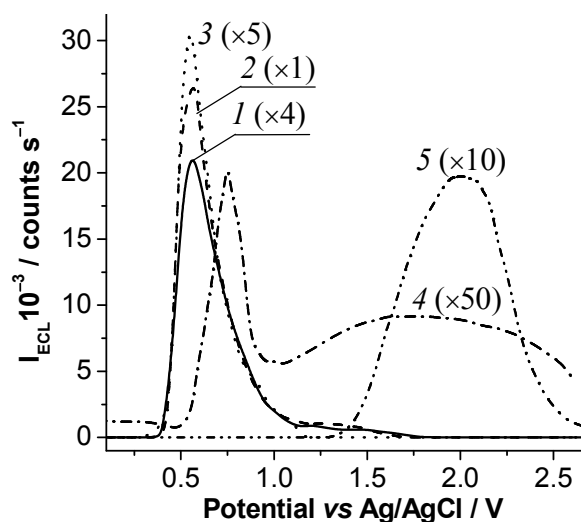
## Electrochemiluminescent (ECL) properties of the thin films of aniline-luminol copolymers on the platinum electrode

Reshetnyak O.V.<sup>1</sup>, Koval'chuk E.P.<sup>1</sup>, Błażejowski J.<sup>2</sup>,  
 Protsyshyn Kh.V.<sup>1</sup>, Pavlyuk V.A.<sup>1</sup>

<sup>1</sup>Ivan Franko National University of Lviv, Lviv, Ukraine

<sup>2</sup>University of Gdańsk, Gdańsk, Poland

Proceeding from the luminescent properties of the luminol (Lum), it can be assumed, that analogous properties possesses also its polymeric form and copolymers. Therefore the thin films of the luminol and aniline (An) copolymer (P(An-Lum)) under the different molar ratio of monomers (C(Lum):C(An) = 10:1, 1:1, 1:10 and 1:25) in the initial mixture were synthesized electrochemically on the platinum electrode under the potentiostatic conditions (TE = +1.2 V vs Ag/AgCl reference electrode) and its electrochemiluminescent properties has



Dependence of the ECL intensity of Plum (1) and P(An-Lum) (2–5) from the electrode potential (duration of polymerization – 15 min; C<sub>0</sub>(Lum) = 0.01 M; C<sub>0</sub>(An), M: 0.0 (1); 0.001 (2); 0.01 (3); 0.10 (4); 0.25 (5)

been studied. The samples of polyluminol (Plum) and copolymers, in accordance with data in [1], were produced in the acid aqueous-DMSO (volume ratio 9:1) medium. ECL of Plum and P(An-Lum) films was studied under the potentiodynamic conditions (s<sub>E</sub> = 5 mV/s) in the alkaline aqueous medium (pH 10.5). The feature of the P(An-Lum) ECL is the presence of the two waves of light radiation, exactly under the +(0.4–1.2) V and +(1.2–2.5) V, on the dependence of the ECL intensity from the electrode potential (see Fig.). The first wave ECL observes for the PLum (curve 1) and copolymers (curves 2–3), which were synthesized under the ratio C(Lum):C(An) = (1–10):1.

The increase of this ratio to 1:10 leads to the origin of the second wave (curve 4), which stays a sole under further increase of aniline contents to the 1:25 ratio (curve 5). Analysis of the results shown, that the source of ECL is direct electrochemical (first wave) or chemical (by the electrochemically generated free radical intermediates, second wave) oxidation of the luminol fragments in the polymeric chains. The high ECL intensity of copolymer's samples argues about the availability of these materials for the use in the sensors of luminescent type.

1. Koval'chuk E.P., Grynchysyn I.V., Reshetnyak O.V., J. Błażejowski // Euro. Polym. J. – 2005. – V. 41. – P. 1315-1325.

## Correlation of deposition conditions and mechanical properties of a-SiC(:H) films deposited by radio-frequency magnetron sputtering technique

Rusavsky A.V., Vasin A.V., Okholin P.M., Rymarenko N.L.,  
Stepanov V.G., Nazarov A.N.

*Lashkaryov Institute of Semiconductor Physics, Kyiv, Ukraine*

Report is focused on the study of mechanical properties of a-Si<sub>1-x</sub>C<sub>x</sub>(:H) layers (density, hardness, residual stress) deposited by radio-frequency magnetron sputtering technique. Hydrogenated a-Si<sub>1-x</sub>C<sub>x</sub>:H films were deposited on Si wafers by magnetron sputtering of SiC target in Ar (93 vol.%) + CH<sub>4</sub>(7 vol.%) gas mixture. Non-hydrogenated a-SiC films were deposited by sputtering of SiC target in pure argon. Deposition temperature was about 200<sup>0</sup>C. A series of the samples have been deposited applying different RF-discharge power. After the deposition some of the samples were thermally treated at atmospheric pressure in dry argon. Nanohardness and bulk density have been measured by nanoindentation, and weighing methods correspondingly while residual stress was estimated from substrate curvature radius (using Stony equation) measured by X-ray diffraction from silicon substrate. Local structure and morphology was examined by FTIR, Raman scattering, atom force microscopy (AFM) and scanning transmission electron microscopy (STEM).

Nonhydrogenated a-SiC exhibited significantly denser and harder structure in comparison with a-Si<sub>1-x</sub>C<sub>x</sub>:H films. It was shown that density of the films and compressive residual stress are directly correlated in both hydrogenated and nonhydrogenated materials. Surface roughness was found to be correlated with bulk density as well. Comparative study of the surface morphology (by AFM) and bulk morphology (STEM) allows to suggest that bulk density and surface roughness are determined by nanoscale growth morphology features appearing due to low deposition temperature (low surface mobility of the atoms and radicals). Annealing of the films in argon at 450<sup>0</sup>C resulted in reduction of compressive stress in a-Si<sub>1-x</sub>C<sub>x</sub>:H while a-SiC layers do not show obvious stress relaxation. Moreover, part of the a-SiC were delaminated after annealing (450<sup>0</sup>C).

Sumarizing of the experimental data we conclude that: (1) density of the SiC(:H) films deposited at lows substrate temperature by radio-frequency magnetron sputtering is mostly determined by nanoscale (20-60 nm) growth features associated with low deposition temperature; (2) incorporation of hydrocarbon reduces bulk density of the material and promote to relaxation of residual compressive stress. Low-stress a-Si<sub>1-x</sub>C<sub>x</sub>:H films have been fabricated by combination of “low RF power” regime and low temperature postdeposition annealing.

## Structure research in the modified composite resins

Ryk L.V., Domantsevich N.I., Yatsyshyn B.P.

*Lviv Commercial Academy, Lviv, Ukraine*

Technical resins have a complex of properties and features that distinguishes them from the traditional materials used in a woodworking industry, and applied, mainly, for agglutination and formation of compositions. Characteristics of such composites define consumer properties of products and demand careful studying. Structure research and physical-mechanical characteristics of glues are important for upgrading during creation of wood-wool composites.

It is positioned that the structure of a surface of urea-formaldehyde resins (UFR) by industrial production KF-MT-15, hardened according to requirements of a technological regime of manufacturing of wood-wool composites, was relief and porous (fig. 1). At the same time use of modified resins lead to reducing of quantity of free formaldehyde in a composition (to 0.1-0.3 vol. %). That's why surface of such resins is more flat, with smaller structure forming (fig. 2). The differences of structure at hardening of two types of resins are connected as with processes of formation and modification in organic materials (activity of components, speed of reactions and other), and with physical and chemical characteristics constituents (initial viscosity, time of gelatinization).



Fig. 1. Microphotography of surface of the hardened unmodified UFR-sample (KF-MT-15). X 300.

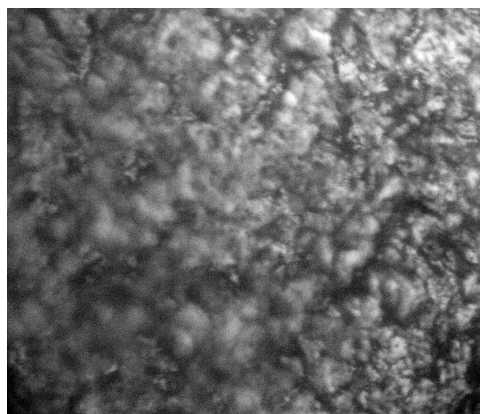


Fig. 2. Microphotography of surface structure of the hardened modified resin sample. X 300.

The increasing of mechanical characteristics (hardness on a bend, hardness on a distention) and improvement of physical indicators (density, hygroscopicity, swelling in water) modified composites materials were established by subsequent physical-mechanical tests of composite wood-wool materials.

## Diffusion instability of homogeneous distribution of lead in lead tin telluride

Saliy Ya.P., Stefaniv N.Ya.

*Vasyl Stefanyk Precarpathian National University, Ivano-Frankivsk, Ukraine*

The alloy  $\text{Pb}_x\text{Sn}_{1-x}\text{Te}$  is the principal material for fabrication of IR photodetectors. A major concern in the growth, processing and use of  $\text{Pb}_x\text{Sn}_{1-x}\text{Te}$  is its stability. Components and defects move easily in this material. Some interdiffusion occurs even during growth of  $\text{PbTe/SnTe}$  superlattices at temperatures as low as  $\sim 200^\circ\text{C}$ . Lead interstitials which are donors and cation vacancies which are acceptors in are both usually present in the alloy and move about during the growth and post-growth treatment, producing some native doping. Usually, as-grown films of  $\text{Pb}_{0.8}\text{Sn}_{0.2}\text{Te}$  are of p-type due to the vacancies, and some post-growth annealing is required to convert them into n-type. However, layers obtained by low-temperature epitaxy may be of n-type as grown.

Although the uniformity of composition of good-quality  $\text{Pb}_x\text{Sn}_{1-x}\text{Te}$  samples grown by different techniques is usually pretty good, the spatial distribution of native dopants may be quite inhomogeneous. The formation of some clusters of Pb atoms on the surface was observed directly for epilayers after post-growth cooling or annealing, and it was suggested that as-grown material contained the Pb atoms inhomogeneously distributed in interstitial positions.

There are a significant number of publications where ideas of non-uniformity have been used to account for several peculiarities in the transport properties of  $\text{Pb}_x\text{Sn}_{1-x}\text{Te}$  alloys.

A mechanism of formation of inhomogeneities in the alloy  $\text{Pb}_x\text{Sn}_{1-x}\text{Te}$  during either post-growth cooling or low-temperature annealing is proposed, based on a diffusion instability in the interacting system which includes cations in lattice sites, lead interstitials and cation vacancies. The principal points of the mechanism are: vacancies follow local variations of alloy composition, being always in local equilibrium; their concentration depends superlinearly on local composition. The uniform distribution of composition and the native dopants becomes unstable under a condition that is likely to be satisfied at temperatures below  $200^\circ\text{C}$  in samples enriched with lead interstitials. We show that the instability should result in the formation of a layered doping profile where the concentration of lead interstitials varies by a factor of 2-3 while the variation of composition is of the order of 10%. Possible consequences of this effect for the electrophysical properties of the alloy are discussed.

## Band gap simulation for $ZrO_2 <Ti>$ nanostructured materials

Savchenko N.D., Shchurova T.N., Opachko I.I.

*Uzhgorod National University, Uzhgorod, Ukraine*

The purpose of the present work is calculation of the band gap for  $ZrO_2 <Ti>$  nanostructured materials promising to be applicable in opto- and microelectronics due to the wide range of possible variation in the band gap.

Calculations were conducted by a method based on linear combination of atomic orbitals and pseudopotential with the use of Hartree-Fock atomic terms [1] in three steps. Tabular values of the covalent radii for Zr (0.175 nm), Ti (0.161 nm) and O (0.042 nm) atoms were taken in the calculations of covalent bonding energy. At the first step, the energy positions of the valence band maximum and conduction band minimum for  $ZrO_2$  and  $TiO_2$ , were found to be -10.3; -5.15; and -9.99; -7.05 eV, respectively. This allowed to define the band

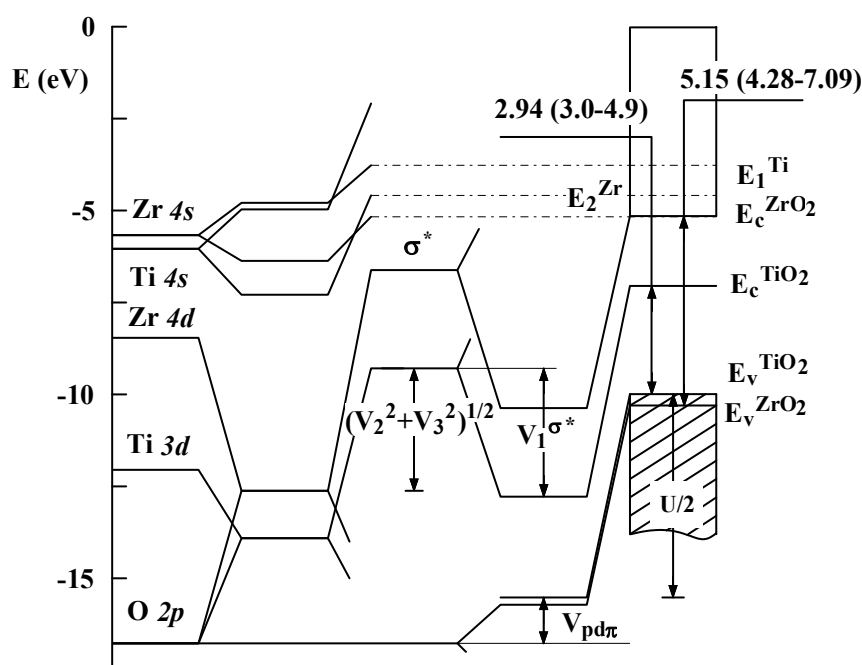


**Figure.** The energy band diagram for  $TiO_2$  and  $ZrO_2$ . Theoretical and experimental data for the band gap taken from literature are given in parentheses in electron-volts.

concentration dependence of the band gap was calculated, assuming that at  $x \leq 0.98$  the band gap of  $ZrO_2 <Ti>$  compound is formed by Ti 3d states. The band gap value of 4.06 eV was found for  $x = 0.98$ . For other  $x$  values the band gaps were determined by linear approximation.

gap values for  $ZrO_2$  (5.15 eV), and  $TiO_2$  (2.94 eV) in the  $\Gamma$ -point of the Brillouin zone. At the second step of the calculations, we determined the energy positions in  $ZrO_2$  band gap of the states induced by a presence of titanium ions. From the value of Ti 4s atomic term the energy of the above-mentioned states is expected to be -4.95 eV. At the third step,

1. Harrison W.A. Elementary Electronic Structure. New Jersey, London, Singapore, Shanghai, Hong Kong, Taipei, Chennai: World Scientific Publishing Co. – 2004.

## Adjustment of native nanostructure of bacteriorhodopsin molecules by low-power cw gas laser irradiance

Savchuk A.<sup>1,2</sup>, Stepanchikov D.<sup>3</sup>, Burykin N.<sup>1</sup>, Korchemskaya E.<sup>1,2</sup>

<sup>1</sup>International Center “Institute of Applied Optics”, Kyiv Ukraine;

<sup>2</sup>Institute of Physics, Kyiv Ukraine;

<sup>3</sup>Zhytomyr State University, Zhytomyr Ukraine

The biological photoreceptor bacteriorhodopsin (BR) is embedded in the purple membranes of the extreme halophilic microorganism *Halobacterium salinarium*. In the purple membrane fragment, BR molecules are coupled at different angles into trimers forming a two-dimensional hexagonal crystalline lattice with a space of 62 Å [1]. The crystalline structure causes astonishing stability of BR toward chemical and thermal degradation. Upon absorbing visual light, a BR molecule undergoes a cycle of the photochemical conversions. The initial form of BR photocycle, bR570, has an absorption peak at 570 nm, and the longest-lived (in film) intermediate M412 has an absorption peak at 412 nm. BR has gained acceptance as the multifunctional nanomaterial [2]. However, the potentialities of a light impact on the creation of nanostructures with BR were not considered previously. In this report the directed photobleaching of one, two or three molecules in the BR trimer through the variation of intensity of linearly polarized light beam is first proposed.

A probability of the phototransformation bR570→M412 depends on the BR molecule orientation in a film plane. The molecules whose long axes are aligned close to the direction of light polarization do absorb light, whereas those with perpendicular orientation to this direction do not absorb light. As a result photoselection of BR molecules takes place under the action of linearly polarized light [3]. The photoinduced dichroism increases initially with increase in the exciting light intensity and reaches a peak value. On further increasing light intensity a decrease in the macroscopic dichroism value comes because the BR molecules oriented perpendicularly to the direction of polarization of light with near-saturation intensity are also capable of phototransformation to the intermediate M412. An experimental dependence of the macroscopic photoinduced dichroism was modeled with regard to the coupling of BR molecules in a trimer at different angles (Fig. 1). From a value of the macroscopic photoinduced dichroism, we determine a quantity of the photobleaching BR molecules in trimers at given light intensity. A calculated probability of a transition in the intermediate M412 of one, two or three molecules in BR trimers as a function of an intensity of the linearly polarized exciting He-Ne laser beam,  $I$ , in the steady-state for the wild type BR is shown in Fig. 2 ( $a = \sigma_{\parallel}^B A^{B \rightarrow M} \tau I \lambda / hc$ , where  $\sigma_{\parallel}^B$  is the absorption cross-section for the

light polarized parallel to a long absorption axis of a molecule for the form bR570;  $A^{B \rightarrow M}$  is quantum yield of bR570  $\rightarrow$  M412 transition;  $\tau$  is the thermal relaxation time of M412;  $\lambda = 633$  nm).

An interaction between the BR molecule and nanoparticle is more efficient for the M412 intermediate than for the initial form bR570. We found that control of a quantity of BR molecules in the M412 intermediate at sites in the hexagonal crystalline lattice with a space of 62 Å could be performed by the low-power cw He-Ne laser irradiance.

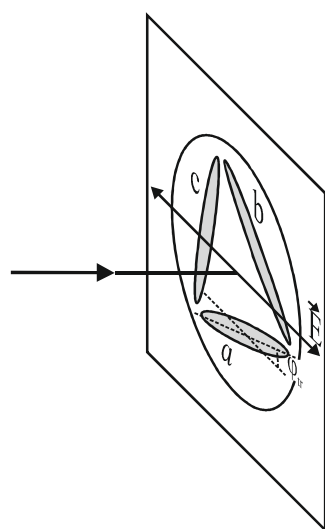


Fig. 1

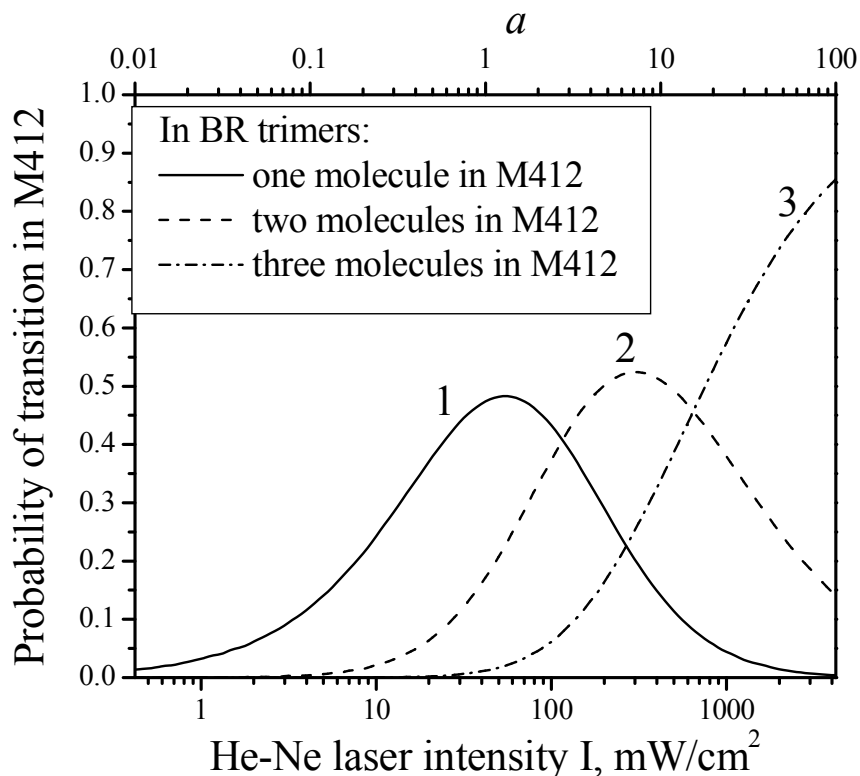


Fig. 2

1. Balashov S.P., Lanyi J.K. "Bacteriorhodopsin" In: Microbial Bionanotechnology (Edited by B. Rehm). – Horizon Press, London, 2006. – P. 339-365.
2. Hampp N. "Nanobiotechnology enables new opportunities in material sciences: bacteriorhodopsin as a first example" In: Bionanotechnology: Proteins to Nanodevices. (Eds.: V. Renugopalakrishnan, R.V. Lewis). - Springer, Dordrecht, Netherlands, 2006. – P. 209-216.
3. Korchemskaya E., Stepanchikov D., Druzhko A., Dyukova T. Mechanism of nonlinear photoinduced anisotropy in bacteriorhodopsin and its derivatives // Journal of Biological Physics. – 1999. – V.24. – P. 201-215.

## Structural and optical properties of $Zn_{1-x}Co_xO$ thin films

Savchuk S.A., Kleto G.I., Tkachuk V.I., Smolinsky M.M., Garasym V.I.

*Chernivtsi National University, Chernivtsi, Ukraine*

In the past decade, ZnO-based diluted magnetic semiconductors (DMSs) doped with transition metals have attracted much attention due to the possibility to induce room temperature ferromagnetism. However, many open questions still remain regarding the origin and mechanisms of ferromagnetic ordering in DMSs. In case of Co doped ZnO thin films, many researchers attributed the observed ferromagnetism to Co clustering. There are also reports, in which ferromagnetic behavior is intrinsic in nature.

In this work,  $Zn_{1-x}Co_xO$  thin films with content of Co  $0 < x < 0.08$  were deposited by RF-plasma sputtering technique. Targets for this technique were prepared by solid state reaction using of ZnO (99.99 %) and Co (99.5 %) powders. X-ray diffraction, atomic force microscopy, optical spectroscopy and magneto-optical Faraday rotation measurements were used for characterization of the grown films. Structural analysis and optical absorption spectra confirm incorporation of  $Co^{2+}$  ions on  $Zn^{2+}$  sites into ZnO lattice for  $x < 0.04$ . Transmission spectra are shown in Fig. 1. The shift of the absorption edge to higher photon energy with the increase of Co content in the  $Zn_{1-x}Co_xO$  oxides can be seen.

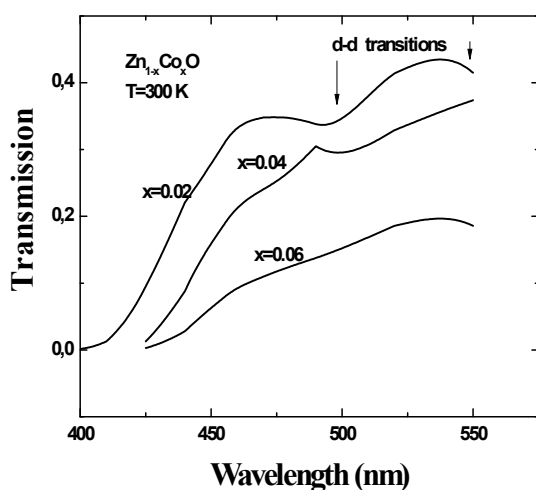


Fig.1. Transmission spectra of  $Zn_{1-x}Co_xO$  thin films.

In longer wavelength part of the spectra additional absorption bands were observed. Three absorption bands are explained within the framework of d-d transitions in ions of  $Co^{2+}$ . In particular, they can be attributed to the following transitions:  ${}^4A_3(F) \rightarrow {}^2E(G)$ ,

${}^4A_3(F) \rightarrow {}^4T_1(p)$  and  ${}^4A_2(F) \rightarrow {}^2A_1(G)$ .

In addition, increasing of Co content led to creation of inclusions in the grown films. Peculiarities were revealed in magnetic field dependence of Faraday rotation, which can be attributed to ferromagnetic ordering for  $Zn_{1-x}Co_xO$  film samples with  $0.04 < x < 0.08$ . Possible mechanisms of the observed ferromagnetism are discussed.

## **Crystalquasichemistry of Point Defects in the Chrystal of Chalcogeniden of Eu: EuS, EuSe, EuTe.**

Shevchuk M.O.

*Vasyl Stefanyk PreCarpathion National University, Ivano-Frankivsk, Ukraine*

Monochalcogenides of Eu belong to the group of magnetic semiconductors and have a number of unqiue properties (1,2). They crystallize in NaCl-structures and can become semiconductor, when the rare-earth ion is divalent, or can become metal, when the rare-earth ion is trivalent.

Monocrystals of EuSa are pellucid in the visible area spectrum and they are green. Clean monocrystals are pellucid with a touch of red.

The conductivity of EuS is always n-type. The attempt to get EuS with the p-type conductivity by using alloying with the univalent metals (K,Na) ended in failure, because adding of this metals renew quantitatively  $\text{Eu}^{2+}$  to  $\text{Eu}^{3+}$

EuSe and EuTe can have as n-type as p-type conductivity, depending on their composition...P-type conductivity arises due to surplus of tellurium in relation to stoichiometry composition of EuX. It is possible to transform the divalent EuTe-coposition into trivalent one, using the all-round pressure.

Pure EuX (X=Se, Te, S) of the stoichiometrical compositions are semiconductors with the high resistance ( $10^8$ - $10^{10}$  Om/sm) by room temperature.

It is possible to change in wide ranges the value of electrical conductivity of europium monochalcogenides and their coefficient of temperature using the alloying; and also to replace the main atom of lattice with the divalent atom that is distinguished by +1. For the alloying as a rule are used the trivalent rare-earth elements which form with Eux solid solutions of substitution. The crystal quasichemical formulas for non-stoichiometrical EuX including their defect sub system. There are the calculations of the concentrations of point defects in the anion and cation sublattices, free bearers and Holl-concentration in this investigation.

*This work to execute according department project (State registration № 0107U006768).*

1. Yarembash E.I., Yeliseev A.A .,Chalcogeniden of rare-earth elements. M. 2Science. – 1975. – 260 p.
2. Obdonchik V.A., Mikhlina T.M.,”Chalcogeniden.” “Scientifical Thought”. Kiev. –1967. – P. 48.

## Electrophysical Properties of Biocomposites Containing Colloidal Silver

Shilov V.M., Voitenko O.Yu., Podolska V.I., Marochko L.G.

*Ovcharenko Institute of Biocolloidal Chemistry, NAS of Ukraine, Kyiv, Ukraine*

Below, we report results of studying the electrophysical characteristics of *Candida albicans* yeast cells in which precipitates of colloidal silver particles are formed by the chemical-microbiological method [1]. According to the spectral analysis the disperse composition of silver in biocomposites demonstrated that nanoparticles with the mean sizes of 1.6-2.5 nm are formed in microorganism matrices. Apparently, nanoparticle sizes are limited by the sizes of chamber formed by glycoprotein macromolecules comprising the structure of cell wall.

We made an attempt to relate the experimental values of electrophoretic velocity and rate of electrorotation with changes in cell wall observed upon the biocomposite formation. In our calculations, we used known electric cell model (isolating cytoplasmic membrane that separates conducting cytoplasm and external solution) supplemented by an external ion-exchange layer that models the cell wall.

A comparison of changes in the dc and ac surface conductivities of cell testifies to the formation of clusters of metal silver nanoparticles in the cell wall. It was estimated that, the ac surface conductivity (at  $4 \times 10^5$  Hz) exceeds the surface conductivity at a dc by a large degree, which causes electrophoresis. The dc conductivity increases with  $\text{AgNO}_3$  concentration, albeit much slower than ac conductivity. An increase in  $\text{Ag}^+$  concentration not only increases the concentration and sizes of silver nanoparticles on cell walls, but also results in the formation of chains and clusters.

The obtained estimate demonstrates that nanosized silver particles act inside the cell wall as perfectly nonconducting particles. Their contribution to surface conductivity is explained only by an increase in the surface charge density on cell walls by the value of the charge of ions adsorbed on particles. The direct current through the clusters still can be ignored.

However, in the case of alternating current of fairly high frequency, the situation can change substantially. The effective conductivity of a cluster is directly proportional to its size  $a_{kl}$ . When the size of cluster is achieved, its effective conductivity at a frequency corresponding to the maximum of the rate of electrorotation exceeds the conductivity of intercellular liquid by an order of magnitude. This cluster, which is composed of metal silver nanoparticles and extended along the cell wall, has a size comparable to the radius of the cell.

1. Shilov V.N., Voitenko E.Yu., Marochko L.G., Podol'skaya V.I. Electric characteristics of cellular structures containing colloidal silver // *Colloid J.* – 2010. – V.72, №1. - P. 125-132.

## On the role of coordination topological defects in reversible photodarkening in As-S thin films

Shpotyuk M.V.<sup>1,2</sup>, Balitska V.O.<sup>1,3</sup>, Shpotyuk O.I.<sup>1</sup>, Iovu M.S.<sup>4</sup>, Vakiv M.M.<sup>1</sup>

<sup>1</sup>Scientific Research Company “Carat”, Lviv, Ukraine

<sup>2</sup>Lviv Polytechnic National University, Lviv, Ukraine

<sup>3</sup>Lviv State University of Vital Function Safety, Lviv, Ukraine

<sup>4</sup>Institute of Applied Physics, Chisinau, Moldova

Chalcogenide glasses (ChG) are known to be widely used in photonics, because of extremely high sensitivity to absorbed light exposure, which induces both irreversible and reversible changes in optical properties [1]. Irreversible changes appearing in as-prepared films are stabilization processes. In contrast, reversible photoinduced processes are assumed to be disordering ones since they can be recovered in reversible way by thermal annealing near glass transition.

Near band-gap photo-irradiation could re-switch covalent chemical bonds in the ChG network producing coordination topological defects (CTD) and introducing additional disorder into the ChG structure responding for the reversible photodarkening effect. Near the 2% increase in the homopolar As-As bonds number in As<sub>2</sub>S<sub>3</sub> thin film under photo-irradiation was detected in [2] by EXAFS method. Unsuccessful attempt to theoretically estimate the probability of photoinduced bond breaking in As<sub>2</sub>S<sub>3</sub> and As<sub>2</sub>Se<sub>3</sub> thin films was done in [3].

We obtained kinetic characteristics of reversible photodarkening effect in As-S thin films. It was shown that these characteristics could be described successfully with first order kinetic functions.

In addition, we theoretically deduce formula for calculation of CTD concentration in ChG. It was shown that CTD concentration depends on energy of broken bond, bond switching energy, correlation energy, optical band-gap and energy of excitation light. Few percents of CTD concentration was shown to be possible in As-S thin films. This result is well-agreed with developed approach to calculation of the numerical criterion of induced structural modification. Our approach is grounded on the assumption that photoinduced structural changes are mainly associated with destruction-polymerization transformations. It was shown that compositional dependences of structural modification numerical criteria could be associated mainly with CTD formation processes.

1. Tanaka K., Saitoh A., Terakado N. Photoinduced phenomena in group VIb glasses // J. Mater. Sci.: Mater. Electron. – 2009. – V. 20. – P. S38-S42.
2. Yang C.Y., Paesler M.A., Sayers D.E. Measurement of local configurations associated with reversible photostructural changes in arsenic trisulfide films // Phys. Rev. B. – 1987. – V.36, 17. – P. 9160-9167.
3. Munzar M., Tichy L. Kinetics of photo-darkening and self-bleaching in amorphous As<sub>2</sub>S<sub>3</sub> and As<sub>2</sub>Se<sub>3</sub> thin films // Phys. Stat. Sol. (RRL). – 2007. – V.1, 2. – P. R74-R76.

## The Structure of superficial tapes of carbon fiber, copper-plated using PbS

Sirenko H.A., Midak L.Ya., Skladanyuk M.B., Soltys L.M.

*Vasyl Stefanyk' Precarpathian National University, Ivano-Frankivsk, Ukraine*

The purpose of work consisted in research of crystalline structure of superficial layers at coverage of carbon fiber by a copper using PbS. The objects of research were carbon fibers of UTM-8 and tekarm without and with coverage by a copper.

The problem of passivity of copper's surface takes on the special significance in copper-plating of high dispersion carbonized fibers, got by chemo-mechano-activating technology. It is connected with high catalytic activity of metallic copper which is settleable on the developed surface of fiber and causes exothermic oxidation-reduce reactions of formation of  $\text{Cu}_2\text{O}$  and  $\text{CuO}$  here.

Sciagrams rotined that surface of modified carbonized high dispersion fiber which is copper-plated by the known formaldehyde technology have the layers of  $\text{Cu}^0$  (hkl 111, 200, 220),  $\text{Cu}_2\text{O}$  (hkl 111, 220, 311, 222) and  $\text{CuO}$  (hkl 002, 200, 202, 113, 310, 222). It is discovered that on the stage of copper-plating by formaldehyde technology  $\text{Cu}_2\text{O}$  and  $\text{CuO}$  appear as a result of both processes: reducing  $\text{Cu}^0$  in the volume of solution of copper-plating and oxidation of the copper's surface on a fiber.

It was succeeded to decrease (for one-layer coverage) or quite remove (for the two-layers coverage) of  $\text{CuO}$  formation and increase of content of  $\text{Cu}^0$  in coverage using modification of formaldehyde technology. The content of  $\text{Cu}_2\text{O}$  in coverage also grows with the increase of amount of coverage on a fiber.

It is set that most lacks of the modified formaldehyde technology can be removed using zinc technology, if reducing of the copper's ions to conduct with zinc powder in sulfate solution. It is shown that duty of coverage of carbon fiber by a copper using zinc and then modified formaldehyde technologies results to almost complete reducing of  $\text{Cu}_2\text{O}$ . These processes take place on two types of carbon fibers (UTM-8 and tekarm) in an identical measure.

It is determined that the smallest crystalline particles of PbS are well settleable on copper-plated carbon fiber, forming dense coverage. The dense layer of  $\text{Cu}^0$  or  $\text{Cu}^0 + \text{Cu}_2\text{O}$  appears at PbS coverage of copper-plated fiber.

It is shown that both variable technologies of causing:  $\text{Cu}$  (by the modified formaldehyde technology) (I layer) +  $\text{Cu}$  (by zinc technology) (II layer) and  $\text{Cu}$  (by zinc technology) (I layer) +  $\text{Cu}$  (by the modified formaldehyde technology) (II layer), have a positive effect with the protective action of PbS (III layer), but it follows to give advantage for technology of  $\text{Cu}$  (by zinc technology) (I layer) + (by the modified formaldehyde technology) (II layer) + PbS (III layer).

## **The thickness of quasisolid nanolayers of polyglycolic liquids-base lubricants on the steel surfaces**

Sirenko H.A., Kuzyshyn O.V.

*Vasyl Stefanyk' Precarpathian National University, Ivano-Frankivsk, Ukraine*

Estimations of lubricating layer thickness and dependence of films thickness of oils on the base of polyglycols on loading and temperature have been considered.

To study nanofilms, formed on the surface of steel, used different classes of polyglycolic liquids: polyethylene glycols ( $M = 200-6000$ ) (PEG-200, PEG-400, PEG-600, PEG-1500, PEG 2000, PEG-4000 PEG-6000), linear propylene glycols ( $M = 200-2000$ ) (Laprol 202 Laprol 602, Laprol 1002, Laprol 2002); branched propylene glycols based on glycerin ( $M = 500-3500$ ) (Laprol 503, Laprol 3003, Laprol 3503); blockpolymer of ethylene/propylene oxides ( $M = 5000$ ) (Laprol 5003); statistical copolymers of ethylene/propylene oxides ( $M = 1500-2500$ ) (Laprol 1502, Laprol 2502-2-70, Orites 210 DS).

Load-carrying ability and antiwear properties of oils were tested at four-ball friction machine (the test was carried out at 1140, 1470, 1495 revolutions per minute (upper ball); for determining sticking load – critical load  $N_{cr}$ , when higher steel wear was observed, – load  $N$  was changed degree by degree from 100-200N to  $N < N_{cr}$  and  $N > N_{cr}$  in the area  $N = N_{cr} - 10-25$  N more).

The criterion of Lancaster was used to evaluate the hydrodynamic effects. The formula for calculating the thickness of lubricating films was found using the criterion of hydrodynamic effects.

Hydrodynamic effects and nanofilms thickness were calculated by the dependence of diameter of the wear spots and critical load at the seizing, with the specific expected load on one ball at Hertz at the beginning of wear, as well as the unit load on a platform at wear seizing. Both calculations give information about the thickness of the lubricant nanofilms at the beginning of sliding as the maximum load and at the end of friction as a result of changes in film thickness due to the specific load and temperature of contact and, consequently, changing physical and chemical properties of oil films on these two factors.

Comparison of different classes of polyglycolic liquids showed significant differences between them in forming nanofilms on the surface due to the peculiarities of molecular structure of these lubricants.

Additional research of viscosity-temperature properties and compressibility of these liquids on the temperature led to the necessity of consideration them in calculation formulas.

## Effect of Se isovalent impurity on ZnO properties

Slyotov M.M., Khomyak V.V., Slyotov O.M., Kosolovsky V.V.

*Yu. Fedkovych Chernivtsi National University, Chernivtsi, Ukraine*

Zinc oxide is one of compounds that are much investigated at present. It is due to the possibility of practical application of ZnO in various optical electronic devices. Of particular importance in formation of their properties are isovalent impurities as shown for the case of classical II-VI compounds. Therefore, it is relevant to study the effect of isovalent impurities on the physical properties of ZnO.

ZnO layers were grown by magnetron sputtering on sapphire substrates with a simultaneous doping by Se isovalent impurity. It allowed comparing the effect of isovalent impurity on the properties of sputtered layers and II-VI compounds obtained by diffusion method.

Doping of ZnO layer by isovalent impurity causes formation of intensive photoluminescence. As in the case of diffusion layers, it is localized in the boundary spectral region (curve 1, Fig. 1). The radiation spectrum is characterized

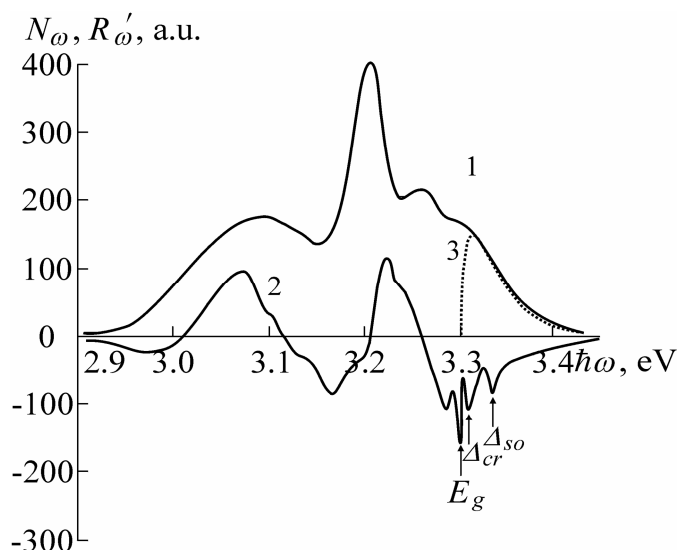


Fig. 1 Spectra of photoluminescence (1),  $\lambda$ -modulated optical reflection (2) and calculated interband recombination (3) of thin ZnO:Se layers.

by several components. Among them, of key importance are interband transitions of free charge carriers, curve 3. The dominant radiation is determined by recombination of excitons bounded to Se isovalent impurity. It is evidenced by the basic characteristic features – shift of maximum  $\hbar\omega_m$  toward the area of larger energies with a decrease in excitation intensity  $L$  and power dependence of intensity  $I \sim L^{1,5}$ . One more band can be observed in the boundary radiation area. The nature of this band can be attributed to recombination

processes with participation of centers that are formed by Se isovalent impurities. One cannot rule out the possibility of excitons annihilation when non-elastically scattered on free charge carriers. Doping by Se impurity is not followed by formation of some other compound. It is evidenced by characteristic parameters of energy structure, found from optical reflection, which refer to ZnO with a hexagonal structure –  $E_g \approx 3.3$  eV,  $\Delta_{cr} \approx 8.2$  meV,  $\Delta_{so} \approx 48$  meV.

## Properties of CdTe, CdO layers and CdO-CdTe heterojunction

Slyotov M.M., Skrypnyk M.V., Kosolovsky V.V., Ulyanitskiy K.S.

*Yu. Fedkovich Chernivtsi National University, Chernivtsi, Ukraine*

The layers of a wide-gap cadmium oxide compound are widely used in various optical electronic devices. Their preparation involves technological processes on single crystals. However, an active role in the manufactured devices is played by thin layers which serve the basis for heterojunctions that are of great practical importance.

The basic CdTe material was prepared in the form of thin films (up to 10  $\mu\text{m}$ ) by thermal evaporation in vacuum ( $10^{-4}$ - $10^{-5}$  torr). CdO heterolayers were prepared by isothermal annealing of CdTe in photoactivated oxygen (quasi-epitaxial build-up). CdO formation is proved by research on  $\lambda$ -modulated optical reflection  $R'_\omega$  (curves 1, 2 in Fig. 1). The energy gap is  $E_g \approx 2.31$  eV, which correlates well with the data reported in the literature. The presence of the second peak at  $\hbar\omega \approx 2.57$  eV is caused by optical transitions with participation of valence subband split-off due to spin-orbital interaction in a cubic structure of CdO. In the reflection spectra there is also certain structural pattern in the boundary area. The character of spectral distribution depends on the doping isovalent Mg impurity (curve 2 in Fig. 1). Mg doping is also responsible for rather intensive luminescence in the boundary area of radiation spectrum  $N_\omega$ . It is determined by recombination processes typical of such impurity type.

Doped layers of CdTe:Mg are characterized by p-type of conductivity, and CdO layers – by n-type. Such anisotype layers form CdO-CdTe heterojunction. It is characterized by rectification coefficient at least  $10^2$ . Typical volt-ampere curves are given on the insert to the figure. Possibilities of practical application of the obtained heterojunctions are discussed.

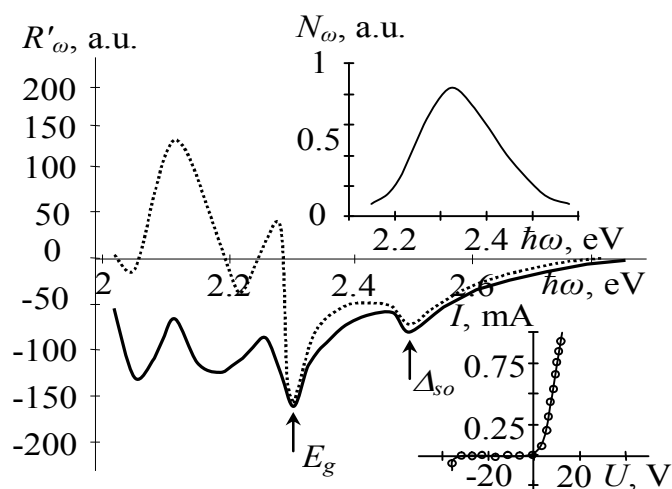


Fig. 1. Spectra of  $\lambda$ -modulated optical reflection (1, 2), photoluminescence (3) of CdO and volt-ampere characteristics of CdO-CdTe heterojunction (4) formed by thin layers.

## **The peculiarities of morphology and charge flow in composites on the base of fluorocontaining polyamides**

Smertenko P.S.<sup>1</sup>, Olkhovik G.P.<sup>1</sup>, Sheludko E.V.<sup>2</sup>, Bryzgin A.R.<sup>2</sup>

<sup>1</sup>*V. Lashkaryov Institute of Semiconductor Physics, NAS of Ukraine, Kyiv, Ukraine*

<sup>2</sup>*Institute of Bioorganic Chemistry and Petrochemistry of NAS of Ukraine, Kyiv, Ukraine*

Current-voltage characteristics of composites on the base of fluorinated polyamide with conductive fillers: fullerene carbon and quasi-crystals (Al 65 %, Cu 23 % and Fe 12 %) were investigated on sandwich and slit structures in two directions of applied electric field. The pressure contact was made by indium pad sized 1 square mm. The characteristics were measured at room temperature in darkness and at illumination with an equivalent of 0.1 sun.

The main peculiarities of I-V characteristics behaviour of composites on the base of quasi-crystal with concentration of 1 %, 5 %, 10 and 20 % are the following:

1) all films have enough high resistivity with resistance from  $10^{10}$  Ohm up to  $10^{11}$  Ohm in darkness and about  $10^9$  Ohm under illumination at applied voltage  $V = 10$  V;

2) the ratio of light to dark currents achieves the value from 5 up to 10;

3) the film resistance is decreased to a 1.6 times with increase of quasi-crystals concentration in composite from 1 % to 10 % to a 4 times when the quasi-crystals concentration in composite is about 20 %;

4) absence of injection of charge carriers from contacts, as on curves the long (more than three orders) saturation regions are observed.

For composites with fullerene carbon there are the following features of I-V characteristics:

1) the composite electroconductivity increases with increase of fullerene carbon concentration from 1 % to 30 %;

2) the photosensitivity of composites to white light decreases with increase of fullerene carbon concentration;

3) the open circuit voltage  $V_{x.x.} = 10-40$  V is observed in composites with fullerene carbon concentration within the range 15 % - 20 %;

4) when fullerene carbon concentration is increased up to 30 %, the volume photosensitivity is disappeared.

In addition the surface morphology of all samples was studied by optical microscopy. This attempt to find the effect of surface morphology on electroconductivity changes was made.

## Temperature dependence of exciton absorption in semiconductor nanocrystals

Smolinsky M.M., Savchuk A.I., Stolyarchuk I.D., Makoviy V.V.

*Yu. Fedkovich Chernivtsi National University, Chernivtsi, Ukraine*

Studies on the peculiarities of the temperature dependence of optical energy gap of semiconductor nanocrystals are of vital importance in a comprehensive research since they provide information on the processes of exciton-phonon interaction under dimensional restriction. As long as quantum-dimensional effects at quantum dots drastically affect the energy levels and phonon spectra which in this case have their peculiarities due to small size and, respectively, small number of atoms, the influence of interfaces and mechanical stresses, this must reflect on the temperature dependence of exciton optical transitions.

In this paper, experimental studies performed on the temperature dependence of optical absorption spectra of nanocrystals of semimagnetic semiconductors CdMnS and PbMnI<sub>2</sub> introduced into polymer matrices. The size of synthesized nanocrystals was evaluated by means of transparent electron microscopy (TEM) and the intensity of optical absorption edge displacement toward the short-wave spectral region. Optical spectra were measured on a spectral set including monochromator MDR-23 and helium optical cryostat. Fig.1 shows absorption spectra of PbMnI<sub>2</sub> nanocrystals recorded at different temperatures. At liquid helium temperature one can observe a whole series of four exciton bands. Spectral analysis makes it possible to interpret this series within exciton transitions for nanocrystals with different discrete dimensions multiple of the thickness of a separate layer of PbMnI<sub>2</sub> crystals. The temperature dependence of exciton peaks has its peculiarities as compared to the bulk crystals. In this paper, the experimental results are explained in the framework of different exciton-phonon interaction mechanisms.

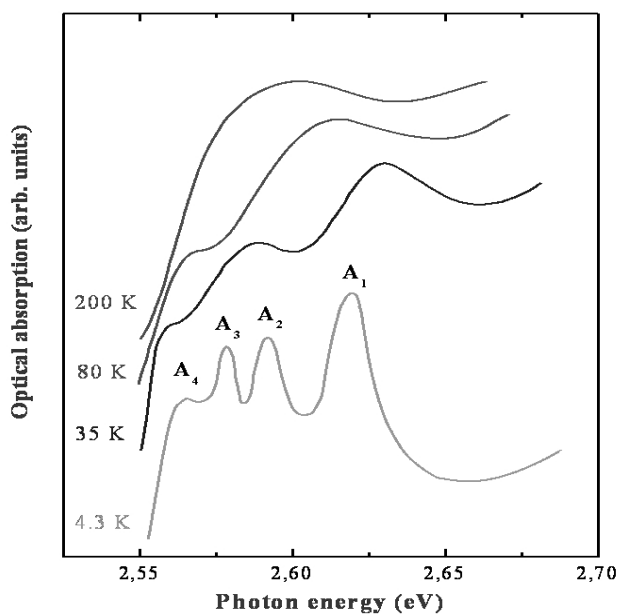


**Fig. 1.** Exciton absorption spectra of PbMnI<sub>2</sub> nanocrystals at different temperatures.

## **Polarization conversion effect in obliquely deposited SiO<sub>x</sub> films and nc-Si-SiO<sub>x</sub> light-emitting nanocomposites**

Sopinsky M.V., Indutnyi I.Z., Michailovska K.V.,  
Shepeliavyi P.E., Tkach V.M.<sup>1</sup>

*V. Lashkaryov Institute of Semiconductor Physics, NASU, Kyiv, Ukraine*

<sup>1</sup>*V. Bakul Institute for Superhard Materials, NASU, Kyiv, Ukraine*

Structural anisotropy of the porous SiO<sub>x</sub> films and nc-Si-SiO<sub>x</sub> light emitting nanocomposites, prepared by oblique deposition of silicon monoxide in vacuum, was studied using polarization conversion (PC) effect. For this purpose a simple method of PC investigation with the use of standard null-ellipsometer is proposed and probed. This method is based on the analysis of the azimuthal angle dependence of the off-diagonal elements of the Jones matrix. The SEM study shows that obliquely deposited SiO<sub>x</sub> films have a porous column-like structure with the column diameter and inclination depending on the deposition angle. Polarimetric investigations revealed that both in-plane and out-of-plane anisotropy were present, associated with the columnar growth. The correlation between the PC manifestations and the SEM results is analyzed. It was found that the tilt angle of columns in obliquely deposited SiO<sub>x</sub> is smaller than predicted by the "tangent rule" and "cosine rule" models.

We applied this polarimetric method to the characterization of SiO<sub>x</sub> films and nc-Si-SiO<sub>x</sub> light emitting nanocomposites, obliquely deposited on c-Si substrates with different orientation of the surface. It has been established that the column tilt angle is greater in samples on c-Si(111) substrate. Greater tilt angle of columns resulted in greater porosity of such systems. So, the systems on c-Si(111) substrate are more susceptible to chemical vapor treatments because the dissolving vapors more easily penetrate in such films.

To considerably increase PL intensity and shift PL peak position of light emitting nc-Si-SiO<sub>x</sub> composites the annealed SiO<sub>x</sub> films are treated by HF vapors. Our experiments on photoluminescence of HF vapor treated systems shown that such transformation of PL spectra run more intensively in the nanocomposites on c-Si(111) substrates. In this case more effective vapor treatment causes higher oxidation of the nc-Si surface and decreasing of nc-Si sizes, more complete passivation of nonradiative traps. As a result, higher PL intensity and some blueshift of PL spectrum compared to the systems on c-Si(100) take place.

These results show important role of the substrate surface in the formation of nanocolumn structure of obliquely deposited films. Further comprehensive study of this effect may give significant contribution to elucidation of the structure formation mechanism in the SiO<sub>x</sub> obliquely deposited films and nc-Si-SiO<sub>x</sub> light emitting nanocomposites.

## **Influence of tunneling on dissociation of electron – hole pairs in PEPC films doped with fullerene**

Soroka A., Dmitrenko O., Kulish M, Zabolotny M., Davydenko N., Studzynsky S., Olasyuk A.

*Taras Shevchenko Kyiv National University, Kyiv, Ukraine*

Charges carrier generation in the base of number of important photophysical and photochemical processes. Molecular structures with a  $\pi$ -conjugate polymer doped fullerene  $C_{60}$  electronic system are characterized by the non uniformity of the electron density distribution, is intensified as a result of an additional intermolecular charge transfer. That is why, a study of inter- and intermolecular charge separation mechanism, as well as an influence of the molecular structure and temperature. About processes of moving of charges carriers it is possible to receive the information by means of spectra of a luminescence. We investigated spectra of a luminescence in PVC and PEPC films doped fullerene  $C_{60}$  at temperatures 77K and 300K. The luminescence was excited by light with length of a wave 5145A and density of a light power (P) 5 – 70 mW/sm<sup>2</sup>. Concentration of  $C_{60}$  made 0.5, 2 and 3 weight percent.

From the made researches follows, that – 1) the form of a spectrum of a luminescence of composites PVC (PEPC) + $C_{60}$  essentially depends both on concentration of fullerene, P and from temperature of a sample; 2) the spectrum of a luminescence of composites PVC + $C_{60}$  cannot be submitted as a linear combination of spectra PVC (PEPC) and  $C_{60}$  from what follows, that in a spectrum of a composite brings contribution CT states. For the theoretical description of features of a luminescence the model which is taking into account stochastic character of movement of carriers of a charge has been developed. The model uses equation of the Agmon – Hopfield. This equation allows taking into account as processes of diffusion so tunnel character at transport of charge carriers. Modelling results correlate with the data of experiments.

## **Hydrophilics properties of plasma modified diamond-like films**

Starik S., Perevertailo V., Gontar O., Kutsay O., Loginova O., Gorohov V.

*Institute for Superhard Materials of the National Academy of Science of Ukraine,  
Kyiv, Ukraine*

The biocompatibility of diamond and diamond-like carbon materials reliably confirmed by a significant number of published clinical research. The use of diamond-like carbon films as biocompatible coatings of various materials and medical products requires providing certain requested properties and the variation of contact angle of such film forming materials. The most promising and modern method of carbon thin film surface modification are low-temperature plasma treatment. The variation of plasma forming gas environment and discharge energy characteristics allow change the surface properties of carbon coatings. The nanodimensional controlled surface layer is transformed only for plasma-chemical processing. Thus the bulk of the carbon coating retains the original mechanical and physical-chemical properties of the modified material.

In this paper, the RF plasma-chemical surface modification of hydrogenated diamond-like films carry out in argon, nitrogen, helium and hydrogen atmosphere.

The variation of RF modified hydrogenated diamond-like carbon film physical properties were investigated by solving the inverse problem of optical spectrophotometry. The reduce of carbon film thickness at plasma-chemical etching was uneven. The average etching rate of diamond-like film was determined for ions of various gases.

The kinetics of low-temperature wettability of the surface modified hydrogenated diamond-like carbon films were investigated by the method of fast cinematography (up to 1200 fps). The spreading process time was in range  $10^{-2} - 10^{-3}$  s. It was faster than for the naturally oxidized surfaces.

The most important result was representing a demonstration of complete wetting. In such case a contact angle is about  $0^\circ$ . It was observed for all investigated samples after the plasma-chemical treatment by low energetic ions.

## **Energy spectrum of one-dimensional ionic conductors described by Pauli statistics**

Stasyuk I.V., Stetsiv R.Ya., Vorobyov O.A.

*Institute for Condensed Matter Physics NAS of Ukraine, Lviv, Ukraine*

The microscopic mechanism of ion transport in one-dimensional Pauli conductor is investigated. We consider a finite ionic chains as the element of some nanostructure as well as the finite ones with periodic boundary conditions which simulating infinite chains. Our attention is paid to superionic conductors that exhibit transitions to high-temperature superionic phases. In a low-temperature phase ions are in the fixed positions while in a superionic phase particles are distributed between several possible positions with equal probability. We investigate the energy spectrum of one-dimensional ionic conductors described by Pauli statistics taking into account ion transfer as well as the short-range non-local correlation between particles. Both commutator and anticommutator Green's functions constructed of Pauli creation and annihilation operators are calculated using exact diagonalization technique on the basis of states of finite ionic chains. The frequency and temperature dependences of one-particle density of states is calculated. The conditions of transitions from dielectric to a superfluid-like state are analyzed. The last can be interpreted as a state that corresponds to a superionic phase.

## Creation, structure and properties of new thermo- and pH-responsible grafted nanolayers

Stetsyshyn Yu.<sup>1</sup>, Zolobko O.<sup>1</sup>, Zemła J., Fornal K.<sup>2</sup>, Kostruba A.<sup>3</sup>, Donchak V.<sup>1</sup>, Harhay H.<sup>1</sup>, Skorobohaty Ya.<sup>3</sup>, Budkowski A.<sup>2</sup>, Voronov S.<sup>1</sup>

<sup>1</sup>*National University «Lvivska Politechnika», Lviv, Ukraine*

<sup>2</sup>*Smoluchowski Institute of Physics, Jagiellonian University, Kraków, Poland*

<sup>3</sup>*Lviv Institute of Physical Optics, Lviv Academy of Commerce, Lviv, Ukraine*

Polymer surfaces, able to change their surface properties under external medium factors, for example, temperature, light, pH etc. are of a great interest for potential applications in numerous areas. Special attention is paid to the surfaces capable to change their properties under action of a several factors simultaneously.

We propose a new approach to formation of nanolayers with dual properties. The surface of a glass plate was treated with ( $\gamma$ -aminopropyl)triethoxysilane (APTES). As a result primary functional aminogroups were immobilized there and peroxide oligoester of a special structure was covalently grafted to this surface due to interaction of these groups with chloranhydride functionalities of oligoester. The thermo-responsible polymer brushes of both poly(*N*-isopropylacrylamide) or poly(three ethylene glycol methacrylate) were grafted to the obtained oligoester nanolayer by method of initiation "from a surface". Therefore, complicated nanolayer consists of thermo-responsible polymer brushes, grafted to pH-responsible oligoester molecules was obtained.

In acid medium, carboxylic groups in oligoester are in nonionic state. Grafted macromolecules adopt a conformation of a statistical ball and surface becomes relatively hydrophobic. In an alkaline medium, due to repulsion of ionized carboxylic groups, macromolecules of oligoester transform into opened out form, and surface becomes hydrophilic. pH- responsible properties of nanolayers are kept even after the grafting of thermoresponsible brushes. Thus, obtained nanolayers possess termo- and pH- responsible properties simultaneously.

The structure of grafted nanolayers on the glass surface was investigated by atomic-force microscopy method. Thickness of the obtained nanolayers and volume fraction of copolymers in grafted nanolayers were calculated using ellipsometric data. The conformation changes of thermoresponsible brushes, grafted to the oligoester nanolayer at different temperatures and pH were shown.

Dual thermo- and the pH-responsible nanolayers could be considered as promising materials for creation of "smart" implants, systems of the controlled interaction with proteins and biosensory systems.

## Production of the chemoelectric currents in Pd-GaP Schottky nano-structures under exposure to hydrogen atoms

Styrov V.V.<sup>1,2</sup>, Simchenko S.V.<sup>1</sup>, Karpov E.G.<sup>3</sup>

<sup>1</sup>*Azov State Technical University, Mariupol, Ukraine*

<sup>2</sup>*Berdyansk State Pedagogical University, Berdyansk, Ukraine*

<sup>3</sup>*University of Illinois, Chicago, USA*

Since the recent discovery of production of electronic flows in Schottky diodes with nanosized “top” metal layer due to ballistic metal-to-semiconductor transport of hot electrons formed by the surface exoergic chemical reaction, e.g. [1], this effect attracts attention of scientists owing to its fundamental and practical potential. Here we investigate a new system of that kind, namely Pd-(n)GaP planar Schottky diode (15 nm Pd-layer) placed in the atmosphere of atomic hydrogen. We found the steady-state current flow through the system under consideration in perpendicular direction to the metal surface on which the hydrogen atoms stationary recombine into molecules.

We elaborated a new approach to measure and boost the value of the chemicurrent by observing the current-voltage characteristic of the Schottky diode in the presence and absence of the atomic flux incident on the structure. Difference  $\Delta I$  in the current magnitude at the same forward voltage applied is a nonequilibrium current (chemicurrent) at the given voltage ( $\Delta I = I_{\text{chemo}}$ ). This value includes some contribution in the total current from a thermal current caused by the temperature gradient between the metal film (heated by the reaction) and the GaP substrate. The nonequilibrium nature of the additional current observed is confirmed by the kinetics measurements: the current drops to its initial value in the absence of atoms practically momentarily once the atoms are “switched off” and jumps immediately to its excited value when atoms are “switched on” (at the given temperature of the structure and the fixed forward voltage bias on the structures). It implies that the “thermal” constituent in the total current is small. We were able to draw some quantitative information about the processes of generation of nonequilibrium chemoelectrons (in fact of electron-hole pairs) in the reaction of recombination of hydrogen atoms on Pd-surface and their travelling in the metal film. The short circuit  $I_{\text{chemo}}$  assuming that the recombination event is responsible for the hot electron birth is as follows:  $I_{\text{chemo}} = \eta_e \chi \gamma j e \Delta S$ , where  $\eta_e$  is the probability of producing the chemoexcited carrier per elementary event of the reaction,  $\chi$  is the probability for hot electrons to reach the Schottky barrier during its travelling through the Pd-film and to surmount the barrier,  $\gamma$  is the coefficient of recombination of hydrogen atoms on Pd,  $j$  – the atomic flux density ( $\text{m}^{-2}\text{s}^{-1}$ ),  $e = 1.6 \times 10^{-19}\text{C}$ ,  $\Delta S$  – is the metal surface area available for the reaction. In one of our experiments at 320 K and zero bias on the p-n junction, we found  $I_{\text{chemo}} = 3 \text{ nA}$ ;  $j = 1 \times 10^{22} \text{ m}^{-2}\text{s}^{-1}$  ( $\Delta S = 10^{-4} \text{ m}^2$ ). For Pd films,  $\gamma = 0.11$  to give  $\eta_e \chi = 0.2 \times 10^{-6}$ .

However, at the forward bias of 1 V the  $I_{\text{chemo}}$  drastically grows reaching 950  $\mu\text{A}$  probably due to increase in the  $\chi$  value. Thus the bias allows us to have gain in the chemicurrent value as large as five orders of magnitude. This result can be of significant importance for the practical applications of nonequilibrium chemicurrents in Schottky nanostructures including sensing and chemical-to-electricity energy conversion.

We may also assume that the chemicurrent is due to adsorption of hydrogen atoms on palladium surface since the heats of adsorption and recombination of H-atoms on Pd lie very closely. So the estimates made above are valid for this assumption as well.

1. Georgen B., Nienhaus H., Weinberg W.H., McFarland E.. Science. – 2003. – 294. – 2521.

## Dependence of the porosity of indium phosphide on the etching time

Suchikova Y.A.

*Berdyansk State Pedagogical University, Berdyansk, Ukraine*

Nanoporous structures are recently increasing applications in various fields of technology because of its unique properties. With a highly developed surface of such semiconductors are considered a number of research groups as a new class of materials that are radically changing their physical properties, reflecting the quantum dimension of the developed structures. In this paper, the degree of porosity of indium phosphide on the conditions of etching.

In the process of electrochemical etching of InP formed porous layers with different degrees of porosity, which is in direct correlation with the conditions of etching.

Table 1 shows the degree of porosity on the etching time, current density at the same time was the same for all samples and was 50 mA/cm<sup>2</sup>.

Table 1

Dependence of the porosity of indium phosphide on the etching time

Sample №	t, min	Porosity, %
1	5	32
2	10	44
3	15	52
4	20	70

Thus degree of InP porosity is directly depend on the etching conditions: the value of porosity is higher, the longer the anodization time of the samples.

This effect can be explained by the fact that at the beginning of etching pores are formed at preferential locations of the semiconductor surface, which are defects, dislocations, cracks and unevenness of the relief. These pores are arranged randomly and branches beneath the surface of the sample. With further increase of the interval etching exits branched pore channels to the surface, the union of small pores in the more massive hole and the formation of new pores, whose appearance is not associated with defects in the crystal lattice crystal.

## Stages of pore formation of porous indium phosphide

Suchikova Y.A.<sup>1</sup>, Kidalov V.V.<sup>1</sup>, Konovalenko A.A.<sup>1</sup>,  
Kirilash A.I.<sup>1</sup>, Sukach G.A.<sup>2</sup>

<sup>1</sup>*Berdyansk State Pedagogical University, Berdyansk, Ukraine*

<sup>2</sup>*National University of Life and Environmental Sciences of Ukraine, Kyiv, Ukraine*

Indium phosphide is technologically important material for producing lasers, diodes, solar cells. At present, special attention is paid to studying the properties of porous InP, since it is a very important material for producing light-emitting diodes and solar cells. Despite the progress made in obtaining the porous layers, so far there is no overall picture of the process of pore formation. This paper presents the observation of pore formation phases of InP by electrochemical etching.

First of all, it should be noted that pore formation is a complex process, accompanied by a number of electrochemical reactions.

- 1) Initially, the etching is observed so-called incubation period - in this period, pore formation does not occur.
- 2) The initial stage of pore formation is characterized by a primary ejection of atoms from the crystal surface. Most likely, snatching occurs in the defective areas of the crystal surface - the location, accumulation of impurities and cracks. This period is characterized by a sharp increase in the etching current density.
- 3) Along with this the formation of the irregular top layer, which can be considered as a porous only in some approximation.
- 4) Formation «crysto» pores begin to ramify beneath the surface of the crystal (Fig. 1a). Nature of the branch is determined by several factors. First, the rate of electrochemical reaction is faster the dissolution occurs, the less branched pores.
- 5) Formation of "curro" long. "curro" pores, on the other hand, grow mainly in the direction of current, i.e. perpendicular to the equipotential lines (Fig. 1b). The depth of germination of this type are far different - from several to tens of micrometers. These pores do not branch and strictly parallel to each other.

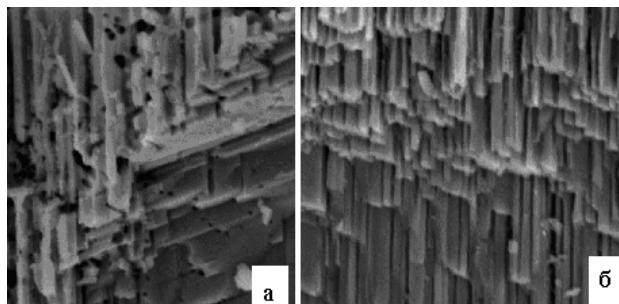


Fig. 1. Image «crysto» (a) and curro (b) pores. These are the basic steps of pore formation of indium phosphide, which may vary depending on the etching conditions and the state of the crystal.

# Influence of doping by rare-earth elements on electrical properties of lithium-iron spinels

Sulym P.O., Gasuyk I.M.

*Vasyl Stefanyk Precarpatian National University, Ivano-Frankivsk, Ukraine*

Analysis of literature data has showed that there are not enough researches of electroconducting and dielectric properties of lithium ferros spinels, doped by ions of rare earth elements (REE), although we know that the replacement of spinel oxides by REE leads to their stabilization. These samples are particularly valuable from the viewpoint of using in the cathode systems of lithium power sources.

Frequency-temperature dependences of the conductive properties of spinel  $\text{Li}_{0.5}\text{Fe}_{2.475}\text{Ln}_{0.025}\text{O}_4$ , ( $\text{Ln} = \text{Pr}, \text{Eu}, \text{Ho}, \text{Er}$ ) are investigated in this paper by the method of complex impedance. This spinel is a perspective active material of cathode for lithium power sources for different purposes.

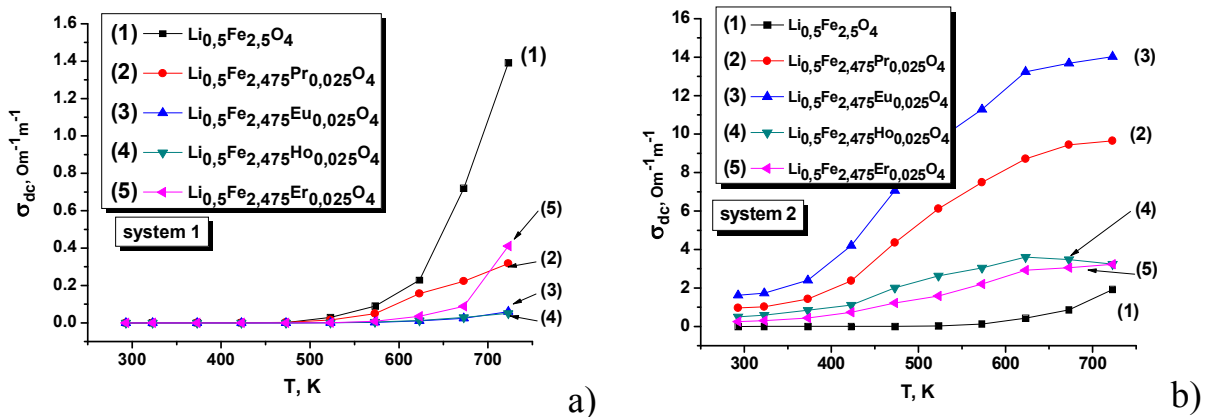


Fig. 1. Temperature dependence of the conductivity of the synthesized samples.

As seen from fig. 1a the dependence of conductivity on temperature for samples slowly cooled after the final sintering (system 1) has a semiconductor character, and the conductivity has a small value. For samples tempered in water after the final sintering (system 2) the dependence of conductivity and numerical value are unchanged only for  $\text{Li}_{0.5}\text{Fe}_{2.5}\text{O}_4$ . For other samples at temperatures above 625 K there is practically horizontal area (output saturation) that can be evidence to change of conduction mechanism to the metallic (fig. 1b). At the same numerical values of conductivity for "system 2" increased approximately to  $10^2$  times compared to "system 1". These differences in numerical values of conductivity are caused by structural changes within the samples, that is confirmed by X-ray and mossbauer researches.

So, we have obtained high conductive cathode materials for lithium-ion power sources with very little doped lithium-iron spinel by ions of rare earth elements.

## Effect of atmospheric oxygen on electrical performance of ZnCdHgTe-based structures

Sydorchuk P., Khlyap H.

*State Pedagogical University, Drohobych, Ukraine*

Environmental effects are unavoidable working conditions for almost all semiconductor devices. How do they influence the performance of the structures?

The abstract presented here attempts to demonstrate experimental results obtained under long-term investigation of ZnCdHgTe-based active elements.

The structures mentioned above are fabricated by various technologies: molecular beam epitaxy, modified liquid phase epitaxy, pulse laser deposition. Atmospheric oxygen starts its effect immediately after finishing the samples preparation and excluding them from the growth chambers (independently of the technology). Room-temperature current-voltage characteristics (IVC) are of special interest.

The data reported here show significant changes in IVCs studied for ZnCdHgTe films prepared by the modified liquid phase epitaxy on single crystal CdTe substrates after more than 3 years storage at normal atmospheric conditions. The as-grown layers had shown no peculiarities except sufficiently high resistance.

After storage the films demonstrated lowering resistance and IVCs typical for heterostructures with a space charge region (i.e. space charge-limited currents, SCLC). The experimental data are analyzed according to the models of SCLC and formation of the oxygen-induced conductivity channels. Fig.1 plots the experimental IVC (curve 1) and a theoretical current-voltage dependence [1].

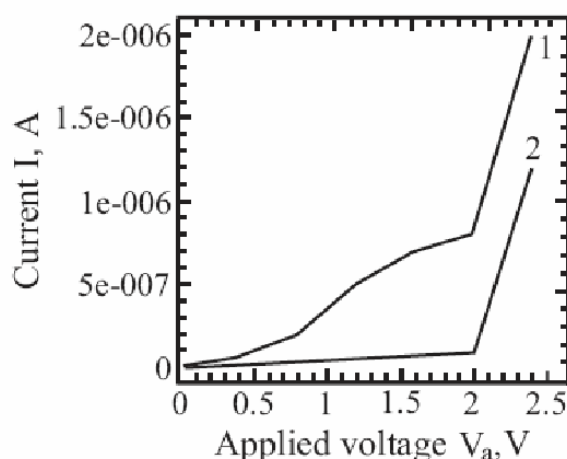


Fig. 1. Current-voltage dependence

1. Khlyap H., Sydorchuk P., Andrukhiv A. Recent Progress in Thin Film Technology // Recent Patents on Materials Science – 2011. – V.4, №.1 – P. 50-55.

## New technique of deposition of continuous TiO<sub>2</sub> films and their photocatalytic properties

Sylenko P.M., Dan'ko D.B., Shlapak A.M., Pylypchuk O.F.,  
Okun' I.Yu., Solonin Yu.M.

*Frantsevich Institute for Problems of Materials Science, National Academy of Sciences of Ukraine, Kyiv, Ukraine*

Titanium dioxide remains one of the most promising photocatalytic materials for water splitting reaction under sunlight. However, it has two essential drawbacks. Firstly, it is large bandgap (about 3 eV) that leads to UV light absorption only (about 4% in solar spectrum). Secondly, such photoanode needs external voltage for water decomposition. These difficulties may be resolved by using the construction of hybrid photoanode, where TiO<sub>2</sub> film is deposited on the surface of solid state solar device [1]. Hybrid photoanode absorbs the whole solar spectrum because the solar cell absorbs the long waves passed through TiO<sub>2</sub>. Solar cell photopotential is added to TiO<sub>2</sub>/electrolyte photopotential that provides the sufficient cathode potential for water electrolysis.

Silicon solar cell stable up to 650°C and chemical vapor deposition (CVD) method for TiO<sub>2</sub> films were used in our work. Island TiO<sub>2</sub> films grew on the Si solar cell surface in contrast to metal substrates (Fig. 1a).

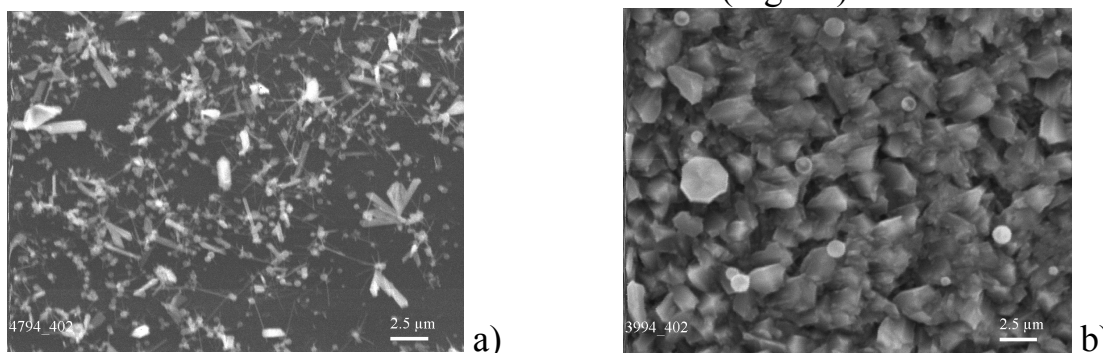


Fig. 1. SEM images of TiO<sub>2</sub> films on Si substrates.  $t_{\text{dep.}} = 3$  h,  $T_{\text{dep.}} = 625^\circ\text{C}$ .

Such hybrid photoanode demonstrated neither photocurrent nor photovoltage due to formation of non conductive oxide films on Si surface in the electrolyte. This difficulty was resolved by thermal deposition of 30-40 nm Ti film on the Si solar cell surface before TiO<sub>2</sub> film formation. Such Ti film served as the catalyst of TiO<sub>2</sub> film growth and then was oxidized itself. Continuous TiO<sub>2</sub> film which protected the substrate from oxidation in the electrolyte was obtained by such a way (Fig. 1b). The efficiency of hybrid photoanodes as a function of TiO<sub>2</sub> film thickness and crystallites dimension was investigated.

1. Miller E.L., Paluselli D., Marsen B., Rosheleau R.E. Development of reactively sputtered metal oxide films for hydrogen producing hybrid multijunction photoelectrodes // *Sol. Energy Mat. & Sol Sells.* – 2005. – 88. – P. 131-144.

## Simulations of OH radicals adsorption at the Si(100) surfaces

Tkachenko A.V., Ananina O.Y.

Zaporizhzhya National University, Zaporizhzhya, Ukraine

The OH adsorption on the surfaces Si(100)-(2×1) with varying degrees of hydrogen coverage have been studied in this work. Were investigated the values of adsorption activation energies for OH particles on Si(100) surfaces. The geometric structure of the adsorbed components and the energies of OH interaction with the surface atoms and with each other were calculated. Modeling of OH adsorption was carried out using semi-empirical method of quantum-chemical modeling MNDO (MOPAC package) and ab-initio Hartree-Fock method included in the software package GAMESS [1,2] for cluster Si<sub>49</sub>H<sub>52</sub> (fig. 1, a) which simulated the surface of Si (100)-(2×1).

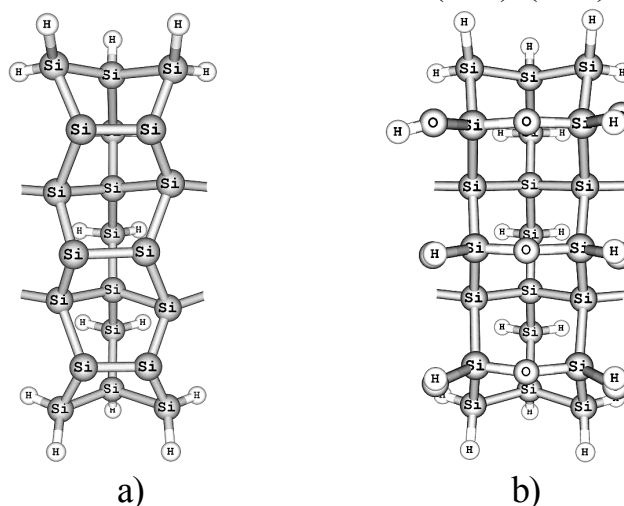


Fig. 1. Cluster Si<sub>49</sub>H<sub>52</sub> a) clean Si(100)-(2×1) surface, b) surface Si(100) with adsorbed OH radicals.

According to the results of the calculations the OH particles can create states on the ordered Si(100)-(2×1) surfaces which have different geometric, energetic and electronic characteristics.

The state with the lowest value of total energy corresponds to the configuration in which the OH particles saturate bounds of both neighboring dimers silicon atoms. There are the bridge-type bounds between silicon and oxygen atoms Si-O-Si (fig. 1, b) formed on the surface.

Adsorption of OH on the hydrogenated surface H/Si(100) requires bigger value of activation energy than it necessary for OH adsorption on clean Si(100) surface. This is due to the desorption of molecular hydrogen from the mono-or dihydride states on the H/Si(100) surface.

1. Klark T. Kompjuternaya ximiya. M. Mir. – 1990. – 231 p.
2. <http://classic.chem.msu.su/gran/gamess/index.html>.

## Synthesis and properties of CdS nanoparticles embedded into thin polymer covering grafted to the solid surface

Tokarev S., Il'chuk G., Kusnezh V., Schevchuk O., Tokarev V.

*Lviv Polytechnic National University, Lviv, Ukraine*

The CdS nanoparticles (NP) embedded into thin polymer layer grafted to the solid surface were fabricated combining several approaches namely self-assembly of surface-active initiator, 'grafting from' radical polymerization, and sol-gel synthesis. The NP synthesis of NP involves several consequent stages comprising: (i) spin-coating of peroxide oligomer on the solid surface; (ii) melting and curing of the peroxide oligomer layer; (iii) formation of grafted brushes at the modified surface via either graft polymerization of acrylic acid (continuous structure) or consequent graft polymerization of styrene and then acrylic acid (mosaic structure); (iv) saturation of grafted polymer layer by ions of  $\text{Cd}^{2+}$ ; (v) finally a treatment by  $\text{H}_2\text{S}$  to form CdS NP inside of grafted polymer layer. The NP obtained were characterized by UV-visible and fluorescence spectroscopy, scanning electron microscopy (SEM), X-ray microanalysis, and atomic force microscopy (AFM).

An effect of structure of the grafted polymer layer onto dimension and distribution of the formed NP was investigated. The CdS clusters size was estimated by both an analysis of optical absorption spectra and AFM. The presence of several cluster fractions with different sizes has been revealed in both matrices with continuous and mosaic structure (table 1). However, it was found that in mosaic polymer matrix, comprised by segregated hydrophilic and hydrophobic areas, thermodynamically more stable clusters with smaller size than in case of continuous matrix.

Table 1

Properties of CdS NP embedded into thin polymer layer

Polymer matrix	$E_1$ , eV	$\text{FWHM}_1$ , eV	$d_1^*$ , nm	N, %	$E_2$ , eV	$\text{FWHM}_3$ , eV	$d_2^*$ , nm	N, %	$d_{\text{av.}}^*$ , nm
continuous structure	2.71	0.33	3.74	85	2.84	0.184	3.15	15	3.65
mosaic structure	2.66	0.214	3.97	38	2.84	0.211	3.13	62	3.45

## **Inhomogeneous magnetic state of thin films of sodium-doped lanthanum manganites**

Tovstolytkin A.I., Matviyenko A.I., Podyalovskii D.Y., Polishchuk D.M.

*Institute of Magnetism, Kyiv, Ukraine*

Rare earth manganites doped with uni- or divalent elements are known to demonstrate phase transformation from ferromagnetic (FM) metal to paramagnetic (PM) insulator, and colossal magnetoresistance effect in the range of this transition [1]. Magnetic and electric properties of the manganites are very sensitive to the particular composition of the sample, internal stress, and structural defects due to strong interplay of different types of interactions in these complex systems [1,2]. In this work, we use ferromagnetic resonance (FMR) technique to probe magnetic state of thin films of sodium-doped lanthanum manganites.

The films (in what follows – LNMO films) fabricated by means of the sputtering of a ceramic target with a nominal composition  $\text{La}_{0.84}\text{Na}_{0.16}\text{MnO}_3$  were investigated in the work. The target was synthesized by means of the standard solid-phase reaction method [2]. The films 750 nm in thickness were deposited on single crystalline  $\text{LaAlO}_3$  (001) substrates. During the deposition the substrates were held at 700°C in an atmosphere consisting of a mixture of argon (20 %) and oxygen (80 %). The pressure of the gas medium was  $7 \cdot 10^{-2}$  torr. After the deposition, the films were subjected to a heat treatment at 900 °C in an ambient atmosphere for 1 hour.

The FMR studies were carried out in the temperature range 110-300 K with the use of X-band ELEXSYS E500 EPR spectrometer.

The results have shown that the formation of FM phase starts at  $T_C^{\text{film}} \cong 265$  K. This value is lower than the Curie temperature of bulk target, from which the films were prepared ( $T_C^{\text{bulk}} \cong 308$  K) [2]. The analysis of the FMR spectra shows that the low-temperature magnetic state of the LNMO films is inhomogeneous and comprises the regions with two different values of magnetization. The magnetizations of each the species have been studied as functions of temperature. The conclusion is made that such peculiar magnetic inhomogeneity originates from the stress which is inhomogeneously distributed over the film volume.

*The work is partially supported by the Joint project of the National Academy of Sciences of Ukraine and Russian Foundation for Basic Research No. 62-02-10.*

1. Haghiri-Gosnet A-M. and Renard J-P. // J. Phys. D: Appl. Phys. – 2003. – V. 36. – P. R127-R150.
2. Yanchevskii O.Z., Tovstolytkin A.I., V'yunov O.I., Durilin D.A., Belous A.G. // Inorg. Mater. – 2004. – V. 40. – P. 744-750.

## The correlation between nanovoid-species structure of amorphous Tellurides of In studied with X-ray diffraction

Tsaly V.Z., Kleto G.I.

*Chernivtsi National University, Chernivtsi, Ukraine*

The idea to study nanovoids in glasses has firstly been proposed during computer modeling of glass network within Monte-Carlo procedure [1], but it was not accepted entirely owing to absence of corresponding experimental confirmations.

Further, S.R. Elliott [2,3], interpreting the nature of the first sharp diffraction peak (FSDP) in  $AX_2$ -type glasses, has assumed the importance of knowledge about nanovoids for glass structure to be understood. It was shown for tetravalent type glasses that analytical the analytical correlation relationship between the FSDP position,  $Q_1$ , and nanovoid diameter,  $D$ , has been presented in the form of  $Q_1 = 1.5 \pi/D$ .

O. Shpotyuk [4], combining the FSDP-related XRD, treated within Elliott's void-based model, and positron annihilation lifetime spectroscopy (PALS) within two-state positron trapping model. By suggesting that the same nanovoids are responsible for both FSDP and PALS data, for  $g\text{-As}_2\text{Se}_3$ , the analytical correlation relationship between  $Q_1$  and  $D$ , has been presented in the form of  $Q_1 = 2.3 \pi/D$ .

In this paper we present the result of combining the XRD investigation [5] and free volume concept [6] apply to amorphous Tellurides of In. The samples were prepared by melt-spinning method. The investigation were carried out using X-ray diffractometer DRON-3, Q-derivatograph and microhardnessmeter PMT-3.

1. Popescu M.A. Hole structure of computer models of non-crystalline materials // *J. Non-Cryst. Solids.* – 1980. – V. 35-36. – P. 549-554.
2. Elliott S.R. Origin of the first sharp diffraction peak in the structure factor of covalent glasses // *Phys. Rev. Lett.* – 1991. – V. 67, N 6. – P. 711-714.
3. Elliott S.R. Extended-range order, interstitial voids and first sharp diffraction peak of network glasses // *J. Non-Cryst. Solids.* – 1995. – Vol. 182. – P. 40-48.
4. Shpotyuk O., Kozdras A., Kavetsky T., Filipecki J. On the correlation between void-species structure of vitreous arsenic selenide studied with X-ray diffraction and positron annihilation techniques // *J. Non-Cryst. Solids.* – 2006. – V. 352. – P. 700-703.
5. Цалий В.З. Структура аморфних стрічок системи  $\text{In}_x\text{Te}_{100-x}$  // *Матеріали ІХ Міжнародної конференції "Фізика і технологія тонких плівок"*, Івано-Франківськ. – 2003. – Т. 2. – С. 59-60.
6. Сандитов Д.С., Бартенев Г.М. Физические свойства неупорядоченных структур.- Новосибирск: Наука, 1982. – 259с.

## The features of temperature dependences of magnetoresistance of $\text{La}_{0.84}\text{Na}_{0.16}\text{MnO}_3$ films

Tsmots V.M.<sup>1</sup>, Pan'kiv L.I.<sup>1</sup>, Pan'kiv I.S.<sup>1</sup>, Tovstolytkin A.I.<sup>2</sup>,  
Matviyenko A.I.<sup>2</sup>, Shchuplyak A.N.<sup>1</sup>

<sup>1</sup>*Drohobych Ivan Franko State Pedagogical University, Drohobych, Ukraine*

<sup>2</sup>*Institute of Magnetism, Kyiv, Ukraine*

In this work the features of temperature dependences of magnetoresistance for the thin film materials of  $\text{La}_{0.84}\text{Na}_{0.16}\text{MnO}_3$  are established.

The discovery of a strong effect of a magnetic field on the electric resistance of complex manganites  $\text{La}_{1-x}\text{A}_x\text{MnO}_3$  ( $A = \text{Ca}, \text{Sr}, \text{Ba}, \text{Na}, \text{K} \dots$ ) has stimulated interest in further study of such systems [1]. Due to colossal magnetoresistance effect, substituted manganites can find practical application in magnetic sensors, elements for information technologies and so on [2]. Recently interesting magnetic and magnetoresistance properties are found in bulk samples, in which the lanthanum atoms are partially substituted by sodium atoms [3], but magnetic parameters of such compounds in thin film condition have not been investigated yet.

In order to obtain the information on the magnetoresistance properties in thin film materials  $\text{La}_{0.84}\text{Na}_{0.16}\text{MnO}_3$ , the measurements of magnetoresistance ( $MR$ ) change with temperature are performed. The investigated samples were prepared by the method of magnetron sputtering on the single crystalline  $\text{LaAlO}_3$  substrates (the temperature of the substrates at deposition – 700 °C). The thicknesses of the films were 20, 100 and 500 nm. The measurement was carried out in the field of 15 kOe in the temperature range of 77-350 K at the parallel and perpendicular sample orientation in the direction of magnetic field.

The analysis of dependences  $MR(T)$  showed the temperature, at which the maximal value of magnetoresistance can be attained, depends on the film thickness (for 20 nm –  $T_{\text{max}} = 230$  K, for 100 and 500 nm –  $T_{\text{max}} = 275$  K). It is found out that the magnitude of the peak  $MR$  increases with the growth of the film thickness. The typical features of the influence of the film thickness and the orientations of the magnetic field on the magnetoresistance properties are determined.

1. Helmolt R.V., Wecker J., Samwer K., Haupt L., and Bärner K. // J. Appl. Phys. – 1994. – 76, 6925.
2. Haghiri-Gosnet A-M. and Renard J-P. // J. Phys. D: Appl. Phys. – 2003. – 36, R127.
3. Tovstolytkin A.I., Tsmots V.M. *et al.* // Low Temp. Phys. – 2010. – 36, 220.

## Dielectric studies of ZnO polycrystalline films

Turko B.I.<sup>1</sup>, Kapustianyk V.B.<sup>1</sup>, Eliyashevskyy Yu.I.<sup>1</sup>, Kulyk B.Y.<sup>1</sup>, Czapla Z.<sup>2</sup>

<sup>1</sup>*Ivan Franko Lviv National University, Lviv, Ukraine*

<sup>2</sup>*Wrocław University, Wrocław, Poland*

ZnO is a technologically important material, which exhibits multifunctional properties for various applications in optoelectronic devices applications, such as solar cell, transparent conducting electrodes and heat mirror [1]. Transparent conducting ZnO films have been extensively studied in recent year.

Zinc oxide films were deposited on the glass substrates with ITO buffer layers by the standard RF-magnetron sputtering using ZnO targets in the argon atmosphere at the gas pressure of  $10^{-3}$  Torr. The RF-power was 100 W, the target-to-substrate distance was 60 mm, the magnet field strength – 0.1 T. The substrate temperature of the sample №1 during sputtering process was 300 °C. The sample №2 was obtained without heating of the substrate. The films thicknesses taken from the ellipsometric studies were found to be approximately 1.2  $\mu\text{m}$ . The crystalline structure of the films was studied using the full-profile data obtained by automated HZG-4A diffractometer intended for examination of polycrystals. The surface morphology of ZnO films was monitored by atomic force microscope.

The dielectric measurements were performed on parallel-sided samples of rectangular form, using automatized setup. The measurements of real part of dielectric permittivity  $\epsilon'$  and dielectric loss  $\tan(\delta)$  were carried out using traditional method of capacitor capacitance measurement. The capacitance was measured using LCR-meter HIOKI 3522-50 LCF HiTester at the frequency range 4 Hz - 100 kHz. The nitric cryostat with the temperature control system of UNIPAN 680 was used for dielectric properties measurements. The crystal sample placed into the cryostat was blown by the nitrogen fume. The temperature was measured using a copper-constantan thermocouple with the margin of error 0.01 K.

Performed X-ray diffraction studies showed that both films are textured along the crystallographic directions [001] perpendicular to its surface. However, the sample №1 has a better crystal quality than sample №2, as the reflex of the plane (002) in the case of the sample №1 is more intense and sharper. Moreover, for sample №1 also observed weak peak from plane (004). The average crystallite size calculated using Debye-Scherrer formula [2] in samples of №1 and №2 is about 53 nm and 26 nm, respectively.

In a nanocrystalline material the majority of atoms reside in the grain boundary or within a few atomic layers from the boundary. The interface regions contain a large concentration of vacancies, vacancy clusters, dangling bonds etc. [3]. Grain boundaries become electrically active as a result of charge trapping by such gap states localized between two adjacent grains. When this

nanocrystalline material is exposed to an electric field, the space charge polarization occurs [4]. For low frequencies, the dipole moment can easily follow the change of electric field. When the particle size of a material decreases the volume of the particle  $V_p$  becomes smaller, but the volume of interface  $V_i$  increases. When  $V_p$  decreases the dielectric relaxation polarization, which appears mainly inside the particle decreases. Also, when  $V_i$  increases the contribution to dielectric constant by space charge polarization and rotation direction polarization, which occur mainly in interfaces, increases [4]. Therefore, dielectric constant of nanostructured materials should be larger than that of conventional materials.

Polarization caused by hopping of charge carriers is exhibited by many materials, especially amorphous semiconductors and glasses, where the charges carriers are localized electrons. In a nanocrystalline material the density of localized trap states in the grain boundary region is very high and one can expect a large polarization by the electron hopping.

Many oxide materials are reported to contain oxygen vacancies at the grain boundaries. An oxygen vacancy is equivalent to a positive charge and hence possesses a dipole moment [4]. In nanostructured materials the density of defects is very high. Therefore the grain boundaries of nanostructured ZnO should be rich in oxygen vacancies and thereby should contain high density of dipoles. Exposed to an external electric field, the dipole moments will rotate leading to an increased rotation direction polarization in nano-ZnO in comparison with conventional materials. Thus, the high value of dielectric constant at low and medium frequencies can be also connected with this type of polarization.

1. Klingshirn C. ZnO: From basics towards applications // *Phys. stat. sol. (b)*. – 2007. – V. 244, №9. - P. 3027-3073.
2. Panasyuk M.R., Turko B.I., Kapustianyk V.B., Lubochkova G.O., Rudyk V.P., Vas'kiv A.P., Davydov V.M. Manufacturing technology, optical and spectral properties of nano-structurized thin ZnO films // *Functional Mater.* – 2005. - V. 12, №4. – P. 746-749.
3. Gleiter H. Nanocrystalline materials // *Prog. Mat. Sci.* – 1989. – V. 33, №4. – P. 223-315.
4. Mo Ch.-M., Zhang L., Wang G. Characteristics of dielectric behavior in nanostructured materials // *Nanostruct. Mater.* – 1995. – V. 6, №5. – P. 823-826.

## Oxidation behavior of carbon-rich a-SiC:H films deposited by radio-frequency magnetron sputtering

Vasin A.V.<sup>1</sup>, Rusavsky A.V.<sup>1</sup>, Okholin P.M.<sup>1</sup>, Kholostov K.I.<sup>2</sup>,  
Bondarenko V.P.<sup>2</sup>, Lysenkov V.S.<sup>1</sup>

<sup>1</sup>*Lashkaryov Institute of Semiconductor Physics, Kyiv, Ukraine*

<sup>2</sup>*Belarusian State University of Informatics and Radioelectronics, Minsk, Belarus*

In the present report oxidation behaviour of carbon-rich a-Si<sub>1-x</sub>C<sub>x</sub>:H layers deposited by radio-frequency magnetron sputtering technique was examined by FTIR, Raman scattering, atom force microscopy (AFM) and scanning transmission electron microscopy (STEM). Carbon-rich a-Si<sub>1-x</sub>C<sub>x</sub>:H films were deposited on Si substrate by magnetron sputtering of SiC target in Ar (93 vol.%) + CH<sub>4</sub> (7 vol.%) gas mixture. Deposition temperature was about 200°C.

A series of the samples have been deposited applying different RF-discharge power. After the deposition the samples were thermally treated at atmospheric pressure in the flow of dry oxygen at temperature up to 700°C. It was shown that increase of discharge power resulted in material with enhanced corrosion resistance. Low corrosion resistance of the layers deposited at low discharge power was shown to be related with excess of carbon incorporation and resulting lower density of the material. To clarify physical mechanism of the oxidation process a samples deposited at moderate discharge power having partially oxidized structure have been analysed in details. A great number of “spot”-like morphological defects (pits) with dimension ranging from 50 nanometres to 50 microns appeared after thermal treatment in oxygen at 600-700°C. Kelvin probe AFM measurements exhibited the work function of the material in the pits is significantly smaller in comparison with surrounding area indicating an obviously different material properties. Comparative analyse of SEM image of the cleavages and AFM surface profile allowed to conclude that “spot”-like defects corresponds to oxidized material while other material is non-oxidized a-Si<sub>1-x</sub>C<sub>x</sub>:H. One of the most surprising observation is conductivity of the oxidized material is larger than that of non-oxidized area.

Summarizing of the experimental data we conclude that: (1) enrichment of the a-Si<sub>1-x</sub>C<sub>x</sub>:H at “low discharge power regime” reduces density and decreases oxidation resistance of the material; (2) oxidation process of the carbon-rich a-Si<sub>1-x</sub>C<sub>x</sub>:H films in the atmosphere of dry oxygen does not follow “layer-by-layer” oxide growth mechanism inherent to bulk crystalline SiC materials. Oxidation in a-Si<sub>1-x</sub>C<sub>x</sub>:H was found to be happen in selective nanoscale areas. Such selective oxidation mechanism is suggested to be a consequence of nanoscale inhomogeneities associated with nanoscale growth features.

## **Research of polymeric periodic structures formation process in photocurable composite materials by interference method**

Vorzobova N.D., Bulgakova V.G., Burunkova J.E., Moskalenko A.I.

*Saint-Petersburg State University of Information Technologies, Mechanics and Optics,  
Saint-Petersburg, Russia*

At present efforts of many leading scientific laboratories are directed on development of new methods and technologies of obtaining volume polymeric micro- and nanostructural elements. Such elements are relevant in various spheres of science and technics (the information and laser technics, communication, instrument making) as photonics elements – photonic crystals, managing and selective elements. Periodic structures can be obtained by interference lithography. Negative photoresist SU – 8 is the basic material used. An important problem of using this material is a problem of removing residual solvent. It is a labor-intensive process of thermal processing. The present work is oriented on using of light-curable composite materials having advantage at thick layers formation without solvent. Also specific material properties (including a large positive change in the refraction index of the material in the process of photopolymerization) define structures characteristics.

The periodic structures were formed by interference method at wavelength of 325 nm. Dependence of structures characteristics on light-curable compositions, exposure parameters, layer thickness and conditions of postexposure processing was investigated.

The following results are produced:

1. Possibility of interference method realization using monomeric compositions and nanocomposites is shown. Periodic structures with submicronic and nanoscale elements and diffraction efficiency up to 60 % were obtained.

2. Connection between diffraction and dimensional characteristics of periodic structures and material properties was established. It is shown that ZnO nanoparticle doping and nanoparticle concentration increasing leads to diffraction efficiency growth.

3. Probable mechanisms and a role of diffusion processes at structures formation are determinated.

## **Relaxation time approximation and variation method in the calculation of kinetic parameters of semiconductors**

Voznyak O.M.<sup>1</sup>, Zukowski P.<sup>2</sup>, Nykyruy L.I.<sup>1</sup>, Lysak A.V.<sup>1</sup>

<sup>1</sup>*Vasyl Stefanyk PreCarpathion National University, Ivano-Frankivsk, Ukraine*

<sup>2</sup>*Lublin University of Technology, Lublin, Poland*

One of the most precise methods for studying of influence of the impurities on electrical properties of material is the analysis of transport phenomena. These well-known approaches, which are based in particular on the use of relaxation time and a variation principle. These approaches are analyzed in the literature from the various positions [1,2].

On the prevailing scattering mechanism in semiconductors usually speak about set of different kinetic effects dependence on the energy of relaxation time, carrier concentration and temperature. Concentration dependence of mobility define of the changing of relaxation time at filling zone, and thermo-power – derivative on the energy of relaxation time in the strongly degenerate semiconductors (semimetals). The distribution function of carriers is obtained by solving the integral equation in the case of elastic scattering. However, in this case, the distribution function of non-equilibrium carriers can be formally expressed in terms of functions, which play the role of relaxation time.

The variational method is used less often than the relaxation time approximation for explain the properties of narrow-gap semiconductor with spatially dependent of dielectric function, but it has several advantages: the method is applicable to account for inelastic carriers scattering on optical phonons, has a simpler mathematical tools. However, the variational method has its drawbacks. Firstly, it is difficult to determine the number of the series for a given precision in the results. Second, it is important to choose a trial function successfully in two, three addition in order to obtain results with reasonable accuracy.

The contributions of individual scattering mechanisms in the calculation of mobility of the charge carrier using variational approach and the time relaxation approximation is analyzed.

It is shown, that the description of transport phenomena by variation method is useful for detailed description is set in known scattering mechanisms. In this case, can restrict of consideration the one scattering mechanism which is most evident in certain concentrations and temperatures. The variation problem is solved for this scattering mechanism, selecting of certain adjustable rates (which have some physical meaning), and is based on these selected coefficients calculation of various kinetic parameters.

1. D.M. Zayachuk. About Dominant Scattering Mechanisms in Lead Telluride // Semiconductor physics (Rus.). – 1997. – V.31, №2. – P. 217-220.
2. P.N. Gorley, V.A. Shenderovsky. Variation Approach in Kinetic Theory. Naukova Dumka, Kyiv. 1992. – 296 p.

## Atomic emission spectroscopy of nanoporous carbon materials

Yaremiy I.P., Yaremiy S.I., Tomyu U.O.

*Vasyl Stefanyk Precarpathian National University, 57, Shevchenko Str.,  
Ivano-Frankivsk, 76000, Ukraine*

Atomic emission spectroscopy is a powerful modern method which allows to perform qualitative and quantitative analysis of various substances. An example of this class of devices is an atomic emission spectrometer SEV-30. One of its main advantages is the usage of the original spectrum source with dependent discharge [1], which allows to reduce the intensity of the continuous background and, consequently, much lower detection limit of elements in comparison with classical methods of atomic emission and atomic absorption.

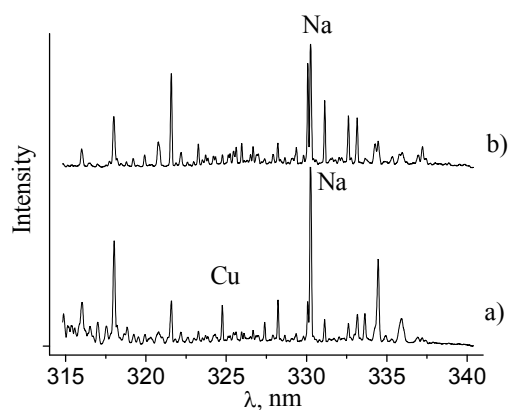


Fig. 1. Emission spectrums of initial (a) and carbonized at 900<sup>0</sup>C and washed out in 30% nitric acid from ashes (b) samples (the wavelength region that has the analytical lines of Cu and Na).

It was determined that the original unmodified powder contained such elements as K, Ca, Na, Mg, Fe, due to their absorption from the soil during growth, and technological impurities Cu and Fe, which were included in the powder during its modification.

*This work was supported by the project UKX-9200-IF-08.*

1. Сапрыкин Ю. А. Аналитические возможности и особенности атомно-эмиссионного анализа с электронным возбуждением атомов в среде гелия при атмосферном давлении / Ю.А. Сапрыкин, Ю.А. Паздерский, Т.А. Бандера // Журнал аналитической химии. – 2003. – Т. 58, № 12. – С. 1251-1258.

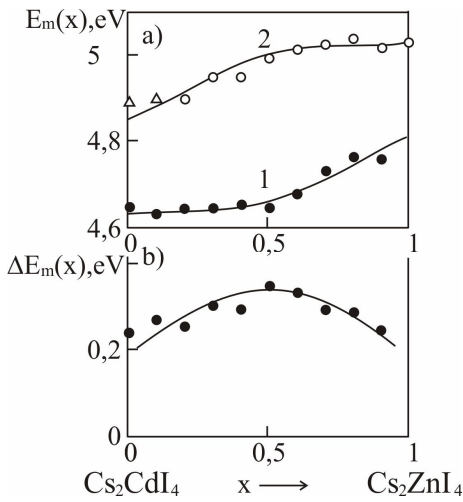
## Absorption spectrums of thin films of solid solutions $\text{Cs}_2(\text{Cd}_{1-x}\text{Zn}_x)\text{I}_4$

Yunakova O.N., Miloslavsky V.K., Kovalenko E.N.<sup>1</sup>

*Kharkiv National University, Kharkiv, Ukraine*

<sup>1</sup>*Kharkiv National University of Radioelectronics, Kharkiv, Ukraine*

The compounds  $\text{Cs}_2\text{CdI}_4$  and  $\text{Cs}_2\text{ZnI}_4$  belong to the layered crystals of the  $\beta\text{-K}_2\text{SO}_4$  type with layers perpendicular to the  $c$  and very close parameters of the crystal lattice, which favors formation of solid solutions  $\text{Cs}_2(\text{Cd}_{1-x}\text{Zn}_x)\text{I}_4$  over the whole range of concentrations. It has been established previously that both compounds are direct band dielectrics, with the low-frequency excitons localized in the structural elements  $\text{CdI}_4^{2-}$  ( $\text{ZnI}_4^{2-}$ ) of the compounds.



The absorption spectra of excitons in thin films of solid solutions  $\text{Cs}_2(\text{Cd}_{1-x}\text{Zn}_x)\text{I}_4$  were found to belong to the persistence type. Analysis of the spectra revealed two excitonic bands  $A^I$  and  $A^{II}$  genetically related to the bands of  $\text{Cs}_2\text{CdI}_4$  and  $\text{Cs}_2\text{ZnI}_4$ . Both bands shift nonmonotonically towards higher frequencies

with increasing  $x$  (fig. 1a), with the inflection points in the dependence  $E_m(x)$ , which is symmetric with respect to  $x = 0.5$ , but the frequency difference between these bands is the greatest at  $x = 0.5$  and the dependence  $\Delta E_m(x)$  is symmetric with respect to this point (fig. 1b).

Fig. 1

Given the structure of crystal lattices of the compounds showed that the concentration dependence of the spectral position of the exciton bands  $A^I$  and  $A^{II}$  is associated with the transfer of excitons between the tetrahedrons  $\text{CdI}_4$  and  $\text{ZnI}_4$  along the  $b$  axis in the solid solutions. Experimental result agrees well with the calculation of energy  $E_{AI}(x)$  and  $E_{AII}(x)$  based on a theory similar to the theory of Davydov's splitting of exciton bands in molecular crystals. On fig. 1.: dots – experiment, solid curves – calculations by Eq. (1).

$$E_{\pm} = \frac{1}{2} [E_1 + E_2 \pm \sqrt{(E_1 - E_2)^2 + 4V_{12}V_{21}}], \quad (1)$$

where  $V_{12}$  and  $V_{21}$  are the matrix elements of the operators  $\hat{V}_{12}$  and  $\hat{V}_{21}$  that take into account transfer of excitons between  $\text{CdI}_4$  and  $\text{ZnI}_4$ . For the molar concentrations  $x = 0$  and  $1$ , the matrix elements  $V_{12}$  and  $V_{21}$  are equal to zero, from here  $V_{12} = x(1-x)\beta_{12}$ ;  $V_{21} = x(1-x)\beta_{21}$ . Considering, that  $\beta_{12}$  and  $\beta_{21}$  are assumed to be independent of  $x$  and equal to each other, we have determined the best fit of the experimental and the estimated dependence of  $\Delta E_m(x)$  at  $\beta = 0.5$  eV.

## Crystallochemistry of point defects and properties of nonstoichiometric GeTe, SnTe.

Jurchyshyn L.D

*Precarpathian National University of Vasyl Stefanyk  
Ivano-Frankivsk, Ukraine*

Germanium and tin tellurides and solid solution on their basis are treated as narrow-gap semiconductors that are broadly used for thermoelectric energy converter [1]. They are phases of a replaceable state with a broad unilateral homogeneity region that is shifted towards tellurium redundancy [2]. The mentioned phase state peculiarities stipulate a high concentration of its own point defects and p-type charge carrier, correspondingly ( $10^{20} - 10^{21} \text{ cm}^{-3}$ ). The point defects of a semiconducting compound crystal-chemical structure significantly determine its conductance type and current carriers concentration, as well as the whole complex of other physicochemical properties [2]. Notice that at present there exists no unified opinion concerning the kind of these defects as well as their charging state [1, 2]. That's why the investigation of concentration dependences properties in a compound homogeneity region is an important issue that demands the study of point defects behavior as well as mechanisms of their appearance and interaction.

In the project crystal-quasichemical formulas for nonstoichiometric p-GeTe compound with tellurium redundancy on condition of two- and four-charged Germanium  $V_{Ge}^{2-}, V_{Ge}^{4-}$  vacancies existence are proposed. Defective subsystem in Germanium selfdoping process is analysed. There is made a conclusion about dominated point defects on the basis of the calculation results comparison of current carriers concentration dependence on deflection amount from stoichiometric composition followed by an experiment.

Though, as the experiment results show, more than two-charge carriers fall to one cation vacancy what indicates existence of not only two-charged but also four-charged Germanium vacancies.

*This work to execute according department project (State registration № 0107U006768).*

1. Korzhuyev M.A. Germanium Telluride and Its Physical Characteristics. Nauka Publishing House, Moscow. – 1986. – 103 c.
2. Freik D.M., Prokopiv V.V., Galushchak M.O., Pyts M.V., Mateik G.D. Crystal Chemistry and Thermodynamics of atomic defects in  $A^{IV}B^{VI}$  Compounds. Pluy P.H., Ivano-Frankivsk. – 1999. – 164 c.
3. L.I. Mezhylovskaya, L.D. Yurchyshyn, L.V. Turovskaya, O.V. Galiuk. Nonstoichiometric GeTe and SnTe compounds defective subsystem and physic-chemical properties peculiarities by. Physics of electronic materials 3<sup>rd</sup> International Conferehce Proceeding. Kaluga, Russia. – 2008. – V.2. – P. 112-114.

## Measurement of uniaxial magnetic anisotropy field of epitaxial ferrogarnet films

Yushchuk S.I., Yuryev S.O.

National University "Lvivska Polytechnica", Lviv, Ukraine

For the rare earth ferrite-garnet epitaxial films (FGEF) the axis of easy magnetization (AEM) is the direction [111] close to the normal of the film plane. To determine the uniaxial magnetic anisotropy field of ferrogarnet films we have developed the magneto-optical method and designed equipment that allows determining this field relatively fast and with sufficient precision.

The proposed technique is based on the determination by of Faraday effect dependence on magnetic susceptibility of the film sample along the axis of easy magnetization  $\chi_{||}$  on behalf of tension constant magnetic fields  $H_{\perp}$  which is perpendicular to this axis.

Simultaneously the constant magnetic field  $H_{||}$  is applied to the sample and parallel to AEM. If the plane polarization light pass through the FGEF in the direction parallel to AEM and in addition to the  $H_{||}$  field apply a small sinusoidal magnetic field with amplitude  $H_{||}^{\omega}$  then the

polarization angle of light that has passed through the sample will be modulation of sinusoidal magnetic field due to Faraday effect. The light intensity is determined by the system consisting of the analyzer light and photodetector. Thus the output photodetector  $V_{out}$  signal will be proportional to the angle of Faraday rotation. And this angle depends on the longitudinal magnetization  $M_{||}$  which is parallel to the direction of light propagation. Since  $M_{||} = \chi_{||}(H_{||} + H_{||}^{\omega})$  (1) the measured photodetector signal is proportional to the susceptibility  $\chi_{||}$ :  $V_{out} \sim \chi_{||} \cdot H_{||}^{\omega}$  (2). To determine the uniaxial anisotropy field  $H_k = \frac{2K_1}{M_s}$  (3) ( $K_1$  - constant crystallographic anisotropy and  $M_s$  - saturation magnetization) it is necessary to draw the curve depending of susceptibility  $\chi_{||}$  of the field  $H_{\perp}$  for various values of  $H_{||}$  and to find the value of  $H_{\perp}^{max}$  in maximum points of  $\chi_{||}$ . The dependence on susceptibility  $\chi_{||}$  of the field  $H_{\perp}$  ( $H_{||} = 100$  E) for  $Y_{2,6}Sm_{0,4}Fe_{3,8}Ga_{1,2}O_{12}$  garnet film is shown in Fig. 1. The

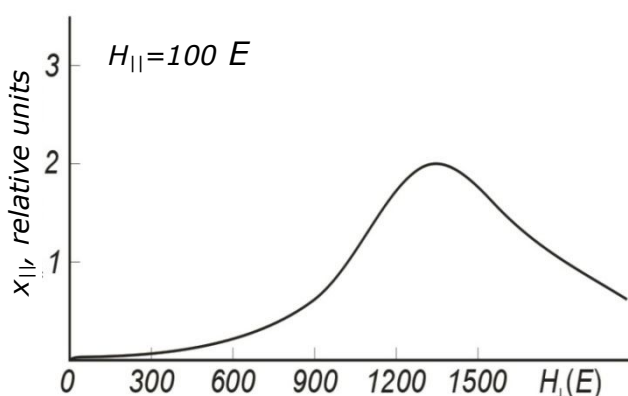
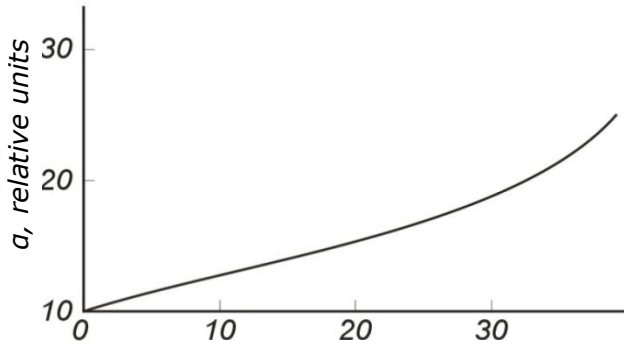


Fig. 1. The dependence on susceptibility  $\chi_{||}$  of the field  $H_{\perp}$  ( $H_{||} = 100$  E) for  $Y_{2,6}Sm_{0,4}Fe_{3,8}Ga_{1,2}O_{12}$  garnet film.

research has shown that with the growing  $H_{||}$  maximum of curve  $\chi_{||} = f(H_{\perp})$  is shifted towards higher values of  $H_{\perp}$ . Thus the field  $H_{\perp}^{\max}$  peak point in the susceptibility curve is a function of  $H_{||}$ . We introduce this function in the form of  $\alpha(H_{||}) = H_{\perp}^{\max}(H_{||})/H'_k$  (4), where  $H'_k = \frac{2K_1}{M_s} - 4\pi M_s$  (5).

Fig. 2 shows the results of calculation according to the function  $\alpha(H_{||})$  of the normalized field  $H_{||}/H_{\perp}^{\max}$ . From Fig. 2 for the corresponding pair of values



$H_{\perp}^{\max}$  and  $H_{||}$  we define corrective coefficient  $\alpha$  and to the (4) we calculate the  $H'_k$  field. To determine the uniaxial anisotropy field  $H'_k$  according to (5) (see also (3)) it is necessary to know the saturation magnetization of ferrogarnet  $Y_{2,6}Sm_{0,4}Fe_{3,8}Ga_{1,2}O_{12}$  determined

Fig 2. The dependence on function  $\alpha(H_{||})$  of the normalized field  $H_{||}/H_{\perp}^{\max}$ .

by independent means. The value of magnetization equal  $4\pi M_s = 180 \text{ Gs}$  for the epitaxial ferrogarnet films grown on a

substrate of single crystal gallium-gadolinium garnet. For this sample uniaxial anisotropy field ( $H'_k = 890 \pm 50 \text{ E}$ ) is determined by the method described above. Measurement accuracy is  $\pm 5\%$ .

## **Spectra-luminescent properties of plasmonic nanocomposites at a low-intensive lamp excitation**

Zamkovets A.D., Pershukevich P.P.

*Institute of Physics, National Academy of Sciences of Belarus, Minsk, Belarus*

Last decades nanocomposites of various types and among them thin films contained of noble metal nanoparticles are under the intensive studying. Inherent plasmon absorption bands in the visible as well as an ability of metal nanoparticles to the strong enhancing the local fields near their surfaces provide for their different practical applications. One of the promising applications of plasmonic nanocomposites may be molecular electronics which is fast developing for last ten years. For this field it is important to supply a possibility of controlling the work parameters of developed devices by low-intensive signals.

In this paper we studied spectra-luminescent properties of plasmonic planar nanocomposites contained of the Ag nanoparticles which were fabricated by a thermal evaporation in a vacuum in the VU-1A set-up. Transmission spectra were registered with the use of the spectrophotometer «Cary 500». Luminescent and excitation spectra were measured at the automatized spectrofluorimeter SDL-2. Excitation was made by a low-intensive lamp radiation (a power density of  $10 \text{ mW/cm}^2$ ). Possibility to compare an illumination intensity of different samples was ensured by their hard fixation and by invariable conditions of a spectra registration.

For densely-packed monolayers of Ag nanoparticles we recorded a luminescent band in the red region of the visible spectral range at the excitation at the wavelength of 450 nm. Band characteristics (its intensity and spectral position) were found to be dependent of a metal surface density.

We analyzed this band features at a placing of a densely-packed monolayer of Ag nanoparticles into KCl and ZnS matrixes. The significant dependence of spectra-luminescent properties of nanocomposites Ag-KCl and Ag-ZnS on an excitation wavelength was demonstrated. It is shown also that a presence of Ag nanoparticles may lead to both an enlarging and a decreasing of a nanocomposite luminescence. The purposeful control of nanocomposite constructive parameters allows changing the degree of an influence on its spectra-luminescent properties.

Among the reasons giving rise to a luminescence of nanocomposites under consideration, the important role may belong to metallic complexes as well as to structure defects which appear into nanocomposites at their formation on substrates at the time of a thermal evaporation of materials.

## Formation of multicharge nanoforms of titanium oxide in films

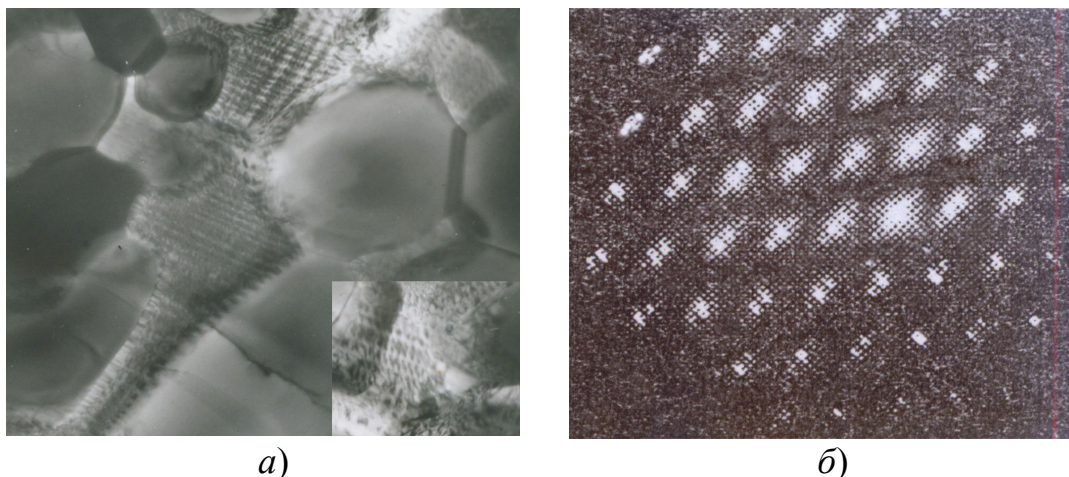
Zaslavskii O.M.

*National University of Bioresources and Nature Management of Ukraine, Kyiv, Ukraine*

Titanium oxide films were given on heated multicrystalline molybdenum substrate by laser evaporation in vacuum. Temperature interval of heating padding was 200-1500°C.

Film structure was analyzed by X-ray investigation, transmission and diffraction electron microscopy.

Was noticed that the amorphous titanium oxide was generated below the substrate temperature of 400°C. If the substrate temperature is higher, the titanium oxide will crystallize in the Anatase form, which coexists in the temperature interval 700-900°C with Rulile. At substrate temperature higher than 900°C the titanium oxide exists only in the Rulile form. The crystal size grows by rising temperature of deposition. Below the deposition temperature of 1400°C deficient phases of the titanium oxide by Oxygen aren't found. A lot of parallel formations are observed at substrate temperature higher than 1400°C in the titanium oxide films. These formations are induced by defects of the crystal packing (fig. 1 *a*). Microdiffraction picture looks like superposition of several systems of reflexes from phases, which are similar to Rutile structure (fig. 1 *b*).



*a)* – microstructure  $\times 135000$ ; *b)* – microdiffraction

Fig. The results obtain from TEM investigation the titanium oxide film at substrate temperature 1400°C

The obtained results indicate about formation of the continuous series of the solid solution  $\text{TiO}_2 - \text{Ti}_2\text{O}_3$ . This solid solution corresponds the nanophase interlacing, which was generated by the oxygen polyhedrons. The oxygen polyhedrons were coordinated around titanium, which was in the oxidation level +3 and +4.

**Electronic structures peculiarities study of  $x\text{-Al}_2\text{O}_3 + y\text{-SiO}_2$   
( $x = 0.2; 0.3; 0.75; 0.96; y = 0.8; 0.7; 0.25; 0.04$ ) nanocomposites  
mixtures**

Zaulychnyy Ya.V.<sup>1</sup>, Ilkiv V.Ya.<sup>1</sup>, Foja O.O.<sup>2</sup>, Dymarchuk V.O.<sup>2</sup>,  
Zarko V.I.<sup>3</sup>

<sup>1</sup>*National Technical University of Ukraine “Kyiv Polytechnic Institute”, Kyiv, Ukraine*

<sup>2</sup>*Frantsevich Institute for Problems of Materials Science of NASU, Kyiv, Ukraine*

<sup>3</sup>*Chuiko Institute of Surface Chemistry of NASU, Kyiv, Ukraine*

Electronic structure peculiarities of  $\text{Al}_2\text{O}_3 + \text{SiO}_2$  mixtures, obtained by mechanical and pyrogenical methods with different oxide ratio, were investigated by means of X-ray emission method. Analysed X-ray emission  $\text{AlL}\alpha$ - and  $\text{SiL}\alpha$ -bands represent distribution of  $\text{Alsd}$  and  $\text{Sisd}$  valence electron states. Obtained spectra were coincided in the single energy scale for analysis.

Sharp decreasing of contribution of  $\text{Alsd}$  electrons, taking part in covalent-bonding states, as well as increasing of electron contribution to non-bonding  $\text{Op}$ -states of studding mixture are revealed by the comparision of X-ray emission  $\text{AlL}\alpha$ - and  $\text{SiL}\alpha$ -bands of pure nanosized  $\text{Al}_2\text{O}_3$ ,  $\text{SiO}_2$  and their mechanical mixtures  $x\text{-Al}_2\text{O}_3 + y\text{-SiO}_2$  ( $x = 0.2; 0.3$  та  $y = 0.8; 0.7$ ). These changes of emission bands are caused by  $\text{Alsd}$  electron transition to  $\text{Op}$  states of  $\text{SiO}_2$  and testify the formation of chemical bonds between  $\text{Al}_2\text{O}_3$  and  $\text{SiO}_2$  under electron bombardment.

Comparison of X-ray emission  $\text{AlL}\alpha$ - and  $\text{SiL}\alpha$ -bands of pure  $\text{Al}_2\text{O}_3$ ,  $\text{SiO}_2$  and their mixtures obtained by means of pirogenical method testifies increacing of valence electron energy redistribution in this composite. Valence electrons energy redistribution effect increases with decreasing of  $\text{Al}_2\text{O}_3$ :  $\text{SiO}_2$  ratio.

Electronic structure investigation reveals that  $x\text{-Al}_2\text{O}_3 + y\text{-SiO}_2$  mechanical mixture heating caused by electron bombardment leads to formation of  $\text{Si} - \text{O} - \text{Al}$  bonds. In case of pirogenical synthesis of  $x\text{-Al}_2\text{O}_3 + y\text{-SiO}_2$  mixtures nanosized composite forms and efficiency of bond formation is much higher.

## Paculiarities of segregation of the *Eu* impurity in the *PbTe:Eu* crystals grown from melt

Zayachuk D.M.<sup>1</sup>, Mikityuk V.I.<sup>2</sup>, Pashuk A.V.<sup>1</sup>, Ulyanitsky<sup>2</sup>,  
Shlemkevych V.V.<sup>2</sup>, Kharko O.V.<sup>1</sup>

<sup>1</sup>*Lviv Polytechnic National University, Lviv, Ukraine*

<sup>2</sup>*Yuriy Fedkovych Chernivtsy National University, Chernivtsy, Ukraine*

For a long time rare earth elements have been successfully used in controlling the physical properties of semiconductors. Semiconductors doped with rare-earth impurities are effective materials in producing light sources whose emission wavelengths are very weakly dependent on temperature. Rare earth elements being used as doping impurities makes it possible essentially decrease the concentration of background impurities in the crystals and films as well as to increase the mobility of free charge carriers. This paper is devoted to the investigation of the behavior of the doping impurity of *Eu* in the *PbTe:Eu* crystals grown from melt by the Bridgman method and doped with *Eu* during the growth process. *Eu* impurity was introduced into the initial charge for the crystals growth within the limits of  $1 \cdot 10^{19} - 1 \cdot 10^{20} \text{ cm}^{-3}$ . Both the longitudinal and diametrical distributions of the doping impurity into the different doped ingots are investigated by the method of roentgen fluorescent element analysis using the analyzer Expert 3L.

It is revealed that character of impurity distribution along and across of the doped ingots is determined by the technological conditions of the crystal growth. Under some conditions the impurity is distributed monotone along the doped ingot whereas under other ones the impurity concentration changes non-monotone along the ingot axis and the concentration profile of impurity has maximum. Generally into the lead telluride crystals grown from melt by the Bridgman method and doped with *Eu* the impurity concentration in the surface layers are some larger than the concentration in the bulk crystal. If the initial impurity concentration into the melt is very small, for example about  $10^{19} \text{ cm}^{-3}$ , practically the whole of impurity can be pushed out on the lateral surface of the crystal ingot. It is possible to establish the specific conditions for growth of the doped crystal under which the impurity behavior will be inversed to mentioned, i.e., the impurity will not be pushed out on the lateral surface but on the contrary will be pulled in the bulk of the crystal spreading along the doped crystals further than usually.

The possible mechanisms of the obtained behavior of the doping impurity of *Eu* into the *PbTe:Eu* crystals grown from melt by the Bridgman method are analyzed.

## Design, nanomodification and characterization of silicon multilayer as optical material

Zubko E.I.

*Zaporizhzhya State Engineering Academy, Zaporizhzhya, Ukraine*

An increase of efficiency of photo-electric converters is the actual task of technology of their making. One the methods of decision of this problem there can be an increase of the amount of the falling light on a solar cell for the decrease of reflection of light from the surface of converters that have a large index of refraction in the area of all incident light. Lately is shown the possibility of replacement of a traditional monolayer of antireflecting coverages by multi-layered, that can work as effective traps for dissipated and reflected light. The multilayer coating samples were fabricated starting from etching of silicon substrates of low resistivity. The electrochemical etch was performed at room temperature with an electrolyte obtained by mixing an aqueous HF with hydrochloric and hydrobromic acid. By the methods of electronic microscopy, XRD and optical spectroscopy were shown that varying of composition of the electrolyte and current density results in nanostructurization of the surface of silicon as layers with different thickness (200-400 nm), morphology and porosity (Fig. 1.).

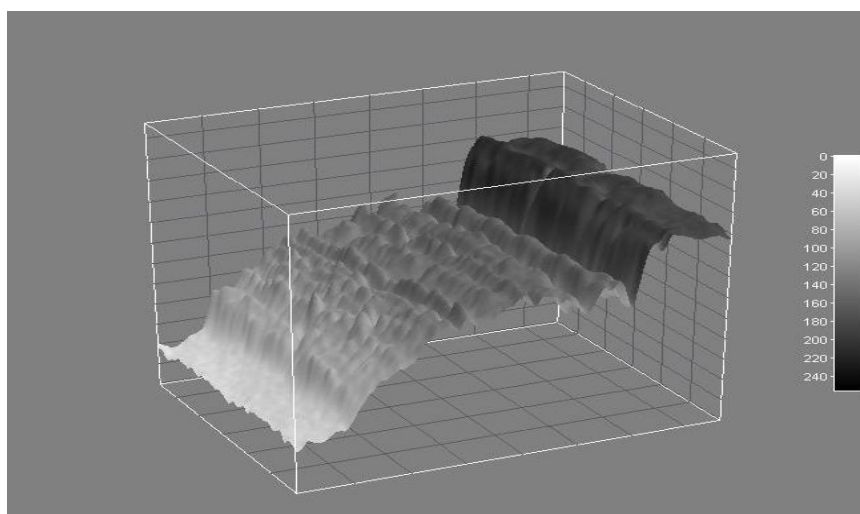


Fig. 1. 3D image of silicon multilayers after modifying.

It is set that thickness of appearing layers were inversely proportional with concentration of components of electrolyte and symbasis of the etching time. It is possible to expect that every subsequent layer will collect sunlight, strengthen an influence previous and to direct him under the most effective for absorption corner, retaining backbeams. As a result it is possible to promote efficiency of the solar cell panel. A mathematical model allowing expecting the index of refraction of realized polylayers and creations on this basis of absorptive materials able to execute the functions of antireflecting coatings is worked out.

**СЕКЦІЯ 4 (усні доповіді)**  
**ТОНКОПЛІВКОВІ ЕЛЕМЕНТИ ЕЛЕКТРОННИХ**  
**ПРИСТРОЇВ, НАНОЕЛЕКТРОНІКА**

17-20 травня 2011 р.

**SESSION 4 (oral)**  
**THIN FILM ELEMENTAL COMPOUNDS FOR**  
**ELECTRONIC DEVICES**

May, 17-20, 2011

## Data Acquisition System for Thermoelectric Generators

Ahiska R.<sup>1</sup>, Mamur H.<sup>2</sup>

<sup>1</sup>*Gazi University, Faculty of Technical Education, Department of Electronics-Computer Education, Ankara, Turkey*

<sup>2</sup>*Cankiri Karatekin University, Vocational High School, Department of Electronics and Automation, Cankiri, Turkey*

Thermoelectric generator (TEG) theoretically may offer many advantages such as being highly reliable, having no moving parts, and being environmentally friendly, when compared with conventional electric power generators [1]. However, wide application of thermoelectric power generation has been limited because of its relatively low heat-to-electricity conversion efficiency. Nowadays, a large number of works concerning thermoelectricity focus on how to improve heat-to-electricity transformation efficiency of thermoelectric materials, that is, how to improve the thermoelectric figure of merit  $ZT$  of these materials [2]. One exception is the TE recovery of waste heat in which it is unnecessary to consider the cost of the thermal input. Consequently, low conversion efficiency is not a serious drawback [3]. Many thermocouples are interconnected electrically in series to increase the operating voltage and thermally in parallel to increase the thermal conductivity, forming a thermoelectric module (TEM). TEM devices can typically be classified into thermoelectric generators (TEGs) and thermoelectric coolers (TECs). TEGs convert thermal energy from a temperature gradient to electrical energy (Seebeck effect) [4].

Measurement of the energy obtained from TEG energy and hot/cold surface temperatures of module measurements usually have been carried out with instant of measurement devices in the TEG systems. All parameters, which are necessary for the calculations of TEGs, both have been instantly tracked and have been recorded thanks to TEG-DAS developed by us.

Experimental setup of TE system has been carried out as in Figure 1. Here, branding Altec two TEGs have been used. Electric heater, which is made of chrome-nickel wire of 500W sizing 5x5cm, has been wrapped to ensure the temperature of hot surfaces. By means of the electric heater, hot surface temperature could be increased up to approximately 200°C. To ensure the cold side surface temperature two radiators sizing 5x5x0,8cm have been done. The cold water has come through these radiators. The cold water temperature, obtained from the circulators, is about 10°C. The electric power, obtained from the TEGs, changing the temperature difference generally has been carried out changing the value of electric heater temperature (hot side temperature  $T_H$ ) due to vary depending on the temperature difference  $\Delta T$  between hot surface temperature  $T_H$  and cold surface temperature  $T_C$ . The electric heater power has been adjusted by an auto transformer branding Artes Electronics. Four T-type thermocouple spot-endings are used for hot/cold surface temperatures of TEGs.

The TEG-DAS has been founded in Figure 2 in order to get continuous registering and tracing of the electrical energy obtained from the TEGs and hot/cold surface temperatures of TEGs. Here, after the hot/cold surface temperatures of TEGs have been measured T-type thermocouples spot-ending, these have been transmitted to the S7-200 CPU224XP Programmable Logic Controller (PLC) branding Siemens, thanks to EM231 expansion module (EM) branding Siemens and connecting four temperature sensors. The analog temperature signals have been converted into digital signals and these signals have been processed with the help of the EM. For sensing amount of current and voltage produced of TEGs, WAS2 CMA 5/10A DC current transmitter branding WeidMüller and MCR-VDC-UI-B-DC voltage transmitter branding Phoenix Contact have been used, respectively. Owing to the used current transmitter and voltage transmitter, can sense current up to 10A DC and voltage up to 550V DC, respectively. The system will be used to the high power of TEGs system planning forward. For sensing the amount of current and voltage, transmitters data have been connected to AI0 and AI2 inputs of PLC. In here, the analog data are converted to the digital data. The power values have been calculated with the help of the PLC program. The OP has been used for these received instantaneous values of all data. These temperature values received from the four different points, temperature difference hot/cold surface interface temperatures, current, voltage and power are monitored in the OP. Calibration of current, voltage and temperatures were carried out with the Fluke 725, Multifunction Process Calibrator device.

Afterwards, these parameters of TEGs have been processed in the PLC, have been transmitted to the SCADA program (Supervisory Control and Data Acquisition) via RS485 communication line. The current, voltage, power, hot/cold surface temperatures and temperature difference have been registered at a second time intervals in the MySQL database. These data have been stored to calculate the conversion of efficiency of TEGs at any time.

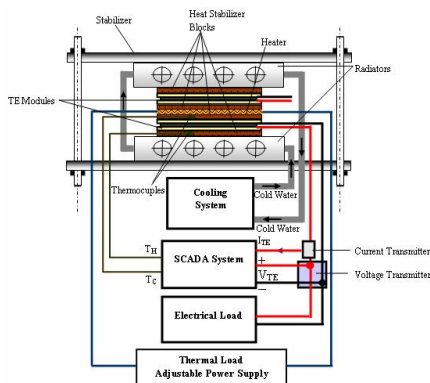


Fig. 1. Experimental setup of TEG system.

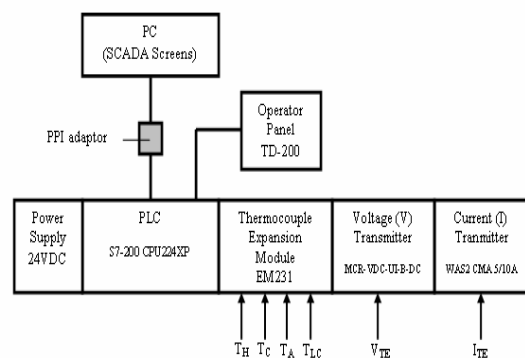


Fig. 2. Setup of TEG-DAS.

A setup of TEG system, approximately 10W, has been implemented and a TEG-DAS system has been successfully developed for continually monitoring

and registering of parameters of TEG used for the calculation of TEG performance values. These measured parameters of TEG, hot/cold surface temperatures, current, voltage and power, have been monitored and registered in the computer, as well as instant values have been observed in the OP. Accuracy tests of these values obtained from measuring values have been done with the calibration devices and Of %5 share of these results of measurement has been seen.

In a later study, these measuring of hot/cold surfaces flows, which are active in the efficiency of TEG, also will be done, at the same time, these amount of hot/cold surface temperature points will be increased.

1. Niu X., Yu J., and Wang, S. Experimental study on low-temperature waste heat Thermoelectric generato // Journal of Power Sources. –2009. – V. 188, № 2.–P.621-626.
2. Tsai H.L., ve Lin, J.M. Model building and simulation of thermoelectric modüle using Matlab/Simulink // Journal of Electronic Materials. –2009. – Cilt 39, –No 9, P. 2105-2111.
3. Lertsatitthanakorn C., “Electrical performance analysis and economic evaluation of combined biomass cook stove thermoelectric (BITE) generator”, – 2007. –Cilt 98, No 8. – P. 1670-1674.
4. Gou X., Xiau H., ve Yang S., “Modeling, experimental study and optimization on low-temperature wasteheat thermoelectric generator system”, Applied Energy, – 2010. – Cilt 87, No 10. – P. 3131-3136.

## **The processes of electron transfer in photosynthetic reaction centers as a standard in nanoelectronics**

Barabash Y.<sup>1</sup>, Zabolotny M.<sup>2</sup>, Serdenko T.<sup>1</sup>

<sup>1</sup>*Institute of Physics of the NAS of Ukraine, Kyiv, Ukraine*

<sup>2</sup>*T. Shevchenko Kyiv National University, Kyiv, Ukraine*

Nanobioelectronics is a new and fast progressing discipline, which integrates achievements of nanoelectronics and molecular biology. Its progress is mainly determined by the development of nanotechnologies. This discipline implies the use of charge transfer processes in biomacromolecules and their assemblies of nanometer size.

In traditional semiconductor electronics charge transfer processes are based on collective interaction in the crystal. In molecular electronics is the charge transfer between individual molecules, or donor-acceptor centers, highly organized molecular ensembles. For electronic circuit, which will consist of a large number of molecules, stability can not be achieved due to the presence of thermal fluctuations. Quick and high quality electronic transfer observed in the structure of reaction centers (RC) – protein complexes that perform directed transmembrane transport in photosynthesis.

RC is a protein with a total weight of  $135 \cdot 10^3$  Da, containing 104 atoms, consists of 6 polypeptide chains and has a number of pigments. When the light quantum excites bacteriochlorophyll dimer (donor), electron is transferred from its excited level successively on monomer bacteriochlorophyll, primary and secondary quinones (acceptor) and falls during 10  $\mu$ s about the opposite side of the membrane. An electron is transmembrane transferred to  $20A^\circ$  with high quantum efficiency. This process is accompanied by conformation changes in the electron transport, which provides long-term existence of the excited state. Therefore it is important to invent an adequate model of electron transfer in biomacromolecules.

The paper studies the kinetics of the absorption spectrum of RCs solutions on wavelength of 865 nm. The detailed analysis of two-level system with different modes of excitation was performed. It showed unsuitability of this model for each fraction. So it is necessary to use higher level systems. For-level model is used. RCs are considered as identical. They show a dynamic response to external influences (changes in the structure), which provides high efficiency of charge transport. The kinetic constants (microscopic speed) are determined. RCs consist of the donor, acceptor and electron transport parts. Future elements of nanobioelectronics should contain the same components similar to macromolecules, which should provide high efficiency of their work.

## A solar cell based on a heterojunction n-TiO<sub>2</sub>/p-CdTe

Brus V.V.<sup>1</sup>, Ilashchuk M.I.<sup>2</sup>, Kovalyuk Z.D.<sup>1</sup>, Maryanchuk P.D.<sup>2</sup>,  
 Ulyanytsky K.S.<sup>2</sup>, Gritsyuk B.M.<sup>2</sup>

<sup>1</sup>*Frantsevich Institute for Problems of Materials Science, NAS of Ukraine,  
 Chernivtsi, Ukraine*

<sup>2</sup>*Yuriy Fedkovych Chernivtsi National University, Chernivtsi, Ukraine*

Solar cells based on heterojunctions, generally consist of a wide-band semiconductor “window” and a solar radiation “absorber”. TiO<sub>2</sub> and CdTe, due to their electrical, optical and operational properties, are well suited to be the “window” and “absorber” materials, respectively [1-3]. The feasibility of TiO<sub>2</sub>/CdTe heterojunctions for photoelectrical conversion is shown in a number of works [4,5], where the ETA-solar cells based on TiO<sub>2</sub>/CdTe heterojunctions were investigated. This paper reports the results of an investigation into the electrical and photoelectrical properties of a solar cell based on a n-TiO<sub>2</sub>/p-CdTe heterojunction fabricated by means of deposition of a TiO<sub>2</sub> thin film onto a freshly cleaved p-CdTe single crystal substrate. The relatively simple methods of ohmic contacts formation were proposed as well as their electric properties were studied. The CdTe single crystals with p-type conductivity were grown by Bridgman method at low cadmium vapor pressure ( $P_{Cd} = 0.02$  bar). The values of specific electrical conductance and majority carriers concentration at 295 K for these crystals were measured to be  $\sigma = 8.9 \cdot 10^{-2} \text{ Ohm}^{-1} \cdot \text{cm}^{-1}$  and  $p = 7.2 \cdot 10^{15} \text{ cm}^{-3}$ , respectively. The TiO<sub>2</sub> thin film was deposited onto the freshly cleaved p-CdTe single crystal substrate (110) with typical dimensions 5×4×1 mm in an universal coating system Laybold – Heraeus L560 by DC reactive magnetron sputtering of a titanium target in atmosphere of argon and oxygen mixture. The measured values of specific electrical conductance and majority carriers concentration at 295 K for the TiO<sub>2</sub> thin film were  $\sigma = 7.1 \text{ Ohm}^{-1} \cdot \text{cm}^{-1}$  and  $n = 4.8 \cdot 10^{18} \text{ cm}^{-3}$ , respectively. The solar cell possessed the open-circuit voltage  $V_{oc} = 0.69 \text{ V}$ , the short-circuit current 6 mA/cm<sup>2</sup> and fill factor  $FF = 0.42$  under 100 mW/cm<sup>2</sup> illumination.

Reasons for the relatively large value of the serial resistance ( $R_s = 820 \text{ Ohm}$ ) were discussed. The good match between the spectral quantum efficiency of the solar cell and the solar radiation spectrum under AM1.5 was noticed.

1. Diebold U. The surface science of titanium dioxide // Surface Science Reports. – 2003. – V. 43. – P. 53-229.
2. Kosyachenko L.A. Problems of photoelectric conversion in thin-film CdS/CdTe devices // Fiz. Tekh. Poluprov. – 2006. – V.40. – P.730-746.
3. Singh R.S., Rangari V.K., Sanagapalli S., Jayaraman V., Mahendra S., Singh V.P. Nano-structured CdTe, CdS and TiO<sub>2</sub> for thin film solar cell applications // Solar Energy Materials & Solar Cells. – 2004. – V.82. – P. 315-330.
4. Ernst K., Engelhardt R., Ellmer K., Kelch C., Muffler H.-J., Lux-Steiner M.-Ch., Konenkamp R. Contacts to a solar cell with extremely thin CdTe absorber // Thin Solid Films. – 2001. – V. 387. – P. 26-28.
5. Ernst K., Belaidi A., Konenkamp R. Solar cell with extremely thin absorber on highly structured substrate // Semicond. Sci. Technol. – 2003. – V.18. – P. 475-479.

## Matrix model of excitation of the thin film bar graph display

Bushma A.V.

*Odesa National Academy of Telecommunications named after O.S. Popov, Odesa, Ukraine*

Most widely used for information display in modern radioelectronic equipment are electron-optical image converters (EOIC) based on thin film elements. Reliability of data presentation with a high level of discreteness can be functionally reached using a bar graph (BG) information model due to its information redundancy. The apparatus component of reliability is provided, first of all, by matrix electric connection of EOIC elements. However, it is not possible to simultaneously excite all the elements necessary to form the BG model. Therefore, used is the dynamic regime to form images, which is usually realized by multi-cyclic scanning the matrix along one of its coordinate. As an alternative, developed were bicyclic methods for synthesizing a BG visual image on the display. Minimization of the number of cycles to excite information area elements considerably increases reliability of data output and lower the level of high-frequency electromagnetic noises caused by EOIC control unit.

In this work obtained are analytical models allowing to describe electrical signals necessary to realize bicyclic excitation of thin film BG display elements.

To realize the bicyclic synthesis of an image, the elements of the matrix set  $\tilde{\mathbf{A}}_{\nu\text{BG}}^{\text{M}}$  with taking limitation into account are separated in two non-intersecting subsets that are excited in different cycles of  $S_{\nu\text{BG}}$  symbol formation. As result, we show that realization of a BG model with bicyclic image formation by separation groups in high-order bits of display matrix can be provided by electrical signals of the following form

$$\begin{aligned} \tilde{\mathbf{A}}_{\nu\text{BG}}^{\text{M}} &= \tilde{\mathbf{A}}_{\nu\text{BG}}^{\text{DM}} = \left[ \tilde{\mathbf{A}}_{\nu\text{BG}}^{\text{DM11}} + \tilde{\mathbf{A}}_{\nu\text{BG}}^{\text{DM21}} \right] \Big|_{T_S} = \\ &= \left\{ \left[ \tilde{\mathbf{E}}_{\nu\text{BG}}^{\text{L11}} \times \tilde{\mathbf{E}}_{\nu\text{BG}}^{\text{H11}} \right] \Big|_{t=t_s+\tau_g-0}^{t=t_s+\tau_g-0} \right\} \cup \left\{ \left[ \tilde{\mathbf{E}}_{\nu\text{BG}}^{\text{L21}} \times \tilde{\mathbf{E}}_{\nu\text{BG}}^{\text{H21}} \right] \Big|_{t=t_s+\tau_g+0}^{t=t_s+2\tau_g-0} \right\}, \end{aligned}$$

where  $\tilde{\mathbf{E}}_{\nu}^{\text{L}q}$ ,  $\tilde{\mathbf{E}}_{\nu}^{\text{H}q}$  are  $m$ - and  $n$ -dimensional vectors of electric signals that control low- and high-order bits of the matrix, respectively;  $t$  is current time of image dynamic synthesis;  $T_S$  – onset of the period of symbol formation,  $\tau_g = T_S/r$  – time interval,  $r$  – the number of cycles to synthesize a visual image on the display. Here,  $\tilde{\mathbf{E}}_{\nu}^{\text{L}q}$  presents a row matrix, while  $\tilde{\mathbf{E}}_{\nu}^{\text{H}q}$  does the column one. The group  $\tilde{\mathbf{A}}_{\nu}^q$  consists of elements placed at the intersection of buses with applied electric stimuli for thin film matrix.

## **Effect of plasma treatment and diamond-like carbon film deposition on CdTe film photoelectrical characteristics**

Klyui N.I.<sup>1</sup>, Kostylyov V.P.<sup>1</sup>, Lukyanov A.N.<sup>1</sup>, Chernenko V.V.<sup>1</sup>,  
Kharchenko N.M.<sup>2</sup>, Nikitin V.A.<sup>2</sup>, Li T.A.<sup>2</sup>, Klyui A.N.<sup>3</sup>

<sup>1</sup>*V.E. Lashkarev Institute of Semiconductor Physics of NAS of Ukraine, Kyiv, Ukraine*

<sup>2</sup>*National Technical University "Kharkiv Polytechnic Institute", Kharkiv, Ukraine*

<sup>3</sup>*Taras Shevchenko Kyiv National University, Kyiv, Ukraine*

To improve the efficiency of photovoltaic energy conversion processes in solar cells (SC) based on CdTe the different active treatments are used under their manufacturing. The aim of this work was to perform comparative study of the effect of active treatments such as annealing in air, chloride treatment, plasma treatment in hydrogen, and diamond-like carbon (DLC) film deposition on photovoltaic characteristics of structures based on CdTe films, deposited in different conditions.

It was shown that chloride treatment of ITO/CdTe structure followed by thermal annealing in air at temperature 430<sup>0</sup>C leads to increasing diffusion length of charge carriers in the CdTe layer.

Thermal annealing at temperature 430<sup>0</sup>C in air only does not affect the value of diffusion length of charge carriers in the CdTe layer, but increases the photosensitivity in the spectral range from 400 nm to the region of sharp decline of the spectral characteristics (about 820 nm). It testifies that surface recombination rate at the CdTe film surface decreases.

Some combinations of the active treatments such as thermal annealing in air, chloride treatment followed by thermal annealing in air, hydrogen plasma treatment and deposition of thin DLC film can increase the diffusion length of charge carriers in the cadmium telluride layer in the ITO/CdTe structures. The effect depends on deposition method (conventional vacuum deposition or deposition in quasi-closed volume).

Besides, it was shown that on the obtained by deposition in a vacuum ITO/CdTe structures that were not subjected to any additional processing or thermal annealing, the hydrogen plasma treatment significantly increases the spectral sensitivity in the spectral range 400-800 nm, and on structures that were subjected to chloride treatment followed by thermal annealing in air the significant increase in spectral sensitivity in mentioned range is achieved after treatment in hydrogen plasma and DLC films deposition.

*This work was supported by STCU project № 4301.*

## **Simulation of nonstandard 3D SOI-Structures for SoC and LoC elements**

Kogut I.T.

*Vasyl Stepanyk Precarpatian National University, Ivano-Frankivsk, Ukraine*

The creation and use of microsystem-on-chip (SoC) and laboratories-on-chip (LoC) has significantly intensified for last years. Traditionally the planar CMOS, bipolar and Bi-CMOS technologies are used for SoC fabrication. These technologies allow to create elements of digital and analog blocks, as well as sensors and actuators. The SOI structures assumed to have better perspectives based on speed, rigidity to external factors, growing degree of integration and for development of device structures with three-dimensional silicon-on-insulator (3D SOI) architectures. The research and investigation of new technological methods fabrication of original SOI-structures are desirable for development of new SoC and LoC elements. This paper presents the simulation results of developed technology for nonstandard local 3D SOI structures formation. This technology allows to create SoC and LoC integrated elements for planar MOS-devices and 3D SOI structures of different types, for example: autoemission microcathodes, hermetical and non hermetical cavities, sensitive elements of acceleration sensors.

Nonstandard local 3D SOI-structures are formed using processes of industrial CMOS-technology: a lithography, local thermal oxidation with masking by a silicon nitride film, isotropic and anisotropic plasma etching, formation of tunnels and cavities in a substrate, etc [1]. Such local structures can be created at proposed places on a silicon substrate according to the device layout. This structure contains 3D SOI element and the element, which can be used for the device structures on bulk silicon. Using the computer simulation we have investigated the electrical characteristics, doping concentrations and charge carriers distribution depending on the gate potential for 3D *n*-channel SOI MOS-transistor, standard and matrix SOI CMOS-transistors with 3D gates, switching elements on Schottky diodes, contact electrodes with 3D surface, elements for high-sensitive integral accelerometers with registration of a field emission current change, hermetical and non hermetical microcavities and micro-channels into a SOI-substrate. The technology developed allows the creation of isolated strips of 3D SOI-structures of any length and isolated areas within each strip. Therefore, defects are not introduced into a surface layer of 3D SOI-structure, thus providing a high crystal perfection and electro-physical properties of silicon.

1. Kogut I.T., Druzhynin A.O., Holota V.I. Architecture and elements of an integrated microsystem on basic matrix crystal with structure of silicon-on-insulator // Visnyk of NU "Lviv Polytechnic" – 2008. – №646. – P. 86-95.

## **Surface purification of CdTe substrates by laser melting**

Kosyachenko S.V, Zakharuk Ya.D., Galochkin A.V., Dremlyuzhenko S.G.,  
Rarenko I.M., Strebegev V.N.

*Yuriy Fedkoivch Chernivtsi National University, Chernivtsi, Ukraine*

Cadmium telluride regions with high density of crystalline structure local violations are places, where point defects are gathered. For defect gettering it is necessary to provide their mobility, in connection with that such gettering method includes heat treatment, a temperature and duration of which are sufficient for defect diffusion from substrate regions (where the devices are formed) into getter region. Point defects, having the large diffusion coefficients, migrate in semiconductor substrate volume during the heat treatment, and hitting into layer with breakdown crystalline structure, precipitate here.

A possibility of CdTe substrate purification from impurities by structure-breakdown layer gettering, formed by laser irradiation, is considered. For profile calculation of diffusive distribution of point defects during heat treatment, and also substrate purification degree after heat treatment, a model, based on diffusion equation with consideration of impurity absorption by dislocations, is proposed. Impurity redistribution task in structure CdTe-Cd<sub>1-x</sub>Hg<sub>x</sub>Te during annealing is solved also. Investigations, carried out on specially prepared samples, confirmed CdTe purification effectiveness by gettering: impurity concentration decreased in 5÷10 times.

## Large low frequency capacitance of a nanocomposite “layered semiconductor – ferroelectric” capacitor under light illumination

Kovalyuk Z.D., Bakhtinov A.P., Vodop'yanov V.N., Netyaga V.V.

*Frantsevich Institute of Material Science Problems, National Academy of Sciences of Ukraine, Chernivtsy, Ukraine*

Composite nanostructures fabricated on the basis of layered anisotropic semiconductor  $p$ -GaSe and ferroelectric  $\text{KNO}_3$  are studied. Multilayer nanostructures were obtained by introducing nanoscale pyramidal ferroelectric inclusions into a layered GaSe matrix [1]. Impedance spectra of the bulk composite GaSe< $\text{KNO}_3$ > nanostructures are investigated in dark and under illumination. It was been founded the processes of accumulation and transport of charge carriers in these structures are due to quantum-dimensional processes in high electrical fields. Such conditions appear because of a switching of electrical polarization and a display of inverse piezoelectric effect in the ferroelectric inclusions. We have found an essential increasing of low frequencies capacity in capacitors prepared on the basis of the nanocomposite material under their illumination at 300K (Fig.1). It may be explained by the Maxwell–Wagner effect in the nanocomposite material and takes place due to surface screening of the electric polarization of ferroelectric single domain nanoparticles with non-equilibrium charge carriers.

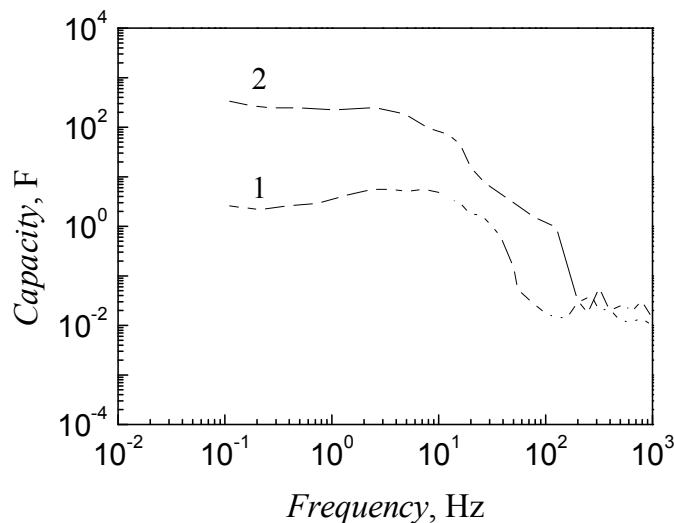


Fig.1. Frequency dependences of the composite nanostructures capacitance in dark (1) and under illumination (2).

1. Bakhtinov A.P., Vodop'yanov V.N., Kovalyuk Z.D., Netyaga V.V., Konoplyanko D.Yu. Carrier transport in layered semiconductor ( $p$ -GaSe) – ferroelectric ( $\text{KNO}_3$ ) composite nanostructures // Semiconductors. – 2011. – V.45, №3. – P. 338-349.

## Electrical properties of InP/InGaAsP double heterostructures

Krukovsky S., Sukach A., Tetyorkin V., Mrykhin I., Mykhashchuk Y.

*Scientific Research Company "Carat", Lviv, Ukraine*

*V. Lashkaryov Institute of Semiconductor Physics NAS Ukraine, Kyiv, Ukraine*

InP-based double heterostructures (DH) with are widely used for manufacture high performance infrared devices for diverse civil and military applications. It is known that these devices suffer from defects of different types in active region. In this report details of manufacture and electrical properties of DH  $n^+$ -InP/n-InGaAsP/ $p^+$ -InP are presented. The emphasize are made on the nature of an excess current in these structures stimulated by deep defects. For this purpose, the dark current is measured as a function of bias voltage and temperature. The measured current-voltage characteristics are theoretically analyzed to determine dominant transport mechanisms.

The investigated DH are grown by liquid phase epitaxy on (001)-oriented  $n^+$ -InP substrates ( $n = (1-3) \times 10^{18} \text{ cm}^{-3}$ ) at a temperature 610-650 °C. The structures consist of n-InP buffer layer, active InGaAsP layer with thickness of 0.6-0.8  $\mu\text{m}$ , undoped p-InP buffer layer and highly doped  $p^+$ -InP:Zn layer ( $p = (2-3) \times 10^{18} \text{ cm}^{-3}$ ). The total thickness of the last two layers was approximately 9  $\mu\text{m}$ . In order to reduce the concentration of uncontrolled background impurities epitaxial layers were doped with Yb. The p-n junction was created by Zn diffusion into the active layer.

In the investigated structures the forward current at low temperatures (77-230 K) may be expressed as  $I = I_0 \exp(qU/E_0)$ , where characteristic energy  $E_0$  has two values depending on the bias voltage. At lower biases it is ranged from 69 meV at 77 K to 78 meV at 230 K. And at higher biases its value was something lower. At temperatures  $T = 230-290 \text{ K}$  the current-voltage characteristics are described by the recombination mechanism with the ideality coefficient 1.9-2.0. The reverse current is shown to be determined by the trap-assisted tunneling via deep defect states in the gap followed by the interband tunneling at high reverse biases.

Experimental data are analyzed in terms of possible participation of extended defects in transport of mobile carriers. Presumably these defects are misfit dislocations which are arised at the heterojunctions.

## **Magnetic switching of magnetic nanofilms and management spin current by pulse laser radiation**

Krupa M.M.

*Institute of Magnetism NASU, Kyiv, Ukraine*

Spintronics belongs to one of the most quickly developing areas of science and technology, it is based on the control of the processes of transfer of spin current between the elements of electronic devices. For spin current control in spintronics devices it is necessary to change the state of magnetization of control and spin filter elements. Usually, one is realized with the help of itself magnetic field of the electric current flowing through special electrodes. At such simple approach there are difficulties of realization of strong enough local magnetic fields in nano- and macro ranges and high-speed controlling the spin currents.

Interesting resources to control the spin current appears when using short laser pulses. Such short laser pulses in magnetic materials can not only create a significant magnetic field in local micro-regions due to the inverse Faraday effect, but to get the directional motion of electrons in the direction of the laser beam due to momentum transfer of photons to electrons. The latter effect is called the photon pressure of laser radiation. Under the action of the photon pressure the reversal of a magnetic low coercitive nanolayer can be obtained in nanofilm heterostructure with two magnetic nanolayers. Such magnetic reversal occurs at the strong enough intensity of laser radiation in a very short time of the order of ten picoseconds. This indicates the prospect of using short laser pulses to control the spin current in spintronics.

Thus, all the foregoing indicates the prospects of using laser pulse radiation in spintronics. It is clear that because of the large light absorption of in magnetic materials, laser beam should be used in the case of thin nanofilm magnetic heterostructures. The latter are just the basic materials to create elements and spintronic devices.

In the presented work we have researched mechanisms of the laser-induced reversal magnetization in single-layered  $Tb_{22}Co_5Fe_{73}$  and three-layered magnetic nanofilms  $Tb_{19}Co_5Fe_{76}/Pr_6O_{11}/Tb_{22}Co_5Fe_{73}$  and  $Co_{80}Fe_{20}/Pr_6O_{11}/Co_{30}Fe_{70}$  under nanosecond and picosecond laser pulse radiation. It is shown the role of the laser-induced spin current in magnetic transformation in the magnetic nanofilms and possibility of fast magnetic reversal in these nanostructures under ultra-short polarized laser pulses that can be used in the new spintronic devices.

## Effect of surface doping of the characteristics of silicon p-n junctions as gas sensors

Ptashchenko F.O.<sup>1</sup>, Ptashchenko O. O.<sup>2</sup>, Dovganyuk G. V.<sup>2</sup>

<sup>1</sup>Odessa National Maritime Academy, Odessa, Ukraine

<sup>2</sup>I.I. Mechnikov National University of Odessa, Odessa, Ukraine

The effect of prolonged exposure of silicon *p-n* junctions in moist ammonia vapors with a partial pressure of 12kPa was studied on *I-V* characteristics of forward and reverse currents, as well as on the characteristics of *p-n* structures as sensors of ammonia, water and ethanol vapors. Kinetics of forward and reverse currents in *p-n* junctions after a change of the ambient atmosphere composition was analyzed.

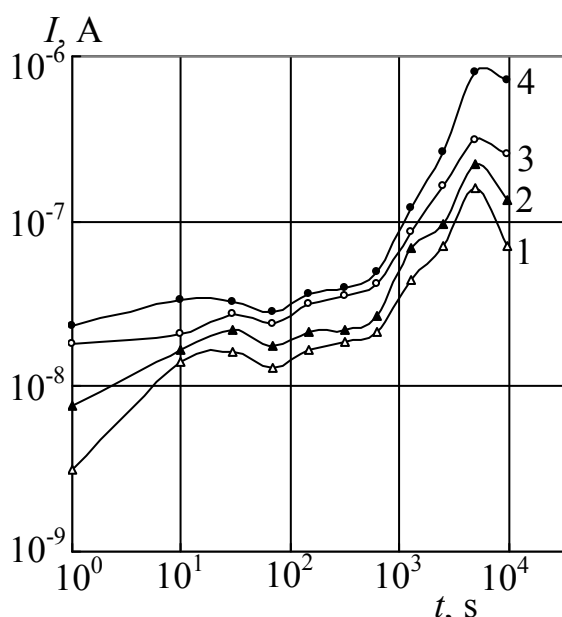


Fig. 1. Change in the reverse current with the duration of the treatment. Measurements were made in air with NH<sub>3</sub> vapors of a partial pressure, Pa: 1 – 50; 2 – 100; 3 – 200; 4 – 500.

increased the additional current, due to adsorption of HNO<sub>3</sub>, H<sub>2</sub>O and C<sub>2</sub>H<sub>5</sub>OH molecules.

The dependence of the reverse current, measured in the ammonia vapors at  $V = -1V$ , on the treatment duration is illustrated in Fig. 1. As a result of this treatment the sensitivity of the *p-n* junction as a sensor of ammonia vapors increased from  $0.05\mu A/kPa$  to  $1.5\mu A/kPa$ .

The enhancing of gas sensitivity of silicon *p-n* junctions as a result of the treatment at high concentrations of ammonia vapors can be explained by the formation of stable donor centers on the crystal surface.

Over the current range 10nA – 1mA the *I-V* characteristics of the direct current of *p-n* junctions, measured in dry air, can be described with the expression

$$I(V) = I_0 \exp(qV / nkT), \quad (1)$$

where  $I_0$  is a constant;  $q$  denotes the electron charge;  $k$  is Boltzmann constant,  $T$  is temperature;  $n \approx 2$  is the ideality coefficient. Such *I-V* characteristics are related to the recombination at deep levels in the depletion layer and at the surface. Adsorption of molecules of HNO<sub>3</sub>, H<sub>2</sub>O and C<sub>2</sub>H<sub>5</sub>OH increased the direct and reverse currents in *p-n* junctions. *I-V* characteristic of the current, caused The prolonged treatment in ammonia vapors practically did not change the *I-V* characteristics, measured in dry air, but significantly

## Review of oxide material application for transparent electronics

Semikina T.V.<sup>1</sup>, Komashenko V.N.<sup>1</sup>, Godlewski M.<sup>2</sup>, Kopalko K.<sup>2</sup>,  
Shmyryeva L.N.<sup>3</sup>, Skorohod I.A.<sup>3</sup>

<sup>1</sup> *V.E. Lashkaryov Institute of Semiconductor Physics, National Academy of Sciences of Ukraine, Kiev, Ukraine*

<sup>2</sup> *Institute of physics PAS, Warsaw, Poland*

<sup>3</sup> *National Technical University of Ukraine "KPI", Kiev, Ukraine*

This paper overviews the tendency of transparent electronics progress. The main ranges of transparent electronics application are sensitive display, flexible displays, organic light emitting diodes (OLED), electroluminescence irradiators, thin films photovoltaic, different electronics and optical coatings. The market of transparent electronics devices is analyzed. NanoMarket estimates the usage of transparent conductive oxide in displays, photovoltaic and light devices on the level of \$9.4 billions dollar to 2015 year.

The physical and electrical properties transparent conductive oxides (TCO) such as ITO, ZnO and other are analyzed. The existing data about p-type ZnO preparation and properties are not repeatable and long time stable that leaves the problem of transparent and conductive p-type material preparation on the top of scientific searching. The development of light emitting diodes on the base of ZnO, thin film transparent transistors and displays demands the elaboration of technology deposition of p-type transparent conductive materials and examples of such elaborations are presented in the paper. The task of exchanging of very expensive films of ITO on ZnO and doped ZnO by Al, Ga and etc. has been still actual. The results of comparison of liquid crystal cells with ITO and ZnO:Al are discussed in review.

The big part is devoted of consideration of different types of solar cell (silicon, organic, thin films) were the layers of transparent conductive films are the part of construction. It is the fact the production of modern solar cell has to use TCO.

The transparent electronics that is partially made on polymer layers needs the low temperature technology of deposition. The original results of electrical properties of thin films of ZnO and ZnO:Al deposited at low temperature by atomic layer deposition (ALD) methods are presented. ALD is examined as perspective technological method for transparent electronics.

## The effect of the semiconductor surface treatment on the photosensitivity of Ni-Hg<sub>3</sub>In<sub>2</sub>Te<sub>6</sub> schottky diodes

Sklyarchuk V.M., Sklyarchuk O.F., Rarenko A.I., Zakharuk Ya.D.,  
Dremlyuzhenko S.G., Koval'chuk M.L., Kolisnyk M.G.

*Yuriy Fedkovych Chernivtsi National University, Chernivtsi, Ukraine*

Direct-zonal Hg<sub>3</sub>In<sub>2</sub>Te<sub>6</sub> semiconductor with band gap by about 0.72 eV – is the perspective material for the photodetectors, sensitive in the spectral region at the wavelength of  $\lambda = 1.55 \mu\text{m}$ , which corresponds the minimal losses in a quartz – basic material for the optical fiber fabrication. In addition, high concentration of the electrically neutral vacancies incident for Hg<sub>3</sub>In<sub>2</sub>Te<sub>6</sub> causes its high radiation stability and insensitivity to many impurities and defects. There is of large scientific and practical interest the development of the fabrication technology of radiation stable photodiodes based on Hg<sub>3</sub>In<sub>2</sub>Te<sub>6</sub>, which can be used in the detectors of visible and IR, X-,  $\gamma$ -,  $\beta$ - and neutron emission and work in the conditions of high radiation.

The results on investigation of photosensitivity of Ni-Hg<sub>3</sub>In<sub>2</sub>Te<sub>6</sub> Schottky photodiodes are presented in this paper. Photodiodes were fabricated on n-type single crystals, grown from the alloys of the especially clean components by the modified method of zonal melting, thermal vacuum evaporation of nickel on surface, pre-irradiated by high energetic argon ions.

Investigations showed, that the regime of previous surface treatment of crystals with stoichiometric Hg<sub>3</sub>In<sub>2</sub>Te<sub>6</sub> vacancies before metal evaporation, allowed to control the spectral photosensitivity (responsivity) form. As known, responsivity

decrease in the  $h\nu > E_g$  energy region is caused by surface recombination. With increase of argon ion energy the concentration of surface levels and surface recombination velocities are decreased, and the responsivity increases in shortwave spectral region, accordingly curves 1,2 on fig. 1.

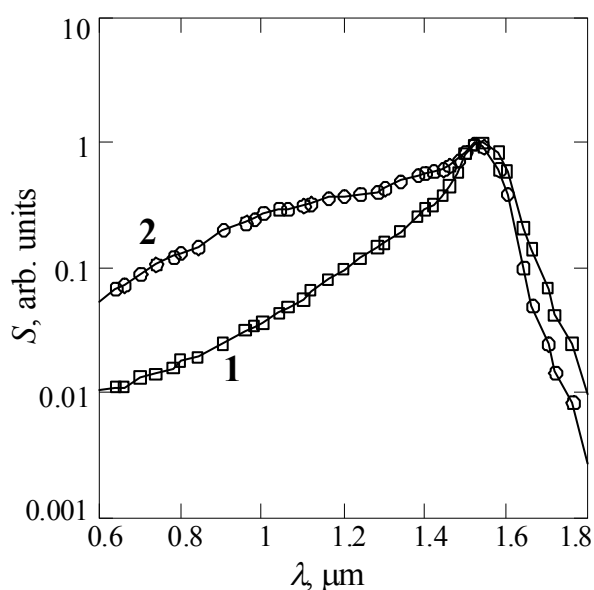


Fig. 1. Responsivity spectra of a Ni-HgInTe diodes fabricated on the surfaces with different pre-treatment regimes.

## Temperature dependence of electroluminescence and charge trapping in Ge and Tb implanted thin SiO<sub>2</sub> films

Tiagulskiy S.I.<sup>1</sup>, Tyagulskiy I.P.<sup>1</sup>, Nazarov A.N.<sup>1</sup>, Nazarova T.M.<sup>2</sup>,  
Lysenko V.S.<sup>1</sup>, L. Rebohle<sup>3</sup>, J. Lehmann<sup>3</sup>, W. Skorupa<sup>3</sup>

<sup>1</sup>*Lashkaryov Institute of Semiconductor Physics, National Academy of Sciences of Ukraine, Kyiv, Ukraine*

<sup>2</sup>*National Technical University of Ukraine "Kyiv Polytechnic Institute", Kyiv, Ukraine*

<sup>3</sup>*Institut für Ionenstrahlphysik und Materialforschung, Forschungszentrum Dresden-Rossendorf, Dresden, Germany*

In this work a comparative study of influence of high temperature on processes of the electroluminescence (EL) and charge trapping in Ge and Tb implanted oxide of metal-oxide-silicon (MOS) structure is performed. The MOS light-emitting devices were fabricated on n-type SiO<sub>2</sub>-Si-structures ( $d_{\text{SiO}_2}=200$  nm for Ge<sup>+</sup> ions implantation and  $d_{\text{SiO}_2}=100$  nm for Tb<sup>+</sup> ions implantation) by the ion implantation with energy of 100 keV. The implanted doses corresponded to 3.0 at % for Ge and 0.5 at % for Tb implantation. To create luminescence centers and to anneal unirradiated defects the rapid thermal annealing at 1000 °C for 6 sec for Ge implantation and thermal annealing at 800-900 °C for 60 min in nitrogen ambient for Tb implantation have been used. Such temperature treatments form correspondingly the Ge and TbO<sub>x</sub> nanoclusters with size near 2-5 nm. The ITO layer was used as a transparent electrode. The EL was studied at constant current regime as a function of injected charge at the same time with measurement of applied voltage to the structure that allowed us to study charge trapping in the dielectric during the device operation. The current-voltage (IV) characteristics of the structures were measured in a joint cycle with the EL intensity (ELI) at a fixed wavelength vs. applied voltage. The EL decay time was measured under constant voltage pulses. All measurements were carried out in temperature range from room temperature up to 200 °C.

It was shown that at high electric field regime the structures show bright blue and green EL with maximum of the EL spectrum at 414 nm and 451 nm for Ge and Tb implantation, correspondingly (Fig.1). The ELI decreases with an increase of measurement temperature (Fig.1) that corresponds to temperature effect on the de-excitation process. The excitation cross-section calculated from ELI-J dependence and decay time measurements demonstrated weak decrease with rise of the temperature.

Electrical quenching of the EL intensity as a function of measurement temperature is depicted with Fig.2 and shows two regions for Ge implanted structures. One region is not depended on temperature, and second one has a strong temperature dependence demonstrating decrease of device life time with increase of measurement temperature. Calculated quenching cross-section, which determines a life-time of light-emitting devices shows activation dependence on measurement temperature with activation energy equals to

0.18±0.02 eV. Applied voltage at electrical quenching of the device increases that corresponds to negative charge trapping in the dielectric during both the first and second steps of the quenching (Fig.2(c)). The Tb implanted structures shows considerably different behavior both EL quenching and charge trapping (Fig.2(b,d)). The model of the electrical quenching in such kind devices is discussed.

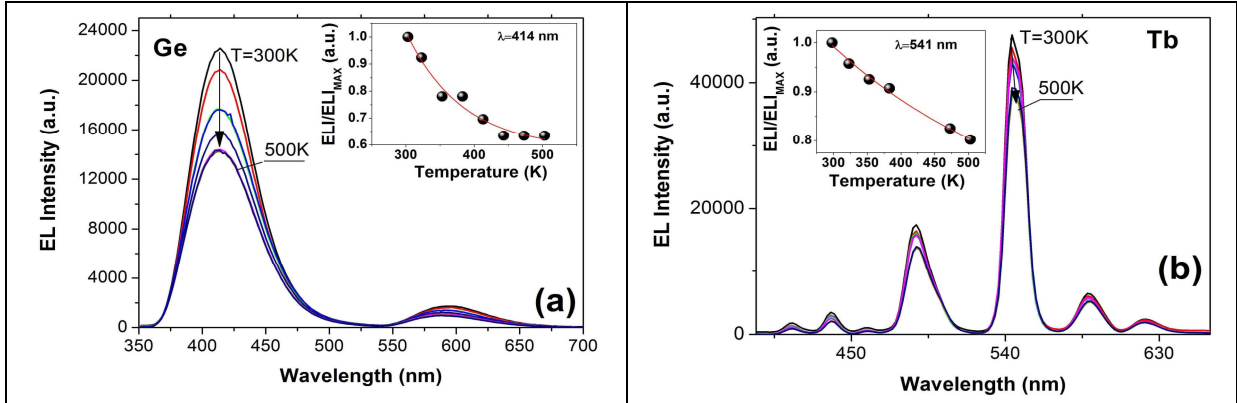


Fig. 1. The EL spectra of the ITO- SiO<sub>2</sub>-nSi structures with Ge (a) and Tb (b) implanted SiO<sub>2</sub> layers as a function of temperature. The inset shows the ELI of the 414 nm and 541 nm line correspondingly for Ge and Tb implanted structures vs. the samples temperature.

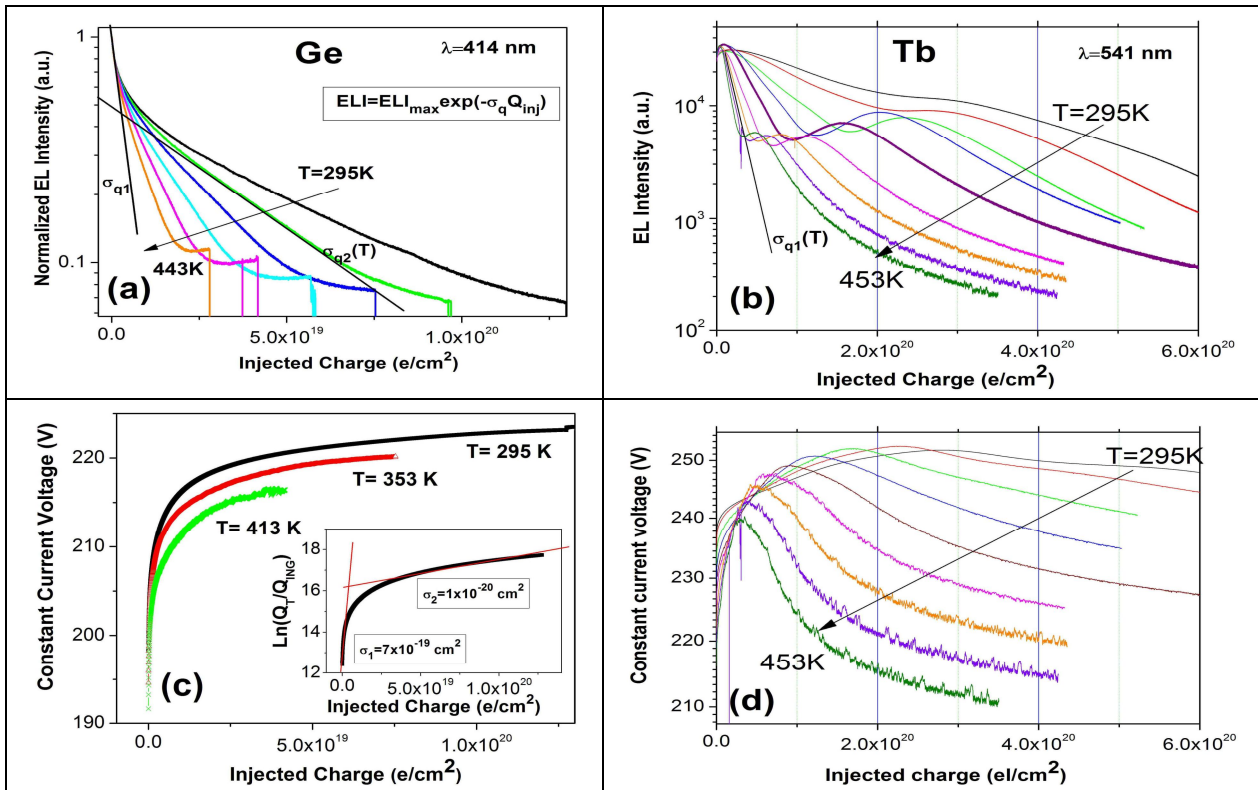


Fig. 2 The ELI of the 414 nm line for the Ge implanted device(a) and of the 541 nm for the Tb implanted one (b) vs. the injected charge as a function of the samples temperature. Constant current voltage applied to the Ge implanted (c) and Tb implanted (d) structure vs. injected charge.

## Changes of the electro-physical parameters of the InGaN/GaN heterostructures of power light-emitting diodes at enhanceable current

Vlasenko A.I.<sup>1</sup>, Veleschuk V.P.<sup>1</sup>, Kysselyuk M.P.<sup>1</sup>, Lyashenko O.V.<sup>2</sup>

<sup>1</sup>*V. Lashkaryov Institute of Semiconductor Physics, NAS of Ukraine, Kyiv, Ukraine*

<sup>2</sup>*Taras Shevchenko Kyiv National University, Kyiv, Ukraine*

From view point of energy-save technologies light-emitting diodes (LED) based on the InGaN/GaN heterostructures, especially power LED with the heterostructure area 1 mm<sup>2</sup> and more is the most perspective sources of light and lighting. But the feature of these heterostructures is more heterogeneous distributing of the internal mechanical strains, dislocations, dopands and component of indium or aluminium in the layers of InGaN and AlGaIn. Therefore the problem of local thermo-mechanical strains appears at passing of the current, concentration of current for to the local low-resistance areas and near-by the contacts, where the local density of current can in ten one times to exceed middle value. It reduces electroluminescence efficiency of LEDs. Also deep levels which play a considerable role in the recombination processes influence negatively, some of them accountable for formation of channels of non-radiative recombination. All of it predetermines the comprehensive study of changes of electric and optical parameters of power LED heterostructures and processes which influence on their stability.

In power InGaN/GaN LED (Golden Dragon+, Osram) found out the change of CVC, unideality factor of CVC  $m$  and derivative of  $m$  on voltage after operating at 500 mA during 1 – 2 months ( $I_{nom} = 350$  mA), that is accompanied diminishing of electroluminescence intensity and defined the defects deep levels. At the differential coefficients of CVC and speeds of recombination found out deep levels, it is here established that levels reveals at  $T = 77$  K. It is discover, that differential factor of inclination of CVC of the power InGaN/GaN light-emitting diodes at direct bias from 0 to 3,2 V changes -  $m = 2,2...8$  and usually has value 5 – 6. It is discovered that CVC InGaN/GaN power LED at  $T = 77$  K  $S$  - like, defined by the deep level. Such type of CVC is defined a transition from the monopolar injection mode to bipolar and is sensible to the defects which create deep levels.

In InGaN/GaN heterostructures found out the infra-red band of electroluminescence, related with the deep level. Found out and investigate the so-called microplasmas - areas of localization of current and according luminescence, which appear in site of the structural defects, in particular dislocations, are in the volume charge area.

## Acoustic emission in light-emitting heterostructures

Vlasenko A.I.<sup>1</sup>, Veleschuk V.P.<sup>1</sup>, Lyashenko O.V.<sup>2</sup>

<sup>1</sup>*V. Lashkaryov Institute of Semiconductor Physics, NAS of Ukraine, Kyiv, Ukraine*

<sup>2</sup>*Taras Shevchenko Kyiv National University, Kyiv, Ukraine*

Light-emitting heterostructures based on the compounds GaN, GaP, GaAs, which are basis of energy-save technologies, more and more pay attention of the technologists and researchers due to improvement of luminescence parameters, reliability and usage at maximally accessible physics-technical parameters and in extreme modes. Exactly processes of degradation and defects-formation, various fluctuation processes and nondeterministic of the threshold parameters at the action of the external fields of this structures imposes the certain limits on their practical application.

One of not many non-destruction experimental method, which can not only discover but also define character and direction of these processes in crystals and functional structures there is acoustic emission (AE) method which is based on registration of the acoustic impulses of noise character from internal sources, in particular at origin and motion of dislocations, at failure of internal mechanical strains at passing of the electric current.

From the complex experimental researches it is established, that on the dynamics of operation of the AE sources in the heterostructures of indicator light-emitting diodes based on the GaP and GaAs compounds have a considerable influence processes of natural ageing, which for time  $\sim 6 \cdot 10^8$  s diminish total AE and AE intensity, raise in 10-20 times maximally admissible density currents, in particular destruction currents and AE origin threshold.

It is reveals that in light-emitting GaP and GaN structures at the densities of currents, that exceed the AE origin threshold, take place simultaneously: operation of AE sources, irreversible change of electroluminescence spectrums, degradation of current-voltage characteristics and fluctuation of quantum yields and current which specifies on the general mechanism of their origin – process of origin and change of the energy state of the structural defects.

Is offered the non-destruction express-method of control of the light-emitting structures and devices, which allows in real-time mode on the AE origin threshold to fix in them degradation and relaxation processes both in the conditions of the long storage and in the conditions of exploitation at the direct current passage and to define the individual maximal parameters of their use, in particular maximal densities of the current which is preceded destruction and to prognoses reliability.

## Nanocomposition membranes for power and information transducers

Yashin A.G., Michailov E.D., Michailova A.M.

*The Saratov state Technical University, Saratov, Russia*

In this work the research of the films based on the acrylate copolymers from aqueous and non-aqueous media are presented. The films obtained from aqueous emulsion have proper physical mechanical properties, optically transparent, chemically resistant to concentrated acid and alkali solutions.

Anionic and cationic acrylate copolymers are referred to hard phase polymer electrolytes (HPPE) with molecular mass of 150-300 thousand arbitrary units. The following three-component copolymers have been studied [1]: 1) Butyl acrylate (ba) – styrene – metacrylic acid (MAA) ( $C_{19}H_{25}O_4$ ) with the implanted cationic surfactants, an equivalent mass of the polymer link is 300 g/mol, hydrophobic anionic polymer; 2) BA – butylmetacrylate (BMA) – MAA ( $C_{16}H_{26}O_6$ ) with the implanted anionic surfactants ( $RSO_3-Na$ ), an equivalent mass of the polymer link is 314 g/mol, hydrophilic anionic polymer; 3) BA – metylacrylate (MA) – MAA ( $C_{31}H_{35}O_6$ ) with the implanted cationic surfactants (R-NCl), an equivalent mass of the polymer link is 300 g/mol, cationic polymer (aqueous emulsions); 4) acrylic acid (AA) – styrene – MAA (non-aqueous copolymer). Emulsion particles dimensions hesitated over 50-300 nm range [2].

The obtained membranes are of 0,03-0,5 mm width, optically transparent, chemically resistant to concentrated alkali solutions, nitric sulphuric and hydrochloric acids, and are dissolved in acetic acid. Permissible heating temperature is up to 333 K. Breaking strength is 50 rgc/cm<sup>2</sup> at 600% elongation

It is not succeeded to modify anionic acrylic copolymers by heteropolyacids. Cationic copolymers (BA – MA – MAA) with the presence of sulphoheteropolyacid (SHPA) possess proper conductivity (see fig. 1).

Films obtained from the copolymer acrylate emulsion AK – styrene – MAA, from non-aqueous solvents (toluene, benzene, isopropylacetate) with tetrahydrofuran additives have conductivity of  $3,6 \cdot 10^{-3} \text{ Om}^{-1} \text{ cm}^{-1}$ , the width of the film is 0,05 mm. The copolymer contains two carbonyl groups able to dissociate in moisture content  $K_{dis}=1,7 \cdot 10^{-4}$ , conductivity is not observed if there is no moisture. The force of carbonic acids depends on the radical electrophyllicity bonded with carboxyl. As mentioned above to form nanoparticles of tetrahydrofuran (THF), forming suspension additive raises conductivity up to  $5 \cdot 10^{-2} \text{ Om}^{-1} \text{ cm}^{-1}$  (fig. 1)

As the result of research it was determined that acrylate copolymers obtained from aqueous anionic and cationic emulsions may be considered as hard polymer electrolytes. Cationic emulsions can be modified by heteropolyacids additives up to 1%, thus improving their physical chemical properties. The optimal moisture contents in the film, obtained from aqueous

electrolyte is 18%. Cationic acrylate copolymers are the most perspective for application.

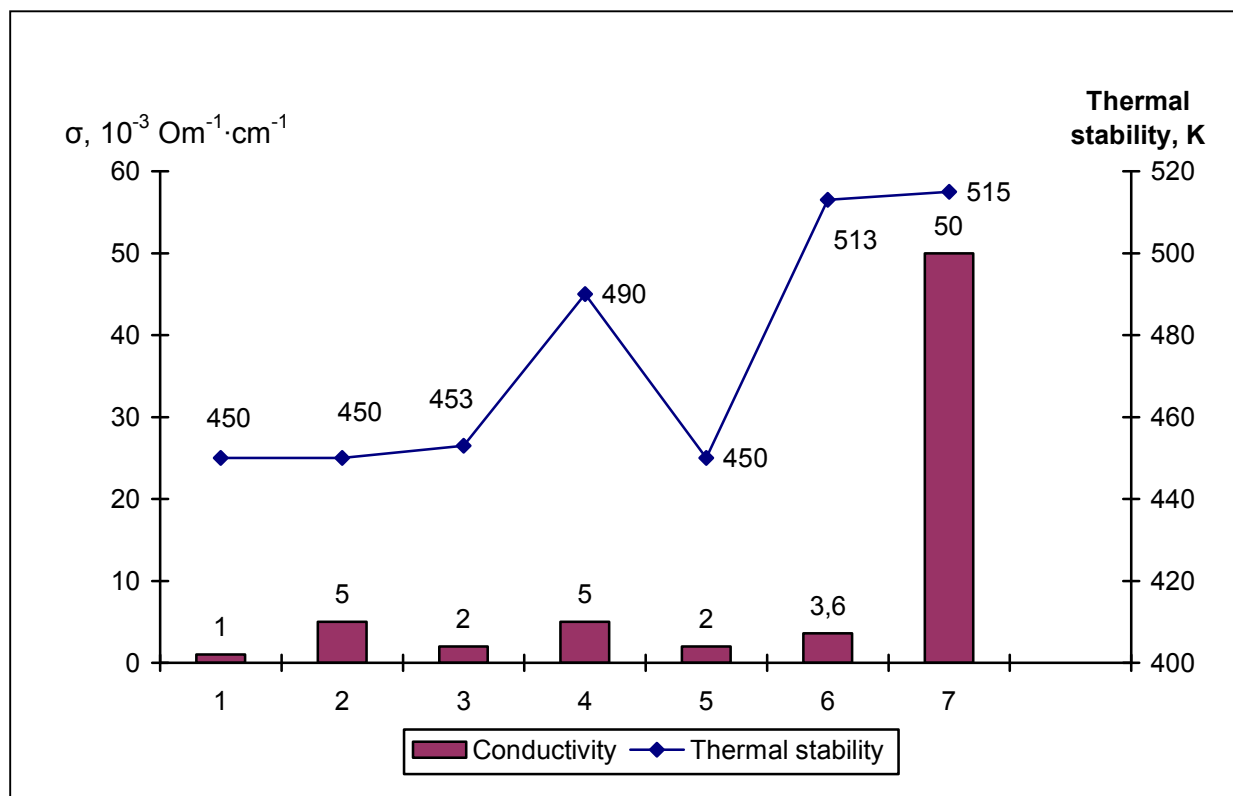


Fig. 1. The influence of obtaining acrylic polymer films method on their properties: 1. BA – styrene – MAA with implanted asurfactant; 2. BA – MA – MAA with implanted asurfactant; 3. BA – MA – MAA with implanted csurfactant; 4. BA – MA – MAA with phosphoric molybdenum acid additive; 5. AK – styrene – MAA; 6. AK – styrene – MAA with phosphoric tungsten acid additive in THF.

The membranes are tested in power source gasanalyser and electrochrome indicators.

1. Smirnova O.A., Michailov D.O., Chernova M.A., Channova G.K., Michailova A.M. // Theses of XIV Russian international conference of physical chemistry and electrochemistry of melted and hard electrolytes. Ekaterinburg. – 2007. – V.II. – P.111.
2. Eliseyeva V.I. Polymer dispersions. M. Chemistry. – 1980. – 296 c.

**СЕКЦІЯ 4 (стендові доповіді)  
ТОНКОПЛІВКОВІ ЕЛЕМЕНТИ ЕЛЕКТРОННИХ  
ПРИСТРОЇВ, НАНОЕЛЕКТРОНІКА**

19 травня 2011 р.

**SESSION 4 (poster)  
THIN FILM ELEMENTAL COMPOUNDS FOR ELECTRONIC  
DEVICES**

May, 19, 2011

## Plasma effect on the CuInSe<sub>2</sub> thin film resistivity

Aktas K<sup>1</sup>, Acar S<sup>1</sup>, Salamov B G<sup>1,2</sup>

<sup>1</sup>Physics Department, Faculty of Sciences, Gazi University, Ankara, Turkey

<sup>2</sup>National Academy of Science, Institute of Physics, Baku, Azerbaijan

Copper indium diselenide has a direct band gap of 1.1 eV, absorption coefficient up to the order of  $10^5 \text{ cm}^{-1}$ . It is expected to be one of the promising absorbing materials for photovoltaic applications, and is usually utilized as heterojunction solar cell in the form of polycrystalline thin films. CIS film could be applied to image pickup devices, as well as solar cells, since high efficient thin-film photoconductors are known to be useful in the photoconductive imaging [1]. A better understanding of the electrical properties of the films is required for a systematic evaluation of the preparation conditions and for the optimization of the film characteristics. The electrical properties of CIS thin films have been studied in detail by several workers [2,3] and all have found dependences between those properties with fabrication and postfabrication processing.

The interaction of various materials, such as metals, semiconductors, dielectrics and polymers, with gas-discharge plasma leads to changes in their behaviour due to surface modification. This phenomenon is widely used in semiconductor technology for etching, film deposition and modification of surface properties [4]. In this work, effect of plasma on the electrical resistivity of CIS polycrystalline film is discussed.

A schematic diagram of the experimental set-up with an ionization cell is shown in figure 1. For experimental test, we used a device proposed in Ref. [5]. The ionization system is mainly a discharge cell containing two electrodes (4 and 6), one of which is a semiconducting photosensitive plate (4). The plate that we used has a circular shape of diameter 20 mm on a glass substrate (3) with a back contact. The soda-lime glass substrate is coated with transparent conductor (ITO) and on top a CIS (4) film of about 0.25  $\mu\text{m}$  thickness is deposited by triple-ionized beam technique in which Cu-, In- and Se-vapor for CIS were ionized and accelerated [6]. During the film-deposition, the acceleration voltages for Cu-, In- and Se-beams were maintained at 2 kV and the electron currents for ionization of the Cu-, In- and Se-beams were varied between 0 mA and 150 mA. Source materials employed were Cu, In and Se of 99.9999% purity. Source temperatures of the three crucibles for Cu, In and Se were 1420°C, 980°C and 320°C, respectively. The substrate temperature was kept at 300°C by an infrared lamp, and the pressure in the vacuum chamber was maintained at less than  $1 \times 10^{-5}$  Torr for deposition period of 90 minutes. This plate is illuminated with IR light (1) which causes an increase in the photoconductivity. A filter (2) is used to allow the desired spectrum to the cathode. In our system the CIS film was chosen as a semiconducting

photocathode (4), which is important in the formation of image by charged particle flux (electron and ion).

A gas discharge gap (5) is formed by a dielectric separator with a thickness varying from 15 to 40  $\mu\text{m}$ . The anode is a disk (diameter 20 mm and the thickness 2 mm) of glass (7) coated with a thin layer of transparent conductor (6)  $\text{SnO}_2$ . The cell is placed into a metallic chamber having windows, in which a residual pressure  $p$  between  $760 \div 28$  Torr can be formed. A voltage of up to 500 V is applied to the electrodes of the cell. By applying a feeding voltage  $V_0$  between the *ITO* contact and the  $\text{SnO}_2$  layer, a discharge is ignited in the gap. This corresponds to a discharge operating in the Townsend regime (this stable form of discharge is employed in spectral image converters with photosensitive *GaAs* detector possessing linear *CVCs*). The measurements are carried out at room temperature. The discharge gap of the cell is occupied by the atmospheric air. Resistivity measurements were carried out with Keithley 2400 sourcemeters.

The resistivity of  $\text{CuInSe}_2$  films was measured at room temperature by two-point probe method before plasma and then the *CIS* thin film expose to plasma process. So resistivity was measured again. It is clear that resistivity which region expose of to plasma treatment is not homogeneous. The variation of the resistivity,  $\rho$ , of *CIS* film shown is numerically given in Table 1. We think especially *In* segregated from surface *CIS* samples during the plasma treatment and consequently *Cu/In* ratio increased. The resistivity is strongly related to the *Cu/In* ratio. The ratio of *Cu/In* increases cause of the decrease in resistivity on the sample. It is seen that from the Table 1, resistivity values decrease by three orders of magnitude after the plasma treatment. This result agrees with the resistivity variations reported previously [7]. In ref [8], they changed of *Cu/In* ratio from 0.9 to 1.1 and observed the resistivity values decrease of five orders of magnitude. The increase of the resistivity when the copper concentration decreases in relation to the indium concentration is a compensation effect due to the excess *In* atoms which act as donors. The observed drastic decrease in resistivity, as the *Cu/In* ratio changes from 0.96 to 1.1, could be attributed to the presence of a high conductivity of  $\text{Cu}_{2-x}\text{Se}$  phase segregated in the grain boundaries. Also, the copper excess causes a whole degeneracy in the deposited films.

CIS Resistivity ( $\Omega\text{cm}$ )	
Before plasma treatment	After plasma treatment
$1.7 \times 10^7$	$1.0 \times 10^4$
	$8.5 \times 10^4$
	$3.5 \times 10^5$
	$1.1 \times 10^6$
	$1.2 \times 10^6$
	$3.3 \times 10^6$

The influence of plasma treatment on the electrical properties of *CIS* thin films was investigated. With the treatment of plasma, resistivity values which region expose of to plasma treatment are not homogeneous and decrease by three orders of magnitude after the plasma treatment. This result may be related to variation of *Cu/In* ratio.

This work was supported by the Gazi University BAP research projects 05/2010-31 and 05/2009-17.

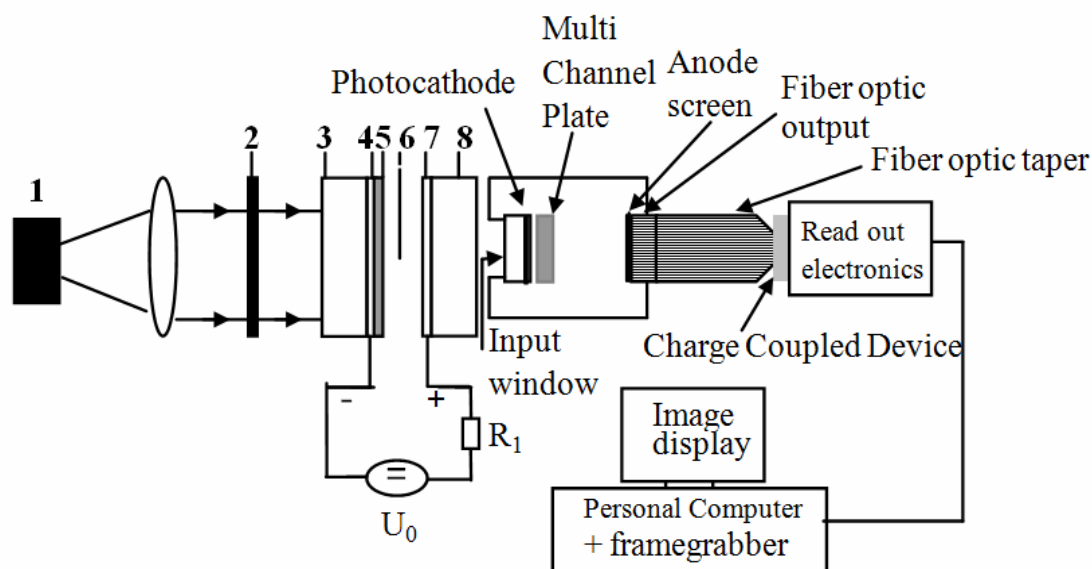


Fig. 1. Experimental setup including an *IR* image converter. Numbers indicate: 1. light source; 2. *Si* filter; 3. flat glass disc; 4. transparent *ITO* conductor; 5. *CIS*; 6. gas discharge gap; 7. planar transparent *SnO<sub>2</sub>* conductor; 8. flat glass disc.

1. Nouti R., Axton R., Herrington C., and Deb S. K. // *Appl. Phys. Lett.* – 1984. – 45. – 668.
2. Isomura S., Kaneko H., Tomioka S., Nakatani I. and Masumoto K. // *Jpn. J. Appl. Phys.* – 1980. – 19. – 23.
3. Ashour A., Akl A.A., Ramadan A.A., Abd K. El-Hady // *Journal of Materials Science: Materials in Electronics.* – 2005. – 16. – P. 599-602.
4. Gurevich E.L., Kittel S., Hergenröder R., Astrov Yu.A., Portsel L.M., Lodygin A.N., Tolmachev V.A. and Ankudinov A.V. // *J. Phys. D: Appl. Phys.* – 2010. – 43. – 275302.
5. Salamov B.G., Colakoglu K. and Altindal S. // *Infrared Phys. Technol.* – 1995. – 36. – 661
6. Tanaka K., Kosugi M., Ando F., Ushiki T., Usui H. and Sato K. // *Jpn. J. Appl. Phys.* – 1993. – 32. – 113.
7. Tuttle J.R., Albin D.S., Noufi R. // *Sol. Cells.* – 1991. – 30 – 21.
8. Akl A.A., Afify H.H. // *Materials Research Bulletin,* – 2008. – 43 – 1539-1548.

## **An electronic switching structure Te-CdTe, formed under pulsed laser irradiation of CdTe**

Dauletmuratov B.K.

*Institute of Semiconductor Physics V.E. Lashkaryov NAS, Kyiv, Ukraine*

The advantage of electric switching elements based on bistable semiconductor structures is the ability to effectively manage their parameters under the influence of external electric and magnetic fields [1].

In the work investigated the influence of the nanosecond ruby laser radiation on the electrical and photoelectric characteristics of crystals of CdTe. Shown that the appearance of a layer Te irradiated CdTe leads to the formation of a bistable structure Te-CdTe with the property multiple electronic switching from high to low resistance state with memory. The presence of switching at liquid nitrogen temperature indicates the electronic mechanism of the phenomenon.

When voltage is applied, the structure from a high state to a low-resistance state when power is off a low-resistance state is retained. For the reverse mixing structure goes to a high state as when power supply high-resistance state is retained, with the memory.

The results of combinational (Raman) scattering testified that on the surface of the film they exist amorphous tellurium. Since in amorphous semiconductors is observed fluctuation of the electrostatic potential, the carriers until the reach of contacts who have been forced to bend around barriers created by the large scatter the conduction band of disordered atoms through separate channels of conductivity, because of what the structure is high resistivity. When voltage is applied forward bias potential holes in the forbidden band bend, resulting in the expense of reducing the height of the potential carrier concentration abruptly increased. A potential hump filled electron plasma, after which the free carriers move along the whole section rather than on a separate channel, and therefore the structure becomes a low impedance. Low-resistance state after the withdrawal of food preserved by the fact that in the amorphous state of tellurium is ions. High-resistance state under reverse bias due to the fact that since the barrier has a polarity reverse bias the barrier height increases, the resulting structure becomes a high-resistance. High-resistance state after the removal of supply indicates that the tellurium ions is neutralized.

1. Baydullaeva V.V., Borsch V.P., Veleschuk A.I., Vlasenko B.K., Dauletmuratov S.N., Levitsky P.E. Mozol Structure Te-CdTe with property electronic switching with memory // Technology and design of electronic equipment (TKEA). – 2007. – V. 71, № 5. – P. 40-43.

## The Pool-Frenkel conduction mechanism in metal-GaP contacts

Demir M., Güzel T., Acar S. and Özer M.

*Physics Department, Faculty of Sciences, Gazi University, Ankara, Turkey*

The formation of metal-semiconductor (MS) contacts widely has been studied because of their technological importance in semiconductor devices. Electrical properties of MS interfaces have been extensively studied in recent years to understand the charge transfer properties. These studies suggest different dominant conduction mechanisms in the MS structures, which include space charge limited current, Poole-Frenkel conduction, and Schottky conduction mechanism [1,2].

Analysis of temperature dependent current-voltage characteristics of Schottky devices allows us to understand different aspects of current transport. In this work we have carried out  $I$ - $V$  measurements in 125-300K temperature range. In order to understand the transport mechanism of the contacts, the dark forward  $I$ - $V$  characteristics were analyzed in terms of the Poole-Frenkel (PF) type conduction [3,4].

The semiconductor substrates used in this work were n-type S-doped GaP single crystals, with a (100) surface orientation, 300  $\mu\text{m}$  thick. The wafer was chemically cleaned using the RCA cleaning procedure with the final dip in diluted HF for 30 s, and then rinsed in deionized water of resistivity of 18 M $\Omega$  cm with ultrasonic vibration and dried by high purity nitrogen. Immediately after surface cleaning, high purity gold (Au) metal (99.999%) with a thickness of 2000 Å was thermally evaporated from the tungsten filament onto the whole back surface of the wafer in the pressure of  $1 \times 10^{-7}$  Torr. Then, a low resistivity ohmic contact was followed by a temperature treatment at 400 °C for 3 min in N<sub>2</sub> atmosphere. The Schottky contacts were formed on the other faces by evaporating gold (Au, 99.999%) with a thickness of 1500 Å as dots with diameter of about 1.0 mm through a metal shadow mask in liquid nitrogen trapped high vacuum system in the pressure of  $1 \times 10^{-7}$  Torr. The  $I$ - $V$  measurements were performed by the use of a Keithley 2400 sourcemeter.

The  $I$ - $V$  characteristics of the device were investigated in the 125-300 K range to identify the dominant charge transport mechanism in this region. The data fit to PF type conduction. Generally, the current-voltage dependence of the device can be expressed as [3,4]

$$I \propto \exp(-E_0/kT) \exp(Z)V^{1/2} \quad (1)$$

where  $Z = n/kT(e^3 \eta / 4\pi \epsilon_0 \epsilon_r d)^{1/2}$ , this equation takes to form Eq. 2 for the PF conduction

$$I \propto G_0 V \exp(-E_0/kT) \exp(Z)V^{1/2} \quad (2)$$

$G_0$  is the conductance of the sample and Eq.2 can be rewritten as

$$\log(I/V) = Y + ZV^{1/2}, \tag{3}$$

where

$$Y = \log(G_0) - E_0 / kT \tag{4}$$

The plots of  $\log(I/V)$  versus  $V^{1/2}$  is shown in Fig. 1. for room temperature. If the conduction is controlled by the PF mechanism a plot of  $\log(I/V)$  versus  $V^{1/2}$  should be a straight line with the intercept and the slope giving the values of  $Y$  and  $Z$ , respectively.

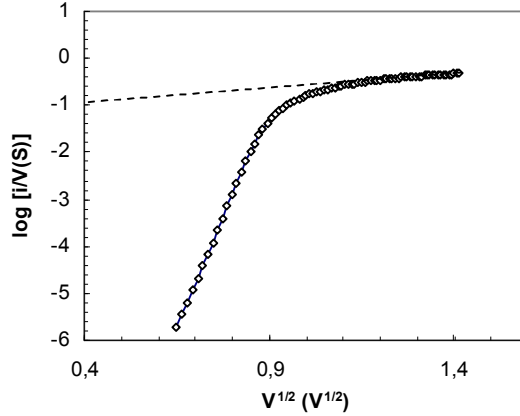


Fig. 1.  $\log(I/V)$  versus  $V^{1/2}$  at room temperature.

If the charge transport mechanism is PF type, according to theory a plot of  $Z$  against  $1/T$  should be a straight line passing through the origin. Also, the plot of  $Y$  against  $1/T$  should be a straight line. The values of  $Y$  and  $Z$  were calculated for each temperature. It can be seen from Fig. 2, the plot of  $Y$  vs  $1/T$  the data gives a good linear fit below 270 K. The values of  $Z$  versus  $1/T$  are plotted in Fig 3 according to theory, this plot is expected to be a straight line passing through origin. This is the case only in the temperature region below 270 K in our sample. It is clear that the data give good fit to PF conduction. The deviation of the experimental data from the low temperature line at 270 K is similar to that in Fig.2, and it indicates a change in the transport mechanism in the about of this characteristic temperature.

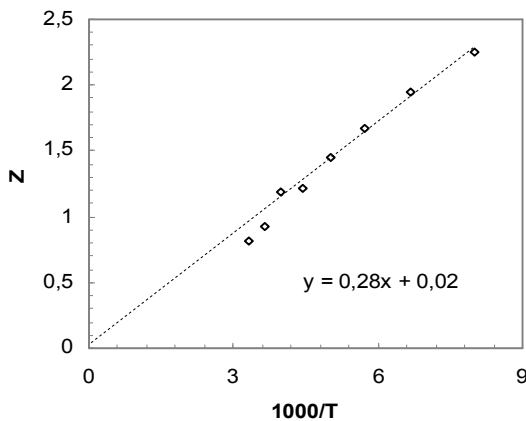


Fig. 2.  $Z$  parameter versus  $1/T$ .

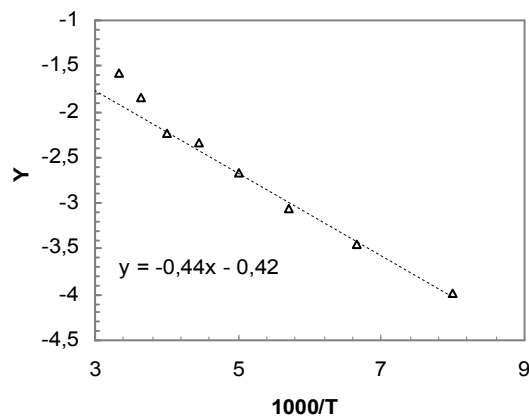


Fig. 3.  $Y$  parameter versus  $1/T$ .

The  $I$ - $V$  characteristics of the metal-GaP contacts have been measured in the temperature range of 125-300 K. The transport mechanism has been investigated in the measured temperature range. Transport mechanism is identified as the Poole Frenkel type in lower temperature range. The transport mechanism changes at a characteristics temperature of about 270 K.

*This work was supported by Gazi University Scientific Research Project (BAP) FEF 05/2009-17.*

1. Hussain A., Akhter P., Bhatti A.S., Shah A.A., Bilal S. // Vacuum – 2010. – 84. – 975.
2. Janardhanam V., Lee H.K., Shim K.H., Hong H.B., Lee S.H., Ahn K.S., Choi C.J. // J. of Alloy. Comp. – 2010. – 146.
3. Mathew X., Enriquez J.P. et al. // Solar Energy Mater. Solar Cell. –2000. – 63. – 355
4. Rakhshani A.E., Makdisi Y., Mathew X // J. of Materials Science Materials in Electronics. – 1997. – 8. – 207

## SOI MOS-transistor with the parted gate

Dovhij V.V.

*Vasyl Stepanyk Precarpatian National University, Ivano-Frankivsk, Ukraine*

The most widespread types of MOS-transistors with silicon-on-insulator structure (SOI) contain the many parasitic effects, one of which bipolar, that present in n-channels SOI MOS-transistors. Reason of this effect is an accumulation of positive charges in a under channel area as a result of impact ionization. Depending on SOI MOS device structures in one cases these effects must be removed, and in other they can be used for the improvement of devices descriptions [1].

In this paper is showed the SOI MOS-transistor construction with the parted gate and contact to the under channel area. In this transistor a gate consists of two parts, between them is a layer of metal which is directly deposited on the buried oxide. Layouts and structure of this transistor is represented on fig.1.

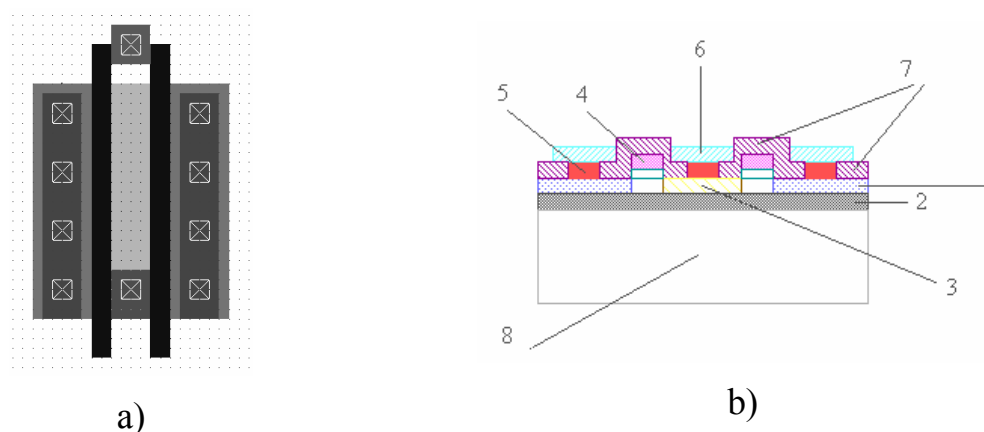


Fig. 1. SOI MOS-transistor with the parted gate: a) layouts; b) cross section: 1 – n+ area; 2 – buried oxide; 3 – metal layer, deposited on buried oxide; 4 – gate; 5 – contact area; 6 – metal layer; 7 – dielectric layer; 8 – Si substrate.

The offered construction of matrix SOI MOS-transistors with a double control have advantage at creating of different devises, such as signal generators, input and output cascades, logical elements. For example, the results of researches output cascade, made on this technology, showed substantially higher speed of switching at simultaneous diminishing of consumable power. Consequently this technology it is enough perspective, have practical application in modern microelectronics.

1. Druzhynin A.A., Kohut I.T., Kenyo H.V. Features of SOI MOS-transistors with a matrix configuration of elements // Optoelectronics and semiconductor technology. – 1994. – Issue 28. – P. 71-74.

## New approaches to measuring of thermoelectric parameters of semiconductor materials

Freik D.M., Terletskyi A.I., Zapukhlyak R.I., Dykun N.I.

*Vasyl Stefanyk Precarpathian National University*

The study of thermoelectric properties of semiconductor materials requires the adequate measuring techniques of thermoelectric parameters. The various measuring methods and their modifications were described in literature elsewhere, however majority from them allows to measure only certain parameters of samples. Such methods, which in the same experiments gives possibility to measure all the spectrum of thermal and electrical parameters of material, deserves special attention. Measuring of thermal conductivity of semiconductor material is the most complicated problem, which requires taking into consideration many physical and technological factors.

It was proposed the theory of stationary absolute measuring method of solid thermal conductivity, which also enables to get in the same experiment additional information about electrical conductivity and thermoelectric power. This method was developed for investigation rather small samples (10 mm × Ø 5 mm) from materials with low thermal conductivity.

It was developed the experimental cell for measuring solid thermal conductivity in the temperature range from a room up to 500 °C, which additionally allows to determine electrical conductivity and thermoelectric power of samples.

Moreover it was indicated on the construction features of measuring cell, which are very important for the high precision of experimental results.

From the results of measuring, the thermal conductivity of samples is calculated according to expression:

$$\chi = \left( \frac{I_{\text{eH}} \cdot U_{\text{eH}}}{T'_{\text{eH}} - T_{\text{eH}}} - \alpha \chi_{\text{is}} \right) \frac{l}{S},$$

where,  $I_{\text{eH}}$ ,  $U_{\text{eH}}$  are the current and voltage which are given on an internal heater;  $T_{\text{eH}}$  - temperature of internal heater in the thermal equilibrium after turning on of external heater;  $T'_{\text{eH}}$  - temperature of internal heater in the new thermal equilibrium after turning on of internal heater;  $l$ ,  $S$  - length and cross-section area of the sample, respectively;  $\alpha \chi_{\text{is}}$  - coefficient, which depends on the construction features of the cell and can be determined using well-known thermal conductivity materials.

## Solar CdSe/ZnSe cells

Gubanova A., Kysselyuk M., Kryskov Ts., Rachkovsky O., Yeremchuk V.

*Ivan Ohienko Kamianets-Podilsky national University, Kamianets-Podilsky, Ukraine*

The active searches of materials for the most effective photovoltaic elements are continuing nowadays. Thin-film Solar cells are important for a large-scale production. They attract relatively a subzero cost (comparatively with single-crystal analogues) and open possibilities of creation of the effective, environmentally sound Solar modules with large area, which will be able to satisfy market necessities.

Cadmium selenide (CdSe) with the bandgap of 1,8 eV was selected for an absorptive layer and zinc selenide (ZnSe) with the bandgap of 2,7 eV was as a high band semiconductor.

The technology of vacuum thermal deposition which was carried out at the temperature of the all-epitaxial besieging was used for growth of layers of Solar cells. In quality lining molybdenum foil which served as a bottom contact for a Solar cell was used.

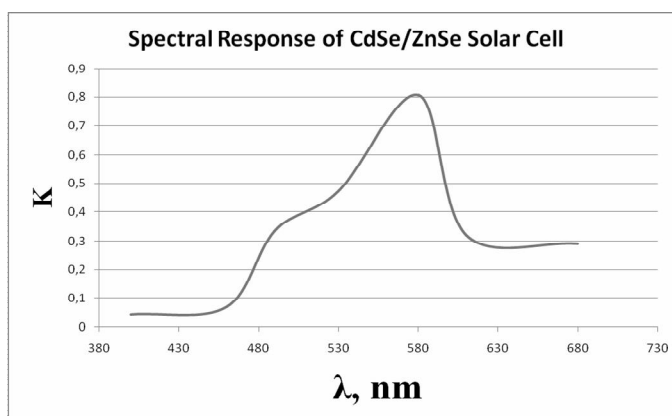
An overhead contact was made rider.

As a source of light for the irradiation of the investigated standard was used lamp of cold luminescence (part of infra-red area was minimized in a spectrum falling like a light stream). Power of radiation presented 2 W. On such conditions the current of short circuit arrived at the value of 78  $\mu\text{A}/\text{cm}^2$ . Maximal tension 0,15 V. Resistance of p-n transition is equal 274 k $\Omega$ .

Volt-current description coincides with the results of numerous researches in the field of Solar energy.

Continuing work can be directed on the creation of overhead semiluent metallic contact (gold, silver and others like that) for the improvement of electric contact. It is necessary to investigate dependence of indexes of sun element on the basis of the chosen connections from the thickness of the besieged films.

1. Martin A. Green, Keith Emery, David L. King, Yoshihiro Hisikawa and Wilhelm Warta. Solar Cell Efficiency Tables // Progress in Photovoltaics: Research and Applications. – 2006. - № 14. –P. 45-51.
2. Allen Rothwarf. Criteria for the design of high efficiency thin film solar cells: Theory and practice // Solar Cells, Volume 21, Issues 1-4, June-August. – 1987. –P. 1-14.



## Kinetics investigation of the semiconductor gas sensor based on heterojunction SnO<sub>2</sub>-Si(p)

Il'chenko V.V., Kravchenko O.I., Telega V.M., Shyshkin M.O.

*The Kiev National University of Taras Shevchenko, Kiev, Ukraine*

Gas sensor was used in the experiment is based on p - n-junction: tin dioxide is a semiconductor with electronic conductivity; silicon is a semiconductor with hole conductivity. SnO<sub>2</sub> film applied on the silicon plate thickness of 0.3 microns in the form of a grid 7x7 by magnetron sputtering. Aluminum and nickel contacts were used as Ohmic contacts. For obtaining nickel contacts on tin dioxide used method of magnetron sputtering. For research of response of gas sensor was used 100% air humidity and dried air environments at the temperature 18 ° C.

Before the point of time  $t=t_1$  rectangular pulses with the period of 10 seconds (duration of 2 seconds) and amplitude -2V are put to the sensor. At the point of time  $t=t_1$  dc voltage -2V is put to the sensor and in the result molecules are collected at the surface of heterojunction. This process produces an increase of sensor current. We have identified approximation sum of 2 exponentials:

$$f(t) = A \left[ 1 - \exp\left(-\frac{t}{\tau_1}\right) \right] + B \left[ 1 - \exp\left(-\frac{t}{\tau_2}\right) \right] + I_1, \tau_2 \gg \tau_1$$

At the point of time  $t=t_2$  sensor should almost completely saturate so  $t_2 - t_1 \cong (2 \div 3)\tau_2$ . Since that point of time rectangular pulses are put on a sensor, envelope curve represents sensor purification from adsorbate and should be approximated with the same formula.

Humid air.

Adsorption:  $\tau_1=11.7s$      $\tau_2=164s$

Desorption:  $\tau_1=15.7s$      $\tau_2=183s$

Dru air.

Adsorption:     $\tau_1=36s$      $\tau_2=619s$

Desorption:     $\tau_1=20s$      $\tau_2=237s$

Probably availability of 2 parallel processes with different time constants may be explained by porous structure of sputtered tin oxide. Some of dipoles fall on sensor surface, another ones percolate inside the sensor due its porous structure. Obviously, in the first case the characteristic times of adsorption and desorption are smaller than one associated with diffusion.

## Porous Bragg mirror as rear reflector for multi-Si solar cells

Ivanov I.<sup>1,2</sup>, Nychyporuk T.<sup>2</sup>, Skryshevsky V.<sup>1</sup>, Makarov A.<sup>3</sup>

<sup>1</sup>National Taras Shevchenko University of Kyiv, Ukraine

<sup>2</sup>Institut National des Sciences, Lyon, France

<sup>3</sup>V. Lashkaryov Institute of Semiconductor Physics NAS Ukraine, Kyiv, Ukraine

Absorption of IR range sunlight in the Si-based solar cells (SC) with standard for solar cell industry thickness of 200 μm is rather small after single-pass through SC. Absorption can be improved by increasing of light path in the bulk of SC. Increasing of light path without increasing of geometrical thickness of SC can be obtained with forming of Bragg mirror (BM) on the rear side of SC (Fig. 1a). One of the ways for BM forming on the rear side of SC is forming of porous silicon (PS) layers or porous TiO<sub>2</sub> nanoparticles layers with high and low porosity. Refractive index of PS covers continuously the range between that of c-Si and air and can be controlled with current density, HF concentration, temperature, wafer resistivity. Refractive index of TiO<sub>2</sub> nanoparticles layers can be controlled using different diameters nanoparticles.

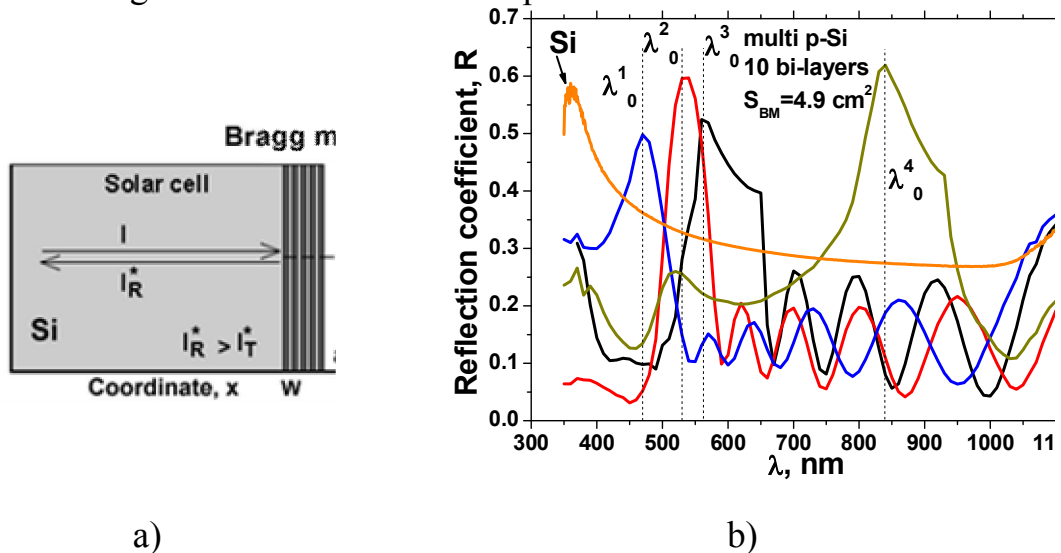


Fig. 1 a) Schematic representation of paths of infrared light with intensity  $I$  inside SC with BM,  $W$  is SC thickness; b) reflection spectrum of porous silicon BM on the multicrystalline p-type wafer ( $\lambda_0^1 = 470 \text{ nm}$ ,  $\lambda_0^2 = 530 \text{ nm}$ ,  $\lambda_0^3 = 562 \text{ nm}$ ,  $\lambda_0^4 = 840 \text{ nm}$ ).

BM was fabricated by electrochemical etching of p-type  $\langle 100 \rangle$  multi-Si wafer in HF/ethanol solution (3:1) at room temperature. PS layers of BM with low and high porosity had reflection indexes  $n_H = 2.2$  and  $n_L = 1.7$ . The maximum reflection coefficient  $R_{\max}$  of 10-bilayer multi-Si based Bragg mirror for  $\lambda_0 = 840 \text{ nm}$  was 61%. Bragg peak width at  $0.5 \cdot R_{\max}$  was 183 nm (Fig. 1b).

*This work practically supported by State Committee on Science, Innovation and Information of Ukraine.*

## Mechanical and adhesive parameters in metal condensate – single crystal silicon system

Juzevych V.M.<sup>1</sup>, Koman B.P.<sup>2</sup>

<sup>1</sup>*G. Karpenko Physicomechanical Institute, Nat. Acad. Sci. of Ukraine, Lviv, Ukraine*

<sup>2</sup>*Ivan Franko Lviv National University, faculty of electronics, Lviv, Ukraine*

Using a console method there was experimentally studied the kinetics of forming the internal mechanical stresses  $\sigma(d)$  in thin films of chromium, copper, gold and aluminium on silicon monocrystalline substrates at different speeds of deposition. The energetic and adhesion parameters have been studied in nanolayers of chromium, copper, gold and aluminium using macroscopic methods in physics. Specific numerical values have been obtained for interphase energy, interphase stretching, adhesion work, interphase charge and energetic characteristic of interphase layer – i.e. the energy of adhesive bonds, which is larger compared with the interphase energy. The regularities of the formation of mechanical stresses at maximum level have been determined. The relationship between the contact and contact – boundary problem has been formulated in order to determine the distribution of free electrical charges in metal and in semiconductor as well as the corresponding mechanical stresses based on the thermodynamic approach to the study of mechanoelectric processes in nanolayers at the interface of metal – semiconductor interface.

For the Si – Me (Cr, Cu, Au, Al), Ge – Me and Ni – Me systems, specific numerical values have been obtained for interphase stress, interphase energy, work of adhesion and for the new energetic characteristic of interphase layer, i.e., the energy of adhesive bonds  $W_{add}$ , which is larger than the interphase energy  $W_m$ .

The energy of adhesive bonds  $W_{add}$  in the Si – Me systems has been determined to be higher than in Ge – Me systems. However, this value is much lower than for the two interacting metals, particularly for Ni – Me.

The interphase charge  $Q_m$  in the Si – Me and Ge – Me systems has been determined not to be subjected to essential changes. It is assumed that self-organizing role of the substrate at the formation of nanocondensates is determined by the value of the difference in electronegativeness of the substrate and condensate materials.

## Layouts features of SOI CMOS gate matrix arrays

Kogut I.T., Dovhij V.V.

*Vasyl Stepanyuk Precarpatian National University, Ivano-Frankivsk, Ukraine*

The major element of gate matrix arrays is a base cell which determines density of elements placing on a chip, features of tracing, degree of elements uses of gate matrix array, electric descriptions, etc. In this paper is presented the research results of the base cell developed authors for SOI CMOS gate array with silicon-on-insulator structure (SOI).

The developed base cell can be applied in layouts planning and technology integrated circuits productions with regular architectures and integrated microsystems-on-chip (SoC) based on SOI CMOS gate array. New in this base cell is its organization with a double location consistently united 3 p- and 3 n-channel transistors and 1 p- and 1 n-channel transistors and by introduction of complete dielectric isolation of such SOI MOS-transistor structures between itself, which allows creating matrices on principle «sea of valves» or «sea of transistors». Advantage of such base cell is the use possibility drain-source area of transistors as connecting elements. The electrical schemes of base cell and layouts examples for logical elements 3OR-NOT and inverter is represented on fig. 1.

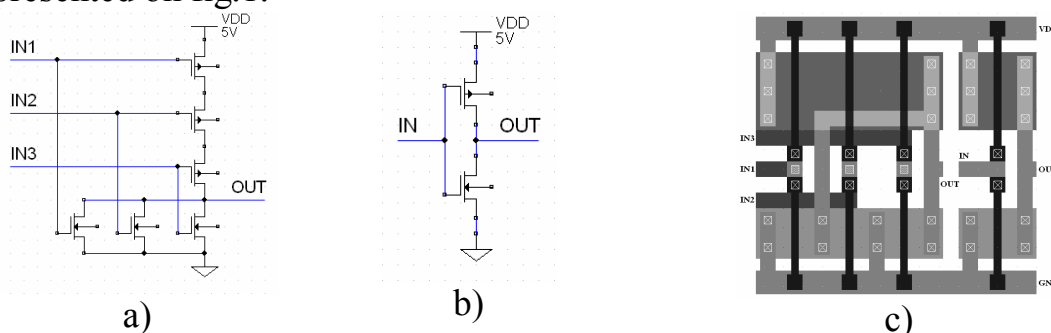


Fig. 1. Electrical schemes and layouts of logic elements 3OR-NOT and inverter with use of offered cell: a) 3OR-NOT element; b) inverter; c) layouts of a) and b) elements.

The results of researches and designs showed that the gate array on the basis of the developed cell have improving frequency and electric descriptions, high density of elements placing on a chip, high coefficient of the transistors uses and improve commutations possibilities.

Such gate array will find application in industrial and in scientifically-experimental researches from optimization of existing and creation of new integrated circuit, and as well as SoC, laboratories-on-chip (LoC) based on SOI CMOS matrix array.

1. Kogut I.T. Elements of microsystems at a basic matrix crystal of the structure of 'silicon-on-insulator' // Dis. of Doctor of Technics degree of NU "Lviv Polytechnic" – 2010.

## **Optical-electronic transducers on the basis of thin film photopiroelectrical sensors**

Kravtsiv M.M., Boychuk V.I., Virt I.S., Medvid M.A.

*Drohobych Ivan Franko State Pedagogical University, Drohobych, Ukraine*

In this work the results of investigation of the optical-electronic transducers on the basis of thin film photopiroelectrical sensors are reported.

The kind of matter exists in which the essential piroeffect, independent on the external electrical field and connected with molecules' structure, is observed. Besides, these materials possess photoconductivity with spectral distribution overlapping with piroeffect in the visible and infrared range.

The organic matter thin films present themselves a conglomerate of the very dispersive single crystals oriented onto the substrate in such way that spontaneous polarization of the whole conglomerate of crystals is directed along normal to the substrate and is different on zero and/or is created upon irradiation. Piroactivity of the films examined at the room temperature is found to be time stable.

By radiation treatment of the photosensitive piroelectric by irradiation flow in the wavelength range resulting in simultaneous photoconductivity and piroeffect, the non-equilibrium carriers at the existence of barrier contacts and local centers upon piroelectrical field create a photoelectric state.

This fact at the proper frequency modulation or spasmodic irradiation from the overlapping spectra range gives possibility to form non-equilibrium carriers which are shifted upon alternating piroelectric field and, being trapped by local levels, create inhomogeneous distribution resulting in internal electrical field. In each point of photopiroelectric the value of field will be determined by exposition of the image and impact of the piroelectrical effect.

By creating the inhomogeneous distribution of photopotential in the photopiroelectric, one can convert the image into the electrical signal after some time using a scanning beam in the fundamental or infrared absorption range.

The time of the relief invisible image in the form of electrical potential and the time its calculation are determined as parameters of the local centers as well as the piroelectrical parameters.

The existence of piroeffect along with photoelectric state discovers a new possibility for practical application of the organic films in the optical memory elements, transducers of optical signal into electrical one, modulators and amplifiers of electrical signals.

## Modified polypyrrole films for determination of aliphatic alcohols in water solutions

Kukla O.L.<sup>1</sup>, Mamykin A.V.<sup>1</sup>, Kurys Ya.I.<sup>2</sup>

<sup>1</sup>*V.E. Lashkarev Institute of Semiconductor Physics of NAS of Ukraine, Kyiv, Ukraine*

<sup>2</sup>*L.V. Pisarzhevski Institute of Physical Chemistry of NAS of Ukraine, Kyiv, Ukraine*

Process of electrochemical obtaining of electroconducting polymers (ECP) in presence of alcohols can be considered as molecular imprinting, where the molecules of alcohol serve as molecules - templates. Starting from the concept of influence of template on the structure of the formed polymer, one can suggest that the films obtaining in such conditions should have a selective sensitivity to the corresponding alcohol. As a functional monomer we used the pyrrole because of its ability to form high stable polymeric films. The synthesis of polypyrrole (PP) films was performed in a 3-electrode undivided cell, a system of gold raster microelectrodes on glass-ceramic substrate was used as the working electrode. Electropolymerization was conducted in the cycling potential regime in the range  $-200 \div 800$  mV with the scanning rate of 50 mV/s in electrolyte, containing 50 mM pyrrole in mixture of 4 ml 0.1 M KCl and 1 ml of isopropanol (using as template).

Measurements of the PP films were conducted in water solutions of different alcohols. Influence of analytes (metanol, ethanol, isopropanol, butanol in different concentrations) was registered as the relative change of current  $\Delta I/I_0$  through a polymeric film.

It was shown that in the range of volume concentrations of alcohols 100  $\div$  5000 ppm the PP films, modified by isopropanol, are sensitive to ethanol, isopropanol and butanol (in contrast to the unmodified films). The response to isopropanol appeared to be the highest and the concentration dependence in the range of 100-2000 ppm makes up 0.3 % of relative conductivity change of the film on each 100 ppm, for ethanol and butanol they are 0.1 % and 0.15 % accordingly. In the range 2000-5000 ppm the responses on ethanol, isopropanol and butanol are practically identical with concentration dependence of about 0.15 % on 100 ppm. At the concentrations of alcohols more than 3000 ppm a saturation of film responses was observed. The lower threshold of sensitivity to the alcohols was limited by noise of transducer base line and makes up for isopropanol near to 100 ppm.

The results obtained show a potentiality for creation of sensor elements based on the modified ECP films that will be selective to define substances in water as well as for creation of some type of electronic tongue based on the array of such films.

## Interference calixarene films as sensitive elements for “optoelectronic nose”

Kukla O.L., Tzyrkunov Yu.A., Matvyenko L.M., Vahula O.O., Fedchenko O.M.

*V.E. Lashkaryov Institute of Semiconductor Physics of NAS of Ukraine,  
Kyiv, Ukraine*

The problem of creation of “optoelectronic nose” is very actual now because of a lot of tasks on the control of various gaseous compounds in the areas of ecology, medicine, biotechnology, food production etc.

As sensitive elements for developed by us “optoelectronic nose” usually served interference calixarene films obtained by thermal vacuum evaporation. Under influence of analyzed gaseous matters the films change optical parameters (thickness and refraction index) that causes change of their color. At the same time the calixarene films of different types possess some different sensitivity to gaseous analytes that allows to realize a principle of "electronic nose" with recognition of separate analytes and gas mixtures.

The basic drawback of a vacuum obtaining of sensitive films are thermal decompositions of calixarene molecules, that does not guarantee the obtaining of films that are identical to structure of initial materials. In addition, such films possess a bad adhesion to substrates and low stability to analytes that diminishes possibilities of sensor reusing.

As an alternative to the above method the centrifuge coating of thin calixarene films was developed. Coatication was conducted on polished silicon substrates from solution, containing mixture of calixarene and binding polymer. Dimethylformamide, acetone and chloroform were served as solvents that provided the centrifuge coating process with required viscosity and speed of evaporation on air. The films of tertbutylcalixarenes C[4]A, C[5]A, C[6]A, C[8]A and calix[4]Ad, calix[6]A with the melting temperature of 300-400<sup>0</sup>C, and row of low temperature calixarenes with the melting temperature of 100-160<sup>0</sup>C were investigated. As connective compounds for films were used photosensitive polymers, it is related to possibility of photolithography for forming of sensor elements of certain type and size.

The measurement results showed that the obtaining interference films possess more high sensitivity to analytes as ones obtained by vacuum evaporation. Besides these films assume heat treatment that considerably improves adhesion without the decrease of sensitivity, good moisture resistance and stability of films to frequent influence of analytes. The possibility of using of the developed technology for production of interference sensor elements for “optoelectronic nose” was shown.

## Dielectric properties of membranous superionic capacitor

Mikhailova A., Motsar A.

*Saratov State Technical University, Saratov, Russia*

High volume properties of systems with sulfosalicylic acid (SSA) and its complexes with a number of rare earth elements and transition metals studied make it possible to use them to create ultra-capacitors (super capacitor).

Has been studied insulating state of super ionic conductors based on polymeric derivatives of sulfonic acids.

The study was conducted on a precision component analyzer WK6430B for the system Ti/SE (SSA). Operating Voltage – 0.5 V, current frequency of 1 Hz to 1 MHz. Measurements were made at  $T = 293$  K,  $P = 101$  kPa.

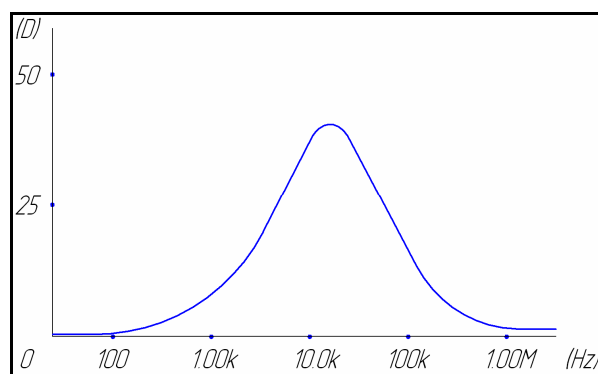


Fig. 1 Frequency dependence of dielectric loss factor of the system Ti/SE (SSA).

The test samples showed that with increasing current frequency dielectric loss (D) begins to rise and reaches its maximum at the current frequency of 25.6 kHz. This is because the material of the samples has a movable component, so that scattering occurs, the charge carriers. That is, at the direction of motion of electric charges in an external electric field, carriers, they acquire from the electric field energy. This energy is wasted in "collisions" carrier and is converted into heat energy. As the frequency of the current value of the dielectric loss factor decreases. This is due to the fact that at high frequency oscillatory movement of charge carriers become smaller in the space of a polymeric conductor and the number of "collisions" of carriers is reduced.

1. Bukun N.G., Rodionov V.V., Mikhailova A.M. // Solid State Ionics – 2000. – 136-137. – P. 279-284.
2. RF Patent № 2400294. Proton-conducting polymer composite. Mikhailova A.M., Kolokolova E.V., Nikitina L.V. 27.09.2010.

## **Self-assembling of low-dimensional Ti systems under conditions of quasi-equilibrium condensation**

Mokrenko A.A.

*Sumy State University, Sumy, Ukraine*

Formation of low-dimensional systems with required characteristics is important task of nanotechnologies. Condensation under conditions near the thermodynamics equilibrium are of great interest due to ability of extreme minimization of free energy of condensate structural fragments and as a result the whole system. With this aim the series of experiments were made on forming of condensates under conditions of quasi-equilibrium condensation at high stationary of technological process. The aim of work is to reveal structure formation mechanisms and form of metal condensates at deposition of low fluxes of ionized substance.

Low-dimensional systems have been produced by ion-plasmas sputtering system, which consists of planar DC magnetron. As the investigated substance titan is chosen. Condensates were obtained on fresh (001) KCl flats and on the glass substrates. It is necessary to emphasize that special attention was devoted to purification of working gas in the vacuum chamber. Due to using of special method of the gas (Ar) purification the pressure of all chemically active gases was less than  $7 \cdot 10^{-7}$  Pa. The power of gas discharge was 6 W, pressure of Ar changed from 2.8 to 5.5 Pa, and temperature of substrates was from 350 to 355 K. It allowed to condensate stationary low fluxes of sputtered substance.

Investigation of structure and phase composition of condensates at the different stages of their forming was made using SEM and TEM, high-energy electron diffraction and X-ray microanalysis. It has been found experimentally that at low power of discharge, consequently, and the low deposited fluxes, on (001) KCl flats there is a transition from polycrystalline films to forming of systems of separate islands on the initial stage of deposition (300 s). During long-term condensation (8 h) and low condensates fluxes morphology of growth surface undergoes changes consisting in a gradual transition from globular to the crystalline structures. In the case of condensation on glass substrates only globular self-similar structures are formed at same conditions.

Nucleation of condensate on crystalline substrates take place only on the active centers of substrate and allows realizing wide spectrum of low-dimension systems. At same conditions nucleation on the glass can take place on the borders of contact of nearby clusters. Thus, conditions of quasi-equilibrium condensation provide atom-by-atom condensate building, that additionally determined by the local redistribution of the condensed fluxes in the system low temperature plasma - condensate. Transitions from globular structure to the system of separate crystals are result of the system energy minimization.

## The In/p-Cd<sub>1-x</sub>Mn<sub>x</sub>Te Schottky barriers fabrication and properties

Petrus' R., Kusnezh V.

*Physics Department of Lviv Polytechnic National University, Lviv, Ukraine*

The In/p-Cd<sub>1-x</sub>Mn<sub>x</sub>Te Schottky barriers (SB) on Cd<sub>1-x</sub>Mn<sub>x</sub>Te solid solutions single crystals were fabricated by the thermal deposition of indium (In) on a smooth surface of freshly cleaved crystal wafer. The temperature of crystal surface during In film (thickness  $d \approx 0,2-0,4$  microns) deposition in vacuum ( $P \sim 10^{-4}$  Pa) does not exceed the room temperature. Under these conditions of In deposition the elemental composition of Cd<sub>1-x</sub>Mn<sub>x</sub>Te solid solution remains unchanged, therefore the SB properties are determined by parameters of contacting phases.

The current-voltage characteristics of the In/p-Cd<sub>1-x</sub>Mn<sub>x</sub>Te SB show the rectification. Rectification coefficient  $K$  (calculated from the ratio between direct and reverse currents at  $U = 2$  V) in these structures has maximum value  $2 \cdot 10^5$  at Mn content  $x = 0$  and decreases to  $10^2$  with increase of Mn content in solid solution to  $x = 0,35$ . Forward direction corresponds to negative polarity of external bias on In barrier contact for all investigated Mn contents. A photovoltaic (PV) effect occurs during illumination of these structures from the side of In barrier contact. The sign of photovoltage of these structures always corresponds to positive polarity on the Cd<sub>1-x</sub>Mn<sub>x</sub>Te wafer, that coincides with direction of rectification determined from current-voltage characteristics. The spectral dependence of relative quantum efficiency of photoconversion  $\eta = f(h\nu)$  (ratio of short-circuit current to the incident photons number) for In/p-Cd<sub>1-x</sub>Mn<sub>x</sub>Te SB with different Mn content ( $x = 0-0,7$ ) was investigated. The absolute maximum of  $\eta(h\nu)$  spectra shifts in the shortwave spectral region with increase of Mn content, which reduces the halfwidth value of  $\eta(h\nu)$  spectra. Thus, the Mn content in Cd<sub>1-x</sub>Mn<sub>x</sub>Te solid solution controls the length of the high photosensitivity spectral range in the fabricated In/p-Cd<sub>1-x</sub>Mn<sub>x</sub>Te surface-barrier structures.

## **SnO<sub>2</sub> nanowires for gas sensing application**

Rednyk A., Haviar S., Vaclavu M., Matolin V.

*Charles University in Prague, Faculty of Mathematics and Physics, Department of Surface and Plasma Science, Prague, Czech Republic*

Metal oxides in the form of nanowires with several nanometers or tens of nanometers in diameter are promising materials for gas sensors. Reducing transverse dimension of sensors leads to new selective properties, i.e. sensitivity for special gases as CO and NO<sub>x</sub>.

The sensor systems were prepared by means of the electron beam lithography and rf sputtering. Morphology of the prepared nanostructures was checked by Secondary Electron Microscope (SEM) and Atomic Force Microscope (AFM). Chemical composition was investigated using X-ray Photoelectron Spectroscopy (XPS). The sensing properties of sensor devices were tested by using a chip testing system based on the four probe measurements. Digitally controlled gas handling system permits to test the devices at gas concentrations below ppm at different working temperatures. Properties of gas sensors will be correlated with model studies of gas interaction with the sensing surfaces.

## SAXS investigation of submicropores in electrochemical capacitors MnO<sub>2</sub> films

Skatkov L.<sup>1</sup>, Gomozov V.<sup>2</sup>, Deribo S.<sup>3</sup>

<sup>1</sup>PCB "Argo", Beer Sheva, Israel

<sup>2,3</sup>NTU "KhPI", Kharkov, Ukraine

MnO<sub>2</sub> porous semiconductor films have been prepared by thermal deposition of Mn(NO<sub>3</sub>)<sub>2</sub> are important materials for application in the electronics engineering as electrochemical capacitor metal-oxide systems. For practical application of MnO<sub>2</sub> in electro chemistry capacitors the characteristics of their submicropores (SMPs) are critically important.

In the present communication the morphology, concentration and size distribution of MnO<sub>2</sub> were investigated by small-angle X-ray scattering (SAXS). The observed SMPs were in the range  $0,1 \leq 2R \leq 100 \text{ nm}$ . We analyzed the following quantities: type of angular distribution; asymptotics and the integral parameters of the dispersion indices of SAXS related to the typical size  $l_n$ ; the typical volume  $V_n$  and the typical SMP shadow area  $f_n$ . The mean square size of the SMP was determined by the tangent technique suggested in [1].

Since the size distribution appeared to be polymodal, we classified the pores into four groups, according to their size:  $2R \leq 1 \text{ nm}$ ;  $1 \text{ nm} \leq 2R \leq 4 \text{ nm}$ ;  $4 \text{ nm} \leq 2R \leq 8 \text{ nm}$ ;  $8 \text{ nm} \leq 2R \leq 50 \text{ nm}$ .

The absence of noticeable anisotropy of SAXS shows the character of the dispersion indices which asymptotically obey the Porod law  $I(s) \sim s^{-4}$  ( where  $I(s)$  is the Intensity of X-ray and  $s$  is diffraction vector ). One can assume that scattering SMPs have no domineering orientation, and they are more equiaxial that macro- and micropores.

However, some difference in the integral parameters  $l_n = 5 \text{ nm}$ ;  $V_n^{1/3} = 5 \text{ nm}$  and  $f = 13 \text{ nm}$  allows us to conclude that SMP axes are quite equal. Absolute values of these are close to the values calculated by the Guinier technique based on another way of averaging pore sizes. This confirms that most SMPs have more or less equal axes, unlike macropores.

It should be noticed that, unlike macro- and micropores, some equiaxial SMPs are closed and filled with gas. Their formation results from both clustering oxygen vacancies shaped in MnO<sub>2</sub> films and fact that solidifying rate during the pyrolysis largely exceeds the the gas emission rate. A part of the emitted gas is therefore trapped in the SMPs.

1. Guinier A. and Fourent C. Small-angle scattering X-rays // Wiley, New York –London. – 1990. – P. 199.

## Structure and electrical conductivity of microcrystalline films Re-Me-Ge

Yatsyshyn B.P.<sup>1</sup>, Yatsyshyn S.P.<sup>2</sup>

<sup>1</sup>*Lviv commercial academy, Lviv, Ukraine*

<sup>2</sup>*National University "Lviv Polytechnic", Lviv, Ukraine*

The forming of structure of microcrystalline films from amorphous condensates has the features, which are bound with technology of receiving and thermodynamic conditions deposition. Structure and the magnetic properties of such materials determine parameters of process of a carrier transport in most cases, which contrast them to massive analogs.

It is installed that microcrystalline condensates, obtained by annealing from amorphous binary compounds  $\text{Fe}_{60}\text{Ge}_{40}$  and  $\text{Fe}_{50}\text{Ge}_{50}$  thin films, also as ternary compounds  $\text{RE}_{27}\text{Fe}_{28}\text{Ge}_{45}$  and  $\text{RE}_{25}\text{Fe}_{25}\text{Ge}_{50}$  (where RE - Rare Earth metal: Sc, La, Y) condensed in vacuum by discrete method condensation of compounds or coordinated evaporation components at large deposition rates ( $v_g = 25 - 28$  nm/s) have small grained crystalline structure. Such films were characterized by the reduced resistivity compare with the amorphous thin films. The ratio of values  $\rho_{\text{amorphous}}/\rho_{\text{microcrystalline}}$  varied from 7,0 for condensates  $\text{Fe}_{50}\text{Ge}_{50}$  to 4,5 for  $\text{Sc}_{25}\text{Fe}_{25}\text{Ge}_{50}$  and  $\text{La}_{25}\text{Fe}_{25}\text{Ge}_{50}$  films, which specifies a considerable residual disorder of films with rare-earth metals. A film obtained at small deposition rates ( $v_g = 5 - 7$  nm/s) and subsequently crystallized, had a large-grained structure. Besides this, there was an opportunity to fix intermediate state (between amorphous and crystalline phase, which we classified as a variety of nanocrystalline form) during crystallization such thin films.

The negligible deflection, which values depends on composition and width of a film, were detected at the analysis of a low-temperature electrical conductivity of crystalline thin film, close to the chemical formula  $\text{REFe}_6\text{Ge}_6$  and  $\text{REFeGe}_2$ . The calculation of a resistivity caused by phonon scattering has shown a deviation from experiment results. It is necessary in this connection, apparently, to take into account such contribution of resistivity caused by magnetic scattering, despite of unmanned f-orbits of RE-elements.

## About the existence of the optimum nano scale thickness of $\text{In}_2\text{O}_3$ films to the response of the gas sensitive heterostructure

Yushchenko A.V.<sup>1</sup>, Lendel V.V.<sup>2</sup>, Telega V.M.<sup>2</sup>, Punkovska C.O.<sup>1</sup>

<sup>1</sup>*Vinnitsa national technical university, Vinnitsa, Ukraine,*

<sup>2</sup>*Kiev University, Kiev, Ukraine*

**Motivation.** One of perspective ways of the creation of gas sensitive structure is the utilisation of heterostructures with nano scale adsorption layers [1]. However the reason of the formation of the response signal of such structure now is not enough investigated. The answer to a question about the correlation of heterostructures properties and properties of the nano scale adsorption- active layer allows making a conclusion about the influence of changes of adsorption-active layers parameters on the formation of current-voltage characteristics parameters of heterostructures [2]. In this work the results of the research of the current-voltage characteristic parameters of the heterostructure with nano scale superthin adsorption- active layers of  $\text{In}_2\text{O}_3$  are represented.

**Results and discussion** .The correlation between changes of the resistance of the superthin film adsorption- active layers and parameters of the current-voltage characteristics of heterostructures in the laboratory atmosphere and ammonia environment at 300 K is received. Relative change of the current through heterostructure (at the maximal change it) depend on the thickness of the adsorption layer and correlate with the maximal change of films resistance from the thickness at identical change of gas environment. The film thickness at which the maximal signal of the response for indium oxide - silicon is observed and indium oxide film on silicon lays about 8-11 nm. The received results allow assuming, that the mechanism of the formation of the response of the heterojunction at change of gas environment is caused changes of properties of the indium oxide film which forms heterojunction.

1. Chehun V., Gul R., Ilchenko L., Yushchenko A. Analysis of composition gas environment on the basis of analysis properties of the current-voltage characteristics of the nanostructure// Proceeding Book of the MICRO SYSTEM Technologies 2005. – Munich, – 2005. – P. 244-251.
2. Yushchenko A., Gel P., Shevchuk A., Thaychuk V. The influence of ammonia gas on the electrophysical properties of Al-p-Si structures with adsorption- active layer  $\text{In}_2\text{O}_3+5\%\text{Sn}$  by a thickness of 2 nm // Nauka I studia. - Przemysl. – 2008. – V.17, Fizyka. – P. 38-41.

ЗМІСТ

Секція 3

Фізико-хімічні властивості плівок та наноструктур

(усні доповіді)

Session 3

Physical-chemical properties of the films and nanostructure

(oral)

<b>Baskevich A.S., Bezpachenko A.V., Bulanyi M.F., Dyadenko A.I., Skuratovskaya O.V., Omelchuk A.R.</b> Photoluminescence of thin films of ZnO obtained from chelate compounds	9
<b>Bilogrodskyy Y.S., Shirinyan A.S., Wilde G.</b> Phase formation during temperature cycling of metal nanoparticles of different shapes	10
<b>Bratus' O., Evtukh A., Kizjak A.</b> Electron transport in nanocomposite SiO <sub>2</sub> (Si) films	11
<b>Budzulyak I.M., Gumenyuk L.M., Solovko Y.T., Ilnytsky R.V.</b> Influence of TiO <sub>2</sub> structure modifications on its sorption properties	12
<b>Busko T.O., Dmytrenko O.P., Kulish M.P., Vityuk N.V., Eremenko A.M.</b> Structural and optical properties of photocatalytic active TiO <sub>2</sub> /ZrO <sub>2</sub> /SiO <sub>2</sub> and TiO <sub>2</sub> /ZrO <sub>2</sub> /SiO <sub>2</sub> /Au films	13
<b>Danylenko M.I., Chernega S.M., Mameka N.O., Velychko A.</b> Structure and hardness of worn layer	14
<b>Dzumedzey R.O.</b> Scattering mechanisms of carriers in crystals doped PbTe: Ga (In, Tl)	15
<b>Dzundza B.S.</b> Sizes effects and electrical parameters in nanostructured films lead chalcogenides	16
<b>Fedorchenko M.I., Nakhodkin M.G.</b> The Sb adsorption on Si and Ge surfaces	17
<b>Gomza Yu.P., Klepko V.V.</b> X-rays diffractometry methods for polymer-containing nanocomposites investigation	18
<b>Gorbach T.Ya., Smertenko P.S.</b> The peculiarities of organic layers growth and electroconductivity in (vitamin B1 or analgine) – patterned silicon hybrids	20
<b>Gorichok I.V.</b> Quantum-chemical and thermodynamic calculation energies of vacancies formation in diamond-like semiconductors	21
<b>Gudyma Iu.V., Maksymov A.Iu.</b> The relaxation under thermal noise in the spin-crossover film	22
<b>Gurgula G.Ya.</b> Crystal defects and their complexes in crystals doped zinc chalcogenides	23
<b>Holomb R.</b> Synchrotron radiation photoelectron and surface-enhanced Raman spectroscopy of As <sub>2</sub> S <sub>3</sub> nanolayers under laser irradiation	24
<b>Ivanova S.E., Omelchenko S.A., Yurchenko N.P., Khmelenko O.V., Gorban' A.A., Lokot' S.A.</b> Production and physical properties of nanostructured films Co-Cu/Cu	25
<b>Kavetsky T.S.</b> Investigation of free volume in glasses, polymer and glass-polymer nanocomposite by positron annihilation technique	26
<b>Khottchenkova T., Malashkevich G., Kiisk V., Sildos I.</b> Synthesis and	27

characterization of Ce <sub>2</sub> O <sub>3</sub> nanoparticles in silica shell	
<b>Kolendovskiy M.D., Kryshstal A.P., Bogatyrenko S.I.</b> Melting and crystallization of Bi, Sn, In films in al matrix	28
<b>Kondrat O., Popovicha N., Holomba R., Mitsaa V., Petrachenkova O., Lyamaevb V., Tsudc N.</b> XPS investigation of laser-induced structural changes in As <sub>50</sub> Se <sub>50</sub> nanolayers	29
<b>Konopelnyk O.I., Aksimentyeva O.I., Demchenko P.Yu.</b> Influence of heavy metal ions on absorption spectra and structure of polyaminoarene films	30
<b>Korniyenko N., Kulish N., Dmytrenko O., Pavlenko O., Brusentsov V., Strelchuk V.</b> Collective chemical bonds of atoms of metals with fullerene molecules C60: theory and experiment	31
<b>Lavrynenko O.M., Natreba S.V., Prokopenko V.A.</b> The kinetic of the formation of magnetite and lepidocrocite on the steel surface depending on the pH values of dispersion medium	32
<b>Lepikh Ya.I., Ivanchenko I.A., Budienskaya L.M.</b> Heterostructure p (Pb <sub>1-x</sub> Sn <sub>x</sub> Se)-n (CdSe) films for far ir spectrum photodetectors	33
<b>Mitin V.F., Lazarov V.K., Lytvyn P.M., Kholevchuk V.V., Matveeva L.A., Kotenko I.E., Mitin V.V., Venger E.F.</b> Effect of deposition rate on properties of thin Ge films on GaAs	34
<b>Mudry S., Boruh I.</b> Contact angle changes at spreading of liquid metals on the surface of amorphous alloys	35
<b>Naseka V., Melnik V., Sarikov A., Oberemok O., Romanyuk B., Litovchenko V., Zlobin S., Popov V.</b> Influence of oxygen state in crystalline Si on the implanted Fe and Ti gettering by Al layer	36
<b>Naseka Yu.M., Rashkovetskyi L.V., Strilchuk O.M., Danilchenko B.O.</b> Defects creation in the LPE Cd <sub>1-x</sub> Zn <sub>x</sub> Te thin films under $\gamma$ -irradiation	37
<b>Nikolaeva A., Konopko L., Huber T., Para Gh.</b> Magnetothermopower and the Magnetoresistivity of Bi Nanowires in Weak and Strong Magnetic Fields	38
<b>Nyzhnykevych V.V., Galuschak M.O.</b> Scattering mechanisms in crystals PbSe p-type conductivity	39
<b>Nykyruy L.I., Mazur M.P.</b> Theoretical basis of calculation of thermoelectric parameters doped crystals of lead chalcogenides	40
<b>Ol'khovskaya S.I., Sipatov A.Yu., Rogacheva E.I.</b> Galvanomagnetic properties of PbSe<Cl> films	41
<b>Pavlenko O., Dmytrenko O., Kulish M., Brusentsov V., Rybiy V., Tkach V., Korniyenko M., Strilchuk V.</b> Structure and vibration properties of C60 with metals	42
<b>Peleshchak R.M., Mats'ko M.B., Odrehivs'ka O.O.</b> Mechanical descriptions of nanoscale tapes are with the structure of zinc-blende	43
<b>Pinchuk-Rugal' T.M., Nechyporenko O.S., Dmytrenko O.P., Kulish M.P., Grabovskyy Yu.E., Zabolotnyy M. A., Mamunya E.P., Levchenko V. V., Strelchuk V.V., Shlapatska V.V., Rugal' O.G.</b> Radiation modification of polyethylene composites of multi-walled carbon nanotubes under irradiation	44
<b>Pozdnyakov D., Borzdov A., Borzdov V.</b> Optimization of topological parameters of cold cathode based on ordered array of (9,9) carbon nanotubes with open ends	45

<b>Prokopiv V.V.</b> Thermodynamics of native point defects in crystals of compounds $A^{IV}B^{VI}$	46
<b>Prokopiv V.V.(Jr.)</b> Features equilibrium phase diagrams and defect subsystem of cadmium, lead and stanum tellurides	47
<b>Pysklynets U.M.</b> Constants of equilibrium of the quasichemical reactions of defects creation in CdTe.	48
<b>Romaka V.A., Stadnyk Yu., Budgerak S., Romaka L., Horyn A.</b> Crystal, electronic structures and properties of TiNiSn semiconductor	49
<b>Rubish V.M., Gera E.V., Pop M.M., Kozusenok O.V., Maryan V.M., Tarnaj A.A., Shtets P.P., Kyrylenko V.K., Durkot M.O.</b> Optical properties of As-Sb-S-I amorphous films	50
<b>Saliy Ya.P.</b> Formation of the subsystem defects in films of compounds $A^{IV}B^{VI}$	51
<b>Samsonenko S.N., Samsonenko N.D.</b> Models of electrical conductivity diamond materials	52
<b>Sarikov A.V.</b> Thermodynamic theory of the phase separation in the non stoichiometric silicon oxide films	53
<b>Shapoval P., Kusnezh V., Yatchyshyn J., Il'chuk G., Guminilovych R.</b> Physical properties of $CuInSe_{2x}S_{2(1-x)}$ thin films	54
<b>Sukhov R., Kryshtal A.P.</b> Size and temperature stability of liquid phase in Ge/Au layered film system	55
<b>Suschenko O.N., Slusar T.V., Legkova G.V., Grebenshikov D.V., Gordienko S.O., Ermolenko V.M.</b> Influence of technological parameters on characteristics of thin films	56
<b>Timukhin Ie.V., Zinchenko V.F., Mozkova O.V., Gorshtein B.A.</b> Optical and operational properties of coatings based on complex fluorides and composites	57
<b>Turovska L.V.</b> Defect formation processes of Pb-Sn-Te thermoelectric material	58
<b>Vaksman Yu.F., Nitsuk Yu.A., Yatsun V.V.,</b> Influence of Iron Impurities on Optical Properties of ZnSe:Fe Films and Layers	59
<b>Virt I.S., Rudyj I.O., Kurilo I.V., Lopatynskiy I.Ye., Dubov Yu.G.</b> Thermal conductivity measurement of $V_2VI_3$ thin films	60
<b>Yurchushyn I.K.</b> Thermoelectric properties of nanostructures compounds IV-VI	61
<b>Yurcovitch N.V, Mar'yan M.I.</b> Hyper sensibility of the dissipative structures and self-organizing processes in gradient non-crystalline materials based on glass-like $Ge_2S_3$	62
<b>Zhylynski V.V., Drozdovich V.B., Zharski I.M., Zhdanok S.A.</b> Electrochemical hydrogen sorption of carbon nanosize materials	63
<b>Zlomanov V.P., Freik N.D.</b> Crystal model of point defects and physical and chemical properties of semiconductor crystals of ZnS	64

### Секція 3

#### Фізико-хімічні властивості плівок та наноструктур.

(стендові доповіді)

#### Session 3

#### Physical-chemical properties of the films and nanostructure

(poster)

- Afanasieva T., Grinchuck O., Koval I., Nakhodkin M.** Molecular oxygen adsorption on  $\text{Ge}_x\text{Si}_{1-x}/\text{Si}(001)$  surface 66
- Afanasieva T.V., Koval I.F., Nakhodkin N.G.** Ab initio calculations of IR spectra in identification of stable and metastable structures of Bi addimer on the  $\text{Si}(001)2 \times 1$  67
- Ahiska R., Freik A., Gorichok I., Nykyruy L.** Growth and Characterization of Thermoelectric Lead Telluride 68
- Ananina O., Yanovsky O., Severina O.** Quantum-chemical study of  $\text{H}_2\text{O}$  molecules adsorption on the graphene 69
- Andreeva A.F., Kasumov A.M., Vlasenko N.A., Goncharenko Y.V.** The concentration and field dependence of the corrosion of steel thin films in acidic medium under a constant magnetic field 70
- Andreeva A.F., Kasumov A.M., Khrinovsky V.Z., Karavaeva V.M.** Spin polarization of electrons in nanoscale films of magnetite  $\text{Fe}_3\text{O}_4$  71
- Antonyuk V.G., Dovga I.V., Bordun I.O.** Cathodoluminescence of thin oxide films for full-coloured Flat Panel Displays (FPD) 72
- Balabai R., Chernikova H.** Quantum-chemical modeling of the oxidation process of ethylene glycol to glyoxal on nanocatalysts of the Cu group 73
- Balabai R., Pisklonov S.** Electronic properties of strained CdTe and ZnTe layers in heterostructure 74
- Balitska V.O., Shpotyuk O.I.** Kinetics of photo-induced transformations in amorphous  $\text{As}_2\text{S}_3$  thin films described in a framework of configuration-coordinate model 75
- Bashev V.F., Ivanov V.A., Litvin B.N., Sergeev G.A., Burdimova A.V., Gudzenko V.N.** Effect of cooling rate on mechanical properties and fine structure parameters of Pb-Sn-Ca alloys 76
- Basov A.G., Dekhtyaruk L.V., Chornous A.M., Shkurdoda Yu.O.** Investigation of electrophysical properties and magnetoresistance in three-layered film systems based on Al and Ni 77
- Beketov G.V., Rashkovetskyi L.V.** Auger spectroscopy of  $\text{Cd}_{1-x}\text{Zn}_x\text{Te}$  LPE-grown epilayers 78
- Bihun R.I., Buchkovska M.V., Stasyuk Z.V.** Quantum electron transport in ultra thin Cu films 79
- Bihun R.I., Stasyuk Z.V., Kravchenko O.E., Koltun N.S.** Size Effect in Optical Properties of Thin Metallic Au Films 80
- Bodiul P., Moloshnik E., Popov I., Curoshu N.** Magnetoresistance and magnetothermo-power in  $\text{Bi}_{1-x}\text{Sb}_x$  wires near the gapless state 81
- Bolesta I.M., Borodchuk A.V., Kushnir O.O.** The morphology of non-percolated silver films 82
- Bolesta I.M., Borodchuk A.V., Kushnir O.O., Kolych I.M., Karbovnyk I.D., Syworotka I.I.** Optical characterization of the ultra-thin silver films 83
- Bordun O.M., Bihday V.G., Kukharsky I.Yo** Cathodoluminescence of thin films based on  $\text{ZnGa}_2\text{O}_4$  84

<b>Borzanytsya D.V., Il'chenko V.V., Lushkin O.E.</b> The influence of an electric field on physicochemical properties of surface layers of lithium niobate	85
<b>Boychuk V.M., Turovska L.V., Mezhylovska L.Yo.</b> Thermodynamics and crystal-chemistry of defect subsystem of PbTe crystals and Pb-Cr-Te solid solutions	86
<b>Boyko V.T., Shpotyuk O.I., Vakiv M.M.</b> Ab initio simulation of nanoclusters in thin As-S films	87
<b>Bukatyuk V.V., Tatarchuk T.R.</b> Obtainment of Nano-Scale Ruby Particles of $Al_{2-x}Cr_xO_3$ Composition	88
<b>Burunkova J. A., Denisyuk I.Yu., Minozhenko O.A.</b> Polymeric thin films of DAST nanocrystals for photonic applications: technology and properties	89
<b>Butariev K.A., Koval I.P., Len Yu.A., Nakhodkin M.G.</b> Influence of annealing on transformation submonolayer coverage of chromium and titanium on Si(001) surface	90
<b>Chelyadyn V.L., Kotsyubynsky V.O.</b> The influence of nanodispersed titanium dioxide hydratation degree on specific capacity of lithium power sources with cathodes on its base	91
<b>Chernyadyev A.Yu., Plachev Yu.A., Vysotsky V.V., Tsivadze A.Yu.</b> Thermochromic behavior of nanoparticles based on aluminum(III) crown-substituted porphyrin in toluene solution	92
<b>Chobanuk V.M., Lishchynskyy I.M., Bachuk V.V. Krynytskiy O.</b> Mechanisms of growth, topology and properties of nanostructures based on lead telluride	93
<b>Chobanyuk V.M., Lysyuk Yu.V.</b> New thermoelectric materials on the based semiconductors nanostructure	94
<b>Chomolyak A.A., Kranjčec M., Studenyak I.P., Vorohta M., Matolin V.</b> Influence of annealing on optical parameters of $cu_6ps_5i$ amorphous thin films	95
<b>Dmitriev A.I. Fedorchenko D.A.</b> The nanocompositions on Van-der-Waals surface of InSe single crystal	96
<b>Dmitruk N.L., Kondratenko O.S., Kotova N.V., Romanyuk V.R.</b> Tuning of surface plasmon resonance in ultrathin gold films by post-growth thermal processing	97
<b>Domantsevych N.I., Aksimentyeva O.I., Martynjuk M.M.</b> Structure and properties of the modified polyethylene films	98
<b>Dudko A.O., Il'chenko V.V., Lushkin O.E.</b> Formation of nanostructured oxides of alkaline earth metals on scandium oxide	99
<b>Dukarov S.V., Sukhov V.N., Churilov I.G.</b> Size effects melting of the condensed metal films	100
<b>Dutka V., Opaynich I., Dutka Yu., Kovalskyi Ya.</b> Monomolecular films and reactivity of diacyl diperoxides. ( <i>Ivan Franko Lviv National University, Lviv, Ukraine; Lviv Polytechnic National University, Lviv, Ukraine</i> ). [172]	101
<b>Dvorina L.A., Dranenko A.S., Koshelev M.V.</b> Obtaining and oxidation of NiSi and NiSi <sub>2</sub> films on single-crystal silicon	102
<b>Dykun N.I.</b> Thermoelectric properties of laminate structures in the PbTe-Cd (Zn) Te, PbTe-Bi(Sb) <sub>2</sub> Te <sub>3</sub>	103
<b>Dynowska E., Makhniy V.P., Melnyk V.V., Khusnutdinov S.V.</b> Optical and	105

structural properties isovalent-substituted cdse layers	
<b>Evmenova A.Z., Odarych V.A., Sizov F.F., Vuichyk M.V.</b> CdTe films structure	<b>106</b>
<b>Fertman E., Beznosov A., Desnenko V., Dolya S.</b> Low temperature magnetic states of the nano phase segregated CMR compound $(Nd_{0.9}Y_{0.1})_{2/3}Ca_{1/3}MnO_3$	<b>107</b>
<b>Freik D.M., Gorichok I.V., Parashchuk T.O., Makovushyn V.I., Bardashevskaya S.D.</b> Thermodynamics of crystal defects in cadmium and lead telluride	<b>108</b>
<b>Freik D.M., Dzumedzey R.O., Mateik G.D., Gevak T.P., Kotyk M.V.</b> Features investigated the influence of Bi, Sb on the kinetic parameters of compounds IV-VI semiconductor crystals	<b>109</b>
<b>Freik D.M., Dzundza B.S., Kostyuk O.B., Letsyn R.B., Arsenych I.I., Gatala I.B.</b> Changing kinetic parameters of IV-VI thin films during their holding in air	<b>110</b>
<b>Freik D.M., Gurgula G.Ya., Freik N.D., Vadyuk M.P., Vintonyak T.P., Zinyuk R.R.</b> Mechanisms of formation and defect subsystem of solid solutions based on zinc chalcogenides	<b>111</b>
<b>Freik D.M., Sokolov A.L., Bilina I.S., Nesteruk O.R.</b> Topology of thin films and nanostructures II-VI, IV-VI received vapor phase methods	<b>112</b>
<b>Freik D.M., Turovska L.V., Andriyshin I. Pokryshka O.Ya., Hrub'yak O.B.</b> Nonstoichiometry and crystal chemistry of defects in lead chalcogenides crystals	<b>113</b>
<b>Freik D.M., Wojcik V., Yurchushyn I.K., Nadruga O.R.</b> Modeling of thickness dependences of thermoelectric parameters for compounds IV-VI	<b>114</b>
<b>Fridman Yu.A., Gorelikov G.A., Klevets Ph.N.</b> Influence of strong inclined anisotropy on the phase states of ultrathin magnetic films.	<b>115</b>
<b>Galchynsky O.V., Gloskovska N.V., Yarytska L.I.</b> Захоплення та делокалізація носіїв заряду в кристалічній системі $CdI_2-PbI_2$	<b>116</b>
<b>Galuschak M.O., Boryk V.V., Tkachuk A.I.</b> Crystal-chemistry of point defects and their complexes and thermoelectric properties of solid solutions	<b>117</b>
<b>Gasuyk I.M., Grabko T.V.</b> On the possibility of using lithium-iron spinels replaced by titanium as a cathode material of chemical power sources	<b>118</b>
<b>Gasynets S.M., Solomon A.M., Azhniuk Yu.M., Yasinko T.I., Guranich O.G., Shpyrko G.N., Gomonnai A.V., Rubish V.M.</b> The study of $(As_2S_3)_{100-x}(Sn_2P_2S_6)_x$ glasses crystallization	<b>119</b>
<b>Gorbenko V.I.</b> Ab-initio study of atomic adsorption on graphene	<b>120</b>
<b>Gorobets S., Gorobets O., Dvoynenko O., Cherednychenko D., Lebeda G.</b> Dendrite Ni self-similar structures received by electrodeposition in the external magnetic field	<b>121</b>
<b>Gorobets S.V., Dvoynenko O.K., Mykhailenko N.O.</b> High gradient ferromagnetic matrix in the form of self alike dendritic Ni nanostructures parameters research	<b>122</b>
<b>Grischenko L., Bezugla T., Zaderko O., Radkevich V., Diyuk V.</b> The surface functionalization of activated carbon carries for nano-scale Pd catalysts	<b>123</b>
<b>Hertsyk O.M., Bojchyshyn L.M., Kovbuz M.O., Pandiak N.L.</b> Modification of nanocrystalline of wares from amorphous metallic alloys	<b>124</b>

<b>Horbenko Y.Yu., Konopelnik O.I., Aksimentyeva O.I., Demchenko P.Yu., Pavlyk M.R.</b> Charge Transport in the nanosystems based on conducting polymers	125
<b>Horley V.V., Kinzerska O.V., Melnyk V.V., Tkachenko I.V.</b> ZnO:Cr heterolayers luminescence	126
<b>Il'chenko V., Kravchenko O., Teslenko S.</b> About the Dependence of Barrier Height on Dioxide Film Thickness in SnO <sub>2</sub> (Pt) – p-Si Heterojunction	127
<b>Il'chuk G., Kusnezh V., Shapoval P., Petrus' R., Guminilovych R.</b> The CdS thin films fabrication and properties	128
<b>Ilashchuk M.I., Orletsky I.G., Parfenyuk O.A., Gavaleshko N.M.</b> Electrical Properties of Anisotypical Heterojunctions of ZnO/p-Cd <sub>1-x</sub> Zn <sub>x</sub> Te	129
<b>Ilashchuk M.I., Orletsky I.G., Parfenyuk O.A., Gavaleshko N.M.</b> Influence of Low-Temperature Annealing on the Properties of Near-Surface Layer of CdTe, Doped with Vanadium	130
<b>Ivankiv L.I., Pastyrsky A.Y., Koltun N.S., Gavryluh V.M.</b> Dissociation mechanism of chemisorbed ethanol molecule on oxide surface	131
<b>Ivlev G.D., Gatskevich E.I., Malevich V.L., Zinovyev V.A., Dvurechenskii A.V.</b> Melting temperature of the nanocluster embedded in rigid matrix	132
<b>Ivlev G.D., Gatskevich E.I., Smagina Zh.V., Dvurechenskii A.V., Nikiforov A.I.</b> Photoluminescence and infrared radiation of Ge/Si heterostructures with quantum dots at nanosecond laser exposure	133
<b>Karachevtseva L., Goltviansky Yu., Konin K., Lytvynenko O., Parshin K., Tsybrii Z.</b> The near-IR light absorption in 2D macroporous silicon structures with SiO <sub>2</sub> nanocoatings	134
<b>Kavetsky T.S., Tsmots V.M., Matlak O.S.</b> On the models of normal indentation size effect in application to chalcogenide vitreous semiconductors	135
<b>Kavetsky T.S., Tsmots V.M., Pankiv L.I.</b> Radiation impact on the concentration of magnetic ordered clusters and paramagnetic centres per clusters in chalcogenide glasses	136
<b>Kharun L.T.</b> Size phenomena in condensed systems	137
<b>Klanichka Yu.V., Mezhylovska L.Yo., Klanichka V.M., Zukowski P.</b> Degradation of structure and physical properties of AIVBVI compounds films under the influence of external factors	138
<b>Klanichka Yu.V., Yavorskiy Ya.S., Klanichka V.M., Yavorskiy R.S.</b> Influence of surface layers on electrical properties semiconductor structures in Petrits' model	139
<b>Klochko N.P., Khrypunov G.S., Volkova N.D., Kopach V.R., Lyubov V.M., Klepikova K.S., Kopach A.V.</b> Pulse plating of zinc oxide nanowires	140
<b>Kondrahova D.M., Synashenko O.V., Protsenko I.Yu., Tkach O.P., Odnodvoretz L.V.</b> Magnetoresistive properties of multilayers based on Fe/Cu and Fe/Pd	141
<b>Kondrat O., Popovich N., Holomb R., Mitsa V., Petrachenkov O., Veres M.</b> Ab initio calculations and Raman spectra of As <sub>2</sub> S <sub>3</sub> , Sb <sub>2</sub> S <sub>3</sub> and Bi <sub>2</sub> S <sub>3</sub> films	142
<b>Kosyak V.V., Opanasyuk A.S., Bukivskij P.M., Gnatenko Yu.P.</b> Optical properties of Cd <sub>1-x</sub> Mn <sub>x</sub> Te films	143

- Kotsyubynsky V.O., Chelyadyn V.L., Ilynskyy R.V., Myronyuk I.F., Mokliak V.V.** Electrochemical intercalation of Li<sup>+</sup> in the dehydrated anatase synthesized by the method of TiCl<sub>4</sub> hydrolysis 144
- Kotsyubynsky V.O., Mokliak V.V., Kolkovskyy P.I., Grubyak A.** Photovoltaic cells based on nondispersed titania sensitized by anthocyanine dyes 145
- Kovalenko M.V., Bovgyra O.V., Kapustianyk V.B.** Ab Initio Study of Gas Adsorption on ZnO Nanotubes 146
- Kozak M.I., Studenyak I.P., Loya V.Yu., Makauz I.I., Fedelezh V.I., Solomon A.M., Zhikharyev V.M., Krafchik S.S., Krasilinets V.M.** Photoinduced bleaching of GeS<sub>2</sub> chalcogenide glass amorphous films 147
- Kozak M.M., Kravchenko O.E., Penyukh B.R.** The conductivity and structure of ultrathin lead and manganese films 148
- Kudanovich A.M., Khairullina A.Ya., Filimonenko D.S., Vorobyova T.N., Parchomenko I.N.** Optical diagnostics of physical-chemical properties and changes in NiO/Al<sub>2</sub>O<sub>3</sub> nanocomposite at different exposures 149
- Kurek E.I., Oliynych-Lysyuk A.V., Raransky M.D.** Research on behaviour peculiarities of a dislocation-impurity subsystem in the thin near-surface Be layers 150
- Kurovets V.V., Yaremiy S.I.** Microhardness of helium implanted monocrystalline materials with a garnet structure 151
- Lepikh Y.I.** Structure and electrico-physical properties of complex compounds on Ge basis 152
- Lishchynskyy I., Klanichka V., Varvaruk V.** Thermodynamic and structural investigations of As<sub>2</sub>S<sub>3</sub>-based glasses with additions of Ag and/or I 153
- Lishchynskyy I., Varvaruk V., Dolibsky M.** Observation of crystallization of (As<sub>0.4</sub>Te<sub>0.6</sub>)<sub>100-x</sub>Ag<sub>x</sub> (x = 0, 5, 15 at. %) glasses 154
- Lisnyak V.V., Yatsimirsky V.K., Safonova V.V., Stratiychuk D.A., Boldyrieva O.Yu.** SEM, TEM examination of surface palladium nanoparticles 155
- Lobko E.V., Kozak N.V., Klepko V.V.** The mobility of the paramagnetic probe in the polyurethane films with various content of neodymium (3+) complex 156
- Loboda V.B., Kravchenko V.O., Shkurdoda Yu.O., Kolomiets V.M.** Conductivity of nanocrystalline alloy CoNi films 157
- Loboda V.B., Kolomiets V.M., Shkurdoda Yu.O., Saltykova A.I., Dekhtyaruk L.V.** The effect of giant magnetoresistance in three-layer nanocrystalline films Fe/Ag/Co 158
- Lop'yanko M.A.** Optimization of technology and simulation of physical processes in thin films II-VI, IV-VI 159
- Lop'yanko M.A., Nykyruy R.I., Mateik G.D.** Structure and physical properties of films of lead chalcogenides obtained from gas-dynamic stream of steam 160
- Lubenets V.A., Lyubchanskii I.L., Gorban O.A., Burkhovetskii V.V., Dvornikov E.A., Volkova G.K., Danilenko I.A., Konstantinova T.E.** Magnetic composite films based on La<sub>0.7</sub>Sr<sub>0.3</sub>MnO<sub>3</sub>/ZrO<sub>2</sub> nanopowders 161
- Lutsyk N.Yu.** Structure and electrical conductivity of amorphous films of the 163

GaSb-GeTe system

<b>Lysenko A.B., Kalinina T.V., Kosinskaya O.L., Zagorulko I.V.</b> Production of nanocrystalline bcc-phase in the $Ce_{79}Ag_{21}$ alloy	164
<b>Lytovchenko V.G., Strikha M.V., Klui M.I.</b> Gap appearance in the distorted multilayer grapheme	165
<b>Magunov I.P., Zinchenko V.F., Stoyanova I.V., Timukhin Ie.V. Stamikosto O.V., Mazur O.S., Kryvda M.Yu.</b> Lanthanide Sulfofluorides as Alloying Additives to Film-Forming Materials $MgF_2$ and $ZnS$	166
<b>Makarovsky N.A., Letyago L.M.</b> Plasma Resonance in Granular Films of the Al-In Alloy	167
<b>Makoviy V.V., Savchuk A.I., Stolyarchuk I.D., Tkachuk P.M., Savchuk O.A.</b> Comparative studies of colloidal nanoparticles and nanocomposites	168
<b>Malyk O.P., Kenyo G.V.</b> Electron scattering on the short-range potential of the crystal defects in GaN	169
<b>Mandzyuk V.I., Myroniuk I.F., Chelyadyn V.L.</b> The cyclic voltametry of nanodispersed tin dioxide	170
<b>Mandzyuk V.I., Nagirna N.I., Povazhnyi V.A., Golovko L.V., Rachiy B.I.</b> Anthracite as electrode material for lithium power sources	171
<b>Mezhylovska L.Yo, Koznyuk A.P., Koznyuk V.P., Korzchenevskiy O.Ye.</b> Crystal-chemistry defects in bromine doped crystals of cadmium tellurides	172
<b>Monastyrskii L.S., Pavlyk M.R., Vaskiv A.P., Yarytska L.I.</b> Features of heat transfer in porous silicon films	173
<b>Morushko O.V., Budzulyak I.M., Rachiy B.I., Yablon L.S.</b> Electron microscopic investigations of nanoporous carbon	174
<b>Mykolaychuk O.G., Romanyuk R.R., Balyts'ka V.O.</b> Radiation-induced effects in non-crystalline GeSe(S) films	175
<b>Myronyuk L.I., Kotsyubynsky V.O., Chelyadyn V.L.</b> Atomic Structure and Morphology of $SnO_2$ Nanoparticles Prepared by Pyrogenic and Liquid-Phase Methods	176
<b>Nagy R.O., Kranjčec M., Hip I., Petrachenkov E.I., Suslikov L.M., Studenyak I.P.</b> Deposition and spectrometric studies of $(Ga_{0.1}In_{0.9})_2Se_3$ thin films	177
<b>Nakhodkin N.G., Kulish N.P., Rodionova T.V.</b> Nanofacet structure of twin boundaries in polysilicon films	178
<b>Nikolaeva A.A. Konopko L.A., Tsurkan A.K., Botnary O.V.</b> Thermoelectric properties of Bi wires in a glass coating with the orientation of C3 along the wire axis	179
<b>Odnodvoretz L.V.</b> Futures of tensoresistivite effect in film materials on the range of elastic and plastic deformation	180
<b>Omelchenko S.A., Plakhtiy E.G., Bulanyi M.F., Kovalenko A.V., Khmelenko O.V., Gorban A.A.</b> The nature of the manganese luminescence centers in thin-film emitting devices	182
<b>Ostapenco E.V., Mazurenko N.I.</b> Formation and properties of anodic aluminum oxide, resulting in a complex electrolyte	183
<b>Philonenko N.Yu., Beryoza Ye.Yu., Baskevich A.S.</b> The study of phase	184

composition for diffusion zone after saturation the surface with both boron and carbon	
<b>Prokopiv V.V., Vanchuk V.B.</b> Nonstructure defects in cadmium telluride	<b>185</b>
<b>Prokopiv V.V.(Jr.), Dumen'ko N.V., Volochans'ka B.P., Pylyponyuk M.A.</b> Influence of cultivation conditions on faulty subsystem in lead telluride films	<b>186</b>
<b>Prysyazhnyuk V.I., Mykolaychuk J.G.</b> Investigation of magnetic properties of films of Gd-Fe system	<b>187</b>
<b>Pylypiv V.M., Grygoruk O.O.</b> Parameters of radiation disordering process of epitaxial YIG films crystalline microstructure at implantation by oxygen ions	<b>188</b>
<b>Raransky M.D., Balazyuk V.N., Melnyk M.I., Kovalyuk Z.D.</b> X-ray diffraction methods for dimensional measurement of nanocrystals – CdMnS, TiO <sub>2</sub> , fullerenes	<b>189</b>
<b>Reshetnyak O.V., Koval'chuk E.P., Błażejowski J., Protsyshyn Kh.V., Pavlyuk V.A.</b> Electrochemiluminescent (ECL) properties of the thin films of aniline-luminol copolymers on the platinum electrode	<b>190</b>
<b>Rusavsky A.V., Vasin A.V., Okholin P.M., Rymarenko N.L., V.G. Stepanov, Nazarov A.N.</b> Correlation of deposition conditions and mechanical properties of a-SiC(:H) films deposited by radio-frequency magnetron sputtering technique	<b>191</b>
<b>Ryk L.V., Domantsevich N.I., Yatsyshyn B.P.</b> Structure research in the modified composite resins	<b>192</b>
<b>Saliy Ya.P., Stefaniv N.Ya.</b> Diffuse instability of the uniform distribution of lead in PbSnTe	<b>193</b>
<b>Savchenko N.D., Shchurova T.N., Opachko I.I.</b> Band gap simulation for ZrO <sub>2</sub> <Ti> nanostructured materials	<b>194</b>
<b>Savchuk A., Stepanchikov D., Burykin N., Korchemskaya E.</b> Adjustment of native nanostructure of bacteriorhodopsin molecules by low-power cw gas laser irradiance	<b>195</b>
<b>Savchuk S.A., Kleto G.I., Tkachuk V.I., Smolinsky M.M., Garasym V.I.</b> Structural and optical properties of Zn <sub>1-x</sub> Co <sub>x</sub> O thin films	<b>197</b>
<b>Shevchuk M.O.</b> Crystallquasichemistry point defects in crystals of europium chalcogenides: EuTe, EuSe, EuS	<b>198</b>
<b>Shilov V.M., Voitenko O.Yu., Podolska V.I., Marochko L.G.</b> Electrophysical Properties of Biocomposites Containing Colloidal Silver	<b>199</b>
<b>Shpotyuk M.V., Balitska V.O., Shpotyuk O.I., Iovu M.S., Vakiv M.M.</b> On the role of coordination topological defects in reversible photodarkening in As-S thin films	<b>200</b>
<b>Sirenko H.A., Midak L.Ya., Skladanyuk M.B., Soltys L.M.</b> The Structure of superficial tapes of carbon fiber, copper-plated using PbS	<b>201</b>
<b>Sirenko H.A., Kuzyshyn O.V.</b> The thickness of quasisolid nanolayers of polyglycolic liquids-base lubricants on the steel surfaces	<b>202</b>
<b>Slyotov M.M., Khomyak V.V., Slyotov O.M., Kosolovsky V.V.</b> Effect of Se isovalent impurity on ZnO properties	<b>203</b>
<b>Slyotov M.M., Skrypnyk M.V., Kosolovsky V.V., Ulyanitskiy K.S.</b> Properties of CdTe, CdO layers and CdO-CdTe heterojunction	<b>204</b>
<b>Smertenko P.S., Olkhovik G.P., Sheludko E.V., Bryzgin A.R.</b> The	<b>205</b>

peculiarities of morphology and charge flow in composites on the base of fluorocontaining polyamides	
<b>Smolinsky M.M., Savchuk A.I., Stolyarchuk I.D., Makoviy V.V.</b>	<b>206</b>
Temperature dependence of exciton peaks of semiconductor nanocrystals	
<b>Sopinsky M.V., Indutnyi I.Z., Michailovska K.V., Shepeliavyi P.E., Tkach V.M.</b>	<b>207</b>
Polarization conversion effect in obliquely deposited SiO <sub>x</sub> films and nc-Si-SiO <sub>x</sub> light-emitting nanocomposites	
<b>Soroka A., Dmitrenko O., Kulish M., Zabolotny M., Davydenko N., Studzynsky S., Olasyuk A.</b>	<b>208</b>
Influence of tunneling on dissociation of electron – hole pairs in PEPC films doped with fullerene	
<b>Starik S., Perevertailo V., Gontar O., Kutsay O., Loginova O., Gorohov V.</b>	<b>209</b>
Hydrophilic properties of plasma modified diamond-like films	
<b>Stasyuk I.V., Stetsiv R.Ya., Vorobyov O.A.</b>	<b>210</b>
Energy spectrum of one-dimensional ionic conductors described by Pauli statistics	
<b>Stetsyshyn Yu., Zolobko O., Zemla J., Fornal K., Kostruba A., Donchak V., Harhay H., Skorobohaty Ya., Budkowski A., Voronov S.</b>	<b>211</b>
Creation, structure and properties of new thermo- and pH-responsible grafted nanolayers	
<b>Styrov V.V., Simchenko S.V., Karpov E.G.</b>	<b>212</b>
Production of the chemoelectric currents in Pd-GaP Schottky nano-structures under exposure to hydrogen atoms	
<b>Suchikova Y.A.</b>	<b>214</b>
Dependence of the porosity of indium phosphide on the etching time	
<b>Suchikova Y.A., Kidalov V.V., Konovalenko A.A., Kirilash A.I., Sukach G.A.</b>	<b>215</b>
Stages of pore formation of porous indium phosphide	
<b>Sulym P.O., Gasuyk I.M.</b>	<b>216</b>
Influence of doping by rare-earth elements on electrical properties of lithium-iron spinels	
<b>Sydorchuk P., Khlyap H.</b>	<b>217</b>
Effect of Atmospheric Oxygen on Electrical Performance of ZnCdHgTe-Based Structures	
<b>Sylenko P.M., Dan'ko D.B., Shlapak A.M., Pylypchuk O.F., Okun' I.Yu., Solonin Yu.M.</b>	<b>218</b>
New technique of deposition of continuous TiO <sub>2</sub> films and their photocatalytic properties	
<b>Tkachenko A.V., Ananina O.Y.</b>	<b>219</b>
Simulations of OH radicals adsorption at the Si(100) surfaces	
<b>Tokarev S., Il'chuk G., Kusnezh V., Schevchuk O., Tokarev V.</b>	<b>220</b>
Synthesis and properties of CdS nanoparticles embedded into thin polymer covering grafted to the solid surface	
<b>Tovstolytkin A.I., Matviyenko A.I., Podyalovskii D.Y., Polishchuk D.M.</b>	<b>221</b>
Inhomogeneous magnetic state of thin films of sodium-doped lanthanum manganites	
<b>Tsaly V.Z., Kleto G.I.</b>	<b>222</b>
The correlation between nanovoid-species structure of amorphous Tellurides of In studied with X-ray diffraction	
<b>Tsmots V.M, Pan'kiv L.I., Pan'kiv I.S., Tovstolytkin A.I., Matviyenko A.I., Shchuplyak A.N.</b>	<b>223</b>
Особливості температурних залежностей магнітоопору плівок La <sub>0.84</sub> Na <sub>0.16</sub> MnO <sub>3</sub>	
<b>Turko B.I., Kapustianyk V.B., Eliyashevskyy Yu.I., Kulyk B.Y., Czaplak Z.</b>	<b>224</b>
Dielectric studies of ZnO polycrystalline films	
<b>Vasin A.V., Rusavsky A.V., Okholin P.M., Kholostov K.I.,</b>	<b>226</b>

<b>Bondarenko V.P., Lysenko V.S.</b> Oxidation behavior of carbon-rich a-SiC:H films deposited by radio-frequency magnetron sputtering	
<b>Vorzobova N.D., Bulgakova V.G., Burunkova J.E., Moskalenko A.I.</b> Research of polymeric periodic structures formation process in photocurable composite materials by interference method	227
<b>Voznyak O.M., Zukowski P., Nykyruy L.I., Lysak A.V.</b> Relaxation time approximation and variational method in the calculation of kinetic parameters of semiconductors	228
<b>Yaremiy I.P., Yaremiy S.I., Tomyn U.O.</b> Atomic emission spectroscopy of nanoporous carbon materials	229
<b>Yunakova O.N., Miloslavsky V.K., Kovalenko E.N.</b> Absorption spectrums of thin films of solid solutions $Cs_2(Cd_{1-x}Zn_x)_4$	230
<b>Yurchyshyn L.D.</b> Crystallochemistry of point defects and properties of nonstoichiometric GeTe, SnTe	231
<b>Yushchuk S.I., Yuryev S.O.</b> Measurement of uniaxial magnetic anisotropy field of epitaxial ferrogarnet films	232
<b>Zamkovets A.D., Pershukevich P.P.</b> Spectra-luminescent properties of plasmonic nanocomposites at a low-intensive lamp excitation	234
<b>Zaslavskii O.M.</b> Formation of multicharge nanoforms of titanium oxide in films	235
<b>Zaulychnyy Ya.V., Ilkiv V.Ya., Foja O.O., Dymarchuk V.O., Zarko V.I.</b> Electronic structures peculiarities study of $x-Al_2O_3 + y-SiO_2$ ( $x = 0.2; 0.3; 0.75; 0.96; y = 0.8; 0.7; 0.25; 0.04$ ) nanocomposites mixtures	236
<b>Zayachuk D.M., Mikityuk V.I., Pashuk A.V., Ulyanitsky K.S., Shlemkevych V.V., Kharko O.V.</b> Peculiarities of segregation of the <i>Eu</i> impurity in the <i>PbTe:Eu</i> crystals grown from melt	237
<b>Zubko E.I.</b> Design, nanomodification and characterization of silicon multilayer as optical material	238

#### Секція 4

**Тонкоплівкові елементи електронних пристроїв, наноелектроніка**  
(усні доповіді)

#### Session 4

**Thin film elements for electronic devices and nanoelectronics**  
(oral)

<b>Ahiska R., Mamur H.</b> Data Acquisition System for Thermoelectric Generators	240
<b>Barabash Y., Zabolotny M., Serdenko T.</b> The processes of electron transfer in photosynthetic reaction centers as a standard in nanoelectronics	243
<b>Brus V.V., Hlasehchuk M.I., Kovalyuk Z.D., Maryanchuk P.D., Ulyanytsky K.S., Gritsyuk B.M.</b> A solar cell based on a heterojunction n-TiO <sub>2</sub> /p-CdTe	244
<b>Bushma A.V.</b> Matrix model of excitation of the thin film bar graph display	245
<b>Klyui N.I., Kostylyov V.P., Lukyanov A.N., Chernenko V.V., Kharchenko N.M., Nikitin V.A., Li T.A., Klyui A.N.</b> Effect of plasma treatment and diamond-like carbon film deposition on CdTe film photoelectrical	246

characteristics	
<b>Kogut I.T.</b> Simulation of nonstandard 3D SOI-Structures for SoC and LoC elements	247
<b>Kosyachenko S.V., Zakharuk Ya.D., Galochkin A.V., Dremlyuzhenko S.G., Rarenko I.M., Strebegev V.N.</b> Surface purification of CdTe substrates by laser melting	248
<b>Kovalyuk Z.D., Bakhtinov A.P., Vodop'yanov V.N., Netyaga V.V.</b> Large low frequency capacitance of a nanocomposite “layered semiconductor – ferroelectric” capacitor under light illumination	249
<b>Krukovsky S., Sukach A., Tetyorkin V., Mrykhin I., Mykhashchuk Y.</b> Electrical properties of InP/InGaAsP double heterostructures	250
<b>Krupa M.M.</b> Magnetic switching of magnetic nanofilms and management spin current by pulse laser radiation	251
<b>Ptashchenko F.O., Ptashchenko O.O., Dovganyuk G.V.</b> Effect of surface doping of the characteristics of silicon p-n junctions as gas sensors	252
<b>Semikina T.V., Komaschenko V.N., Godlewski M., Kopalko K., Shmyryeva L.N., Skorohod I.A.</b> Review of oxide material application for transparent electronics	253
<b>Sklyarchuk V.M., Sklyarchuk O.F., Rarenko A.I., Zakharuk Ya.D., Dremlyuzhenko S.G., Koval'chuk M.L., Kolisnyk M.G.</b> The effect of the semiconductor surface treatment on the photosensitivity of Ni-HgInTe Schottky diodes	254
<b>Tiagulskiy S.I., Tyagulskiy I.P., Nazarov A.N., Nazarova T.M., Lysenko V.S., Rebohle L., Lehmann J., Skorupa W.</b> Temperature dependence of electroluminescence and charge trapping in Ge and Tb implanted thin SiO <sub>2</sub> films	255
<b>Vlasenko A.I., Veleschuk V.P., Kysselyuk M.P., Lyashenko O.V.</b> Changes of the electro-physical parameters of the InGaN/GaN heterostructures of power light-emitting diodes at enhanceable current	257
<b>Vlasenko A.I., Veleschuk V.P., Lyashenko O.V.</b> Acoustic emission in light-emitting heterostructures	258
<b>Yashin A.G., Michailov E.D., Michailova A.M.</b> Nanocomposition membranes for power and information transducers	260

#### Секція 4

#### Тонкоплівкові елементи електронних пристроїв, наноелектроніка (стендові доповіді)

#### Session 4

#### Thin film elements for electronic devices and nanoelectronics (poster)

<b>Aktas K., Acar S., Salamov B.G.</b> Plasma effect on the CuInSe <sub>2</sub> thin film resistivity	262
<b>Dauletmuratov B.K.</b> An electronic switching structure Te-CdTe, formed under pulsed laser irradiation of CdTe	265

<b>Demir M., Güzel T., Acar S., Özer M.</b> The Pool-Frenkel conduction mechanism in metal-GaP contacts	<b>266</b>
<b>Dovhij V.V.</b> SOI MOS-transistor with the parted gate	<b>269</b>
<b>Freik D.M., Terletskyi A.I., Zapukhlyak R.I., Dykun N.I.</b> New approaches to measuring of thermoelectric parameters of semiconductor materials	<b>270</b>
<b>Gubanova A., Kyselyuk M., Kryskov Ts., Rachkovsky O., Yeremchuk V.</b> Solar CdSe/ZnSe cells	<b>271</b>
<b>Il'chenko V.V., Kravchenko O.I., Telega V.M., Shyshkin M.O.</b> Kinetics investigation of the semiconductor gas sensor based on heterojunction SnO <sub>2</sub> -Si(p)	<b>272</b>
<b>Ivanov I., Nychyporuk T., Skryshevsky V., Makarov A.</b> Porous Bragg mirror as rear reflector for multi-Si solar cells	<b>273</b>
<b>Juzevych V.M., Koman B.P.</b> Mechanical and adhesive parameters in metal condensate – single crystal silicon system	<b>274</b>
<b>Kogut I.T., Dovhij V.V.</b> Layouts features of SOI CMOS gate matrix arrays	<b>275</b>
<b>Kravtsiv M.M., Boychuk V.I., Virt I.S., Medvid M.A.</b> Optical-electronic transducers on the basis of thin film photopiroelectrical sensors	<b>276</b>
<b>Kukla O.L., Mamykin A.V., Kurys Ya.I.</b> Modified polypyrrole films for determination of aliphatic alcohols in water solutions	<b>277</b>
<b>Kukla O.L., Tzyrkunov Yu.A., Matvyenko L.M., Vahula O.O., Fedchenko O.M.</b> Interference calixarene films as sensitive elements for “optoelectronic nose”	<b>278</b>
<b>Mikhailova A., Motsar A.</b> Dielectric properties of membranous superionic capacitor	<b>279</b>
<b>Mokrenko A.A.</b> Self-assembling of low-dimensional Ti systems under conditions of quasi-equilibrium condensation	<b>280</b>
<b>Petrus' R., Kusnezh V.</b> The In/p-Cd <sub>1-x</sub> Mn <sub>x</sub> Te Schottky barriers fabrication and properties	<b>281</b>
<b>Rednyk A., Haviar S., Vaclavu M., Matolin V.</b> SnO <sub>2</sub> nanowires for gas sensing application	<b>282</b>
<b>Skatkov L., Gomofov V., Deribo S.</b> SAXS investigation of sub-micropores in electrochemical MnO <sub>2</sub> films	<b>283</b>
<b>Yatsyshyn B.P., Yatsyshyn S.P.</b> Structure and electrical conductivity of microcrystalline films Re-Me-Ge	<b>284</b>
<b>Yushchenko A.V., Lendel V.V., Telega V.M., Punkovska C.O.</b> About the existence of the optimum nano scale thickness of In <sub>2</sub> O <sub>3</sub> films to the response of the gas sensitive heterostructure	<b>285</b>

Наукове видання

**Фізика і технологія тонких плівок та наносистем**

**Матеріали  
XIII міжнародної конференції**

МКФТТПН-XIII

**Physics and Technology of Thin Films and Nanosystems**

**Materials  
of the XIII International Conference**

ІСРТТФН-XIII

Редактор *Дмитро Фреїк*

Технічний редактор *Богдан Дзундза*

Комп'ютерна верстка *Богдан Дзундза, Олександр Соколов, Віктор Борик,  
Лілія Туровська, Ігор Юрчишин, Любов Юрчишин,  
Андрій Ткачук, Лідія Харун*

Відповідальний за випуск *Олександр Соколов*

*Усі матеріали подані у авторській редакції*

Підписано до друку 22.04.2011.

Формат 60x84<sub>16</sub>. Папір офсетн. Гарнітура “Таймс”.

Умовн. друк. арк. 16,6. Тираж 250.

Видавництво

Прикарпатського національного університету імені Василя Стефаника,  
вул. С. Бандери, 1, м. Івано-Франківськ, 76000.

Тел. 8(0342) 71-56-22.

E-mail: [vdvcit@pu.if.ua](mailto:vdvcit@pu.if.ua)

**Ф 83 Фізика і технологія тонких плівок та наносистем. Матеріали XIII Міжнародної конференції: У 2 т. – Т. 2.** / За заг. ред. Заслуженого діяча науки і техніки України, д.х.н., проф. **Фреїка Д.М.** – Івано-Франківськ: Видавництво Прикарпатського національного університету імені Василя Стефаника, 2011. – 300 с.